UNIVERSITY OF SOUTHAMPTON

FACULTY OF NATURAL AND ENVIRONMENTAL SCIENCES

School of Biological Sciences

Effect of anionic lipids on ABC transporters

by

Megha Rai

Thesis for the degree of Doctor of Philosophy

Sep 2018

UNIVERSITY OF SOUTHAMPTON

ABSTRACT

FACULTY OF NATURAL AND ENVIRONMENTAL SCIENCES

School of Biological Sciences

Thesis for the degree of Doctor of Philosophy

EFFECT OF ANIONIC LIPIDS ON ABC TRANSPORTERS

Megha Rai

The role of ATP-Binding Cassette (ABC) transporters in multidrug and agrochemical resistance has been a rising concern across medicine and agriculture. One way to tackle such resistance would be to target the interactions of lipids in the bilayer with the transmembrane helices of the transporters. As a prelude to such studies, it is first necessary to identify specific lipid binding sites at the membrane lipid interface that modify transport activity and could serve as potential inhibitor targets. In this study, the difference in the effects of anionic, neutral and cationic phospholipids has been demonstrated through the varying ATPase activity of Sav1866 and McjD. Furthermore, specific binding sites for anionic phospholipids that contain a cluster of positively charged residues on the cytoplasmic side of McjD was revealed using fluorescence quenching technique. Upon removal of the positive residues, the binding affinity for the anionic lipids was lost. Due to the nature of the technique, only a single tryptophan residue on the protein was required. Therefore, a systematic study comprising of site-directed mutagenesis was used to find the optimal replacement for the endogenous tryptophans to produce an active mutant. Subsequent inactive mutants were characterised using a crosslinking technique to compare their conformational status with the wild-type protein. Another aspect of this study was to purify Sav1866 and McjD using detergent-free styrene maleic acid (SMA) to preserve their native environment, which is often disturbed by using detergents. The SMA purification generated pure protein with a comparable yield to the detergent purification. Lastly, as part of the CASE studentship with Syngenta, a eukaryotic ABC transporter, Mdl1 was purified and characterised. The work produced was at its preliminary stage *en route* to elucidating its mechanism in fungicide resistance.

Table of Contents

List of Figures

Chapter 1 General Introduction

Chapter 2 General Materials and Methods

Chapter 3 Determining conservative substitutions for tryptophan residues in Sav1866

Chapter 4 Conformational changes of Sav1866 in response to nucleotides, detergents and lipids

Chapter 5 Effect of lipid head groups on ABC transporters

Chapter 6 Expression and purification of eukaryotic ABC transporter, Mdl1

List of Tables

Chapter 2 General Materials and Methods

Chapter 3 Determining conservative substitutions for tryptophan residues in Sav1866

Chapter 4 Conformational changes of Sav1866 in response to nucleotides, detergents and lipids

Chapter 5 Effect of lipid head groups on ABC transporters

DECLARATION OF AUTHORSHIP

I, Megha Rai declare that this thesis and the work presented in it are my own and has been generated by me as the result of my own original research.

Effect of anionic lipids on ABC transporters

I confirm that:

This work was done wholly or mainly while in candidature for a research degree at this University;

Where any part of this thesis has previously been submitted for a degree or any other qualification at this University or any other institution, this has been clearly stated;

Where I have consulted the published work of others, this is always clearly attributed;

Where I have quoted from the work of others, the source is always given. With the exception of such quotations, this thesis is entirely my own work;

I have acknowledged all main sources of help;

Where the thesis is based on work done by myself jointly with others, I have made clear exactly what was done by others and what I have contributed myself;

None of this work has been published before submission.

Signed:

Date:

Acknowledgements

Malcolm, you have been the greatest supervisor one could ever ask for, and for that I thank you from the bottom of my heart. Accepting this PhD was one of my happiest and proudest moments, and I have been so lucky to have you as my mentor and a friend. Your positive charisma and enthusiasm always made the journey a little brighter. Thank you for the support from the beginning till finishing up this thesis.

A big thank you to John, who not only helped me get trained and get ready for this project but was also a great friend to be with in the lab (especially with the everlasting protein preps). Tony, who has been an immense help for this project, thank you for your time and patience! Howard, thank you for your support and guidance, and thank you for the demonstrating opportunity! Neville, thank you for all your support with the equipment in the lab, and also our chemical synthesis project. I would also like to thank the team at the University of Birmingham and Syngenta, especially Naomi for letting us work with you and Darren for looking after me. It was a pleasure knowing you. A special thanks to my project students and the technicians. You guys were superb!

This journey would not have been as joyful without my friends in Southampton: (in no particular order) Luke, Mike, Prutha, Emily, Itzia, Alison, Grace, Roshan, Ben, Andy, Moritz, Matt and Jack, thank you all for your kind support!

Thank you to mum and dad for always being there for me! And thank you to all my friends and family for believing in me!

Ninu, I am proud of you!

Thank you Luchi! I could not have asked for a better partner to share this journey with.

And lastly, thank you, Coco, for keeping me company while writing my thesis!

Abbreviations

ABC	ATP-binding cassette
CMC	Critical micelle concentration
di(C18:1)EPC	1,2-dioleoyl-sn-glycero-3-ethylphosphocholine
di(C18:1)lysyl PG	1,2-dioleoyl-sn-glycero-3-[phospho-rac-(3-lysyl(1-glycerol))]
di(C18:1)PA)	1,2-dioleoyl-sn-glycero-3-phosphate
di(C18:1)PC	1,2-dioleoyl-sn-glycero-3-phosphocholine
di(C18:1)PE	1,2-dioleoyl-sn-glycero-3-phosphoethanolamine
di(C18:1)PG	1,2-dioleoyl-sn-glycero-3-phospho-(1'-rac-glycerol)
DTT	Dithiothreitol
EDTA	Ethylenediaminetetraacetic acid
EPI	Efflux pump inhibitors
Fe/S	Iron/Sulphur
IPTG	Isopropyl ß-D-1-thiogalactopyranoside
LDH	Lactic dehydrogenase
MATE	Multidrug and toxic compound extrusion family
MDR	Multidrug resistant
MFS	Major facilitator superfamily
MscL	Mechanosensitive channels
NADH	Nicotinamide adenine dinucleotide
NBD	Nucleotide binding domain
OGNG	Octyl glucose neopentyl glycol
PBS	Phosphate buffer saline
PEP	phosphoenolpyruvate
PIP2	Phosphatidylinositol 4, 5- bisphosphate
PK	Pyruvate kinase
RND	Resistance nodulation division
SMALP	SMA lipid particles
SMR	Small multidrug resistance
TEMED	N,N,N',N'-Tetramethylethylenediamine
tetra(C18:1)CL	1',3'-bis[1,2-dioleoyl-sn-glycero-3-phospho-glycerol
TMD	Transmembrane domain
WT	Wild-type

Chapter 1 General Introduction

One of the major challenges in medicine and agrochemical industry today is overcoming the biological resistance to a wide range of drugs and agrochemicals resulting in the failure of treatments for cancer and infection as well as the failure to protect crops from weeds and pests (El-Awady et al., 2017). Multidrug resistance (MDR) efflux pumps are one of the key players in conferring such resistance due to their ability to export a wide variety of drugs and chemicals out from the cell (Borges-Walmsley, McKeegan, & Walmsley, 2003). Their ubiquitous distribution from bacteria to plants and animals, and their ability to accommodate a range of structurally dissimilar compounds have raised concerns over lack of strategies available to tackle the effects of these proteins (Marquez, 2005; Srivalli & Lakshmi, 2012).

Efflux pumps are divided into five categories according to their structure and function (X.-Z. Li & Nikaido, 2009). All efflux pumps except for adenosine triphosphate (ATP) binding cassette (ABC) superfamily utilise either a proton (H^+) or a sodium (Na^+) gradient to transport substrates (Fluman & Bibi, 2009).

i. Major facilitator superfamily

Major facilitator superfamily (MFS) efflux proteins form the largest group of secondary active transporters. They are subdivided into several families with uniport, antiport and symport transport mechanisms. Six subfamilies of MFS have been identified to have roles in the multidrug transport with a H^+ antiport mechanism (Saier & Paulsen, 2001). The 12 transmembrane drug/H^+ antiporter 1 family (DHA-1) and 14 transmembrane DHA-2 are the most common MFS transporters in bacteria (Fluman & Bibi, 2009). MFS proteins are involved in both intrinsic (pre-existing resistance independent of previous exposure to drugs (G. Zhang & Feng, 2016)) and acquired resistance (evolved resistance post-exposure to drugs as a result of random mutation or transfer of external resistance genes (Munita & Arias, 2016)). For example, Bmr from *Bacillus subtilis* provides intrinsic resistance through gene amplification in the presence of its substrate, which activates its expression. In *Staphylococcus aureus* (*S. aureus*), there are 3 MFS proteins, NorA, QacA and QacB that are involved in acquired resistance to cationic compounds and quinolone (reviewed by (Fluman & Bibi, 2009)).

ii. Multidrug and toxic compound extrusion family

The multidrug and toxic compound extrusion family (MATE) transporters are versatile as they can use either a H^+ or a Na^+ electrochemical gradient to transport compounds. MATE transporters characterised to date can only transport cationic compounds but not anionic compounds (Lu, 2016). An example of this type of transporter is NorM from *Vibro parahaemolyticus*, known to have resistance towards streptomycin and doxorubicin (Baugh, Ekanayaka, Piddock, & Webber, 2012; Y. Morita, Kataoka, Shiota, Mizushima, & Tsuchiya, 2000; Yuji Morita et al., 1998).

iii. Small multidrug resistance family

As the name suggests, small multidrug resistance family (SMR) are a group of small proteins with sizes ranging from 104 to 115 amino acids with only four transmembrane α helices (Paulsen et al., 1996). EmrE from *Escherichia coli* (*E. coli*) is a classic example of an SMR protein that uses the H^+ antiport system to transport cationic hydrophobic compounds such as tetracycline and tetraphenylphosphonium, providing resistance to these agents (Yerushalmi, Lebendiker, & Schuldiner, 1995).

iv. Resistance nodulation division superfamily

In the resistance nodulation division superfamily (RND), efflux of the substrate is driven by a H^+ gradient. Members of this superfamily are known to contribute towards antibiotic resistance and are widely found in Gram-negative bacteria. The large periplasmic domain of the RND protein is able to form complexes with outer membrane proteins and periplasmic adaptor proteins to export substrates past the outer membrane (Nikaido & Takatsuka, 2009). Examples include AcrB from *E.coli* (Murakami, 2008) and MexAB-OprM from *Pseudomonas aeruginosa* (Jeannot et al., 2008).

v. ATP-binding cassette superfamily

ATP-binding cassette superfamily (ABC) proteins transport a diverse range of substrates using energy from ATP hydrolysis (Higgins, 1992). ABC importers play vital roles in the uptake of nutrients, peptides and ions into cells in prokaryotes, but they do not provide this role in eukaryotes (Rees, Johnson, & Lewinson, 2009). There are seven families of ABC transporters in humans involved in various cellular events such as lipid and cholesterol transport and regulation of ion channels. Mutations in these ABC transporter proteins have been reported to result in diseases such as cancer, cystic fibrosis and diabetes (Rees et al., 2009). Permeability (P)-

glycoprotein is one of the most widely studied ABC transporters due to its significant role in pumping out chemotherapeutic drugs from cancer cells (Borst & Elferink, 2002).

1.1 Current strategy to regulate multidrug resistance

There has never been a greater demand for effective efflux pump inhibitors (EPIs) to counteract multidrug resistance (Marquez, 2005). The current methods include using inhibitors to bind to the efflux pumps to prevent the export of drugs (Ahmed, Borsch, Neyfakh, & Schuldiner, 1993) or they could form complexes with the drug substrates so they can no longer be transported by the efflux pumps (Zloh, Kaatz, & Gibbons, 2004). Alternatively, inhibitors could also hinder the supply of energy, i.e. from ATP hydrolysis or electrochemical gradients (Zloh et al., 2004).

When it comes to tackling antibiotic resistance in bacteria, several potent EPIs have been shown to inhibit the activity of particular efflux pumps, but none have been successful in clinical trials (Opperman & Nguyen, 2015). Similarly, in cancer cells with chemotherapy resistance, P-glycoprotein inhibitors have been too toxic for use in the clinic. Increasing members of ABC transporters are being recognised to have essential roles in insecticide/pesticide resistance (Epis et al., 2014; Yu et al., 2017), but yet there are no effective ways to overcome such resistance.

This thesis will investigate a novel mechanism of modulating ABC transporters by characterising the effects of anionic lipids on the protein. In the study model system, the protein is reconstituted into defined lipid bilayers, and the lipid binding sites on the protein are examined using fluorescence assay as described in the following sections. The regulatory effect of the lipid binding on the ABC protein will provide targets for the design of inhibitors, which would complement the activity of drugs and agrochemicals.

1.2 Molecular structure and properties of ABC transporters

ABC transporters have a generic four domain structure as shown in Figure 1.1. Two domains are embedded in the lipid bilayer and are called the transmembrane domains (TMDs). They are highly hydrophobic and form a pathway for substrate transport. The other two domains are found on the cytoplasmic side of the membrane. These domains bind ATP and couple its hydrolysis to the transport of substrates. Hence, these are the nucleotide binding domains (NBDs) (Higgins, 1992).

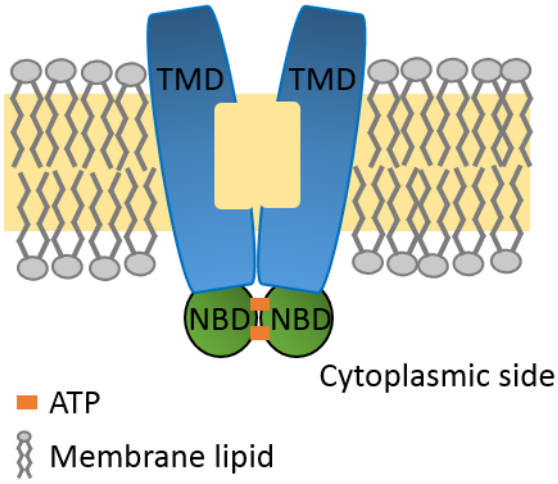

Figure 1.1 A schematic representation of an ABC transporter. The transmembrane domains (TMD) are embedded in the lipid bilayer, and the two nucleotide domains (NBD) are located on the cytoplasmic side, where they bind two ATP molecules (orange rectangle). The central cavity between the two TMD provides a translocation pathway for substrate transport.

ABC transporters are divided into three classes based on the organisation of their TMDs (Figure 1.2) (Rees et al., 2009). Type I ABC importer have the TMD fold type similar to *A. fulgidus* Mod BC protein and type II ABC importers are similar to *E. coli* BtuCD. In importer ABC transporters, the TMDs are expressed as separate subunits (Locher, 2016). On the other hand, ABC exporters have their NBDs fused to the TMDs at their C terminal and so can act as half transporters. Some even have all four domains fused together as with ABCB1 or ABCB4 (Locher, 2016). ABC exporters have a similar fold to Sav1866 TMD (Locher, 2016). The half transporters can either homodimerise or heterodimerise as in the case of LmrA and TAP1/TAP2 respectively (Zolnerciks, Andress, Nicolaou, & Linton, 2011). The number of helices and the structural arrangement of those helices are different in each group due to various substrate specificity (Rees et al., 2009). Nevertheless, the TM helices are all connected via coupling helices in all types of ABC transporters, which play a key role in transmitting conformational changes to the TMDs (Locher, 2016; Rees et al., 2009).

NBDs are structurally more conserved than TMDs (Rees et al., 2009). There are five short sequence motifs that make up the NBDs as shown in Figure 1.3. They are Walker A motif, conserved glutamine in the Q loop, a signature motif that is unique to ABC transporters, Walker B motif and a histidine residue in the H loop or the switch region (Dassa, 2011). NBDs have two domains. The larger of the two domains, Rec A like domain contains two β sheets and six α helices with a Walker A motif (GXXGXGK(S/T)) and a Walker B motif (Φ Φ Φ Φ D) (Φ is a hydrophobic residue) (Dassa, 2011; Davidson, Dassa, Orelle, & Chen, 2008). The smaller domain is the helical

domain, which contains the signature motif, LSGGQ motif (linker peptide or C motif) (Davidson et al., 2008). The ATP binding site is at the interface between the two domains (Rees et al., 2009). The two domains in the NBD are connected by two intracellular loops (ICLs) (Davidson et al., 2008; Dawson & Locher, 2006). The conformational changes induced by the ATP binding at the NBD is conveyed through these ICLs to the transmembrane domain (Dawson & Locher, 2006).

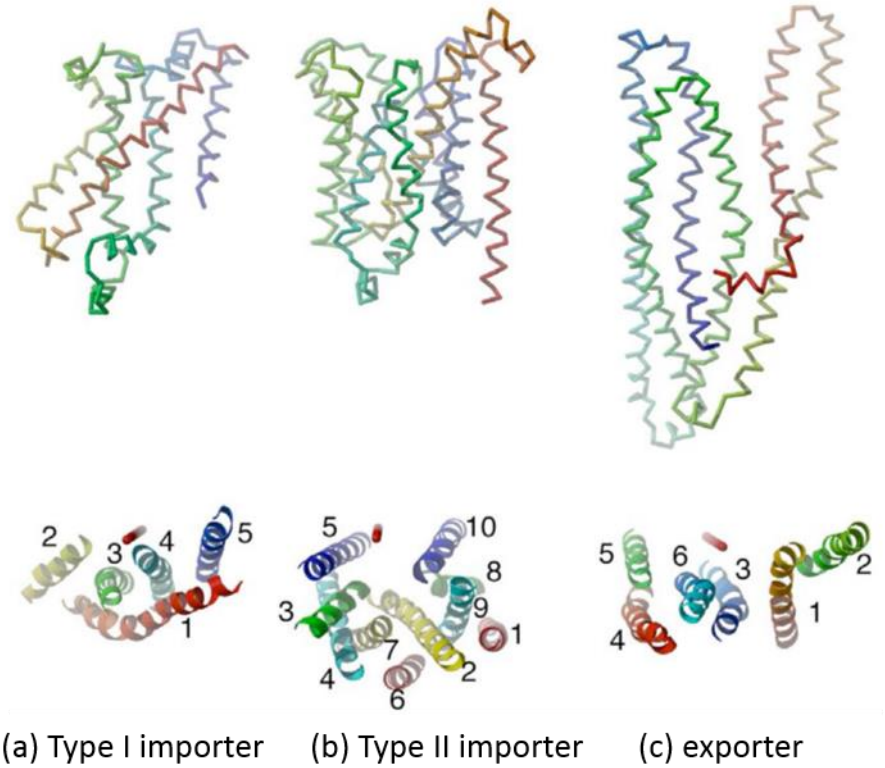

Figure 1.2 The three classes of transmembrane domains (TMDs) in ABC transporters. Type I importer fold of MetI, (b) Type II importer fold of BtuC and (c) ABC exporter fold of Sav1866. The top representation of polypeptides illustrates the organisation of the TMDs with red at the N-terminal to blue at the C-terminal (orientation vertical to the plane of the membrane bilayer). The bottom illustrations show the same polypeptides in ribbon diagrams viewed from the periplasmic side rotated 90˚ from the top view. Image edited from (Rees et al., 2009).

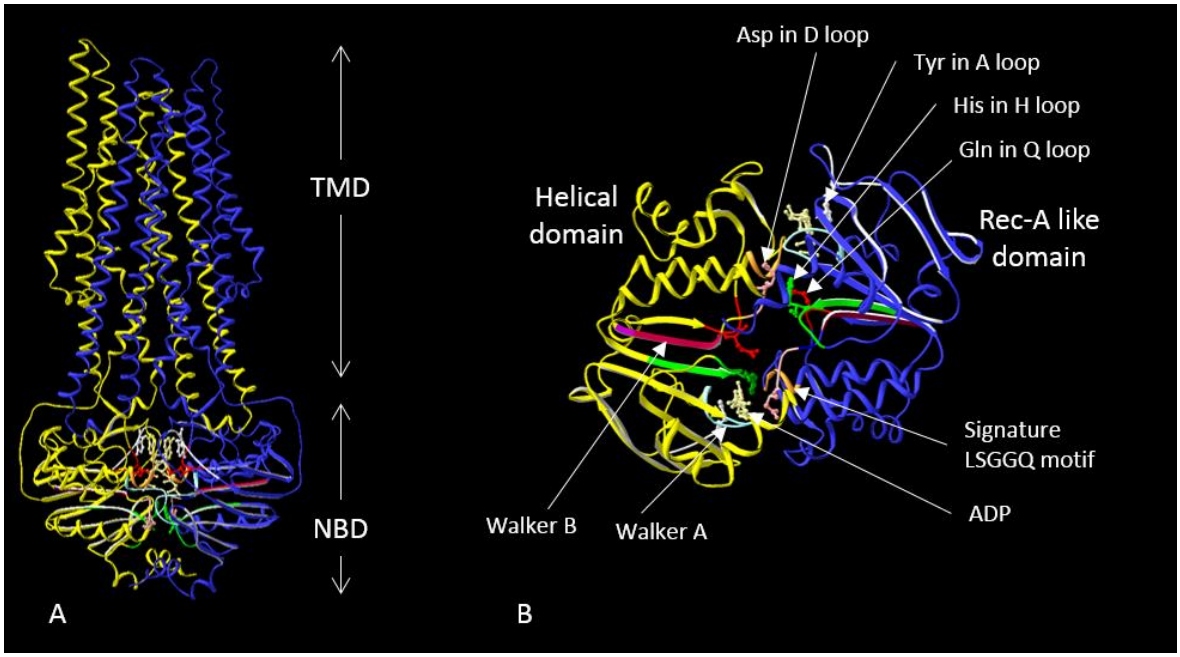

Figure 1.3 Crystal structure of Sav1866 with bound ADP (PDB: 2HYD). (A) The two monomers are shown in blue and yellow with each containing a TMD and a NBD. (B) NBD of Sav1866 highlighting the conserved motifs, shown from the cytoplasmic view. NBD is divided into two domains, the Rec-A like domain, which consists of the Walker A (cyan) and Walker B motif (red), and helical domain containing the signature LSGGQ motif (orange). During ATP binding, the signature LSGGQ motif is aligned opposite to the Walker A motif of the Rec-A like domain. An ADP molecule is shown in light yellow. The loops contain a single conserved residue that helps orient and stabilise the ATP molecule for its hydrolysis. Figure is edited using Swiss-PdbViewer software (4.1.0).

The binding of ATP to the NBD aligns the residues of the Walker A motif in the cis-NBD to the signature LSGGQ motif of the trans-NBD (Higgins & Linton, 2004; Seeger & van Veen, 2009) as shown in Figure 1.3. This particular alignment of the motifs is called head to tail (Locher, 2009).

In the helical domain, the γ phosphate of the ATP molecule interacts with the conserved glutamine of the signature LSGGQ motif of the other NBD (Higgins & Linton, 2004).

Walker A is a glycine-rich motif, which has electrostatic interactions with the α and β phosphates of the ATP molecule. Hence, it is also referred to as the phosphate binding loop or P loop (Jones & George, 2004). The A loop, which precedes the Walker A motif provides aromatic residues, usually a tyrosine that helps pack against the purine ring of the adenine (Locher, 2016; Seeger & van Veen, 2009).

The aspartate from Walker B is responsible for maintaining the geometry of the active site through hydrogen bonds with the magnesium ion (Jones & George, 2004). Downstream of the Walker B motif are the H loop and D loop, which help coordinate the γ phosphate of the ATP

molecule (Lopez-Marques et al., 2015). The conserved histidine residue from the H loop forms hydrogen bonds with the γ phosphate of the ATP molecule, which is necessary for hydrolysis. In addition, the H loop forms a bridge between the Walker A and D loop interface suggesting a regulated coupling between binding of ATP molecule and formation of a dimer (Davidson et al., 2008).

The conserved glutamine in the Q loop also interacts with the ATP and hydrolytic water (Higgins & Linton, 2004) and makes contact between the γ phosphate of ATP molecule with the TMDs (Seeger & van Veen, 2009).

ABC transporters utilise two ATP molecules per reaction cycle. However, the number of substrates transported per cycle is unknown. Nevertheless, it is thought that one ATP molecule is hydrolysed per substrate when two small substrates are transported. When a bigger substrate is transported, two ATP molecules are hydrolysed (Dawson & Locher, 2006).

In this thesis, Sav1866 and McjD are used as model ABC proteins to characterise the regulatory effects of specific lipids on the protein in order to explore alternative methods of overcoming multidrug resistance.

1.2.1 Sav1866

Sav1866 is an ABC multidrug transporter protein from *S. aureus* (Dawson & Locher, 2006), and a bacterial homologue of human ABC transporter, P-glycoprotein, with 28% sequence similarity (Zolnerciks, Wooding, & Linton, 2007). Since the crystal structure of Sav1866 was published, it has been used in homology modelling of other ABC transporters (O'Mara & Tieleman, 2007; Zolnerciks et al., 2007).

Sav1866 is a half ABC transporter with fused TMD (amino acid residue 1-320) at the N terminus and NBD (amino acid residue 337-578) at the C terminus as shown in Figure 1.3 (Dawson & Locher, 2006). The two monomers dimerise to form a full transporter (Dawson & Locher, 2006). Its dimensions are 120 Å long, 65 Å wide and 55 Å deep in size. There are 12 transmembrane helices and between them are the intra and extracellular loops. There are 2 ATP binding sites at the interface between the P loop of one NBD and ABC signature motif of the other NBD, which is highly conserved among ABC transporters (Dawson & Locher, 2006).

In Sav1866 (Figure 1.3), the open conformation has two wings opening up towards the extracellular side, and each wing is made up of TM1 and TM2 from one subunit and TM3 and TM6 of the other subunit. (Dawson & Locher, 2006). There is a large cavity at the interface between

the 2 TMDs, accessible from the outer leaflet. At the level of the inner leaflet, the cavity consists of mainly polar and charged amino acids from helices of TM2-TM5, providing a hydrophilic surface. This suggests that the cavity may not have a high affinity for hydrophobic compounds as substrates (Dawson & Locher, 2006).

Although the physiological substrates of Sav1866 are unknown, compounds such as Hoechst 33342, tetraphenylphosphonium, vinblastine and verapamil have been shown to enhance the basal ATPase activity of the protein by almost two-fold (Velamakanni, Yao, Gutmann, & van Veen, 2008). Lactococcal cells that expressed Sav1866 showed resistance to Hoechst 33342 compared to control cells in cytotoxicity assays. Moreover, the resistant cells were found to be sensitised by verapamil, a human ABC modulator (Velamakanni et al., 2008). The same study also showed the transport of amphiphilic cationic ethidium by Sav1866, which was shown to be inhibited by verapamil.

1.2.2 McjD

McjD is an antibacterial peptide transporting ABC protein from *E.coli* (Choudhury et al., 2014). The antibacterial peptide, Microcin J25 (MccJ25) is a cyclic peptide that binds to the bacteria's RNA polymerase, preventing transcription (Rebuffat, Blond, Destoumieux-Garzon, Goulard, & Peduzzi, 2004). This self-defence system of the bacteria is encoded by the *mcjABCD* gene cluster (Solbiati et al., 1999). *mcjA* encodes the precursor for the MccJ25, which is then modified by proteins encoded by *mcjB* and *mcjC*. Finally, *mcjD* encodes the ABC transporter for its export (Duquesne et al., 2007). In addition to MccJ25, Hoechst 33342 was also shown to stimulate the ATPase activity of detergent purified McjD and McjD reconstituted in proteoliposomes (Choudhury et al., 2014).

The structure of McjD is similar to Sav1866; a homodimer arrangement with an N terminal TMD (6 TMs) and a C terminal NBD. It is 124 Å long, 55 Å wide and 51 Å deep (Choudhury et al., 2014). The crystal structure of McjD in the presence of an ATP analogue, AMP-PNP and $MgCl_2$ showed dimerised NBDs in an ATP bound state (Figure 1.4 A). The TM helices formed a large cavity that is occluded from both sides, which is different from the previous outward-facing Sav1866 structures (Dawson & Locher, 2006, 2007; Mehmood et al., 2016). The occluded state was also verified by crosslinking studies. Cysteine residues were introduced in the extracellular loop, residue L53C, connecting TM1-TM2 and TM1'-TM2' to allow for intermolecular crosslinking (Figure 1.4 B). In the presence of ATP and AMP-PNP, cross-linked dimers were formed representing an occluded state (Choudhury et al., 2014).

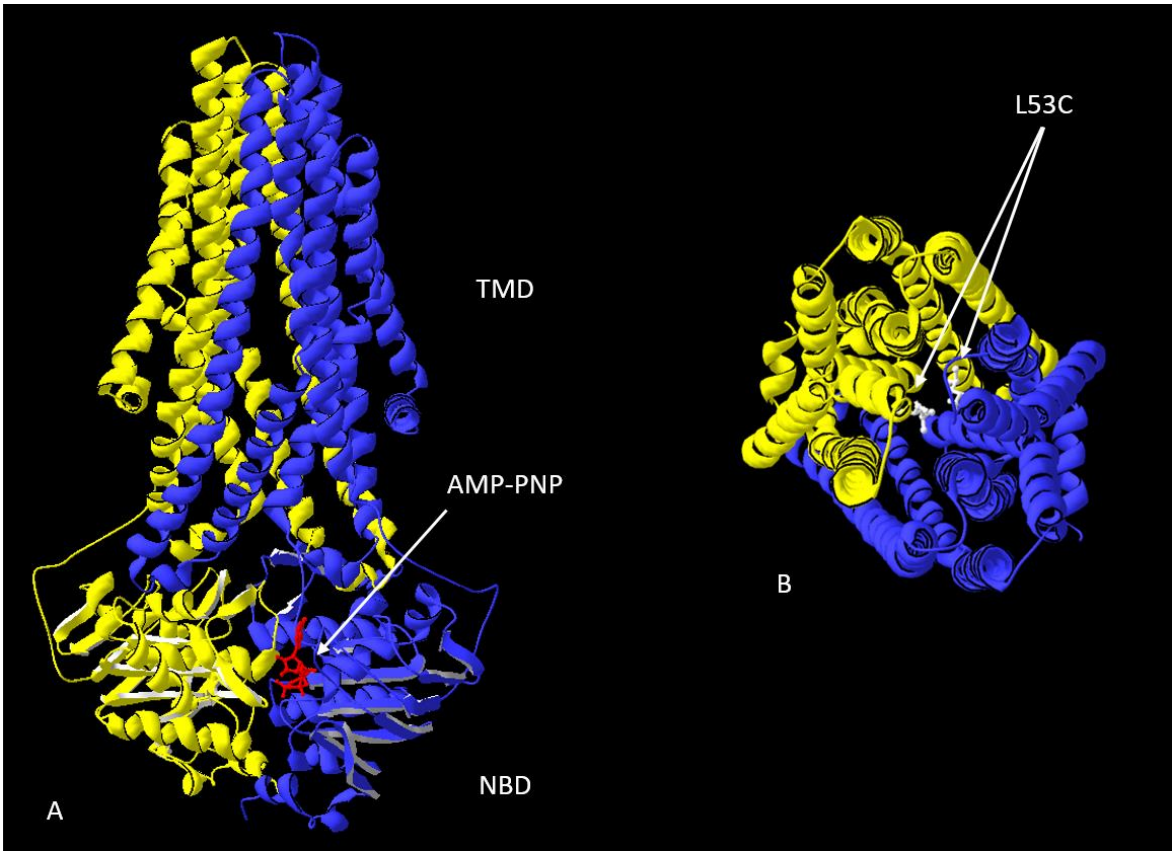

Figure 1.4 Crystal structure of McjD with bound AMP-PNP (PDB: 5EG1). (A) The two monomers are shown in blue and yellow with each containing a TMD and a NBD. (B) L53C connecting TM1-TM2 and TM1'-TM2' to allow for intermolecular crosslinking, shown from the periplasmic view. Figure is edited using Swiss-PdbViewer software (4.1.0).

Following the review of the model proteins, Sav1866 and McjD, the next section will give an overview of the various types and properties of membrane lipids found in bacteria, eukaryotes and archaea, and their regulatory effects on the proteins embedded within the membrane.

1.3 Membrane lipids

Biological membranes are physical barriers surrounding cells and organelles. They have evolved to protect the cell from hostile environment and simultaneously provide selective passage of nutrients into the cell and remove toxic waste products from the cell (Silhavy, Kahne, & Walker, 2010). They are also a site for energy production that uses chemical or charge gradients and plays a central role in signal transduction (Gustot, Smriti, Ruysschaert, McHaourab, & Govaerts, 2010). There are some specialised membranes too such as the myelin sheath in nerve cells that provide electrical insulation, and rod cell membranes that capture photons (Luckey, 2014).

Lipids are biomolecules that are highly soluble in organic solvents (Berg, Tymoczko, & Stryer, 2002). There are three kinds of lipids in the bio-membrane; glycolipids, cholesterols and phospholipids (Berg et al., 2002) as shown in Figure 1.5 .

i. Glycolipids

Glycolipids are derived from sphingosine (amino alcohol group with long, unsaturated hydrocarbon chain (Berg et al., 2002), where the hydroxyl group of the sphingosine backbone is linked with one or more sugars, and the amino group is acylated by a fatty acid. The simplest form of glycolipid is cerebroside, which has an attached glucose or galactose residue. In the plasma membrane of eukaryotes, the sugar unit of the glycolipid faces the extracellular side (Berg et al., 2002).

ii. Cholesterols

Cholesterol is a steroid-based lipid with a tetracyclic fused ring containing a double bond between carbons 5 and 6, an iso-octyl hydrocarbon side chain attached at carbon 17, and a hydroxyl group on carbon 3. The trans-configuration of the tetracyclic rings makes cholesterol a planar and a rigid molecule with a flexible iso-octyl side chain (Ohvo-Rekilä, Ramstedt, Leppimäki, & Peter Slotte, 2002). Cholesterol molecules are situated parallel to the fatty acid chains while the hydroxyl group interacts with the phosphate head group of the phospholipids (Berg et al., 2002). The packing of the cholesterol lipids in the membrane increases its order and density, resulting in a more robust membrane with less permeability (Ohvo-Rekilä et al., 2002).

iii. Phospholipids

Phospholipids are the major constituents of membrane bilayers and will be the major focus of this project. There are two types of phospholipid, phosphoglycerides and sphingomyelins. Phosphoglycerides consist of a glycerol backbone with two fatty acyl chains esterified at positions carbon 1 and carbon 2. A phosphate is attached to the glycerol backbone by a phosphoester bond at position carbon 3, and the phosphate can be further modified with a range of alcohol containing groups (Huijbregts, de Kroon, & de Kruijff, 2000). The lipid tails contain two uneven hydrocarbon chains; the acyl chain attached to carbon 1 is usually saturated with 16-18 carbons and the other acyl chain attached to carbon 2 is unsaturated with 18-20 carbons (Koynova 2013). The unsaturated acyl chain usually contains between one and six double bonds in a cis configuration, which can cause a disordered conformation in the hydrocarbon chains affecting the packing of the lipids (Seelig & Seelig, 1977).

In bacteria, phospholipids are synthesised by enzymes at the plasma membrane (Huijbregts et al., 2000). Phosphatidic acid is the main precursor for the synthesis of phosphoglycerides in bacteria (Huijbregts et al., 2000). Other phospholipids (choline, ethanolamine, and glycerol) form when phosphatidic acid is esterified by other alcohols as shown in Figure 1.6.

Phospholipids carry charges on their phosphate head group. They can be negatively charged anionic lipids such as phosphatidylglycerol and cardiolipin; neutral, zwitterionic lipids such as phosphatidylethanolamine; or positively charged cationic lipids, lysyl- phosphatidylglycerol (Huijbregts et al., 2000; Luckey, 2014; Sievers et al., 2010).

Sphingomyelins, on the other hand, consist of a sphingosine backbone with an amino group attached to an acyl chain by an amide linkage. The acyl chain is often longer than the ones in phosphoglycerides with 20-24 carbons (Ohvo-Rekilä et al., 2002). The primary hydroxyl group of the sphingosine backbone is attached to a phosphate group through an ester link. As with the phosphoglycerides, the phosphate can be further modified (Berg et al., 2002).

Recent studies on membrane lipids and changes in their composition, fluidity and phases have revealed their role in conferring resistance to a range of drugs and chemicals (Khandelwal et al., 2018; Kohli, Smriti, Mukhopadhyay, Rattan, & Prasad, 2002; Peetla et al., 2010; Prasad, Chandra, Mukhopadhyay, & Prasad, 2006). Significant differences were observed in the lipid composition, compactness and fluidness between doxorubicin-sensitive (an anti-cancer agent) and resistant breast cancer cells (Peetla et al., 2010). Doxorubicin-resistant cancer cells were richer in sphingomyelin, phosphatidylinositol, cholesterol and cholesterol esters. This increased the rigidity of the membrane bilayer and packing density, which was hypothesised to cause a decrease in drug uptake as the drugs were found to have strong hydrophobic interactions with the bilayer surface (Peetla et al., 2010). A similar effect was observed in azole-resistant *Candida albicans,* where an enhancement in phosphatidylethanolamine led to increased rigidity of the plasma membrane (Dawaliby et al., 2016), and consequently reduced the movement of azoles into the cells (Khandelwal et al., 2018). Such modulatory effects of membrane lipids and their synergistic interactions with membrane proteins in conferring resistance to various drugs (Elliott et al., 2005; Kohli et al., 2002; Peetla et al., 2010) can be utilised to overcome resistance.

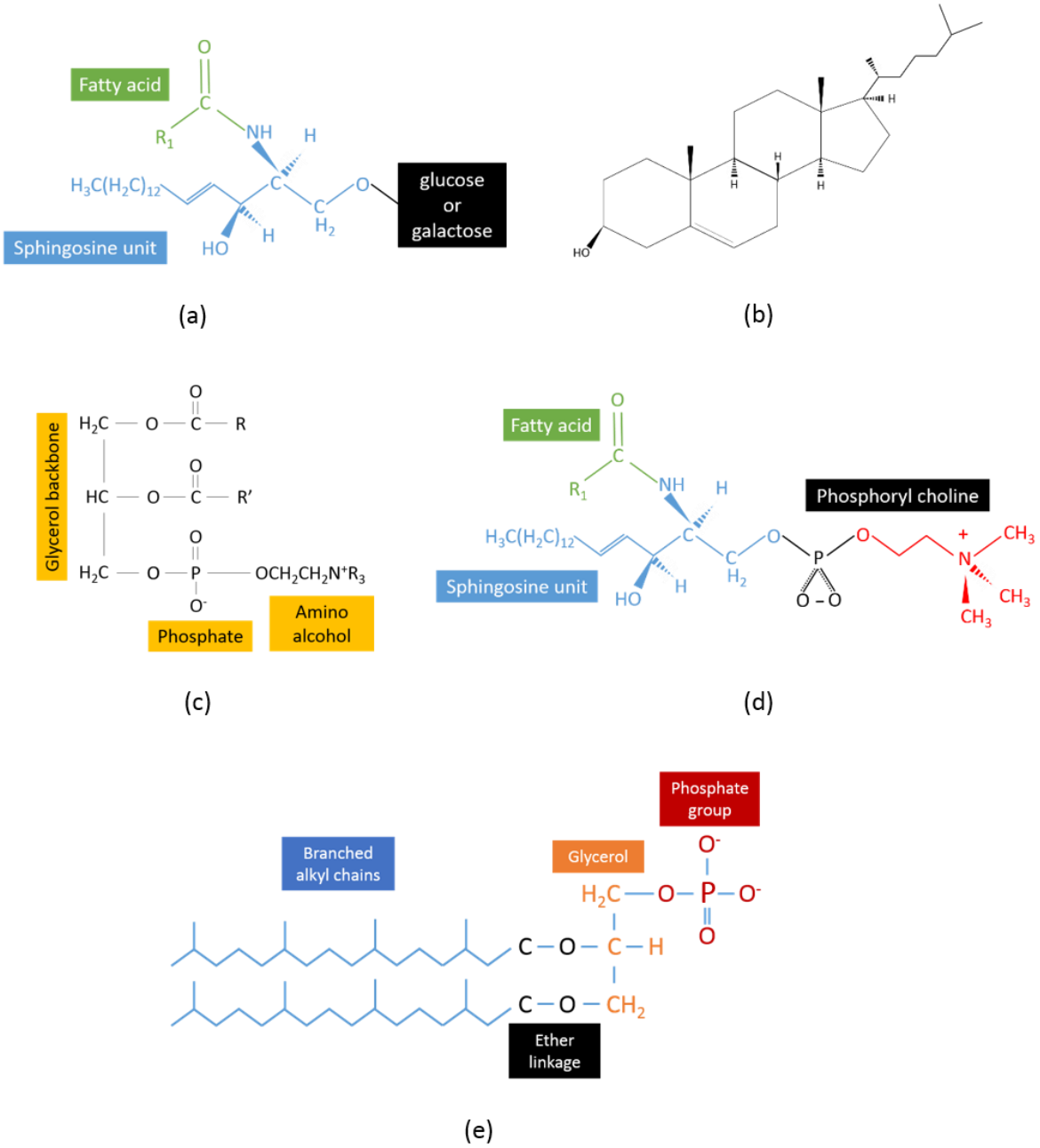

Figure 1.5 Molecular structure of different lipids found in the membrane. (a) Glycolipid (cerebroside) with a sphingosine backbone (blue), a fatty acid (green) acylated at the amino group and a sugar unit attached to the hydroxyl group (black). (b) Cholesterol with a hydrocarbon chain and a hydroxyl group at either side of the four hydrocarbon rings. (c) Phosphoglyceride with a glycerol backbone, two fatty acid chains at C-1 and C-2, and a phosphate group at C-3 that can be further modified with alcohol groups. (d) Sphingomyelin with a sphingosine backbone (blue), a fatty acid (green) acylated at the amino group and a phosphoryl choline group attached to the hydroxyl groups. (e) Phospholipid from archaea showing phosphate head group in red attached to glycerol in orange. The branched alkyl chains are attached to the glycerol with an ether bond (black). Pictures are edited from (Ball David W, 2012).

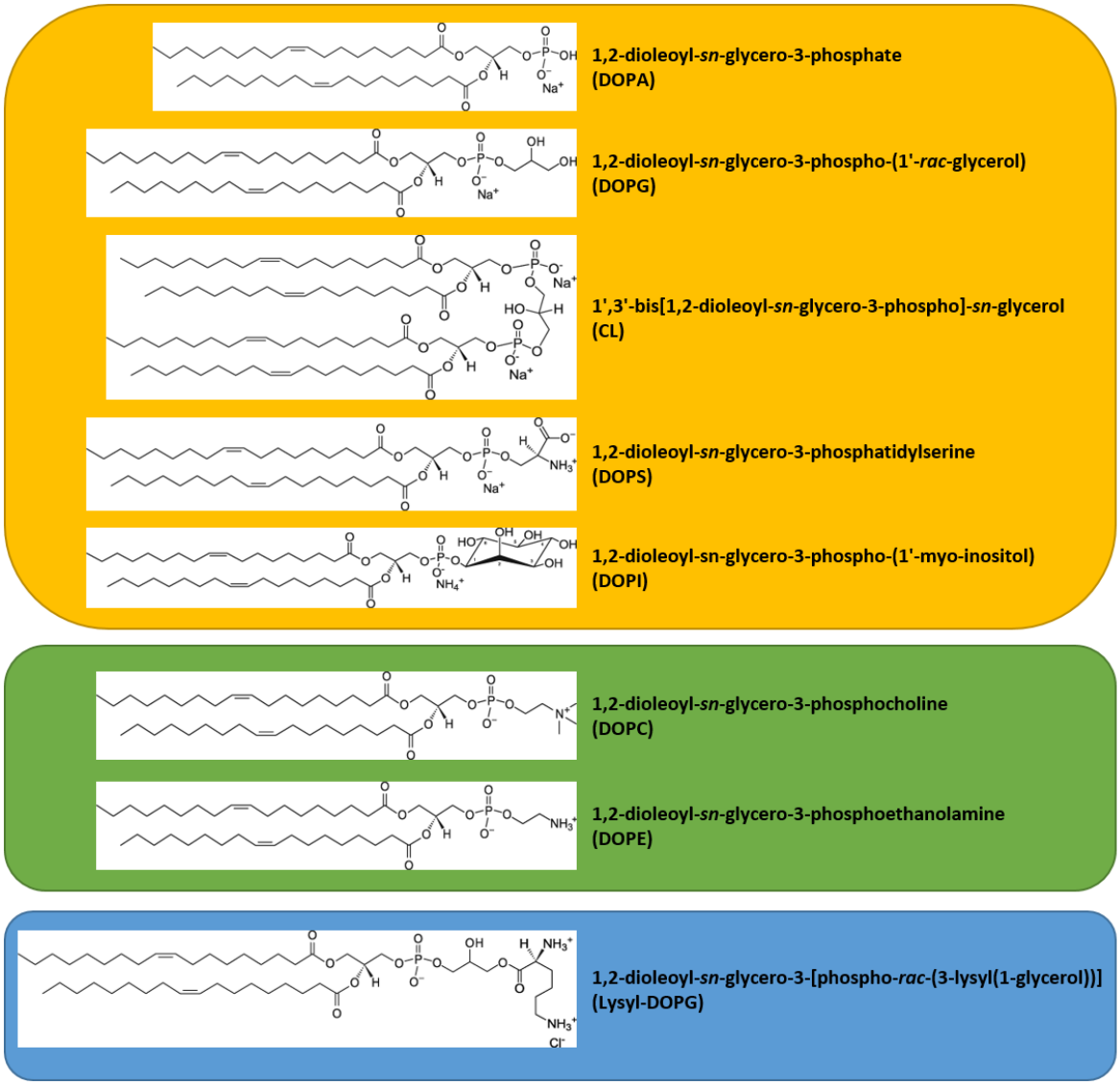

Figure 1.6 Molecular structures of phospholipids. Anionic (negatively charged) lipids are displayed in the top yellow box. Lipids displayed in the middle green box are zwitterionic (neutral), and an example of a cationic (positively charged) lipid is shown in the bottom blue box. Images obtained from Avanti Polar Lipids.

1.3.1 Variation of lipids in bacteria, eukaryotes and archaea

1.3.1.1 Bacteria

Gram-negative bacteria have two membranes; an inner plasma membrane and an outer cell wall. The cell wall consists of the outer membrane, a thin layer of peptidoglycan and periplasm as shown in Figure 1.7. The outer membrane is mainly made up of glycolipids and lipopolysaccharides unlike the inner membrane, which consists mainly of phospholipids. There are lipoproteins (lipids attached to proteins at the N terminal) and β barrel proteins such as porins

located on the outer membrane that allow transport of small molecules and ions (Silhavy et al., 2010).

Gram-positive bacteria only have one cell membrane made up of lipids, mainly phospholipids and integral membrane protein surrounded by a thick peptidoglycan layer (30-100 nm) (Silhavy et al., 2010) as shown in Figure 1.7. There are units of disaccharide N-acetyl glucosamine-N-acytylmuramic acid crosslinked by pentapeptide side chains present in the peptidoglycan layer, which makes the membrane rigid (Silhavy et al., 2010).

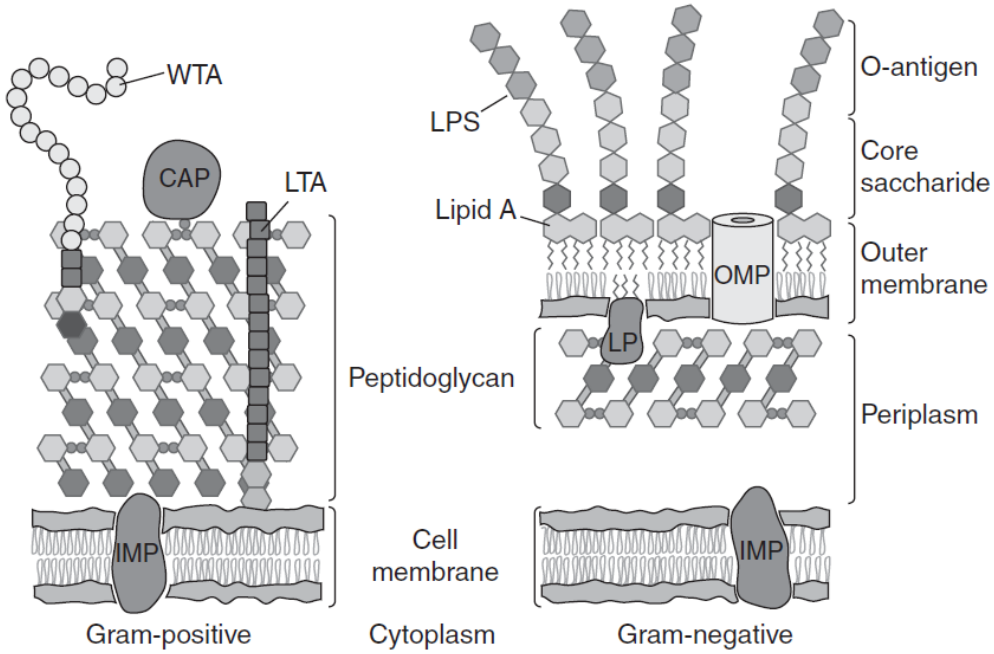

Figure 1.7 A schematic representation of the cell envelopes of Gram-positive and Gram-negative bacteria. Gram-positive cell envelope contains a thicker peptidoglycan than Gram-negative. Gram-negative has an additional outer membrane. IMP- integral membrane protein; CAP- covalently attached protein; OMP- outer membrane protein; LP- lipoprotein. Figure adapted from (Silhavy, Kahne, & Walker, 2010).

Lipid composition is variable within Gram-positive and Gram-negative bacteria. In *E. coli* (Gram-negative bacteria), 70-80% of the phospholipids in the bilayer is neutral phosphatidylethanolamine. Anionic phosphatidylglycerol makes up to 15-20%, and anionic cardiolipin is less than 5% of the membrane (Huijbregts et al., 2000; Raetz, 1978). The *S. aureus* (Gram-positive bacteria) bilayer, however, contains virtually no neutral lipids consisting of 36% phosphatidylglycerol, 7% cardiolipin and 57% cationic lysyl phosphatidylglycerol (Pasupuleti, Schmidtchen, & Malmsten, 2012). The composition of phospholipids also varies during the log and stationary phase of bacterial growth. For example, cardiolipin tends to accumulate in the

stationary phase in *S. aureus*, and phosphatidylglycerol decreases in *E. coli* during stationary phase (Cronan, 1968). The variability in lipid composition during bacterial growth suggests a mechanism for adapting to the changing environment, but may also have a secondary effect on the biological activity of the membrane proteins.

1.3.1.1 Eukaryotes

Phosphoglycerides (Figure 1.5 and Figure 1.6) are the major constituents of eukaryotic cell membrane including phosphatidylcholine, phosphatidylethanolamine, phosphatidylserine, phosphatidylinositol and phosphatidic acid (Van Meer, Voelker, & Feigenson, 2008). The positioning of lipids in the membrane is dependent on their structure. Phosphatidylcholine is the most abundant lipid (50%) (Van Meer et al., 2008). Their primary role is to maintain the integrity of the cellular membrane (Ohvo-Rekilä et al., 2002) due to their strong tendency to form bilayers (Yeagle, 2016). Phosphatidylethanolamine being a cone-shaped lipid is found to be accumulated on the cytoplasmic side of the plasma membrane and also on vesicles to promote membrane fusion (Panatala, Hennrich, & Holthuis, 2015). The cell membrane also contains sphingomyelin, which is structurally different from the phosphoglycerides. The trans-unsaturated tails of sphingomyelins help the lipid tails to pack closely, resulting in the membrane adopting a gel phase (Van Meer et al., 2008). Cholesterols, which are not found in prokaryotes help modulate the fluidity of the membrane (Van Meer et al., 2008).

In addition to the plasma membrane, eukaryotes have internal organellar membranes, which are absent in prokaryotes (Luckey, 2014). However, mitochondrial lipids resemble the lipids found in bacteria. The mitochondria synthesise phosphatidic acid and phosphatidylglycerol to form cardiolipin, which is found in the inner membrane analogous to its location in the bacterial plasma membranes (Van Meer et al., 2008). The majority of lipids are synthesised at the endoplasmic reticulum and modified by enzymes located within the Golgi apparatus. They are then transported to their respective sites by vesicle trafficking (Van Meer et al., 2008). This means that membrane proteins are exposed to dynamic changes in their lipid environment as they undergo vesicular trafficking from the endoplasmic reticulum to the cell membrane (Bogdanov, Dowhan, & Vitrac, 2014).

1.3.1.2 Archaea

Archaeal membranes differ from bacterial and eukaryotic membranes (Figure 1.5). Their membranes are adapted to extreme environments. They have non-polar chains attached to the glycerol via an ether bond compared with the corresponding ester bonds in bacterial and

eukaryotes phosphoglycerides, making these bonds less susceptible to hydrolysis. Moreover, the alkyl chains are also branched with fewer double bonds, probably reducing the problems associated with oxidation. Archaeal membranes can contain monolayers consisting of two hydrophilic head groups joined together by a long chain of 40 carbon atoms (Lazaridis, 2001).

1.3.2 Lipid polymorphism

Lipids are amphipathic molecules with hydrophobic domains and polar (hydrophilic) head groups. When lipid molecules are placed in an aqueous environment, the hydrogen bonds holding the water molecules together are broken, causing an endothermic reaction (Lazaridis, 2001). The dissociation of the surrounding water molecules and their hydrogen bonds cause a significant increase in entropy resulting in a negative Gibbs free energy [$\Delta G = \Delta H - T\Delta S$]. This process of spontaneous formation of hydrophobic clusters in an aqueous system is called the hydrophobic effect (Atkins & De Paula, 2006). Therefore, lipids are arranged so that the hydrophobic domains are shielded from water, and the polar head groups form either hydrogen bonds or ionic interactions with the water molecules (reviewed by (William Dowhan, Bogdanov, & Mileykovskaya, 2008)).

In addition to the hydrophobic interactions between lipids, there are other kinds of interactions that help stabilise the membrane bilayer. Van der Waals attractions between the hydrophobic tails allow them to pack closely, while the lipid head groups have electrostatic interactions and hydrogen bonds with the water molecules (Berg et al., 2002).

Amphipathic molecules exist as monomers in solution at low concentration. The increase in their concentration causes instability of monomers as the unfavourable interaction of the hydrophobic hydrocarbon chain with water overcomes the favourable interaction of the polar domain with water. The optimum concentration at which the monomers form micelles is called the critical micelle concentration (CMC) (Vance & Vance, 2008). Having a larger hydrophobic domain lowers the CMC for a given lipid due to an increase in the hydrophobic effect. However, an increase in the size or charge of the polar head group increases the CMC as the head groups cause steric hindrance when brought together (reviewed by (William Dowhan & Bogdanov, 2002)).

The shape of an amphipathic molecule is an important factor in determining the structural phase adopted by the lipid when it aggregates under the influence of the hydrophobic effect (Dowhan William, 2002) as shown in Figure 1.8. The polymorphic phases of lipids are described below.

i. Micelles (H_I)

Detergents and lysophospholipids (phospholipids with one alkyl chain) are known to form inverted cone-shaped micelles due to the head domain being larger than the hydrophobic domain. Phospholipids with less than eight hydrocarbon chain also form micelles (Vance & Vance, 2008). The micelles can be arranged in a rod like structure, where the hydrophobic fatty acid tails point towards the centre of the rod and the polar head groups on the outside, forming hexagonal arrays, H_I phase (A. G. Lee, 2000).

ii. Lamellar

Phosphatidylcholine is cylindrical, meaning the head group is proportional to its hydrophobic domain. Therefore, it readily forms a bilayer (Dowhan William, 2002). Physiologically, most lipids exist in lamellar or bilayer phase, more commonly so in lamellar liquid crystalline phase (Lα) than lamellar ordered gel phase (Lβ) (Lewis & McElhaney, 2013). The hydrocarbon chains are mostly extended and in all-trans conformation when in an ordered gel phase. In the crystalline phase, the hydrocarbon chains adopt a gauche conformation allowing increased intra and intermolecular motion (Lewis & McElhaney, 2013). The transition from ordered gel to disordered liquid crystalline bilayer can be caused by many factors including changes in temperature, pressure, hydration, ionic strength and pH (Lewis & McElhaney, 2013). Unsaturated and branched alkyl chain increase the fluidity, but short alkyl chain decreases fluidity (Vance & Vance, 2008). Many organisms alter the chain length of their hydrocarbon tails to adapt to the variation in temperature in their environment (Koynova 2013).

iii. Hexagonal (H_{II})

Phosphatidylethanolamine is cone-shaped due to its relatively small head group surface area compared to its hydrophobic domain (Cullis & De Kruijff, 1978). The cone-shaped lipids are arranged in a rod-like shape, with the polar head groups at the centre of the rod, and hydrophobic fatty acid tails pointing outwards (Figure 1.8). Such an arrangement is called the hexagonal (H_{II}) phase (A. G. Lee, 2000). As phosphatidylethanolamine tends to exist at hexagonal (H_{II}) phase above 10 ˚C, at physiological temperature, it tends not to form a bilayer. This implies that in biological membranes such as of erythrocytes, where 30% of its lipid composition is phosphatidylethanolamine, the membrane is disordered. However, the presence of bilayer-forming lipids such as phosphatidylcholine, only 30% of which is required in a mixture of non-bilayer forming lipids, pushes the membrane to form a bilayer structure (Cullis & de Kruijff, 1979).

iv. Lipid cubic phase

Lipid cubic phase is a more complex system. Lipids can be ordered into two types of lipid cubic phase; micellar and bicontinuous. In the micellar cubic form, lipids are arranged in micelles in a cubic lattice. The bicontinuous form is in a curved bilayer form in a 3 dimensional structure with a continuous network of lipid and aqueous channels (Epand, 1998; Luzzati, 1997). The bicontinuous system is also used for protein crystallisation as proteins diffuse into the hydrophobic parts of the cubic phase. The nucleation process and growth of crystals have been observed to be efficient due to the large surface area between the lipid and aqueous interface (Landau & Rosenbusch, 1996).

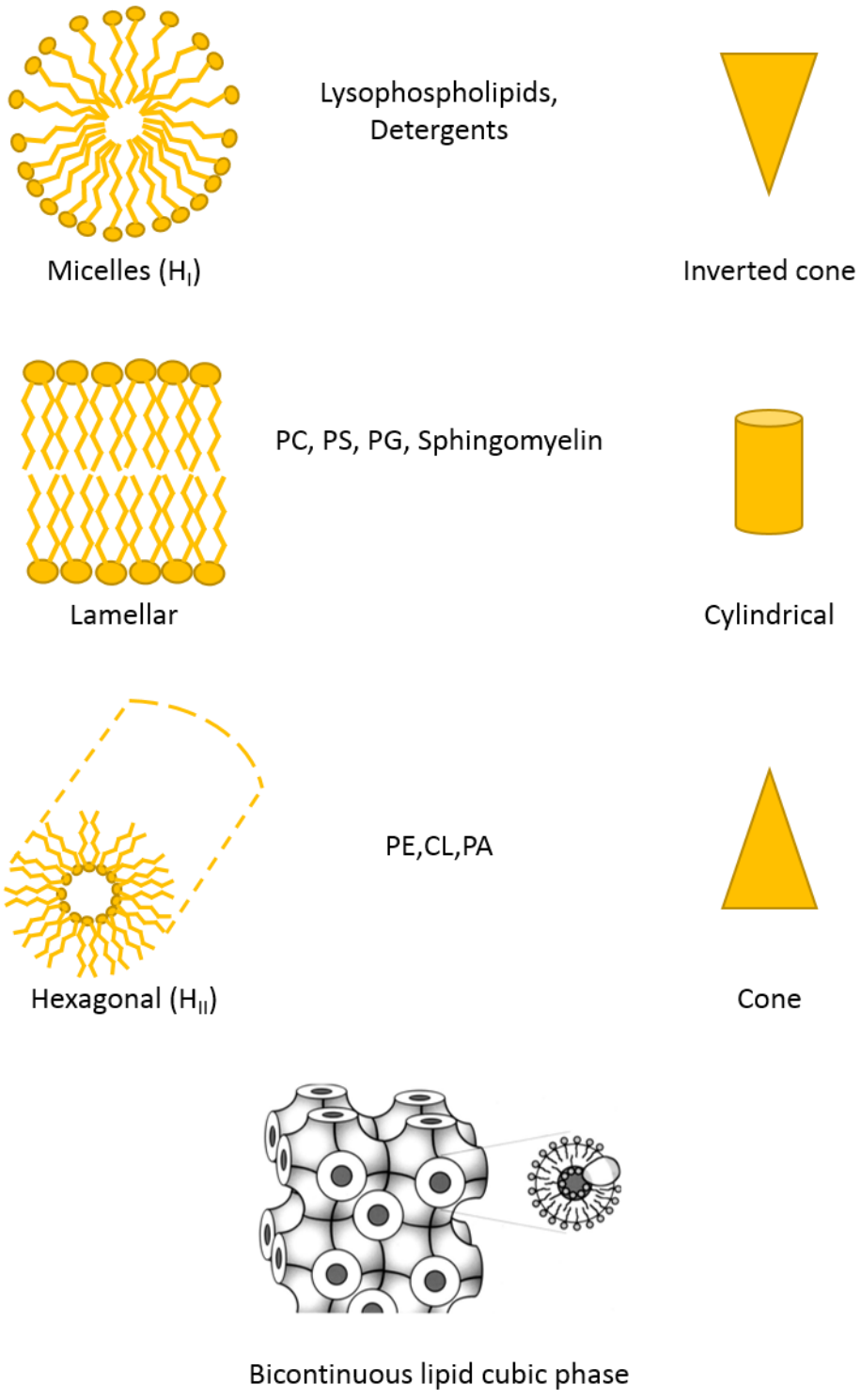

Figure 1.8 Polymorphic phases of lipids. Amphipathic detergents form micelles. Cylindrically shaped lipids (phosphatidylcholine (PC), phosphatidylserine (PS), phosphatidylglycerol (PG)) form lamellar bilayers. Conically shaped lipids (phosphatidylethnaolamine (PE), cardiolipin (CL), phosphatidic acid (PA)) undertake a hexagonal form (H_{II}). Lipids in the bicontinuous lipid cubic phase arranged in a 3 dimensional structure. The zoomed in figure on the right shows the orientation of the protein in the membrane. Picture adapted from (Dowhan William, 2002; Landau & Rosenbusch, 1996).

1.3.3 Lipid asymmetry

Lipids are distributed asymmetrically in the membrane between the two leaflets (Van Meer et al., 2008). The asymmetry of the membrane bilayer is maintained by enzymes that translocate the lipids from one leaflet to the other; flippase (inward movement), floppase (outward movement) and scramblase (bidirectional movement) (Allhusen & Conboy, 2016; Cronan, 1968). In eukaryotic cells, phosphatidylcholine and sphingomyelin are located mostly in the outer leaflet, and phosphatidylserine and phosphatidylethanolamine are located on the cytoplasmic side of the bilayer (Ikeda, Kihara, & Igarashi, 2006; Segawa et al., 2014).

The asymmetry of phospholipids has functional significance. When the asymmetry is disrupted, i.e. phosphatidylserine is translocated to the outer leaflet and exposed to the surface of the cell, a phagocytosis signal is conveyed (Bratton et al., 1997; Huang et al., 2016; Van Meer et al., 2008; Verhoven, Schlegel, & Williamson, 1995), and is also a signal for blood coagulation (Bevers, Comfurius, van Rijn, Hemker, & Zwaal, 1982). Similarly, cardiolipin, which is concentrated in the inner leaflet of the inner mitochondrial membrane and plasma membrane of bacteria is found to accumulate in the outer leaflet of the membrane in cells undergoing mitophagy. In the event of removal of the cardiolipin synthase gene, there was a decrease in cells undergoing mitophagy in primary neuron cells. This suggests that the imbalance in the asymmetry of cardiolipin in the bilayer could be a signal for mitophagy of mitochondria (X. X. Li, Tsoi, Li, Kurihara, & He, 2015).

1.4 Lipid-protein interactions

The variation in the composition of phospholipids and their asymmetry in the membrane may have a direct or an indirect effect on the proteins embedded within the membrane, which may lead to altered biological activity. Studying the interactions between membrane proteins and lipids can help us learn more about the protein's structure and function, which are vital for understanding fundamental biological processes (Liu, Cong, Liu, & Laganowsky, 2016).

There is complexity in the arrangement of lipids surrounding a protein in the membrane. There is the bulk lipid which covers the membrane, and there are annular lipids that are in close proximity to the protein. The composition of annular lipids and bulk lipids maybe different (Simmonds et al., 1982). Lipids that bind specifically to protein at their interface are the non-annular lipids (Simmonds et al., 1982; Simmonds, Rooney, & Lee, 1984). Our understanding of these interactions has come from various techniques including but not limited to mutagenesis, mass spectrometry, fluorescence studies, crystallisation and nuclear magnetic resonance (Choudhury et al., 2014; East & Lee, 1982; Manajit, Hermann, Gebhard, & Klaus, 1992; Mehmood et al., 2016).

There are two types of proteins that associate with the lipids in the membrane. Integral membrane proteins (IMP) have one or more segments inserted into the phospholipid bilayer (Lodish, Berk, & Zipursky, 2000). The membrane-spanning domains of the IMP are either α helices or multiple β strands (Lodish et al., 2000). Some IMPs attach themselves to the phospholipid bilayer via covalent interactions with the fatty acids, which is embedded in the membrane, while others are bound by hydrophobic interactions, salt bridges and hydrogen bonds (Tsukihara et al., 1996).

Peripheral membrane proteins are not embedded in the hydrophobic region of the bilayer. Instead, they interact with the integral membrane proteins or the lipid polar head groups within the bilayer. They are often recruited to the cell membrane for cell signalling and membrane trafficking (reviewed by (Cho & Stahelin, 2005)).

1.4.1 Effects of anionic lipids on membrane proteins

Negatively charged anionic lipids consist of less than 30% of total lipids in eukaryotic membranes (W. Dowhan, 1997). There is growing evidence for anionic lipids, which are usually found to be concentrated on the inner leaflet of the bilayer, on membrane protein structure (Schmidt et al., 2015), orientation (Van Klompenburg, Nilsson, von Heijne, & de Kruijff, 1997) , translocation (de Vrije, de Swart, Dowhan, Tommassen, & de Kruijff, 1988) and regulation of their function (Marius et al., 2008; Rapedius et al., 2005). In addition, anionic lipids are essential for the action of antimicrobial peptides (Zasloff, 2002), phagocytosis (Fadok et al., 2000), DNA replication (Mizushima et al., 1996) and curvature sensing (Hirama et al., 2017).

1.4.1.1 Translocation of membrane proteins

The restriction in the location of protein synthesis requires for proteins to be translocated to their respective functional destinations. The proteins are guided by their N-terminal signal peptide, which consists of positively charged residues, a hydrophobic central core and a polar cleavage site (Zheng & Gierasch, 1996). Anionic phospholipids help the signal peptide insert into the membrane by interacting with the positively charged residues on the signal peptide (Leenhouts, Wijngaard, Kroon, & Kruijff, 1995).

The translocation of protein complexes into the membrane is mediated by pre-protein translocases. The Sec system is a classic example of such translocases. The ATPase subunit Sec A forms complex with integral membrane proteins, SecYEG that forms the channel, to transport proteins from one side of the membrane to the other (Bassilana & Wickner, 1993; Nishiyama, Mizushima, & Tokuda, 1993). Anionic phospholipids promoted interactions of SecA with the

membrane (Breukink, Demel, de Korte-Kool, & de Kruijff, 1992; Lill, Dowhan, & Wickner, 1990) and SecYEG (Hendrick & Wickner, 1991) in addition to stimulating its ATPase activity (Lill et al., 1990). Translocation of proteins was severely hampered in the absence of anionic phospholipids (de Vrije et al., 1988; Lill et al., 1990). However, introducing anionic phospholipids to the membrane bilayer restored translocation (Van Klompenburg et al., 1997)

1.4.1.2 Orientation of membrane proteins

Anionic lipids have been shown to influence the orientation of a signal peptidase, Lep. Lep is found on the inner membrane of *E.coli*, and its role is to remove signal peptides from translocated precursor proteins (Van Klompenburg et al., 1997). Lowering the concentration of anionic lipids below the wild-type level allowed the positively charged residues on the N terminal of Lep to move more freely across the membrane. On the other hand, increasing the anionic content prevented the positive residues on the N terminal from passing through the membrane. This suggests that the electrostatic interactions between positively charged residues on the protein and negatively charged anionic lipids orientate the transmembrane domains of the protein with respect to the bilayer (Van Klompenburg et al., 1997).

The orientation of the transmembrane of bacterial proteins in the membrane is primarily dictated by the positive-inside rule, where the positive residues are predominantly located on the cytoplasmic side of the membrane (G. von Heijne, 1989; Gunnar von Heijne, 1992). However, it does not apply to all membrane proteins (Bogdanov, Xie, Heacock, & Dowhan, 2008). The role of phospholipids in the orientation of proteins in the membrane has been demonstrated by the phosphatidylethanolamine dependent topology of lactose permease, LacY. In *E.coli* lacking phosphatidylethanolamine, LacY was found to be inverted in the membrane bilayer and introducing phosphatidylethanolamine back into the bilayer reversed LacY to its native orientation (Bogdanov, Heacock, & Dowhan, 2002). Similar observations were made with other proteins such as phenylalanine permease, PheP (W. Zhang, Bogdanov, Pi, Pittard, & Dowhan, 2003) and γ-aminobutyric acid (GABA) permease, GabP (W. Zhang, Campbell, King, & Dowhan, 2005).

1.4.1.3 Regulation of protein activity

Cardiolipin is a unique anionic phospholipid due to its four acyl chains and two negatively charged head groups. Its association with membrane proteins has been resolved in crystal structures of proteins that are involved in the electron transport chain (Fiedorczuk et al., 2016; Lange, Nett, Trumpower, & Hunte, 2001; Shinzawa-Itoh et al., 2007; Yankovskaya et al., 2003). Cytochrome bc_1

complex is an oligomeric enzyme that couples transfer of electrons to the translocation of protons across the membrane (Trumpower & Gennis, 1994). Removal of lipids associated with the bovine cytochrome bc_1 complex using phospholipase A_2 rendered the protein inactive (Gomez & Robinson, 1999; Schagger et al., 1990). However, upon addition of exogenous cardiolipin mixed with phosphatidylcholine and phosphatidylethanolamine restored the protein's activity (Gomez & Robinson, 1999). This highlights the synergy between the neutral and anionic lipids as neither could restore the protein's activity on their own.

In terms of binding affinity, cardiolipin showed stronger binding to the cytochrome bc_1 complex compared to phosphatidylcholine or phosphatidylethanolamine. The location of the cardiolipin has been revealed to be in between the crevices of the transmembrane helices suggesting a specific binding site for the lipid. This has been vital for the stabilisation of the protein complexes through ionic interactions between the cardiolipin head group and the positive residues on the protein (Gomez & Robinson, 1999; Schagger et al., 1990; M. Zhang, Mileykovskaya, & Dowhan, 2002).

Electrostatic interactions between anionic lipid, phosphatidylglycerol head group and positively charged arginine side chains at the monomer-monomer interface in the potassium ion channel, KcsA (Valiyaveetil, Zhou, & MacKinnon, 2002) have been observed. In addition, fluorescence quenching studies have indicated nonannular binding sites at the protein-protein interface specifically for anionic lipids (Marius et al., 2008). These negatively charged lipids were found to be critical for the opening of the channel and conductance of ions (Marius et al., 2008; Valiyaveetil et al., 2002).

Large conductance mechanosensitive channels (MscL) are operated by the tension in the surrounding membrane, which leads to the opening of the channel (Booth, Miller, Muller, & Lehtovirta-Morley, 2015; A. M. Powl, East, & Lee, 2005). The residues in the channel move away from the centre of the structure to open the channel, through which various solutes are transported according to their chemical gradient (Booth et al., 2015). It has been shown that anionic lipids such as phosphatidylglycerol, phosphatidic acid and cardiolipin enhance the activity of the MscL channel (Andrew M. Powl, East, & Lee, 2008). A specific anionic lipid binding site has also been demonstrated on the cytoplasmic side of MscL, where the positively charged cluster of residues was present (Andrew M. Powl et al., 2008).

Highly negatively charged anionic lipids, Phosphatidylinositol 4, 5- bisphosphate (PIP_2) and long-chain acyl-CoA esters (LC-CoA) have been shown to activate potassium channels such as K_{ATP} and

Kir (Fan & Makielski, 1997; Hilgemann & Ball, 1996; Larsson, Deeney, Bränström, Berggren, & Corkey, 1996). In addition, the lipid tail is used to tether it to the membrane during interaction with the protein for its activation (Schulze, Rapedius, Krauter, & Baukrowitz, 2003; Shyng & Nichols, 1998; Tucker & Baukrowitz, 2008). Mutagenesis studies have revealed that the basic residues are important for the affinity of negatively charged PIP_2 binding on Kir. These sites of contact between PIP_2 and Kir consists of clusters of basic residues located close to the membrane interface (Logothetis, Jin, Lupyan, & Rosenhouse-Dantsker, 2007). However, these binding sites were also found to be suitable for the binding of LC-CoA but causing inhibition instead of activation of Kir. The mechanism behind the inhibition was suggested due to the displacement of the PIP_2 from the binding site (Rapedius et al., 2005), and the inability of LC-CoA to stabilise the open state of the channel (Rapedius et al., 2005).

1.5 Exploiting the fluorescence property of tryptophan to study lipid-protein interactions

From the lipid-protein interactions discussed in 1.4, it is evident that lipids, especially anionic lipids have a regulatory effect on membrane proteins. In this study, the effects of anionic lipids on the regulation of Sav1866 and McjD are examined using a fluorescence quenching assay to have a better understanding of alternative methods of overcoming multidrug resistance.

Fluorescence is a form of luminescence, emitted by excited electrons on singlet states, S_1 and S_2 that are returning to the ground state, S_0. Each state has different vibrational levels that are numbered. Following excitation, when electrons rapidly relax to the lowest vibrational level of S_1, a non-radiative transition (Valeur, 2001) occurs. This is called internal conversion (Lakowicz, 2006). The electrons then return from the S_1 to the ground state, emitting a longer and lower energy wavelength due to the loss of energy during the internal conversion. This is called the Stoke's shift. Molecules can also transit from S_1 to the excited triplet state, T_1, creating an intersystem crossing (Lakowicz, 2006). This phenomenon is often depicted in a Jablonski diagram in Figure 1.9.

The electron in the excited orbital has the opposite spin to the one in the ground orbital, which allows it to return to the ground state. This, in turn, emits a photon at an emission rate of $10^8\ s^{-1}$. However, if the electron in the excited orbital has the same spin as the one in the ground orbital, the emission is much slower, in the millisecond to the second period. This process is called phosphorescence (Lakowicz, 2006).

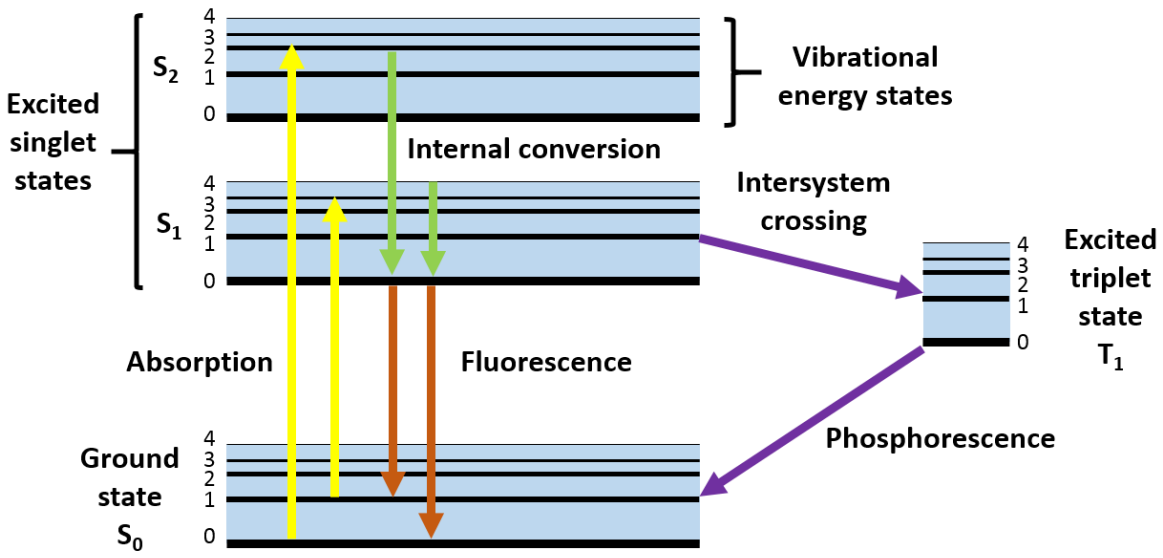

Figure 1.9 The Jablonski diagram. Electrons are excited from the ground state (S_0) to the singlet excited state (S_1 and S_2) in yellow. Each state has different vibrational energy states denoted by the numbers. Internal conversion is the process whereby the excited electrons relax to the lowest vibrational level of S_1 releasing non-radiative energy depicted by the green arrows. The electrons then return to the ground state emitting light (red arrows) at a lower energy wavelength due to loss of energy during the internal conversion. This is called the Stoke's shift. Excited electrons can also relax to the excited triplet state T_1 creating an intersystem crossing, and upon returning to the ground state, phosphorescence is emitted. Figure adapted from (Lakowicz, 2006).

1.5.1 Biochemical fluorophores

Usually, fluorescent compounds are aromatic and depending on the extent of their conjugation, the absorption and fluorescent spectra shift to longer wavelengths (Valeur, 2001). In proteins, the intrinsic fluorescence property of tryptophan is highly sensitive to its environment and has been exploited to study the conformational changes of the protein, its ligand interactions, and interactions with other proteins and lipids (Raja, Spelbrink, de Kruijff, & Killian, 2007; Rasmussen et al., 2007).

Tryptophan has an emission maximum near 350 nm in water and is highly sensitive to solvent polarity (Lakowicz, 2006). Following excitation to higher vibrational levels of the excited singlet state, S_1, the electrons relax to the lowest vibrational energy level as shown in Figure 1.9. The solvent molecules reorient themselves around the excited fluorophore. This process of solvent relaxation lowers the energy level of the excited state, reducing the energy gap between the ground and excited states, and resulting in a longer wavelength emission (Lakowicz, 2006).

The emission of tryptophan alters according to the conformation of the protein. When the tryptophan is buried within the native protein structure, the emission is blue shifted. Conversely, if the protein has lost its folding, the exposed tryptophan emits towards the red spectrum (Lakowicz, 2006).

The indole ring of the tryptophan contributes towards the absorption and emission of ultraviolet light more than the other two aromatic amino acids, tyrosine and phenylalanine. This is due to tryptophan having the highest extinction coefficient (Lakowicz, 2006). Despite having a similar quantum yield (photons emitted: photons absorbed) to tryptophan, the emission spectrum for tyrosine is much narrower. Besides, its fluorescence is quenched within the protein complex by peptide chains and tryptophan residues. Phenylalanine, on the other hand, has a low quantum yield, so its emission is often not observed in proteins. Hence, the fluorescence emission of a protein is mainly due to the tryptophan residues (Lakowicz, 2006).

1.5.2 Fluorescence quenching

Fluorescence quenching is a process by which the fluorescence intensity is decreased (Lakowicz, 2006). There are several mechanisms of quenching (Albani, 2004; Lakowicz, 2006).

1. Collisional quenching
    - During collisional quenching, the excited-state fluorophore comes into contact with another molecule (quencher) reducing its fluorescence intensity. Halogens such as iodide and bromide can act as collisional quenchers.

2. Static quenching
    - Static quenching occurs when the fluorophore is in its ground state, and forms a non-fluorescent complex with the quencher.

3. Resonance Energy transfer
    - Energy transfer is distance dependent between an excited donor and an acceptor, whereby the fluorescence intensity of the donor is reduced as the energy is transferred onto an acceptor. The fluorescence emission spectrum of the donor must complement the absorption spectrum of the acceptor.

In this thesis, bromine atoms on fatty acyl chains are used to quench the fluorescence of a strategically placed tryptophan on ABC transporters that are reconstituted in a mixture of brominated and non-brominated phospholipids (5.2.9). The quenching of the fluorescence would

indicate that the brominated lipids are binding close to the site where the tryptophan has been placed. The replacement of brominated phospholipid from the vicinity of the tryptophan with a non-brominated phospholipid would reduce the level of quenching (East & Lee, 1982). Thus, the experiment would allow to investigate a specific site on the protein providing affinity for lipid binding, which in turn regulates the protein's activity. Such binding site could be exploited as targets for much needed ABC transporter inhibitors.

Chapter 2 General Materials and Methods

2.1 Materials

Anatrace

- n-Dodecyl-β-D-maltopyranoside (DDM)

Avanti Polar Lipids

- 1,2-dioleoyl-sn-glycero-3-phosphocholine (di(C18:1)PC)
- 1,2-dioleoyl-sn-glycero-3-phosphate (di(C18:1)PA)
- 1,2-dioleoyl-sn-glycero-3-phospho-(1'-rac-glycerol) (di(C18:1)PG)
- 1',3'-bis[1,2-dioleoyl-sn-glycero-3-phospho-glycerol (tetra(C18:1)CL)
- 1,2-dioleoyl-sn-glycero-3-phosphoethanolamine (di(C18:1)PE)
- 1,2-dioleoyl-sn-glycero-3-ethylphosphocholine (di(C18:1)EPC)
- 1,2-dioleoyl-sn-glycero-3-[phospho-rac-(3-lysyl(1-glycerol))] (di(C18:1)lysyl PG)

Calbiochem

- Imidazole

Duchefa

- Chloramphenicol

Expedeon

- InstantBlue Protein Stain

New England Biolabs

- *BamHI*
- Molecular weight marker 1Kb DNA ladder
- *NdeI*

GE Healthcare Life Sciences

- Amersham Protran Premium 0.2 NC (western blot membrane)
- HisTrap HP column (1 ml and 5 ml)

LI-COR

- Duo Pre-stained Protein ladder

Melford

- Acrylamide/bis-Acrylamide, 37.5:1 Solution
- Agarose
- Ampicillin Sodium Salt
- Glycerol
- Isopropyl ß-D-1-thiogalactopyranoside (IPTG)
- Kanamycin Monosulphate
- L-Serine
- N,N,N',N'-Tetramethylethylenediamine (TEMED)
- Phosphate Buffer Saline (PBS)
- Tryptone
- Yeast Extract

Merck Millipore

- Amicon Ultra-15 Centrifugal Filter
- Potassium hydroxide
- Sodium phosphate
- Sodium Phosphate Dibasic Molecular Biology Grade
- Sterile disposable 0.22 µm filters
- Tris Molecular Biology Grade

Promega

- DpnI
- Glycerol Molecular Biology Grade
- *Pfu* DNA Polymerase
- PureYield™ Plasmid Maxiprep system
- T4 DNA Ligase enzyme
- Wizard® *Plus* SV Minipreps DNA purification system

Protean

- TEV Protease

Thermo Fisher Scientific

- Bolt® Empty Mini Gel Cassettes
- Di-Potassium hydrogen orthophosphate (K_2HPO_4)

- Dithiothreitol (DTT)
- Ethylenediaminetetraacetic acid (EDTA)
- Hydrochloric acid ACS reagent
- Nalgene™ Rapid-Flow™ Sterile Disposable Bottle-Top Filters with PES Membrane
- Potassium dihydrogen orthophosphate (KH_2PO_4)
- SeeBlue® Plus2 Protein Standard
- Sucrose

All other reagents were from Sigma unless stated otherwise.

2.2 Methods

2.2.1 Sterilisation

Any equipment used for microbiological techniques, agar and media were sterilised by autoclaving at 121˚C for 20 minutes. Antibiotic stocks (Ampicillin 100 mg/ml, Kanamycin 50 mg/ml in analytical grade water and Chloramphenicol 34 mg/ml in ethanol) were sterilised using a 0.22 µm disposable filter.

2.2.2 DNA Preparation

2.2.2.1 Vectors

The *sav1866* gene was a kind gift from Roger Dawson and Kasper Locher. The gene was introduced into pET-19b (Novagen) expression vector between the NdeI and BamHI multiple cloning sites as described in (Dawson & Locher, 2006) and shown in Figure 2.1. The recombinant protein contains a decahistidine affinity tag at the N terminus for purification. pET-19b also provides ampicillin resistance so pET-19b: s*av1866* clones can be selected easily.

The *mcjD* gene was a kind gift from Konstantinos Beis. The gene was cloned into a pWaldo-GFPd expression vector, a derivative of a standard pET28 (a+) vector, between NdeI and BamHI multiple cloning sites as described in (Smith et al., 1985) and depicted in Figure 2.2. The recombinant protein contains a GFP-octahistidine affinity tag at the C terminus. In addition, a TEV cleavage site is also included prior to the GFP tag for its removal after purification. pWaldo-GFPd expression vector provides kanamycin resistance useful for selecting pWaldo-GFPd: m*cjD* clones.

Both vectors, pET-19b and pWaldo-GFPd provide regulation of inducible protein expression due to the lac operon system and high expression levels under the T7*lac* promoter. The use of T7*lac* promoter prevents basal expression of the recombinant protein. The plasmids contain *lac*

repressor (lacI), which acts on both *lac*UV5 promoter of the host chromosome to prevent transcription of T7 RNA polymerase gene and also on the *lac* operator downstream of the T7 promoter in the vector to prevent transcription of the target gene.

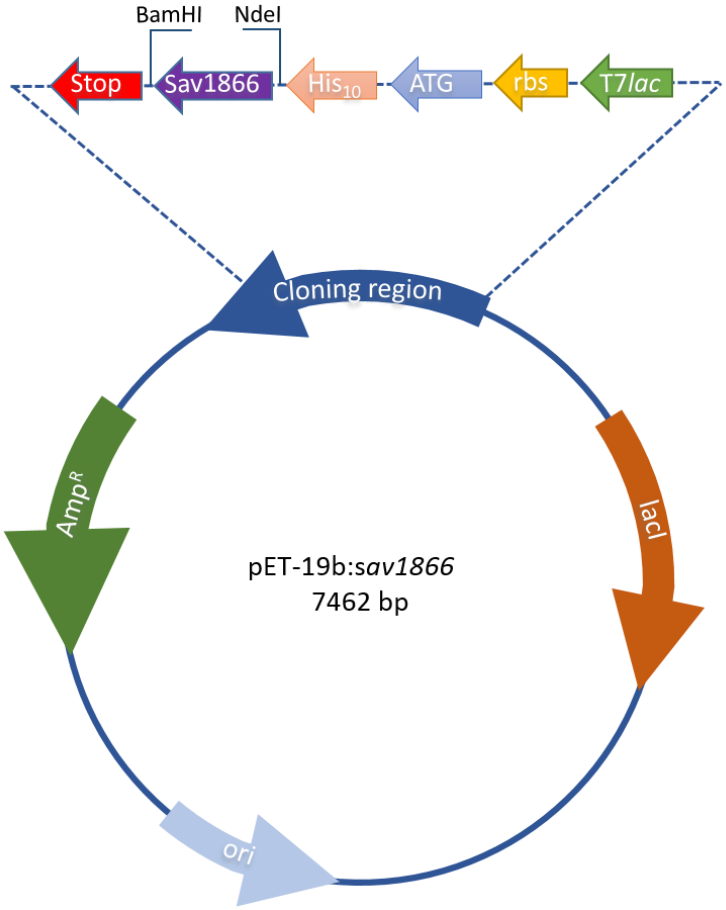

Figure 2.1 pET-19b: *sav1866* protein expression plasmid. The *sav1866* gene was inserted into pET-19b (7462 bp) expression vector (Novagen) using NdeI and BamHI multiple cloning sites. The gene is regulated by T7*lac* promoter and lac operon system that is inducible. The vector provides ampicillin resistance, useful for selection and an N-terminal decaHistidine tag.

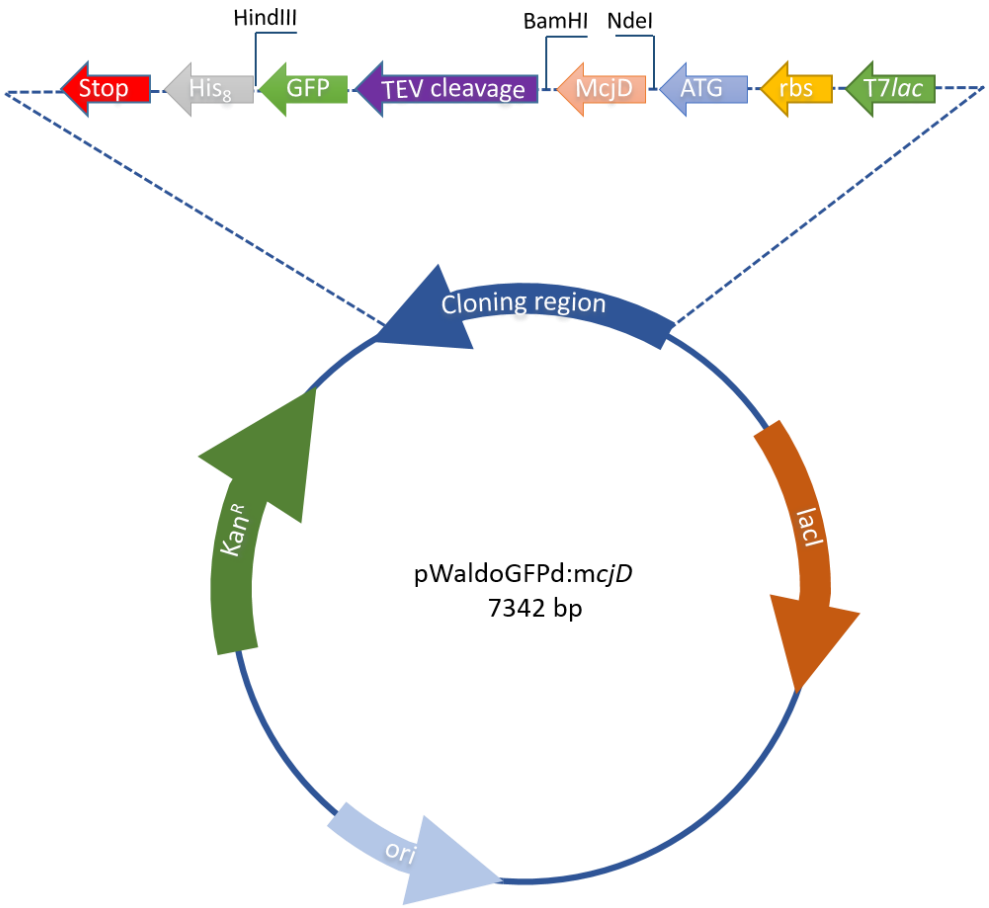

Figure 2.2 pWaldoGFPd:*mcjD* protein expression plasmid. *mcjD* was cloned into pWaldoGFPd vector (7342 bp) using cloning sites NdeI and BamHI. The resulting recombinant protein consisted of McjD with a GFP and octa-Histidine tag at the C-terminal. The gene is regulated by the T7*lac* promoter and is inducible because of the lac operon control. The vector provides kanamycin resistance, which is used for pWaldoGFPd: McjD selection. In addition, a TEV cleavage site prior to GFP tag allows its removal after purification.

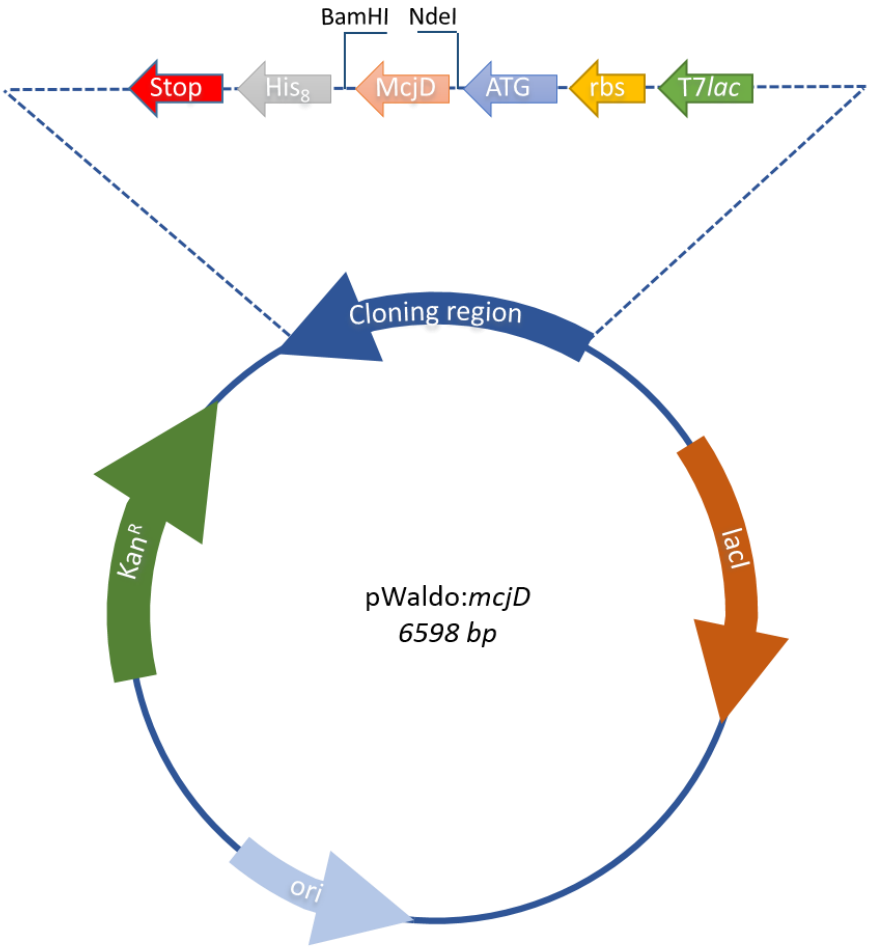

Figure 2.3 pWaldo: *mcjD* expression plasmid. The gfp tag between cloning sites BamHI and HindIII was removed as described in 2.2.2.52.2.2.2. The resulting recombinant protein consisted of an octa-Histidine tag at the C-terminal.

2.2.2.2 Restriction enzyme digest

For DNA analysis, BamHI (Biolabs, R0136L) and NdeI (Biolabs, R0111L) enzymes were used to cut the *sav1866* gene from the pet19b vector in NEBuffer 3.1 (Biolabs, B72035). 1000 ng of DNA was used along with bovine serum albumin (BSA) (Biolabs, B9000S) to prevent adhesion of enzymes to the tube and double distilled water. For McjD, BamHI and HindIII (Biolabs, R0104S) were used to remove the *gfp* from the pwaldoGFPd plasmid (Figure 2.3).

2.2.2.3 Separation of DNA fragments by agarose gel electrophoresis

DNA samples were separated on a 1% agarose gel in TE buffer (10mM Tris, 1mM EDTA) containing 0.005 % Safeview (NBS-SV1). The DNA samples were mixed with loading dye (Biolabs, B70215) and then loaded onto the gel. A 1kb DNA ladder was used as a reference, and the electrophoresis conditions were 100 V for 30 minutes.

2.2.2.4 Extraction and purification of DNA

10 µg of DNA was cut at 37˚C for 6 hours with restriction enzymes. DNA fragments were separated on a 1% agarose gel. The separation of the gene and plasmid was viewed under ultraviolet light. The required plasmid or gene was then cut out of the gel and transferred to a 1.5ml microcentrifuge tube. A ball of glass wool was placed at the bottom of 0.5ml microcentrifuge tube, and the gel fragment was inserted. The gel fragment was then snap frozen in liquid nitrogen for approximately 5 minutes. A small hole was made in the bottom of the tube with a syringe needle and it was placed inside another 1.5 ml microcentrifuge tube. The combined tubes were then centrifuged for 5 minutes at 13000 g. Next, 5 volume of Buffer PB was added to 1 volume of sample collected through the glass wool. The diluted sample was then transferred to a QIaquick column, which was placed in a 2 ml collection tube. The column was centrifuged for 60 seconds, and the flow-through was discarded. The column was washed with 0.75ml Buffer PE and centrifuged for 2 minutes. Finally, the column was placed in a fresh 1.5ml microcentrifuge tube, and 40µl of double distilled water was used to elute DNA by centrifuging at 13000 g for a minute.

2.2.2.5 DNA Ligation

For *mcjD* following removal of the *gfp* gene, a set of primers (forward 5'- GATCCGGCGGCAGCA -3' and reverse 5'- AGCTTGCTGCCGCCG-3') were used to create complementary sticky ends at the BamHI and HindIII sites for ligation. The primers were annealed by incubating 1 µg of each primer in 50 µl of T4 ligase buffer at 85˚C for 10 minutes and letting it cool down to room temperature. The annealed primers were phosphorylated at 5' end using T4 polynucleotide kinase (10 units, Biolabs) and 1 mM ATP in T4 PNK reaction buffer in a 50 µl reaction. The reaction mix was incubated at 37˚C for 30 minutes.

The insert and the plasmid were mixed together and incubated at 16˚C overnight in ligation buffer containing 800 IU of T4 DNA ligase [Biolabs]. Following ligation, salts were removed by loading the ligation reaction onto a Millipore membrane filter (0.25 µM VSMP) floating on a pool of 50 ml 10% glycerol. The membrane was left gently stirring for 25 minutes at room temperature, before being transferred to a 0.5 ml microcentrifuge tube.

2.2.2.6 QuickChange™ site-directed mutagenesis using PCR

Site-directed mutagenesis (Figure 2.4) was done according to the QuickChange™ protocol from Stratagene. PCRs were performed in 0.5 ml thin-walled microcentrifuge tubes in a total volume of 50 µl. 50 ng of DNA template was added to 5µl 10x reaction buffer, 125ng of forward and reverse oligonucleotide primers listed in section 0, 1µl of dNTP (25mM), 1µl of PfuTurbo DNA polymerase

[Promega] (2.5U/ µl), 1µl of DMSO and sufficient double distilled water to bring the volume to 50µl. The PCR conditions were as follows:

95˚C for 30 sec;

Then 25 cycles of

95˚C for 30 sec

x˚C for 1 minute [x dependent on primer]

72˚C for 18 minutes

After the last cycle, the sample was maintained at 4˚C.

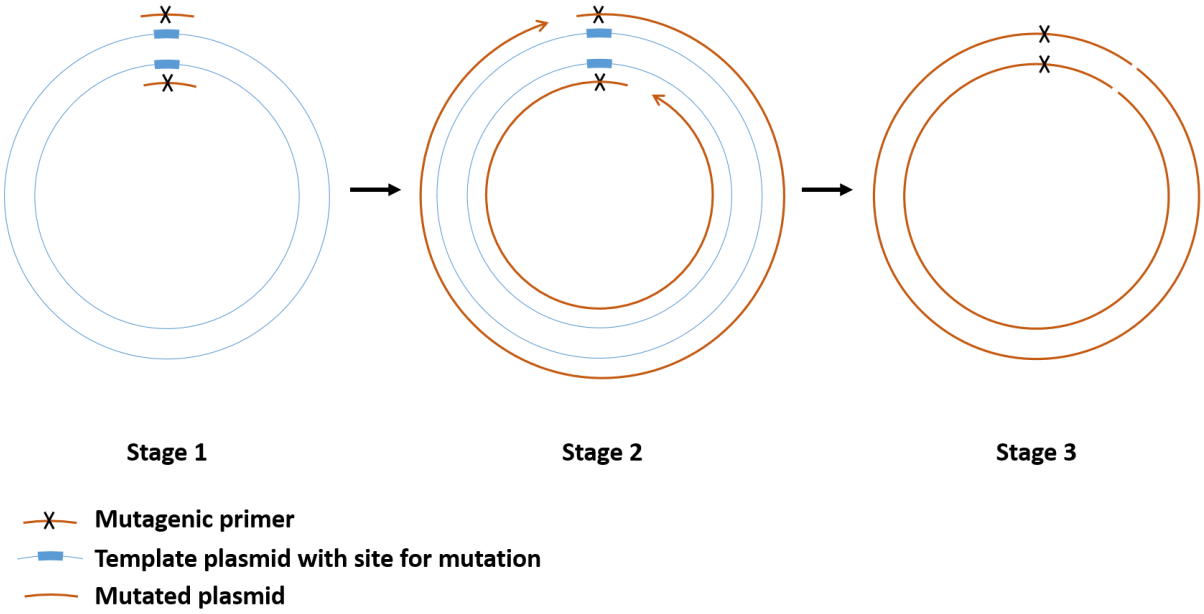

Figure 2.4 QuickChange™ site-directed mutagenesis. In stage 1, the parental DNA is denatured and the forward and reverse oligonucleotide primers, designed to contain the mutation, bind to the site for mutation on the parental template plasmid at the annealing temperature. In stage 2, the elongation of the new strand is carried out by PfuTurbo DNA polymerase. Finally, in stage 3, a new mutated plasmid is formed with a nick at the end of the plasmid, which is later repaired once transformed. The parental DNA plasmid is digested by DpnI enzyme selectively due to the presence of methylated DNA.

2.2.2.7 Small scale purification of plasmid DNA Quick Protocol

Cell Lysis Solution		**Neutralisation Solution**	
0.2M	NaOH	4.09M	guanidine hydrochloride
1%	SDS	0.759M	potassium acetate
		2.12M	glacial acetic acid

Cell Resuspension Solution		**Column Wash Solution**	
50mM	Tris-HCl (pH 7.5)	162.8mM	potassium acetate
10 mM	EDTA	22.6mM	Tris-HCl (pH 7.5)
100µg/ml	RNase A	0.109mM	EDTA (pH 8.0)

Table 2.1 Reagents used in Promega Wizard® Plus SV Minipreps

A single bacterial colony was transferred to 5 ml Luria Broth (LB) media containing the antibiotic ampicillin and incubated at 37˚C with shaking overnight. 4 ml of the culture was centrifuged for 5 minutes by spinning at 13,000 g at room temperature. The remaining 1 ml of the culture was used to make a glycerol stock. The pellet was re-suspended thoroughly in 250µl resuspension solution. 250µl of cell lysis solution was then added to the sample and inverted to mix. Next, 10µl of alkaline protease solution was added and mixed. After 5 minutes of incubation at room temperature, 350µl of neutralisation solution was added and centrifuged at 13000 g for 10 minutes at room temperature. The cleared lysate was filtered using a spin column into a collection tube by centrifuging at 13000 g for 1 minute at room temperature. 750µl of wash solution was then added to the spin column and centrifuged for 1 minute at 13000 g. This step was repeated with a further 250µl of wash solution and centrifuged at 13000 g for 2 minutes at room temperature. For elution, the spin column was transferred to a sterile 1.5 ml microcentrifuge tube, and 50µl of nuclease-free water was added and centrifuged at 13,000 g for 1 minute at room temperature. The concentration of the DNA was determined by measuring the absorbance of the sample at 260nm and 280nm using a Nanodrop 2000c spectrophotometer.

2.2.2.8 Large-scale purification of DNA

4µl of DH5α cells containing the gene was cultured in 200 ml of LB media supplemented with the antibiotic, ampicillin and incubated at 37˚C overnight. The cell culture was centrifuged at 7,700 g

for 10 minutes. The pelleted cells were then thoroughly suspended in cell resuspension solution by vortex. 12 ml of cell lysis solution was then added and inverted to mix. After incubating at room temperature for 3 minutes, 12 ml of neutralisation solution was added and the tube inverted gently to ensure precipitation of cellular debris. Finally, the solution was centrifuged at 17,000 g for 20 minutes at room temperature. For plasmid DNA purification, a vacuum manifold was used with a blue PureYield™ clearing column stacked on top of a white PureYield™ Maxi binding column. One half of the lysate was poured into the blue PureYield™ clearing column, and maximum vacuum was applied until the lysate passed through both the clearing and binding columns. This step was repeated with the remaining lysate. The vacuum was then slowly released, and the blue PureYield™ clearing column was discarded. The binding white PureYield™ Maxi Binding column was then washed with 5 ml of endotoxin removal wash and pulled through the column using the vacuum, followed by 20 ml of column wash. Then, the binding column was allowed to dry for 5 minutes using the vacuum. The binding column was then placed into a fresh 50 ml centrifuge tube, and 1.5 ml of nuclease-free water was added for elution. The tube was centrifuged in a swinging bucket rotor at room temperature at 2000 g for 5 minutes. DNA concentration was measured using a Nanodrop 2000c spectrophotometer.

2.2.2.9 DNA sequence analysis

Plasmid DNA was extracted using Promega Wizard® Plus SV Miniprep kit described above in section 2.2.2.6. 750 ng of DNA sample was sent to Eurofins for sequencing using a combination of T7 promoter primer and a list of forward and reverse sequencing primers listed below. The results from sequencing were analysed using SeqBuilder software and also kalign feature from the www.ebi.ac.uk website.

Primer	**Primer sequence 5'-3'**
T7 promoter primer	TAATACGACTCACTATAGGG
Sav1866 Primer 1	AGGATTCTTGCATGAACGTG
Sav1866 Primer 2	ACTTGCCACAGGGATATG

Table 2.2 List of oligonucleotide sequencing primers for Sav1866. T7 promoter Fwd primer was used to sequence the 5' of the gene followed by the Fwd and Rev primers listed below to sequence the pET-19b: *sav1866* gene.

Primer	Primer sequence 5'-3'
T7 promoter primer	TAATACGACTCACTATAGGG
McjD Primer 1	ATTGAACTCTTTACTTGCTG
McjD Primer 2	ATCTCCGGCTCGCAAATTA
McjD Primer 3	AACGGCATGACTTTTTCAAG
McjD Primer 4	CTGGCGTTGAAAGAAGAATG

Table 2.3 List of oligonucleotide sequencing primers for McjD.T7 promoter Fwd primer was used to sequence the 5' of the gene in combination with the Fwd and Rev primers listed below to sequence the pWaldoGFPd: McjD gene.

2.2.3 Molecular Biology

2.2.3.1 *Escherichia coli* (*E. coli*) strains

The pET-19b: *sav1866* and pWaldo: *mcjD* vectors were used to transfect *E. coli* strains DH5α and BL21 (λDE3) pLysS. DH5α cells were used for performing mutagenesis and cloning and BL21 (λDE3) pLysS cells were used for protein expression. BL21 (λDE3) pLysS strain contains a chloramphenicol resistance plasmid, which also provides T7 lysozyme, inhibiting T7 RNA polymerase.

2.2.3.2 Transformation of DH5α cells

Electrocompetent DH5α cells from -80˚C storage were thawed on ice. 4µl of DNA was added to 60µl of DH5α cells in an electroporation cuvette. The micropulsar (BIORAD) was set to bacteria EC2. Immediately after the DH5α cells were electroporated, 1 ml of SOC solution (20 g bacto-tryptone, 5 g bacto yeast extract, 0.5 g NaCl, 250 mM KCl, pH 7, 2 M $MgCl_2$, 1M glucose per litre) was added to the cuvette and the contents of the cuvette transferred to a 20ml sterilin tube. After 30 minutes at 37˚C shaking at 200 rpm, the DH5α cells were transferred onto LB plates containing ampicillin.

2.2.3.3 Transformation of BL21 (λDE3) pLysS cells

Competent BL21 cells were thawed on ice. 4µl of DNA was added to 60µl of BL21 cells and flicked gently to mix. The BL21 cells were then placed on ice for 30 minutes and heat shocked at 42˚C for 60 sec. The cells were placed back on ice for 2 minutes and 200µl of SOC was added to the

mixture. After 30 minutes of incubation at 37˚C shaking at 200 rpm, the BL21 cells were plated out onto LB plates containing the antibiotics, ampicillin and chloramphenicol.

2.2.4 Small-scale protein expression

1 µl of BL21 glycerol stock was used to inoculate 5 ml LB media containing ampicillin and chloramphenicol. The culture was left overnight at 37˚C shaking. Then, 1 ml of the overnight culture was used to inoculate 10 ml of LB media containing ampicillin and chloramphenicol and incubated at 37˚C until the O.D reached 0.6. 100 µl of IPTG was used to induce gene expression, and the temperature was reduced to 25˚C. 1 ml of cell culture was centrifuged at 17,000 g for 5 minutes, and the pellet was resuspended in 30 µl homogenisation buffer (300 mM Sucrose, 100 mM Imidazole, DNaseI). 5-10 µl of the cell suspension was mixed with 10 µl Tricine SDS sample buffer and 2µl of sample reducing agent.

2.2.5 Large-scale protein expression and purification

2.2.5.1 Growth of Cells

A litre of Terrific Broth [12 g Bacto tryptone, 24 g Bacto yeast extract, 4 ml glycerol and 900 ml water] was prepared in a baffled flask and autoclaved for sterilisation. After cooling, the flask was then supplemented with sterile filtered phosphate buffer [0.17 M KH_2PO_4 and 0.72 M K_2HPO_4 (Fischer Scientific)] and 1% glucose. For Sav1866, 100 mg ampicillin and 34 mg chloramphenicol were added to each flask and inoculated with 5 µl of BL21 glycerol stock containing the pet-19b: *sav1866* gene. For McjD, 50 mg kanamycin and 34 mg chloramphenicol were added to each flask followed by 5 µl of BL21 glycerol stock containing the pWaldoGFPd: *mcjD* gene. The flasks were incubated at 37˚C overnight shaking at 200 rpm.

2.2.5.2 Protein expression

From the overnight inoculated flasks, 70 ml of culture (for Sav1866) and 25 ml (for McjD) was used to inoculate other baffled flasks and incubated at 37˚C for an hour shaking at 200 rpm until the O.D reached 0.8 (for Sav1866) and 0.4 (for McjD) at 600 nm. Then, 1 mM IPTG was added to induce gene expression; at the same time, the temperature was then lowered to 25˚C for overnight incubation.

2.2.5.3 Isolation of crude membrane

The overnight culture was transferred to centrifuge bottles and centrifuged at 12,000 g at 4˚C for 20 minutes. The supernatant was discarded, and the pellet was homogenised using a tissue homogeniser in homogenisation buffer (50 mM Tris pH 8.2, 500 mM NaCl, DNAse 1 (3.96 unitz/

ml) prepared according to (Cardew & Fox, 2010)) using 5 ml of homogenisation buffer per 1 g of cell pellet. The homogenised solution was then run through a French pressure cell press at 35 kPa at 4˚C twice to disrupt the cell membranes. Then the solution was centrifuged at 12,000 g as earlier. The supernatant was then re-centrifuged at 100,000 g for 45 minutes at 4˚C to isolate the crude membranes.

2.2.5.4 Protein purification

Following the centrifugation, the supernatant was discarded, and the pellet was suspended in 20 ml solubilisation buffer (100 mM sodium phosphate pH 8.0, 200 mM NaCl, 15% glycerol, 20 mM imidazole, 1.5% n-Dodecyl-β-D-maltopyranoside (DDM)) for every 1 g of wet membrane. After the solubilisation step, the solution was centrifuged at 100,000 g at 4˚C for 25 minutes. This step pellets larger protein complexes and undisrupted cell membranes. The volume of the supernatant was measured, and solid imidazole was added to bring the imidazole concentration to 20 mM.

2.2.5.4.1 His-tag affinity chromatography

A His-Trap Column [GE Healthcare] was attached to a peristaltic pump in a cold room (4˚C). The column was first washed with 5 x column volume (CV) of wash buffer (100 mM sodium phosphate pH 8.0, 200 mM NaCl, 15% glycerol, 50 mM imidazole, 0.05% DDM). The protein supernatant was run continuously through the His-Trap column overnight at 4˚C. The next day, the column was further washed with 40 x CV of wash buffer before the protein was eluted using elution buffer (100 mM sodium phosphate pH 8.0, 200 mM NaCl, 15% glycerol, 500 mM imidazole, 0.05% DDM). The His-Trap column was washed with wash buffer followed by Milli-Q-water and stored in ethanol at 4˚C.

2.2.5.4.2 Buffer exchange using a PD-10 column

To prepare the column, the column storage buffer was first removed and then washed with equilibration buffer [10 mM Tris pH 8.2, 100 mM NaCl, 0.05 % DDM] five times. Then, a 2.5 ml protein sample was passed through the column, and the supernatant was discarded. Finally, the protein was eluted using 3.5 ml of equilibration buffer.

2.2.5.4.3 Determination of protein concentration (BCA assay)

Protein concentration was measured following the Pierce™ BCA Protein Assay kit protocol. The colourimetric detection of protein quantity is based on the biuret reaction, where Cu^{+2} is reduced to Cu^{+1} by the protein in an alkaline medium. Two molecules of bicinchoninic acid (BCA) chelate with one cuprous ion giving a purple coloured product (Smith et al., 1985), which absorbs strongly at 562 nm. BSA standards (0 – 2000 µg/ml) were prepared using the same buffer in buffer

exchange 2.2.5.4.2. 10 µl of BSA standards and protein samples were mixed with 200 µl of 50:1 (Reagent A: B) in a 96 well plate. The reaction was allowed to develop for 30 minutes at 37˚C. After incubation, the absorbance was measured using a FLUOstar OPTIMA plate reader. The absorbance is directly related to the amount of protein in the sample, Beer-Lambert law $A=\varepsilon cl$ (Swinehart, 1962). A standard curve was plotted for the BSA after correcting for the blank (200 µl of 50:1 (Reagent A: B) and buffer), and the protein concentration was estimated from the standard curve.

2.2.5.4.4 Protein storage

After the buffer exchange, the protein solution was concentrated using a Millipore Amicon Ultra – I5 filter of 100 kDa MW cut off. Finally, the concentration of the purified protein was adjusted to 5 mg/ml and snap frozen using liquid nitrogen in 50 µl aliquots for storage at -80˚C.

2.2.6 Size exclusion chromatography

A Superdex 200 10/300 GL (GE Healthcare) column was used for size exclusion chromatography, and the trace was observed using the AKTA system. All buffers were filtered and degassed before use. The column was pre-washed with water followed by the equilibration buffer [0.05% DDM Ana Grade in 1 x PBS]. 500 µl protein sample was centrifuged at 13000 g for 5 minutes and injected using a Hamilton. The protein was equilibrated with the equilibration buffer whilst running at 0.4 ml/min. 0.5 ml fractions were collected.

2.2.7 SDS-PAGE 1 phase gel

2X gel buffer was prepared using 160 mM Tris-Cl pH 7.4, 0.2 M Serine, 0.2 M Asparagine and 0.2 M Glycine. For 10% gel, 4 ml of 2X gel buffer was mixed with 2 ml of 40% acrylamide, 2 ml of dH_2O, 32 µl 10% APS and 16 µl TEMED. The running buffer was prepared with 25 mM Tris base, 192 mM Glycine and 0.1% SDS. The samples were mixed with 10µl Tricine SDS sample buffer (2x) and 2µl of NuPAGE® reducing agent (10x) before loaded onto the gel. A constant voltage was applied to the gel for 90 minutes at 125V.

2.2.8 Western blot

Nitrocellulose membrane was rinsed in double distilled water and then immersed in transfer buffer (25 mM Tris, 190 mM glycine, 20% methanol). The gel was transferred onto the membrane at 100 V for 2 hours in the cold room. Following the transfer, the membrane was blocked using a blocking solution (5% semi-skimmed milk, in 1 x PBS Tween 0.05%) overnight. The next day, the membrane was washed with 1 x PBS Tween 0.05% for 10 minutes thrice. The membrane was then

incubated with a mouse monoclonal anti-Histidine (anti-His) antibody [Thermo Scientific] (diluted 1:1000) for an hour shaking. The membrane was then washed with 1 x PBS Tween 0.05% thrice and incubated with secondary antibody, goat anti-mouse conjugated with 800nm fluorophore [Molecular probe] for an hour. Finally, the membrane was washed 3 times in 1 x PBS Tween 0.05%.

2.2.9 Gel and western blot analysis

SDS-PAGE gels were stained using InstantBlue Protein stain (Coomassie protein stain). Protein gels and western blots were scanned using an Odyssey Licor Scanner. DNA agarose gel was scanned using G box Syngene and Gene snap software. ImageJ software version 1.46r was used to analyse both gels and membranes.

2.2.10 ATPase activity assay

The ATP hydrolysis was measured using a coupled reaction. The reaction was performed in a cuvette containing Hepes buffer (40 mM Hepes, 100 mM KCl, 5.2 mM $MgSO_4$), 9 mM ATP, 5 mM phosphoenolpyruvate (PEP), 0.6 mM NADH, 7.5 IU pyruvate kinase (PK) and 18 IU lactic dehydrogenase (LDH)).

The reaction is monitored using the oxidation of NADH at 340 nm, which is coupled to the hydrolysis of ATP to ADP by the protein. The coupling enzyme, PK, converts PEP into pyruvate by transferring a phosphate from PEP to ADP. The pyruvate is then converted to lactate by LDH by oxidising NADH to NAD^+ as show in Figure 2.5.

A U-3010 Spectrophotometer was used to measure the oxidation of NADH. Using the software, UV Solutions (Version 1.2) a Time Scan was performed at 340nm, with sampling interval at 0.2 seconds and path length of 10 mm.

ATPase activity was measured using the equation below:

$$ATPase\ activity\ rate = \frac{rate\ of\ A_{340nm}\ signal\ loss\ \times vol\ in\ cuvette}{mol\ \varepsilon\ NADH\ \times Protein\ in\ cuvette}$$

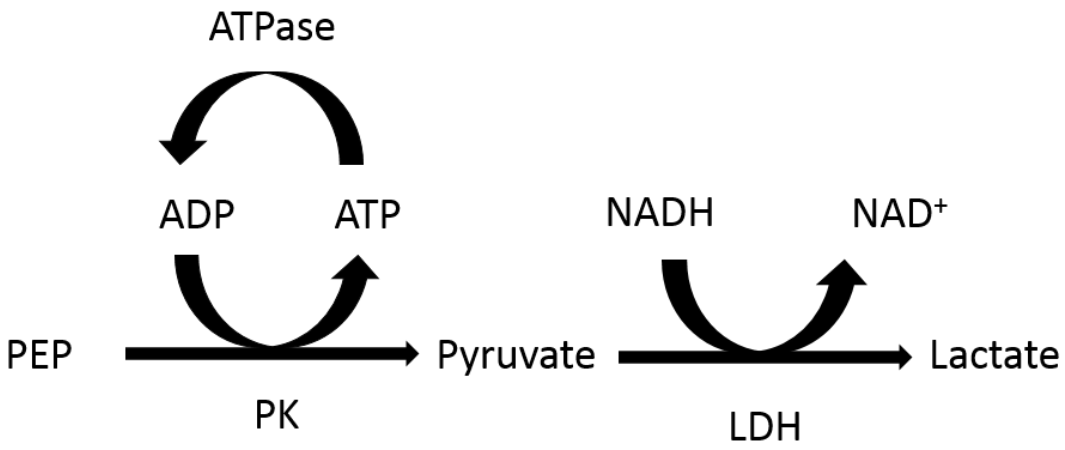

Figure 2.5 ATPase coupled reaction. The hydrolysis of ATP by an ATPase protein is coupled to the oxidation of NADH. The change in absorbance of the oxidation of NADH is measured at 340 nm. Pyruvate kinase (PK) transfers a phosphate from phosphoenolpyruvate (PEP) to the ADP to produce pyruvate and ATP. The pyruvate is then converted into lactate by lactate dehydrogenase (LDH) by oxidising NADH to NAD^+.

2.2.11 Lipid preparation

Lipids were purchased from Avanti Polar Lipids. They were dissolved in chloroform at 20 mg/ml concentration and stored at -20˚C sealed with N_2 gas.

0.6 µmol of lipid was dried onto the wall of the glass vial using a jet of nitrogen. 20 mM of potassium cholate was dissolved in 400µl of reconstitution buffer (20 mM Hepes, 1 mM EGTA, pH 7.2) and added to the glass vial. After sealing the vial with nitrogen gas, it was incubated for 10 minutes at approximately 40˚C while vortexing every 2 minutes for 20 sec. Next, the lipid was sonicated in a sonicator bath (Ultrawave U100) for 6 minutes or until the lipid suspension went clear.

When a mixture of two different lipids was used, the lipids were prepared separately as described and later mixed in appropriate ratios. The mixture was incubated at 40˚C for 20 minutes and allowed to cool to room temperature.

2.2.12 Reconstitution of Sav1866 and McjD in synthetic lipids

0.4 mg protein from a 5 mg/ml stock was added to the lipid suspended in 400 µl of reconstitution buffer and left at room temperature for 15 minutes.

2.2.13 Nickel beads recharge in Nickel His-Trap column

The Ni column was first stripped with 5 x CV of stripping buffer (20 mM sodium phosphate, 0.5 M NaCl, 50 mM EDTA, pH 7.4) and then washed with 5 x CV of binding buffer (20 mM sodium phosphate, 0.5 M NaCl, 20 mM imidazole, pH 7.4). Next, the column was washed with 5 x CV of distilled water. To recharge the column, 2.5 ml of 0.1M $NiSO_4$ in distilled water was used for a 5 ml column. The column was further washed with 5 x CV of distilled water followed by 5 x CV of binding buffer. Finally, 30% ethanol was run through the column and before storage.

Chapter 3 Determining conservative substitutions for tryptophan residues in Sav1866

3.1 Introduction

Tryptophan (Trp) fluorescence is a versatile tool to study protein folding, its conformational changes and its interactions with other proteins and lipids (Raja et al., 2007; Rasmussen et al., 2007). The presence of multiple Trps in membrane proteins can create complexity in the fluorescent signals. Therefore, often site-directed mutagenesis is used to replace endogenous Trps with non-fluorescent amino acids. The challenge lies in choosing the right amino acid that compensates for the loss of the replaced Trp and helps retain the protein's structure and function.

Membrane proteins tend to contain more Trp residues than soluble proteins and are usually concentrated at the periplasmic side of the membrane (Heijne, 1994; Schiffer, Chang, & Stevens, 1992). The amphipathic nature of Trp allows it to reside in the membrane interface (Braun & von Heijne, 1999; Gaede, Yau, & Gawrisch, 2005), anchoring the protein to the membrane (Babakhani, Gorfe, Gullingsrud, Kim, & Andrew McCammon, 2007; Landolt-Marticorena, Williams, Deber, & Reithmeier, 1993; Ulmschneider & Sansom, 2001; Yau, Wimley, Gawrisch, & White, 1998). The aromatic ring is a hydrogen bond acceptor, creating links between the amino group of the indole group with the phosphate head groups and ester oxygen of the lipids (Suzuki et al., 1992). In addition, the indole group of the amino acid possesses an electrical quadrupole moment creating partial negative charge above and below the plane of the ring, which allows it to bind cations such as arginine (Arg) side chains that are vital for maintaining the protein's folding and stability (Gallivan & Dougherty, 1999).

In the literature, many mutagenesis studies have been conducted on various proteins to find the optimum replacement for Trp (see Table 3.1). For example, Trp at position 178 in phosphatidylinositol-specific phospholipase C from *Bacillus cereus* is involved in stabilising the active site by forming hydrogen bonds with its neighbouring Arg residue (Gassler, Ryan, Liu, Griffith, & Heinz, 1997). Mutating the Trp at 178 to alanine (Ala) destabilised the structure by increasing the random coil and losing its β barrel (Feng, Wehbi, & Roberts, 2002). However, a tyrosine (Tyr) replacement maintained the structure of the protein with lower activity than the wild-type. This emphasises the role of the aromatic Trp in stabilising the active site of the protein

(Gassler et al., 1997). In addition, Trps at position 47 and 242 were found to be particularly important for the binding of lipids at the interface. Mutating these residues to Ala decreased the activity of the enzyme dramatically. However, an isoleucine or a phenylalanine (Phe) replacement was comparable to the wild-type. This highlights the importance of the hydrophobic interactions maintained by the two Trps that help the protein to be anchored in the membrane (Feng et al., 2002).

The role of Trp has also been highlighted by studies of MscS channels in *E.coli* where Trp 16 (close to the periplasm) is found to be essential for the gating of the channel whereas, Trps at the subunit interface enhanced the stability of the protein. Substitution of these Trp residues with leucine (Leu) was detrimental to the protein structure and the gating mechanism. This may be because Leu is unable to act as an anchor in the head group region of the membrane as opposed to other aromatic replacements (Phe or Tyr), which produced activities comparable to the wild-type (Rasmussen et al., 2007). Similarly, Trp in dimeric glutathione transferase was found to be important for the packing of the two domains and the stability of the protein structure. Replacing the Trp with a Phe did not have any impact on the secondary structure of the protein but was reported to be less stable than the wild-type. (Wallace, Burke, & Dirr, 2000).

P-glycoprotein consists of 11 endogenous Trp residues and replacing them with Phe caused significant loss of function of the protein. Although the Trp-less mutant retained some multidrug resistance to drugs such as vinblastine and verapamil, the activity was very low compared to the wild-type (Kwan et al., 2000). An alternative study conducted a more expanded substitution of Trp to Tyr and Leu (Swartz, Weber, & Urbatsch, 2013). Substitution of Trps with other amino acids was determined based on the position of the residue in the protein. Trps at the protein interface were replaced with Tyr to compensate for the anchoring of the protein in the lipid bilayer, while the ones in the coupling helices were replaced with Phe. Unfortunately, the substitution of Trp at position 228 (in the transmembrane helix) to Tyr produced truncated proteins, but a Phe replacement was better for its expression of the full-length protein. Furthermore, single Trp mutants that were equally as active as the wild-type P-glycoprotein were combined into quadruple mutants, which still retained activity (Swartz et al., 2013).

In other cases where the endogenous Trp have been replaced with Phe in proteins such as the outer membrane protein A (Kleinschmidt, den Blaauwen, Driessen, & Tamm, 1999) and lac permease (Menezes, Roepe, & Kaback, 1990), the substitution of Trp did not have any significant effect on the structure and the function of the protein. This suggests that the replacement with an alternative aromatic compound was sufficient for the protein to retain their native attributes.

However, others have reported the significance of Trp residues on the stability of the protein structure and in ligand binding (Kumar et al., 2007; Sirangelo, Tavassi, Martelli, Casadio, & Irace, 2000; Wallace et al., 2000). In fact, Trp to Phe substitution showed poor expression in lactose permease of *E. coli* (see Table 3.1), where Trp at position 151 was found to be critical for substrate binding and when mutated to either Phe or Tyr, the affinity for the substrate was reduced (Vázquez-Ibar, Guan, Svrakic, & Kaback, 2003).

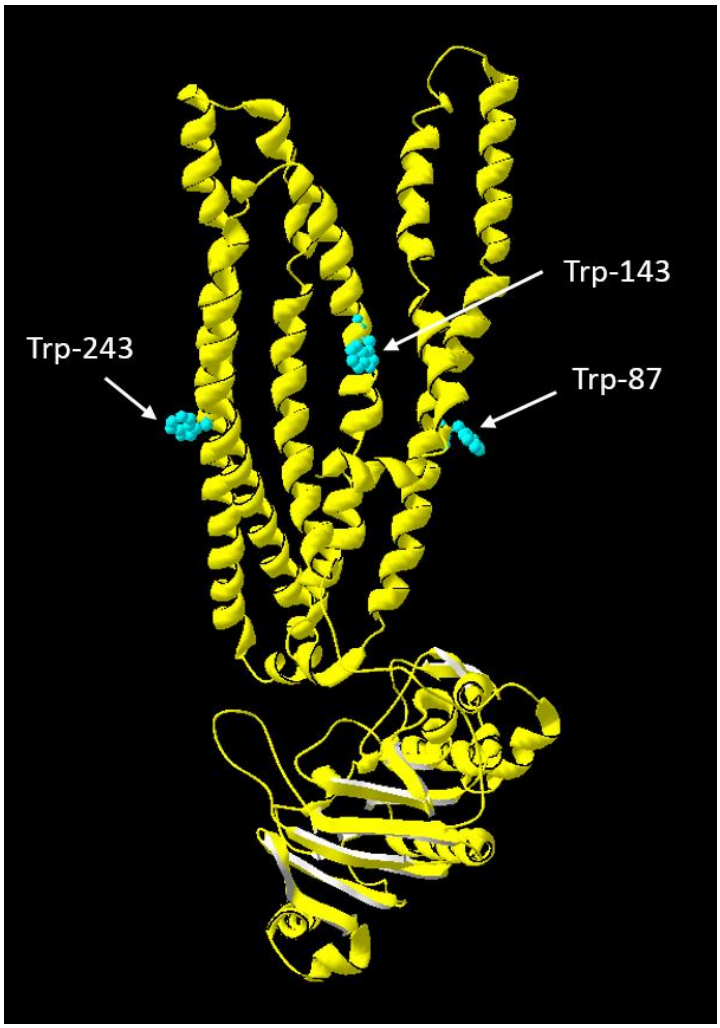

Figure 3.1 Schematic representation of Sav1866 monomer (PDB: 2HYD). The endogenous Trp-87, Trp-143 and Trp-243 are shown. Figure is edited using Swiss-PdbViewer software (4.1.0).

In this chapter, the three endogenous Trp of Sav1866 (Trp-87, Trp-143 and Trp-243; shown in Figure 3.1) are individually replaced with non-fluorescent amino acids to find the optimum replacement. The single Trp mutants that retain ATPase activity are combined together to produce Sav1866 with no Trp. This systematic approach led to creating a Trp-less Sav1866 with ATPase activity indicating that the mutant retains proper folding resembling its native conformation.

Protein	No. of Trp	Trp location	Trp substitution	Consequences of substitution	Reference
Na^+/H^+ antiporter NhaA	8	7 near lipid interface and 1 in the middle of the TM helix	Phe, Cys	No effect on antiport activity	(Kozachkov & Padan, 2011)
Lactose Permease	6	TM and periplasmic	Tyr	No effect on activity except for Trp 151 (involved in substrate binding), which loses affinity for substrate binding	(Vázquez-Ibar et al., 2003)
Outer membrane protein A	5	β barrel near the lipid head group	Phe	Mutants able to fold successfully compared to wild-type	(Kleinschmidt et al., 1999)
Diacylglycerol kinase	5	Predicted to be close to the glycerol region of the bilayer	Leu	Significant effect on activity; however, W25,112 retained 75% activity	(Clark, East, & Lee, 2003)
Mechanosensitive channel	3	W16 (periplasm), W240 & W251 (subunit interface)	Tyr, Phe, Leu, Gln, Gly, Leu	Combination of W16Y W240F W251F produced a wild-type like mutant	(Rasmussen et al., 2007)
Phosphatidylinositol-specific phospholipase C	7	W47 & W242 exposed at the active site, rest buried within the proteins	Ala, Phe, Ile	Ala mutants had significantly reduced activity. Replacement with Phe or Ile produced an active protein	(Feng et al., 2002)

Table 3.1 Replacement of Trps in membrane proteins. TM- transmembrane

3.2 Methods

3.2.1 Construction of plasmids

The preparation of plasmid vectors with s*av1866* gene has been described in section 2.2.2. Site-directed mutagenesis was used to create the mutants. All the mutagenic oligonucleotides have been listed in Table 3.2, and the mutated site has been underlined.

Mutation		**Primer sequence 5'-3'**
W87Y	Forward	ATATTTGGCGCAATACACAAGTAATAAAATATTGTATG
	Reverse	TATTTTATTACTTGTGTATTGCGCCAAATATTGACG
W87F	Forward	ATATTTGGCGCAATTCACAAGTAATAAAATATTGTATG
	Reverse	TATTTTATTACTTGTGAATTGCGCCAAATATTGACG
W87R	Forward	TTGGCGCAACGTACAAGTAATAAAATATTGTATGATATAC
	Reverse	TATTACTTGTACGTTGCGCCAAATATTGACGTATAAATTC
W87L	Forward	ATATTTGGCGCAACTGACAAGTAATAAAATATTGTATG
	Reverse	ATTACTTGTCTGTTGCGCCAAATATTGACGTATAAATTC
W143Y	Forward	TTAATGAATATTTATTTAGATTGTATAACAATTATTATTG
	Reverse	TATACAATCTAAATAAATATTCATTAACCCGGTTAAAATG
W143F	Forward	TTAATGAATATTTTTTTAGATTGTATAACAATTATTATTG
	Reverse	TATACAATCTAAAAAAATATTCATTAACCCGGTTAAAATG
W143R	Forward	TTAATGAATATTCGTTTAGATTGTATAACAATTATTATT
	Reverse	TATACAATCTAAACGAATATTCATTAACCCGGTTAAAATG
W243Y	Forward	CGTTGAAACATACAAGATATAATGCCTATTCCTTTGCCGC
	Reverse	GCAAAGGAATAGGCATTATATCTTGTATGTTTCAACGCAC

W243F	Forward	CGTTGAAACATACAAGATTTAATGCCTATTCCTTTGCCGC
	Reverse	GCAAAGGAATAGGCATTAAATCTTGTATGTTTCAACGCAC
W243R	Forward	CGTTGAAACATACAAGACGTAATGCCTATTCCTTTGCCGC
	Reverse	AAGGAATAGGCATTACGTCTTGTATGTTTCAACGCACGTG
W243L	Forward	ACATACAAGACTGAATGCCTATTCCTTTGCCGC
	Reverse	ATAGGCATTGAGTCTTGTATGTTTCAACGCACG

Table 3.2 Synthetic oligonucleotides used for QuickChangeTM site-directed mutagenesis. The sites used to create mutations in *sav1866* are underlined.

3.2.2 Transformation of *E.coli* DH5α cells and BL21 (λDE3) pLysS cells

The protocol for transformation of *E.coli* DH5α cells and BL21 (λDE3) pLysS cells are described in the General materials and methods section 2.2.3.

3.2.3 Sav1866 protein expression and purification

The protocol for protein expression and purification has been described in section 2.2.5.

3.2.4 Reconstitution of Sav1866 in synthetic lipids

Preparation of synthetic lipids and protocol for reconstitution have been described in section 2.2.11.

3.2.5 ATPase activity assay

The protocol for measuring ATPase activity has been described in section 2.2.10.

3.3 Results

3.3.1 Sav1866 tryptophan mutant expression and purification

Sav1866 has three native Trps at positions 87,143 and 243 as shown in Figure 3.1. Initially, each Trp was replaced with a Leu resulting in Sav1866 W87LW143LW243L. However, this mutant was inactive. Therefore, to create a Sav1866 mutant with no Trps, i.e. Trp-less, and ideally with ATPase activity, a systematic approach of removing each Trp by replacing it with a Tyr, Phe, or Arg was conducted.

All the single mutants, except for W243R, were expressed by *E.coli* BL21 cells. However, the level of expression varied according to the mutation and was lower than the wild-type (WT) (data not shown). Sav1866 WT and the active single Trp mutants, W87Y, W243Y and W243F, purified to homogeneity as indicated by a single band at ~ 70 kDa in Figure 3.2. A band at 25 kDa for W143R indicates the presence of breakdown products of the protein. Another band at ~ 90 kDa could be explained by the association of a full monomer of W143R with the rest of the breakdown product.

The active single Trp mutants were combined to create double Trp mutants. Sav1866 W87YW143R, W143RW243F showed the same bands at ~ 25 kDa and 90 kDa as W143R on the western blot indicating breakdown products of the mutant. Sav1866 W87YW243F purified to homogeneity, but Sav1866 W87YW243Y failed to express (data not shown).

Following the active double Trp mutants, a triple mutant, Sav1866 W87YW143RW243F was expressed and purified. However, breakdown products were evident as seen earlier with other W143R mutants.

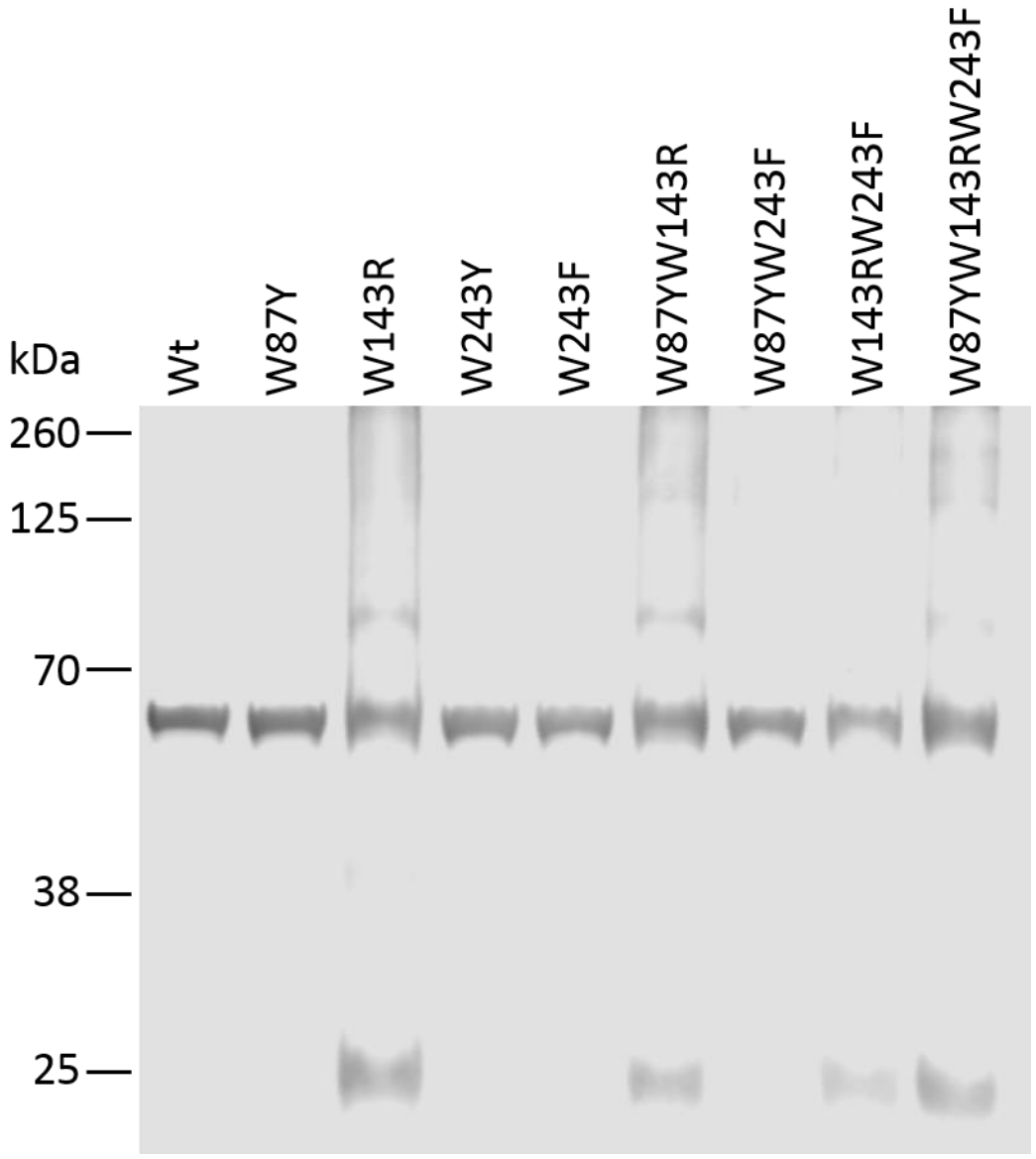

Figure 3.2 Purified Sav1866 wild-type (Wt) and active Trp mutants. 7.5 µg of Sav1866 protein (band at 70 kDa) was analysed by western blot and detected using the anti-His antibody. The molecular weight marker is shown on the left.

3.3.2 Sav1866 single tryptophan mutant basal ATPase activity

Following the expression of the single Trp mutants, the purified proteins were tested for their ATPase activity using the coupled assay described in 2.2.10. In addition, the mutants were supplemented with phosphatidylcholine (DOPC) to study the lipid's effect on their ATPase activity.

The basal ATPase activity of purified Sav1866 WT was 0.48 µmolmg^{-1}min^{-1}, which was increased when the protein was reconstituted in DOPC (0.94 µmolmg^{-1}min^{-1}).

When the Trp at position 87 in Sav1866 was replaced with a Tyr, the ATPase activity of the mutant was the highest at 1.35 µmolmg^{-1}min^{-1} when in DOPC and 0.64 µmolmg^{-1}min^{-1} in detergent as shown in Table 3.3. Replacing W87 with a Phe, Leu or an Arg rendered the mutant inactive (data not shown).

The ATPase activity of Sav1866 when Trp at 143 was substituted with an Arg was 0.4 µmolmg^{-1}min^{-1} for both when in detergent and when reconstituted in DOPC (Table 3.3). Replacing W143 with Tyr, Phe or Leu inhibited the mutant's activity (data not shown).

When replacing Sav1866 Trp at 243 with a Tyr, the ATPase activity when reconstituted in DOPC was 0.49 µmolmg^{-1}min^{-1} and in detergent was 0.10 µmolmg^{-1}min^{-1}. Substituting W243 with a Phe produced a similar level of ATPase activity as shown in Table 3.3. However, W243R and W243L lost their ATPase activity (data not shown).

	ATPase activity in detergent (µmolmg^{-1}min^{-1})	**ATPase activity reconstituted in DOPC (µmolmg^{-1}min^{-1})**
WT	0.48 ± 0.08	0.94 ± 0.06
W87Y	0.64 ± 0.13	1.35 ± 0.13
W243Y	0.10 ± 0.06	0.49 ± 0.05
W143R	0.45 ± 0.04	0.42 ± 0.05
W243F	0.20 ± 0.08	0.49 ± 0.13

Table 3.3 Basal ATPase activity of Sav1866 WT and active single Trp mutants in detergent and reconstituted in DOPC. The ATPase activity was measured using the oxidation of NADH at 340 nm coupled with the hydrolysis of ATP by Sav1866.

3.3.3 Double and triple tryptophan mutant basal ATPase activity

The single Trp mutants that retained their ATPase activity were combined to produce double and subsequently triple Trp mutants (Table 3.4).

Sav1866 W87YW143R had comparable ATPase activity rates of 0.3 µmolmg^{-1}min^{-1} when in detergent and reconstituted in DOPC. Sav1866 W87YW243F was inactive in detergent but had 0.36 µmolmg^{-1}min^{-1} ATPase activity in DOPC. Sav1866 W143RW243F also had comparable activity rates in detergent and DOPC (~0.4 µmolmg^{-1}min^{-1}).

Finally, the triple mutant, Sav1866 W87YW143RW243F, had 0.5 µmolmg^{-1}min^{-1} activity in both detergent and DOPC.

	ATPase activity in detergent ($\mu molmg^{-1}min^{-1}$)	ATPase activity reconstituted in DOPC ($\mu molmg^{-1}min^{-1}$)
W87YW143R	0.27 ± 0.01	0.26 ± 0.01
W87YW243F	0.07 ± 0.04	0.36 ± 0.06
W143RW243F	0.36 ± 0.07	0.46 ± 0.11
W87YW143RW243F	0.50 ± 0.06	0.52 ± 0.07

Table 3.4 Basal ATPase activity of Sav1866 double and triple Trp mutants in detergent and DOPC. The ATPase activity was measured using the oxidation of NADH at 340 nm coupled with the hydrolysis of ATP by Sav1866.

3.4 Discussion

The intrinsic fluorescence property of Trp is a useful tool to study conformational changes of the protein and its interactions with other proteins or lipids (Raja et al., 2007; Rasmussen et al., 2007). One of the techniques that exploits Trp's intrinsic fluorescence property is fluorescence quenching by brominated phospholipids. This technique provides information on the number of binding sites for phospholipids and their relative binding affinity towards the protein (East & Lee, 1982; A. M. Powl et al., 2005). Membrane proteins usually contain several Trp residues (Heijne, 1994; Schiffer et al., 1992). Usually, only a single Trp on the protein is required for the optimal analysis of the fluorescence quenching data. Therefore, site-directed mutagenesis is often used to substitute Trps with other amino acids that ideally do not alter the protein's structure, stability and function.

3.4.1 Expression and purification of Sav1866 mutants

The purpose of this study was to create a Trp-less Sav1866 mutant, which retained its activity. Using site-directed mutagenesis, the three native Trps at positions 87, 143 and 243 were substituted individually with Tyr, Phe, Arg or Leu. All the single mutants except W243R were expressed successfully. Following the results from ATPase activity of the single mutants, double and triple mutants were created.

From the western blot analysis, breakdown products at 25 kDa were observed for all Sav1866 mutants containing the W143R mutation. As a result, in addition to the Sav1866 monomer band at 70 kDa, another higher molecular weight band was observed. This was considered to be an association between the Sav1866 monomer and the breakdown product.

3.4.2 Basal ATPase activity of Sav1866 single tryptophan mutants

From previous mutagenesis studies, Tyr was considered a suitable replacement for Trp due to its ability to anchor onto the membrane bilayer using its polar side chain (Chamberlain, Lee, Kim, & Bowie, 2004; Granseth, von Heijne, & Elofsson, 2005; Liang, Adamian, & Jackups, 2005). Similar effects were observed when Trps at positions 87 and 243 were replaced with Tyr. W87Y had higher ATPase activity than the WT in both detergent and DOPC reconstitution, but W243Y had 21% of WT ATPase activity in detergent and 53% in DOPC. However, Trp at position 143 did not have ATPase activity when replaced with Tyr. This suggests that the effect of Tyr substitution is dependent on the position of Trp on the protein.

All the active mutants had at least double or higher rates of ATPase activity when reconstituted in DOPC than in detergents except for Sav1866 W143R, which had comparable rates under both DOPC reconstitution and when in detergents. This suggests that lipid reconstitution did not have any stimulatory effects on the ATPase activity of Sav1866 W143R.

Replacement of W87 and W243 with Arg caused the protein to lose its activity. Simulation studies have revealed extensive hydrogen bonding between Arg in membrane proteins and the phosphate head groups of phospholipids in the membrane (L. Li, Vorobyov, & Allen, 2013) suggesting Arg's role in facilitating membrane perturbations for cell-penetrating peptides (Amand, Fant, Norden, & Esbjorner, 2008; Herce & Garcia, 2007). In this study, the interface binding of Arg (Hristova & Wimley, 2011; L. Li et al., 2013) was proposed to compensate for the loss of membrane anchoring through Trp. However, only W143 could tolerate the Arg substitution.

Replacing Trp with Leu rendered all mutants inactive. Leu was chosen due to its bulky hydrophobic nature. In previous cases, substituting Trp residues with Leu in KcsA did not affect the opening of the channels (Marius et al., 2008). However, Sav1866 did not tolerate Trp to Leu mutation.

The aromaticity of Phe was a suitable reason to replace Trp with Phe. Although Phe does not provide interfacial binding like Trp (Braun & von Heijne, 1999), previous studies have shown that Phe was a good substitution for Trp (Kleinschmidt et al., 1999; Kozachkov & Padan, 2011; Menezes et al., 1990; Swartz et al., 2013). Phe replacement was only tolerated by W243, albeit the ATPase activity was almost half of the WT.

3.4.3 Basal ATPase activity of Sav1866 double tryptophan mutants

The ATPase activity results from single active Sav1866 Trp mutants were used to create double mutants. The highest ATPase activity was retained by Sav1866 W143RW243F with 75% of activity in detergent and 49% activity in DOPC compared to the WT. Similarly, Sav1866 W87YW143R retained 57% ATPase activity in detergent and 28% activity in DOPC compared to the WT. Lastly, Sav1866 W87YW243F only retained 15% of ATPase activity in detergent and 38% activity in DOPC compared to the WT. Interestingly, all double mutants containing W143R substitution had comparable ATPase activity rates in detergent and DOPC similar to what was observed for the single Sav1866 W143R mutant.

3.4.4 Basal ATPase activity of Sav1866 tryptophan-less mutants

Finally, the Trp-less Sav1866 W87YW143RW243F mutant was active and had a higher rate of ATPase activity than some of its single and double mutant counterparts. In addition, as with the single and double W143R mutants, the Trp-less mutant, Sav1866 W87YW143RW243F also did not seem to be affected by lipid reconstitution as no change in ATPase activity was observed.

3.5 Conclusion

Trp is a useful reporter tool in a protein. However, multiple Trps in membrane proteins make it difficult to study the signals from discrete areas of the membrane protein. Using site-directed mutagenesis, various amino acid replacements were evaluated starting with single mutants moving onto creating a Trp-less Sav1866 mutant. After strategic replacement of the three native Trps in Sav1866, an active Trp-less mutant, Sav1866 W87YW143RW243F was created, which retained almost half of the ATPase activity rate when reconstituted in phosphatidylcholine compared to the wild-type.

Sav1866 W87YW143RW243F, a Trp-less mutant, can be used to introduce a new Trp on the protein in order to conduct fluorescence quenching assays to study lipid binding on the protein. Since the mutant still retains its activity, it indicates that it maintains proper folding, resembling its native conformation.

The mutagenesis studies of Trp residues presented here highlight the importance of systematic examination of individual Trp mutation and subsequent combinations of the active mutants to produce Trp-less active mutants. There is no clear evidence for formulated conservative substitutions of Trps as the substitution that produced an active mutant was dependent on the position of the Trp on the protein.

Chapter 4 Conformational changes of Sav1866 in response to nucleotides, detergents and lipids

4.1 Introduction

Mutating amino acids in proteins does not always guarantee an active mutant protein. In Chapter 3 several amino acids were tested to replace the native tryptophans of Sav1866, but only a few were successful in retaining an active protein, i.e. the mutant was able to hydrolyse ATP. Where the effects result in a reduction of the ATPase activity, it seems unlikely that misfolding or other changes in the structural organisation of Sav1866 has taken place. However, in those mutants which are inactive, there are numerous mechanisms by which this might occur. For example, Sav1866 mutants could misfold, in which case it would be incapable of undergoing organised conformational changes in response to nucleotides such as ATP. Alternatively, the Sav1866 mutant could be locked in a particular conformation, unable to complete its catalytic cycle. In order to verify the latter, this chapter explains the use of a crosslinking technique to analyse the conformation of the Sav1866 mutants and compare it to the wild type protein. In addition, the conformation of the Sav1866 protein and the mutants are assessed in the presence of nucleotides, detergents, native lipid conditions and reconstituted lipids.

ABC transporters utilise the energy from ATP hydrolysis to transport substrates from one side of the membrane to the other (Higgins et al., 1990). The mechanism by which the transporters transfer the energy to bring conformational changes and transport the substrate is still under debate. Two hypotheses for the molecular mechanism of ABC transporters are discussed below.

4.1.1 The Switch Model

The switch model (see Figure 4.1) also known as “Tweezers like” (Chen, Lu, Lin, Davidson, & Quiocho, 2003) and “Processive clamp” (Van Der Does & Tampé, 2004) is based on the principle that ABC dimers have the ability to possess two different conformations. An outward-facing conformation is where the dimer is open to the periplasmic region, and ATP molecules are sandwiched between the two monomers. The other conformation is an inward-facing, open to the cytoplasmic side, and the bound ATP is hydrolysed to ADP and Pi (George & Jones, 2012; Higgins & Linton, 2004).

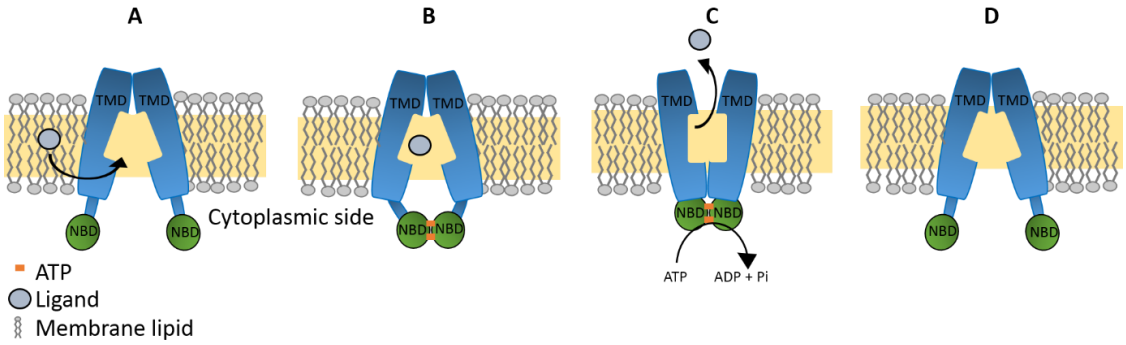

Figure 4.1The Switch Model (A) The cycle starts with the binding of a ligand on the transmembrane domain (TMD) in an inward-facing conformation. (B) The binding of ATP molecules next brings the nucleotide binding domains (NBDs) close together. (C) Once the ATP molecules are hydrolysed, the protein adopts an outward-facing conformation, and the energy is used to transport the ligand on the other side of the membrane. (D) Finally, the protein is restored back to the inward-facing conformation.

In Figure 4.1, the catalytic cycle is initiated by the binding of the substrate in the central cavity of the inward-facing protein. As a result, conformational changes in the nucleotide binding domains (NBDs) enhance the affinity for ATP binding (Higgins & Linton, 2004). At this stage, the NBDs are in an open conformation (Locher, 2016). ATP molecules bind to the two NBDs that are now in close contact, and the transmembrane domains (TMDs) form a V-shape (Higgins & Linton, 2004) (see Figure 4.1). The protein shifts to an outward-facing conformation (Higgins & Linton, 2004). The outward-facing state has a low affinity for any bound substrates due to the changes in the helix arrangement in the TMD (Locher, 2016). In the Sav1866 ADP bound structure, the central cavity was observed to be hydrophilic (Dawson & Locher, 2006), which is unsuitable to retain the hydrophobic substrate. Hence, this leads to the release of the substrate to the external side of the membrane or partitioning into the membrane itself (Locher, 2016).

The ATP is hydrolysed, and ADP and phosphate (Pi) are released, which pushes the NBDs apart in the inward-facing conformation. This is due to the electrostatic repulsion between ADP and Walker A motif of one NBD and the interaction between Pi and the signature motif of another NBD (Higgins & Linton, 2004; Moody, Millen, Binns, Hunt, & Thomas, 2002). Therefore, following the hydrolysis of ATP, the conformation of the protein shifts from outward to inward-facing (Dawson & Locher, 2006; Rees et al., 2009). The coupling helices connecting the NBDs to the TMDs are thought to be essential for the conformational changes of the TMDs (Locher, 2016).

Outward-facing and inward-facing conformations have been demonstrated by two homologous ABC importers, BtuCD (Locher, Lee, & Rees, 2002) and HI1470/1 (Pinkett, Lee, Lum, Locher, &

Rees, 2007) respectively. The presence of the two conformations suggests an alternating access mechanism (Jardetzky, 1966) for the transport of the substrate from one side of the membrane to the other. However, the lack of any nucleotides or ligands in the structure highlights the absence of the driving factor for the change in conformation. The authors suggested that the use of detergents could have a possible effect on the equilibrium between inward and outward-facing conformations (Pinkett et al., 2007).

Once the protein is restored back to its resting state, it is not clear as to whether the NBDs have a wide separation between them or stay in close contact. It has been suggested that the changing of ADP for a new ATP would require the opening of the NBDs to facilitate the exchange (Locher, 2016). From 3D cryo-electron model of BmrA, where the protein was in a nucleotide-free state reconstituted in lipid bilayers, the NBDs were separated, and the TMDs formed a V shape in the inward-facing conformation (Fribourg et al., 2014). Similar structures have been observed using the double electron-electron resonance technique for MsbA (P. Zou, Bortolus, & McHaourab, 2009; P. Zou & McHaourab, 2009; Ping Zou & McHaourab, 2010) and P-glycoprotein (Wen, Verhalen, Wilkens, McHaourab, & Tajkhorshid, 2013), where the inward-facing proteins have separated NBDs. Crystal structures of P-glycoprotein and MsbA with an inward-facing conformation and separated NBDs (Aller et al., 2009; Jin, Oldham, Zhang, & Chen, 2012; A. Ward, Reyes, Yu, Roth, & Chang, 2007) have also been reported.

In some cases, before the protein undertakes the outward-facing conformation, it has been shown to have an intermediate state, where ATP is bound to the NBD, and an occluded state is reached. This intermediate state has been demonstrated in crystal structures of McjD (Lin, Huang, & Chen, 2015) and PCAT (Lin et al., 2015) bound to AMP-PNP and ATP-γs respectively in the absence of a substrate. Both sides of McjD were found to be inaccessible. This was reconfirmed using crosslinking studies, where cysteine residues were introduced at the interface between the two McjD monomers which were thought to come in close contact in an occluded state. More importantly, this cross-linked state was unaffected by the presence of substrates, suggesting that the observed occluded state crystal structure of McjD is not due to lack of substrates (Choudhury et al., 2014). However, the authors proposed an outward-facing structure for the PCAT1 protein in the presence of a substrate in order to release it (Lin et al., 2015).

4.1.2 Constant contact model

The evidence from the crystal structures with separated NBDs have been criticised for not reflecting physiological conditions as the experiments were conducted in detergents and not native lipid bilayers (reviewed by (Fribourg et al., 2014)). The importance of lipids is demonstrated

in ABC exporters where ATP hydrolysis is only stimulated by substrates in the presence of lipids (Locher, 2016). In addition, as the ATP levels at physiological conditions (3 - 5 mM) is much higher than the affinity for ATP for ABC transporters (0.1 – 1 mM), it has been speculated that the NBDs stay in contact throughout the catalytic cycle and only have a transient phase in the absence of the nucleotide (reviewed by (Fribourg et al., 2014)). Therefore any apo or ADP bound state would be very short-lived *in-vivo*, which suggests that structures crystallised with ADP bound or no nucleotides do not represent physiological conditions. Other studies where the NBDs have been physically separated with a nanobody or a viral peptide in ABCB1 (A. B. Ward et al., 2013) and TAP (Oldham et al., 2016) respectively, the proteins have lost their activity due to their inability to close the NBDs together (Locher, 2016). Structures with a bound substrate (glutathione) of ScAtm 1 and NaAtm 1 have revealed an inward-facing conformation with NBDs in close contact (J. Y. Lee, Yang, Zhitnitsky, Lewinson, & Rees, 2014; Srinivasan, Pierik, & Lill, 2014).

Constant contact model (Figure 4.2) is based on alternating ATP hydrolysis in each NBD with one open site for ATP hydrolysis while the other remains closed with bound ATP. Following ATP hydrolysis, the site closes, and the other site opens and continues with the cycle alternatively (Senior, Al-Shawi, & Urbatsch, 1995; Senior & Bhagat, 1998).

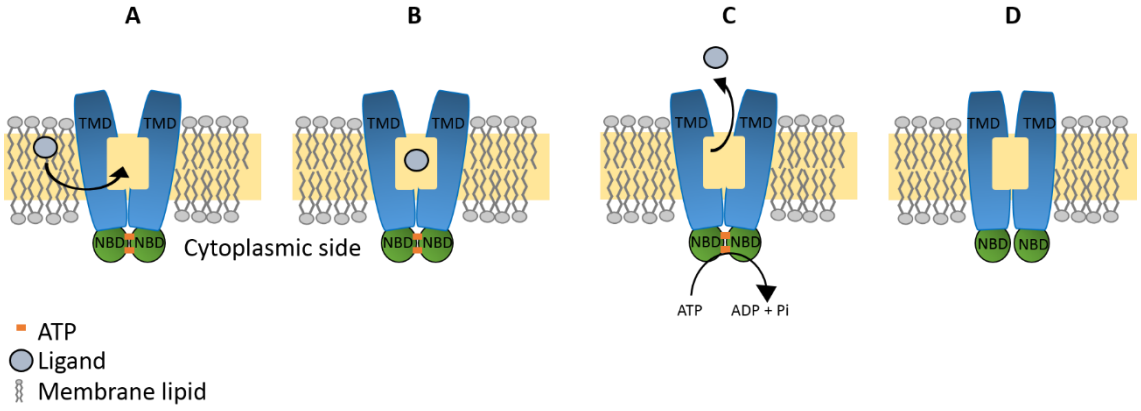

Figure 4.2 Constant Contact Model. (A) The cycle starts with an ATP bound to the outward-facing conformation. (B) The ligand binds to the transmembrane domain (TMD) cavity. (C) ATP is hydrolysed, and the energy is used to transport the ligand to the other side of the membrane. (D) The protein is now restored where the nucleotide binding domains (NBDs) are pushed apart slightly, and the TMD external wings are brought closer together.

In this proposed mechanism, LLO flippase PglK has been used as a model ABC exporter, which transports lipids. The cycle begins with an ATP bound to the NBD, and the protein is in an outward-facing conformation. Once the substrate (lipid) binds to the cavity of the TMD, ATP is hydrolysed, and inorganic phosphate is released, which drives the separation of the NBDs and

brings the external wings of the TMDs together. As the substrate is released, a new substrate binds again, and the ADP is released so that a new ATP molecule can rebind (Locher, 2016).

Crystal structure of inward-facing ABC transporter TM287-TM288 from *Thermotoga maritima* revealed that the NBDs remained in contact (Hohl, Briand, Grütter, & Seeger, 2012) in contrast to previous studies on inward-facing conformations. Crosslinking studies on LmrA revealed contacts between the NBDs in the absence of ligands and nucleotides as opposed to the "Switch Model", which assumes bringing the NBDs close together only in the presence of ATP (P. M. Jones & George, 2015). Crosslinking of the NBDs at their C terminals of P-glycoprotein allowed the protein to retain its drug-stimulated ATPase activity. This suggests that the NBDs do not undergo large conformational changes following ATP hydrolysis (Verhalen & Wilkens, 2011) as opposed to the 30 Å separation between the NBDs observed in the apo and drug bound crystal structures of P-glycoprotein (Aller et al., 2009).

The previous chapter (Chapter 3) has shown that the mutation of Trp residues of Sav1866 has a range of effects on the protein's ATPase activity. In this chapter, the conformational changes of Sav1866 and its mutant variants are examined using a crosslinking technique that provides information about the conformation of the dimeric protein. In order to do this, two further cysteine mutants have to be produced, A281C and Q208C, which are in close proximity in the Sav1866 dimer in the inward-facing and outward-facing conformation respectively (see Figure 4.4).

4.2 Methods

4.2.1 Construction of plasmids

Cysteine residues were introduced at position 281 or 208 in wild-type and mutant constructs of *sav1866* using QuickChange™ site-directed mutagenesis (see General Materials and Methods 2.2.2.6 for methods). Mutagenic primers used are listed in Table 4.1.

Mutation		Primer sequence 5'-3'
A281C	Forward	CACAGTAGGTACACTTTGCGCATTTGTTGGATACTTAGAG
	Reverse	AAGTATCCAACAAATGCGCAAAGTGTACCTACTGTGATTG
Q208C	Forward	TCTTGCATGAACGTGTTTGTGGTATTTCAGTCGTTAAAAG
	Reverse	TTAACGACTGAAATACCACAAACACGTTCATGCAAGAATC

Table 4.1 Synthetic oligonucleotides used for QuickChange™ site-directed mutagenesis The sites used to create mutations in Sav1866 are underlined.

4.2.2 Transformation of DH5α cells and BL21 (λDE3) pLysS cells

The protocol for transformation of DH5α cells and BL21 (λDE3) pLysS cells are described in the General materials and methods section 2.2.3.

4.2.3 Sav1866 protein expression and purification

The protocol has been outlined in the General Materials and Methods section 2.2.4.

4.2.4 Preparation of crude membrane

The crude membrane was harvested as described in 2.2.4 and was re-suspended in 1 x phosphate based saline, PBS (137 mM Sodium Chloride, 2.7 mM Potassium Chloride and 11.9 mM Phosphate) solution at 0.4 g/ml concentration and stored at -20˚C in 20 µl aliquots.

4.2.5 Reconstitution of Sav1866 cysteine mutants in synthetic lipids

Preparation of synthetic lipids and protocol for reconstitution have been described in section 2.2.11.

4.2.6 Crosslinking using copper phenanthroline

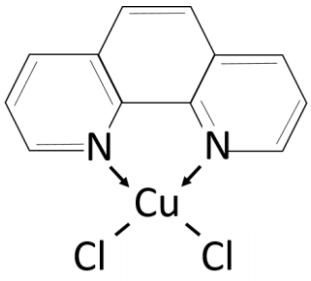

Figure 4.3 Copper phenanthroline is used as an oxidising agent to form cross links between complementary cysteine residues of Sav1866 in order to determine the conformation status (inward-facing or outward-facing).

Crosslinking reactions were performed using purified Sav1866 protein, Sav1866 protein in crude *E.coli* membrane and Sav1866 protein reconstituted in defined synthetic lipid bilayers. In a reaction volume of 30 µl in a microcentrifuge, Sav1866 protein or Sav1866 protein reconstituted in synthetic lipid was diluted to 0.5 mg/ml in a buffer containing 40 mM K-Hepes, 100 mM KCl, and 5 mM $MgSO_4$ at pH 7.2. For crude membrane, the final concentration was 20 mg/ml diluted in 1 x PBS. 10 mM of nucleotides, ATP, ADP or AMP-PNP was added with or without 10 mM sodium orthovanadate (Vi) to the mixture. The crosslinking reaction was initiated by adding 0.5 mM copper phenanthroline (Figure 4.3), which was prepared fresh by mixing 0.36 M 1, 10 phenanthroline in methanol and 0.24 M copper sulphate in 2:1 (v/v) ratio and diluted 8 fold. The reaction was incubated for 20 minutes at room temperature. 4 µl of the reaction mixture was mixed with 4 µl SDS loading dye without dithiothreitol (DTT) to run on an SDS-PAGE gel, which was stained using InstantBlue Protein stain (Coomassie protein stain). For western blot, the SDS-PAGE gel was transferred to a nitrocellulose membrane. Mouse-monoclonal anti-His antibody [Thermo Scientific] primary and goat anti-mouse conjugated with 800nm fluorophore [Molecular probe] secondary antibodies were used to visualise the bands. The intensity of the bands was then analysed using ImageJ software version 1.46r (Schneider, Rasband, & Eliceiri, 2012).

4.3 Results

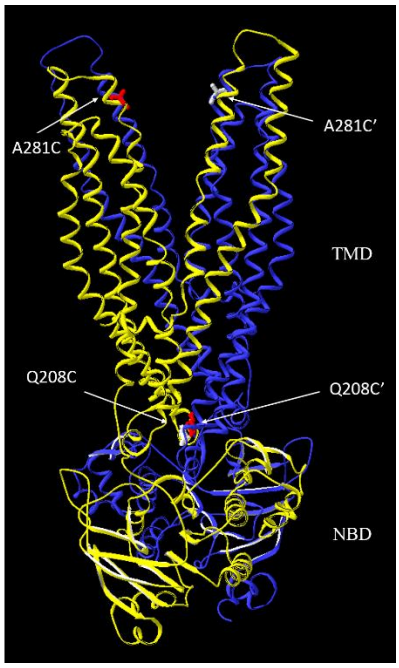

Figure 4.4 Location of crosslinking sites on Sav1866. Two cysteine residues (A281C and Q208C) have been introduced into Sav1866. Crosslinking at position 208 represents an outward-facing conformation. On the contrary, crosslinking at position 281 represents an inward-facing conformation. TMD – transmembrane domain, NBD – nucleotide binding domain (PDB: 2HYD)

A cysteine residue at positions 208 and 281 (Figure 4.4) was introduced using site-directed mutagenesis (see 4.2.1) to the wild-type, single Trp mutants and triple Trp mutants of Sav1866 (listed below), which have different rates of ATPase activity (see Chapter 3).

1. Sav1866 A281C
2. Sav1866 Q208C
3. Sav1866 W87LW143LW243LA281C
4. Sav1866 W87LW143LW243LQ208C
5. Sav1866 W87YA281C
6. Sav1866 W87YQ208C
7. Sav1866 W143LA281C
8. Sav1866 W143LQ208C
9. Sav1866 W243YA281C
10. Sav1866 W243YQ208C

As Sav1866 is a homodimer, both monomers had the mutated cysteine at the same position. The cysteine at position 208 at the end of helix four is adjacent to the periplasmic space, and the

cysteine at 281 on top of helix 6 is located on the opposite end of the protein closer to the extracellular side of the protein as shown in Figure 4.4. Samples were treated with copper phenanthroline as an oxidising agent to form a crosslink between the monomers either at position 208 or 281. Crosslinking of the cysteines at 208 would indicate an outward-facing Sav1866 whereas, crosslinking at 281 cysteines would indicate an inward-facing Sav1866 (see Figure 4.4). In addition, this study would provide information on the structural stability of inactive Sav1866 mutants, despite the loss of ATPase activity, by comparing the crosslinking outcome with the wild-type.

Crosslinking experiments were conducted on Sav1866 that was prepared in three different ways.

i. Detergent purified Sav1866
ii. Sav1866 in crude *E.coli* membrane
iii. Sav1866 reconstituted in phosphatidylglycerol (DOPG) and phosphatidylcholine (DOPC)

The addition of nucleotides was also tested to monitor their effect on the crosslinking (see Methods 4.2.6).

Crosslinked dimers migrated at a slower rate due to their higher molecular weight than the monomer on the SDS-PAGE gel. The relative intensity of the monomer and dimer bands were analysed using ImageJ software version 1.46r (Schneider et al., 2012).

Wild-type Sav1866 has a cysteine residue at position 146 in transmembrane helix 3 (Dawson & Locher, 2006). When the two monomers form a dimer, the cysteine residues are not in close proximity and cannot form a disulphide bridge (data not shown).

4.3.1 Difference in crosslinking between detergent purified Sav1866 and Sav1866 in crude membrane

To examine the effect of detergents on the ability of Sav1866 to form a dimer, and its conformation status, a comparative study between detergent purified Sav1866 (referred to as “purified protein”) and detergent free Sav1866 in crude *E.coli* membrane (referred to as “protein in crude membrane”) was conducted.

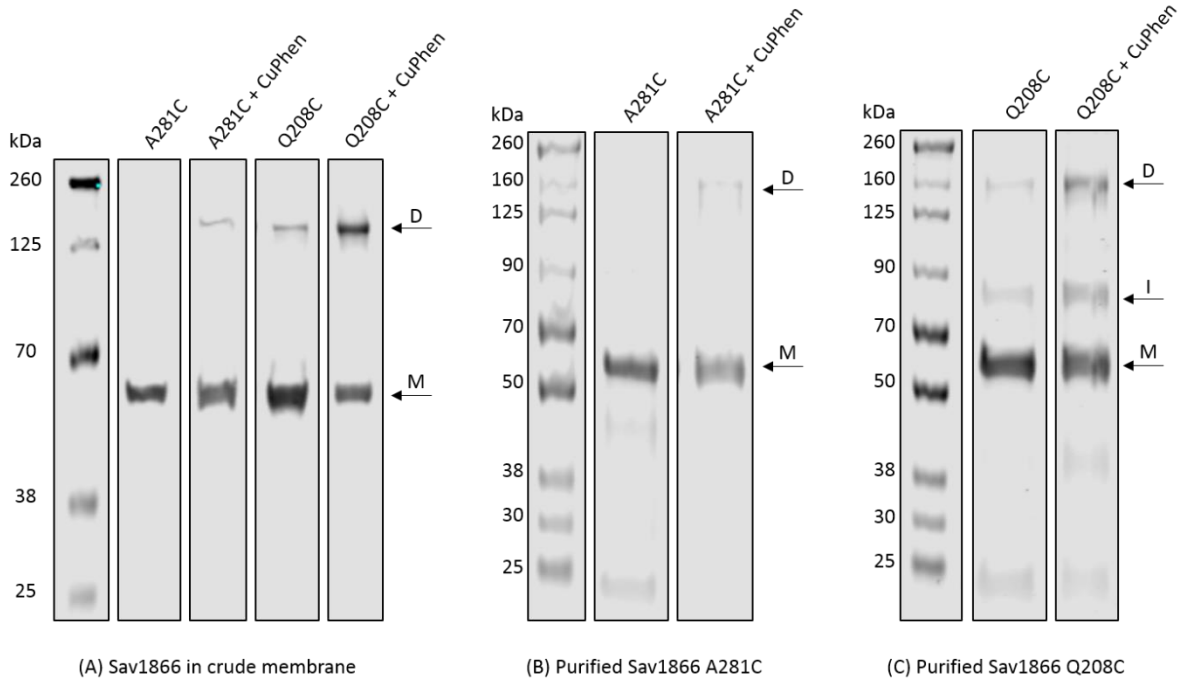

Figure 4.5 Crosslinking of Sav1866 in (80 µg) crude membrane and (2 µg) purified form. Sav1866 cysteine mutants were treated with 0.5 mM copper phenanthroline (CuPhen) as an oxidising agent to allow the formation of dimers (D) from the monomers (M). Sav1866 in crude membrane was separated on an SDS-PAGE gel and transferred onto a western blot, where it was detected using the anti-His antibody as shown in (A). Purified Sav1866 was separated on an SDS-PAGE gel and visualised using Instant Blue as shown in (B). Molecular weight markers are shown on the left in kDa.

Figure 4.5 shows Sav1866 A281C only forms crosslinked dimers (6.1 %) through the cysteine residues at 281 in the presence of copper phenanthroline (CuPhen) as an oxidising agent in both crude membrane and purified conditions. In the absence of CuPhen, only a single band for the monomer of Sav1866 A281C is observed.

Sav1866 Q208C, however, forms spontaneous dimers (8.9 %) as observed in the absence of CuPhen. The addition of CuPhen to the protein increased the level of crosslinked dimers to 48.3 % formed at position 208 adjacent to the periplasmic space in both crude membrane and purified conditions. Purified Sav1866 Q208C also showed intermediate (I) products around 90 kDa both in the presence and absence of CuPhen. Smaller bands around 25 kDa are also seen for purified Sav1866 Q208C, which may represent breakdown products of the protein.

4.3.1.1 Effect of nucleotides on the crosslinking of detergent purified Sav1866 and Sav1866 in crude membrane

For Sav1866 A281C and Q208C, crosslinking reactions with copper phenanthroline as an oxidising agent were performed under the following conditions:

i. Nucleotide-free
ii. ATP
iii. ATP and vanadate (ATP.Vi)
iv. ADP
v. ADP and vanadate (ADP.Vi)

For the rest of the Sav1866 mutants, the same method of crosslinking was applied under conditions (i), (ii) and (iii). The respective bands from western blot images have been cropped and aligned for clarity purposes.

4.3.1.1.1 Sav1866 A281C and Q208C crosslinking

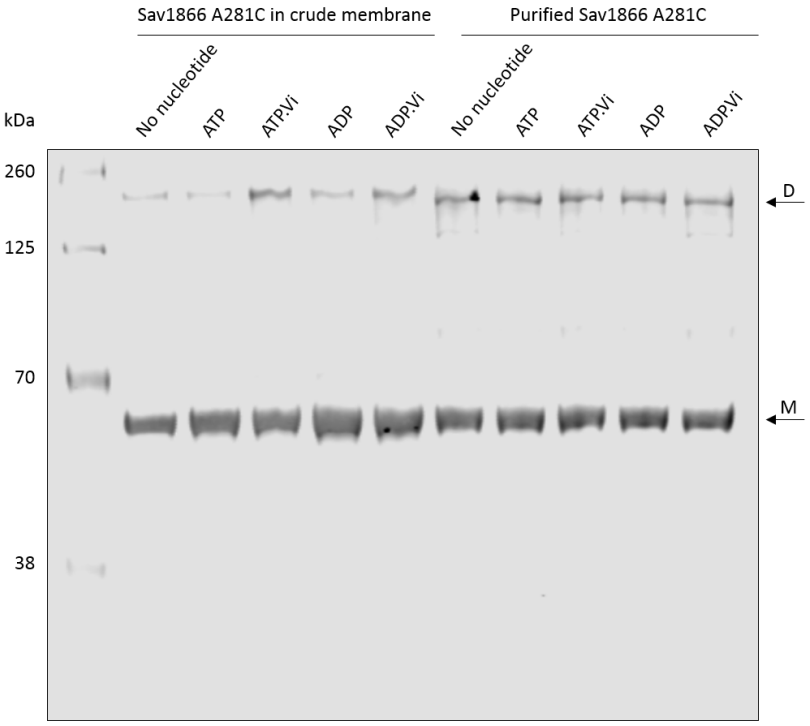

Figure 4.6 Crosslinking of Sav1866 A281C in crude membrane (80 μg) and purified Sav1866 A281C (2 μg) under different nucleotide conditions. Anti-His antibody was used to detect Sav1866 on the western blot. The arrows indicate the monomer (M, MW of 67.6 kDa) and the crosslinked dimer (D, MW of 135 kDa) of the protein. 0.5 mM copper phenanthroline was used for the crosslinking reaction as an oxidising agent. The molecular marker is on the left lane in kDa. Experiments were repeated three times with similar results.

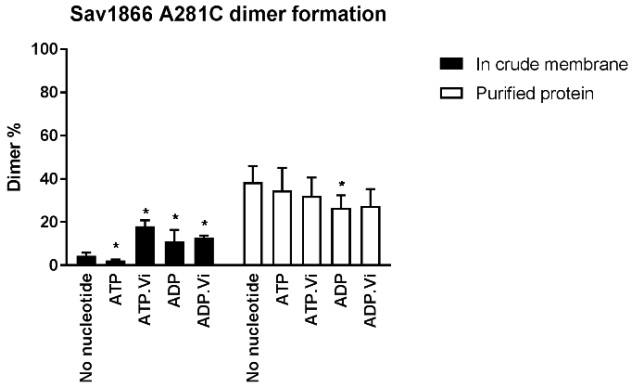

Figure 4.7 Densitometry analysis of crosslinked Sav1866 A281C in crude membrane (black bars) and purified protein (open bars) under different nucleotide conditions. The values are presented as a mean of dimer % with respect to the total Sav1866 A281C protein and error bars represent S.E (n=3). The statistical analysis was performed using a paired t-test. Asterisk indicates statistically different values between the basal and the nucleotide-induced conditions (*P < 0.05). ImageJ software was used for the densitometry analysis of the protein bands.

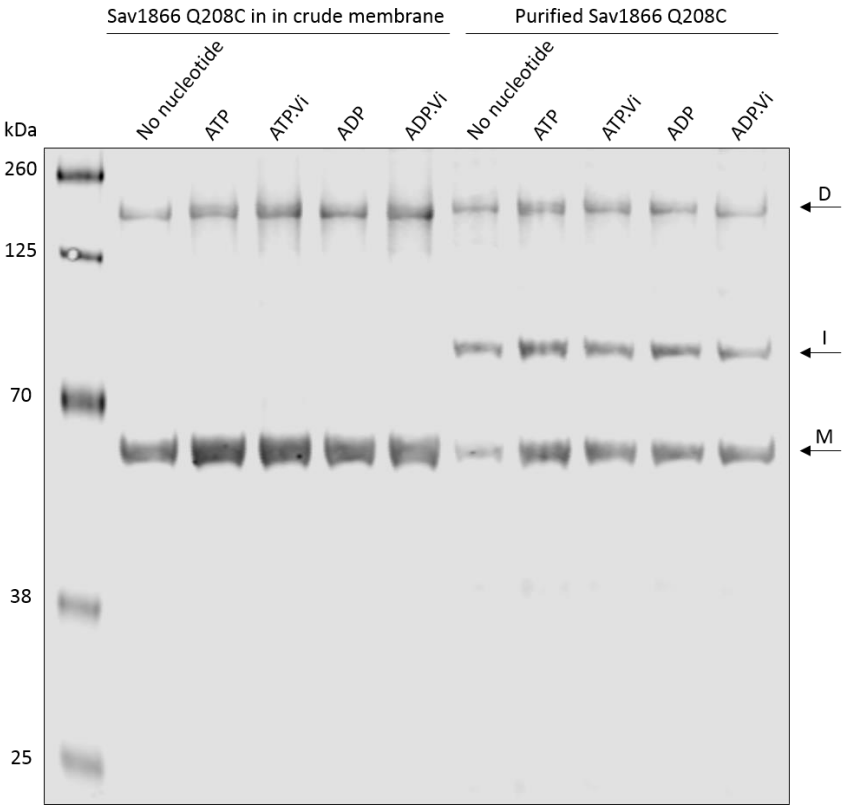

Figure 4.8 Crosslinking of Sav1866 Q208C in crude membrane (80 µg) and purified Sav1866 Q208C (2 µg) under different nucleotide conditions. Anti-His antibody was used to detect Sav1866 on the western blot. The arrows indicate the monomer (M, MW of 67.6 kDa), intermediate product (I, MW of ~90kDa) and the crosslinked dimer (D, MW of 135 kDa) of the protein. 0.5 mM copper phenanthroline was used for the crosslinking reaction as an oxidising agent. The molecular marker is on the left lane in kDa. Experiments were repeated three times with similar results.

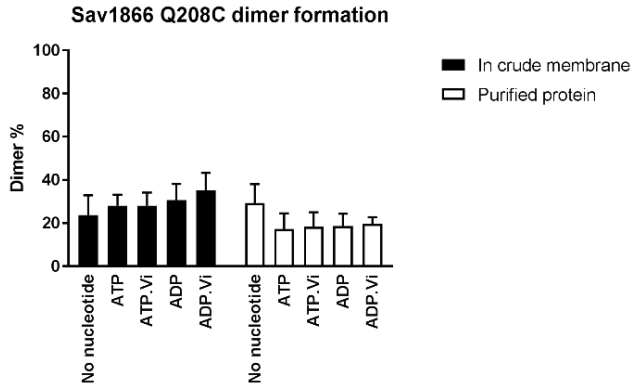

Figure 4.9 Densitometry analysis of crosslinked Sav1866 Q208C in crude membrane (black bars) and purified protein (open bars) under different nucleotide conditions. The values are presented as a mean of dimer % with respect to the total Sav1866 Q208C protein and error bars represent S.E (n=3). The statistical analysis was performed using a paired t-test. ImageJ software was used for the densitometry analysis of the protein bands.

Crosslinks of Sav1866 in crude membrane and detergent purified Sav1866 have been compared in Figure 4.6. From densitometry analysis (Figure 4.7) of Sav1866 A281C in crude membrane, in the absence of nucleotides, approximately 4% of the Sav1866 A281C was crosslinked. The addition of nucleotides brought significant changes to the levels of the crosslinked dimers. Adding ATP lowered the crosslinked dimer to 2%. However, co-incubation with ATP.Vi, ADP and ADP.Vi increased the level of crosslinked dimers to 18%, 11% and 13% respectively.

For detergent purified Sav1866 A281C, the level of crosslinked dimers is considerably higher than Sav1866 A281C in crude membrane. However, the effect of nucleotides is less discriminatory. In the absence of nucleotides, 39% of purified Sav1866 A281C form dimers. The addition of ATP and ATP.Vi has a similar effect, with 35% and 32% of dimer formation respectively, while ADP and ADP.Vi have slightly lower levels of dimers at 26% and 27% respectively. Only in the presence of ADP was there a significant difference compared to the control (nucleotide-free condition).

From Figure 4.8, Sav1866 Q208C in crude membrane did not experience significant changes in dimer formation when nucleotides were added as the levels of crosslinked dimers are similar compared to the nucleotide-free condition (24%). Nevertheless, the addition of ADP.Vi led to the highest level of crosslinked dimers (35%), followed by ADP (30%), ATP.Vi (28%) and ATP (28%).

In purified Sav1866 Q208C, adding nucleotides (ATP, ATP.Vi, ADP and ADP.Vi) decreased the amount of crosslinked dimers formed to approximately 20% from 30% for the nucleotide-free condition.

4.3.1.1.2 Sav1866 W87LW143LW243LA281C and W87LW143LW243LQ208C crosslinking

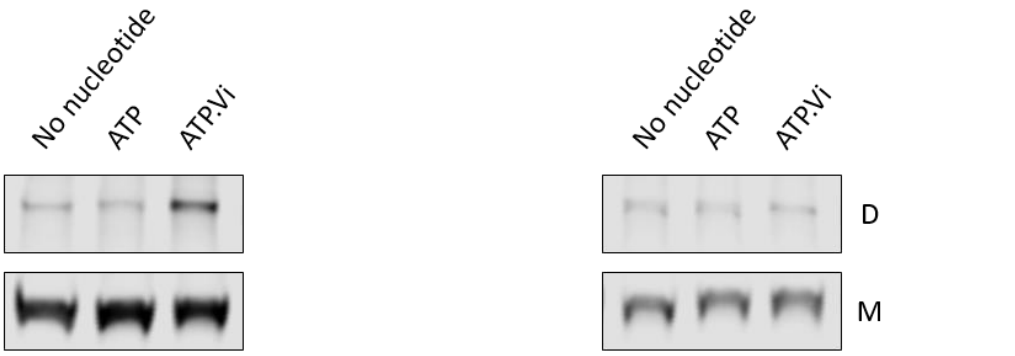

(A) Sav1866 W87LW143LW243LA281C in crude membrane

(B) Purified Sav1866 W87LW143LW243LA281C

Figure 4.10 Crosslinking of Sav1866 W87LW143LW243LA281C in crude membrane (A, 80 µg) and purified Sav1866 W87LW143LW243LA281C (B, 2 µg) under different nucleotide conditions. Anti-His antibody was used to detect Sav1866 on the western blot. The lower panel shows the monomer (M, MW of 67.6 kDa) and the top panel shows the crosslinked dimer (D, MW of 135 kDa) of the protein. 0.5 mM copper phenanthroline was used for the crosslinking reaction as an oxidising agent. Experiments were repeated three times with similar results.

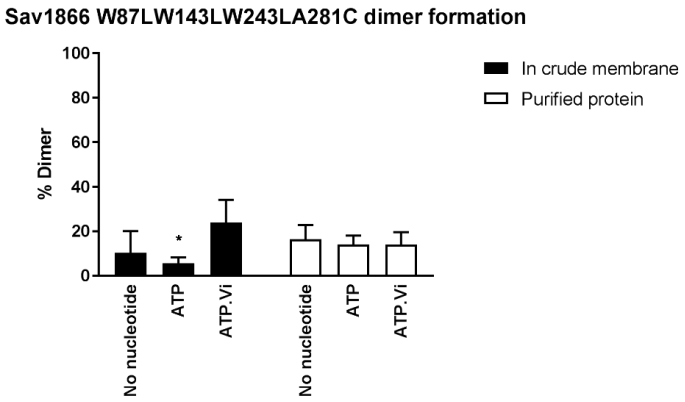

Figure 4.11 Densitometry analysis of crosslinked Sav1866 W87LW143LW243LA281C in crude membrane (black bars) and purified protein (open bars) under different nucleotide conditions. The values are presented as a mean of dimer % with respect to the total Sav1866 W87LW143LW243LA281C protein and error bars represent S.E (n=3). The statistical analysis was performed using a paired t-test. Asterisk indicates statistically different values between the basal and the nucleotide-induced conditions (*$P < 0.05$). ImageJ software was used for the densitometry analysis of the protein bands.

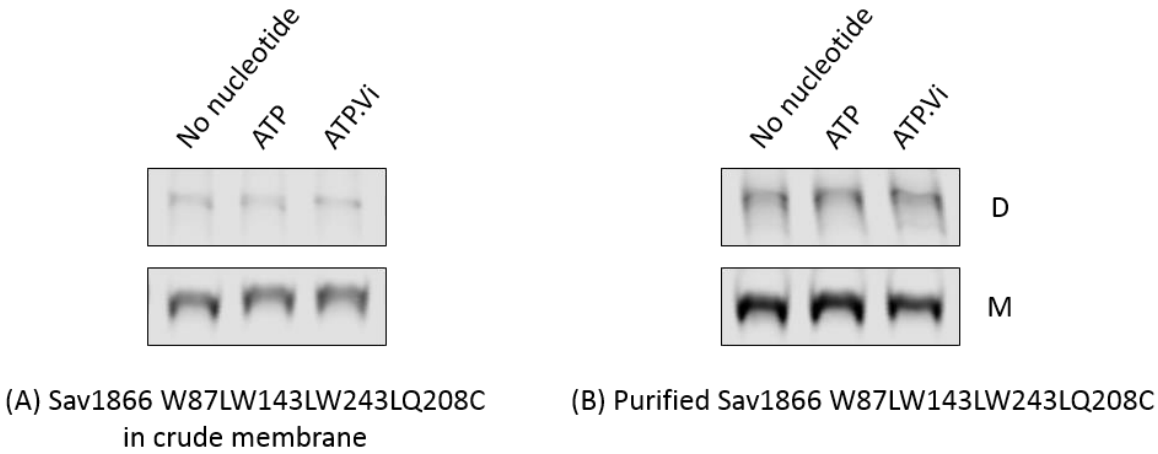

Figure 4.12 Crosslinking of Sav1866 W87LW143LW243LQ208C in crude membrane (A, 80 µg) and purified Sav1866 W87LW143LW243LQ208C (B, 2 µg) under different nucleotide conditions. Anti-His antibody was used to detect Sav1866 on the western blot. The lower panel shows the monomer (M, MW of 67.6 kDa) and the top panel shows the crosslinked dimer (D, MW of 135 kDa) of the protein. 0.5 mM copper phenanthroline was used for the crosslinking reaction as an oxidising agent. Experiments were repeated three times with similar results.

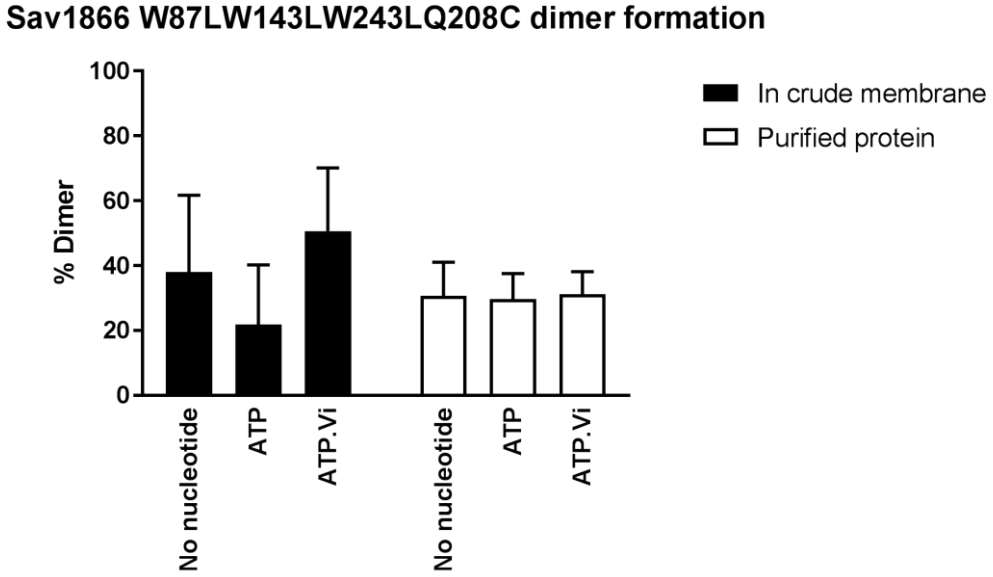

Figure 4.13 Densitometry analysis of crosslinked Sav1866 W87LW143LW243LQ208C in crude membrane (black bars) and purified protein (open bars) under different nucleotide conditions. The values are presented as a mean of dimer % with respect to the total Sav1866 W87LW143LW243LQ208C protein and error bars represent S.E (n=3). The statistical analysis was performed using a paired t-test. ImageJ software was used for the densitometry analysis of the protein bands.

In Figure 4.10, it is clear that co-incubation of Sav1866 W87LW143LW243LA281C in crude membrane with ATP.Vi increases the level of crosslinked dimer (24%) in comparison to the nucleotide-free condition (10%). ATP, however, lowered the level of crosslinked dimer (5.6%) and was significantly different from the nucleotide-free condition.

For purified Sav1866 W87LW143LW243LA281C, the levels of crosslinked dimers are unchanged in the presence of ATP or ATP.Vi compared to the nucleotide-free condition (~14%).

From Figure 4.12, under the nucleotide-free condition, 38 % of Sav1866 W87LW143LW243LQ208C in crude membrane form dimers. The level of dimer formation increases to 50% in the presence of ATP.Vi but decreases to 22% when ATP is added. The errors were such that none of these differences was significantly different.

Levels of crosslinked dimers formed for purified Sav1866 W87LW143LW243LQ208C in the presence of ATP and ATP.Vi are similar to nucleotide-free condition (~30%).

4.3.1.1.3 Sav1866 W87YA281C and W87YQ208C crosslinking

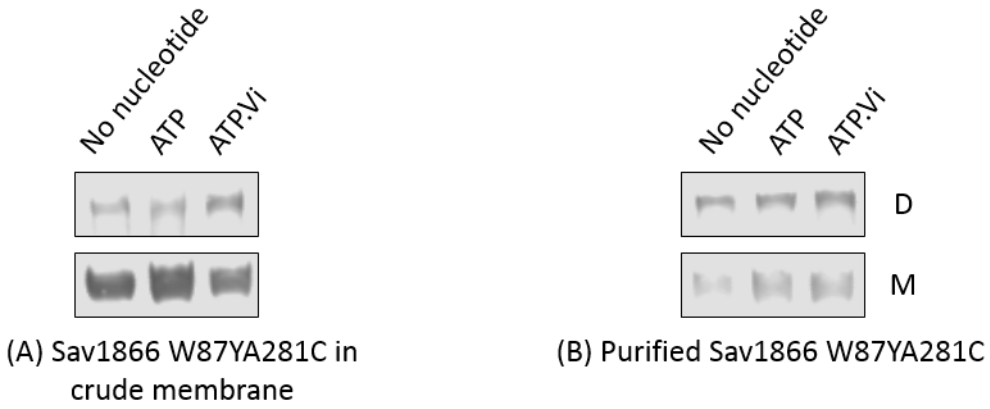

Figure 4.14 Crosslinking of Sav1866 W87YA281C in crude membrane (A, 80 µg) and purified Sav1866 W87YA281C (B, 2 µg) under different nucleotide conditions. Anti-His antibody was used to detect Sav1866 on the western blot. The lower panel shows the monomer (M, MW of 67.6 kDa) and the top panel shows the crosslinked dimer (D, MW of 135 kDa) of the protein. 0.5 mM copper phenanthroline was used for the crosslinking reaction as an oxidising agent. Experiments were repeated three times with similar results.

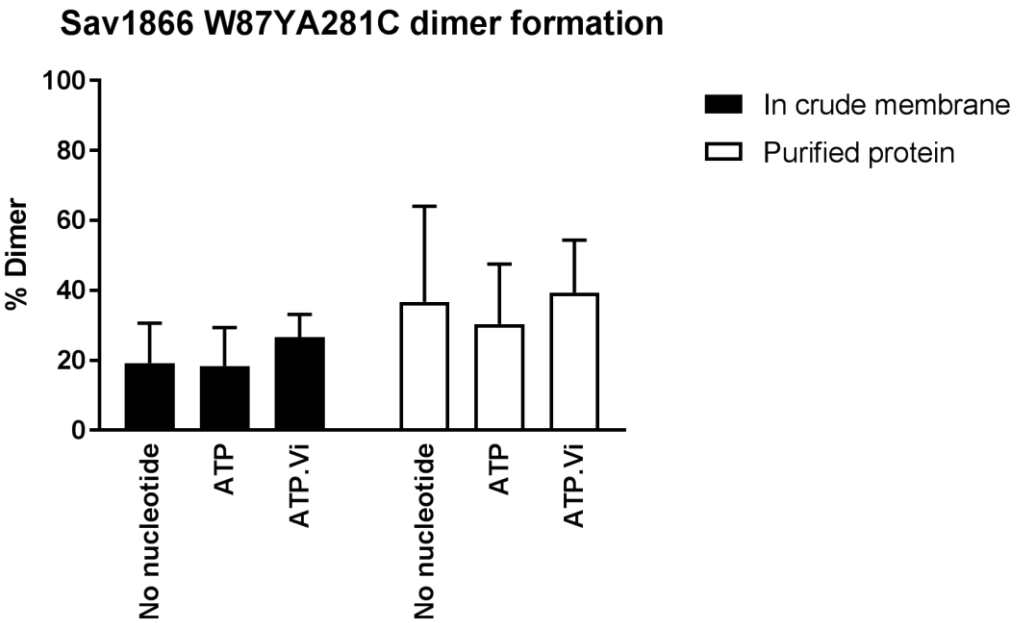

Figure 4.15 Densitometry analysis of crosslinked Sav1866 W87YA281C in crude membrane (black bars) and purified protein (open bars) under different nucleotide conditions. The values are presented as a mean of dimer % with respect to the total Sav1866 W87YA281C protein and error bars represent S.E (n=3). The statistical analysis was performed using a paired t-test. ImageJ software was used for the densitometry analysis of the protein bands.

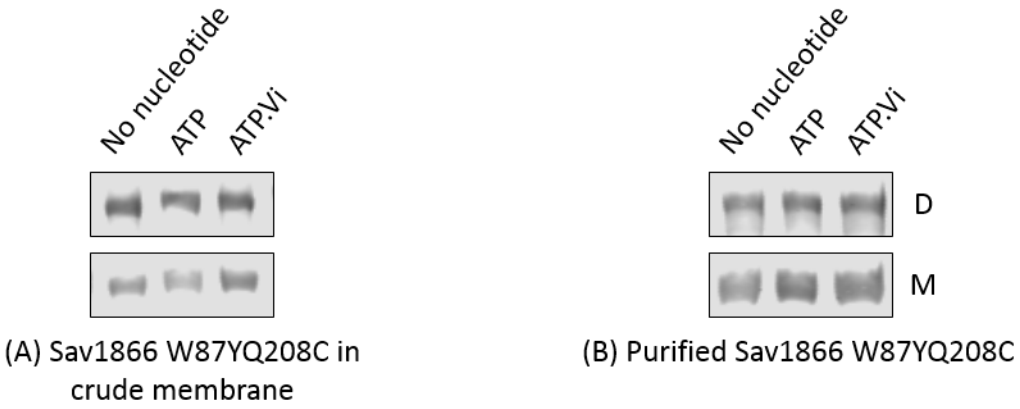

Figure 4.16 Crosslinking of Sav1866 W87YQ208C in crude membrane (A, 80 µg) and purified Sav1866 W87YQ208C (B, 2 µg) under different nucleotide conditions. Anti-His antibody was used to detect Sav1866 on the western blot. The lower panel shows the monomer (M, MW of 67.6 kDa) and the top panel shows the crosslinked dimer (D, MW of 135 kDa) of the protein. 0.5 mM copper phenanthroline was used for the crosslinking reaction as an oxidising agent. Experiments were repeated three times with similar results.

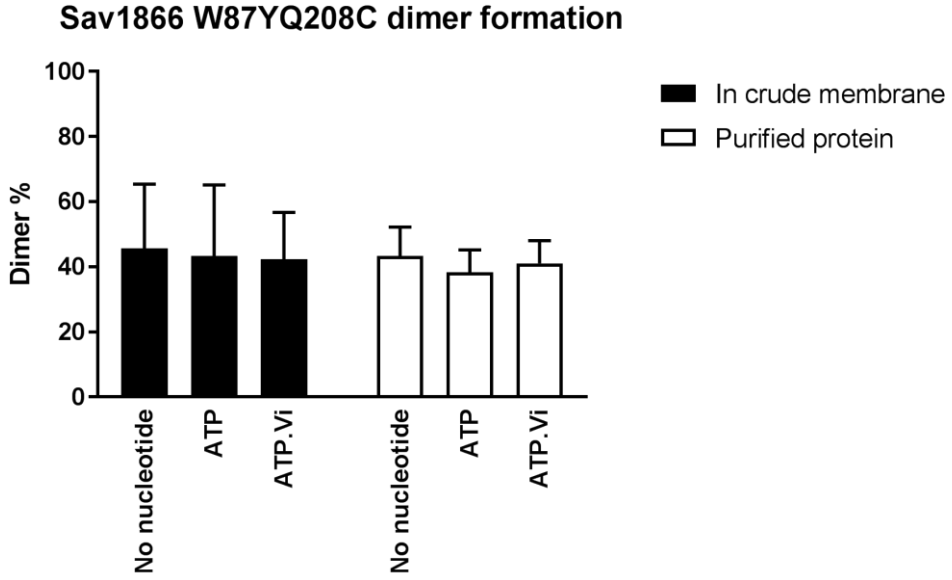

Figure 4.17 Densitometry analysis of crosslinked Sav1866 W87YQ208C in crude membrane (black bars) and purified protein (open bars) under different nucleotide conditions. The values are presented as a mean of dimer % with respect to the total Sav1866 W87YQ208C protein and error bars represent S.E (n=3). The statistical analysis was performed using a paired t-test. ImageJ software was used for the densitometry analysis of the protein bands.

Sav1866 W87YA281C in crude membrane showed similar levels of crosslinked dimers (~19%) formed in the presence of ATP and nucleotide-free conditions. However, co-incubation with ATP.Vi increased the levels of crosslinked dimers to 27%.

For purified Sav1866 W87YA281C the levels of crosslinked dimers for both nucleotide-free condition and addition of ATP.Vi were comparable ~ 38%, and the addition of ATP decreased the dimer level slightly to 30%.

Figure 4.16 and Figure 4.17 show very little changes in levels of dimer formation for Sav1866 W87YQ208C in crude membrane and purified Sav1866 W87YQ208C in the presence of ATP or ATP.Vi and in the absence of nucleotides. The level of dimers formed were ~40% for both samples of the Sav1866 W87YQ208C protein.

4.3.1.1.4 Sav1866 W143LA281C and W143LQ208C crosslinking

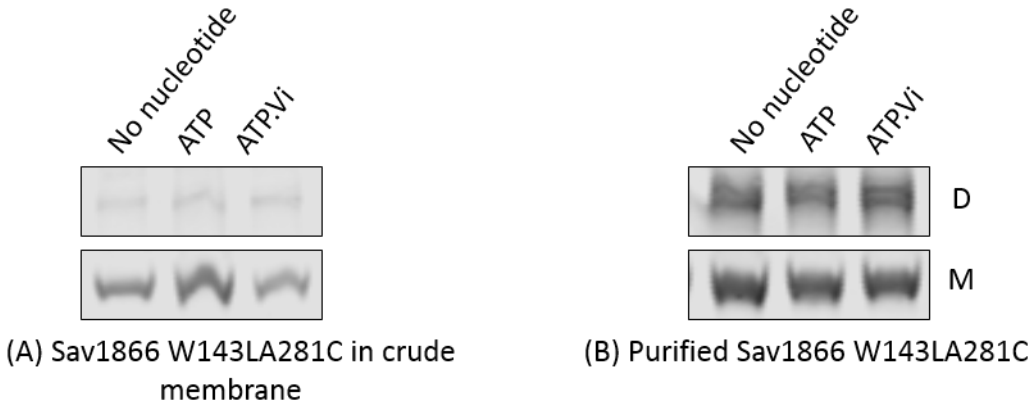

(A) Sav1866 W143LA281C in crude membrane

(B) Purified Sav1866 W143LA281C

Figure 4.18 Crosslinking of Sav1866 W143LA281C in crude membrane (A, 80 µg) and purified Sav1866 W143LA281C (B, 2 µg) under different nucleotide conditions. Anti-His antibody was used to detect Sav1866 on the western blot. The lower panel shows the monomer (M, MW of 67.6 kDa) and the top panel shows the crosslinked dimer (D, MW of 135 kDa) of the protein. 0.5 mM copper phenanthroline was used for the crosslinking reaction as an oxidising agent. Experiments were repeated three times with similar results.

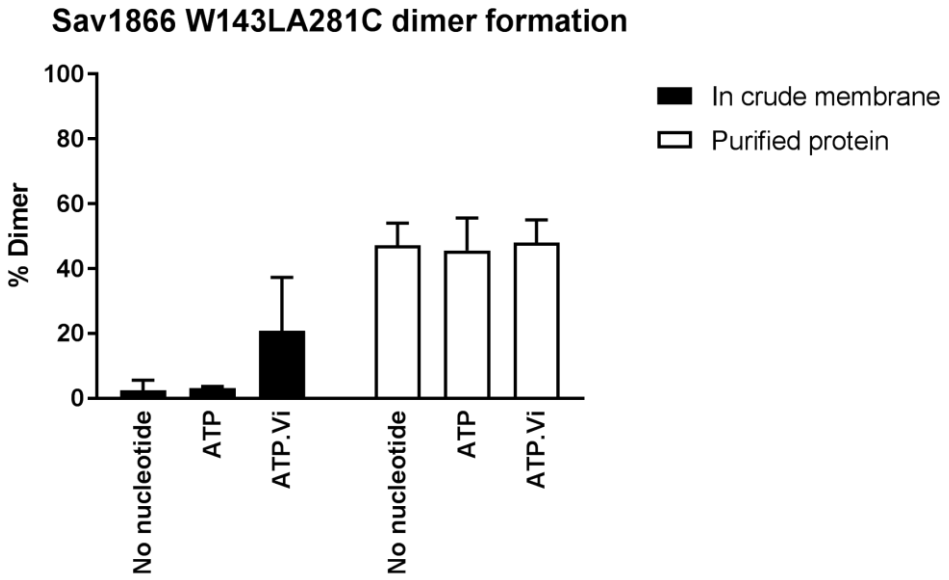

Figure 4.19 Densitometry analysis of crosslinked Sav1866 W143LA281C in crude membrane (black bars) and purified protein (open bars) under different nucleotide conditions. The values are presented as a mean of dimer % with respect to the total Sav1866 W143LA281C protein and error bars represent S.E (n=3). The statistical analysis was performed using a paired t-test. ImageJ software was used for the densitometry analysis of the protein bands.

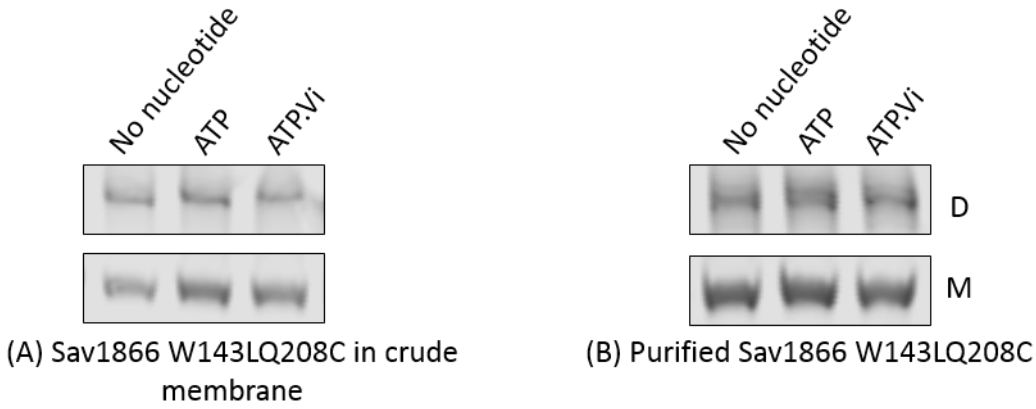

Figure 4.20 Crosslinking of Sav1866 W143LQ208C in crude membrane (A, 80 µg) and purified Sav1866 W143LQ208C (B, 2 µg) under different nucleotide conditions. Anti-His antibody was used to detect Sav1866 on the western blot. The lower panel shows the monomer (M, MW of 67.6 kDa) and the top panel shows the crosslinked dimer (D, MW of 135 kDa) of the protein. 0.5 mM copper phenanthroline was used for the crosslinking reaction as an oxidising agent. Experiments were repeated three times with similar results.

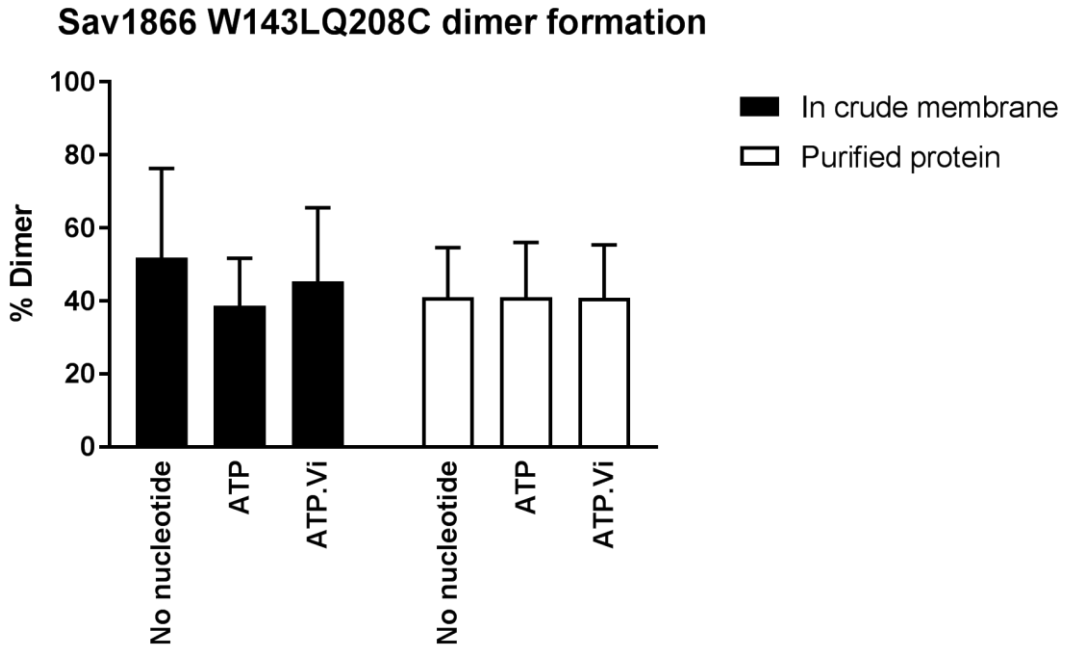

Figure 4.21 Densitometry analysis of crosslinked Sav1866 W143LQ208C in crude membrane (black bars) and purified protein (open bars) under different nucleotide conditions. The values are presented as a mean of dimer % with respect to the total Sav1866 W143LQ208C protein and error bars represent S.E (n=3). The statistical analysis was performed using a paired t-test. ImageJ software was used for the densitometry analysis of the protein bands.

From the densitometry analysis of Sav1866 W143LA281C dimer formation in Figure 4.19, the levels of dimers formed for Sav1866 W143LA281C in crude membrane in the absence of nucleotide and the presence of ATP is very low (~3%). In the presence of ATP.Vi, the dimer levels increase up to 21%.

For purified Sav1866 W143LA281C, however, the levels of dimers formed are higher than for Sav1866 W143LA281C in crude membrane but remain unchanged in the presence or absence of nucleotides (ATP and ATP.Vi) ~46%.

From Figure 4.20 and Figure 4.21, it is clear that the presence or absence of nucleotides (ATP and ATP.Vi) does not change the levels of dimers formed significantly. For both Sav1866 W143LQ208C in crude membrane and purified Sav1866 W143LQ208C, the levels of dimers formed is between 40% and 50%.

4.3.1.1.5 Sav1866 W243YA281C and W243YQ208C crosslinking

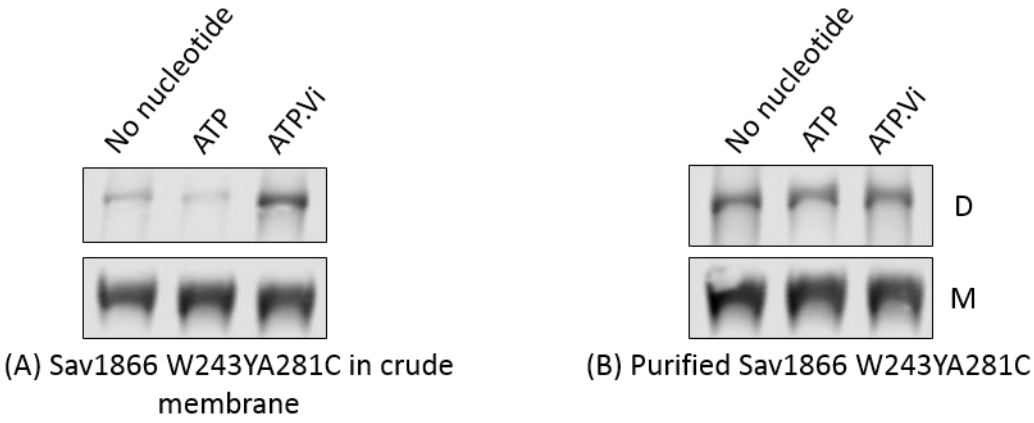

(A) Sav1866 W243YA281C in crude membrane

(B) Purified Sav1866 W243YA281C

Figure 4.22 Crosslinking of Sav1866 W243YA281C in crude membrane (A, 80 µg) and purified Sav1866 W243YA281C (B, 2 µg) under different nucleotide conditions. Anti-His antibody was used to detect Sav1866 on the western blot. The lower panel shows the monomer (M, MW of 67.6 kDa) and the top panel shows the crosslinked dimer (D, MW of 135 kDa) of the protein. 0.5 mM copper phenanthroline was used for the crosslinking reaction as an oxidising agent. Experiments were repeated three times with similar results.

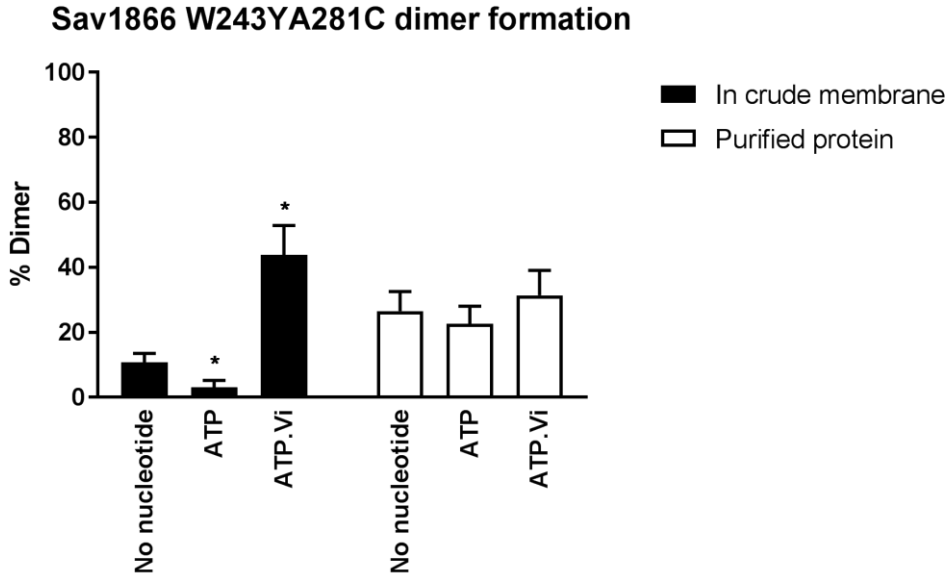

Figure 4.23 Densitometry analysis of crosslinked Sav1866 W243YA281C in crude membrane (black bars) and purified protein (open bars) under different nucleotide conditions. The values are presented as a mean of dimer % with respect to the total Sav1866 W243YA281C protein and error bars represent S.E (n=3). The statistical analysis was performed using a paired t-test. Asterisk indicates statistically different values between the basal and the nucleotide-induced conditions (*P < 0.05). ImageJ software was used for the densitometry analysis of the protein bands.

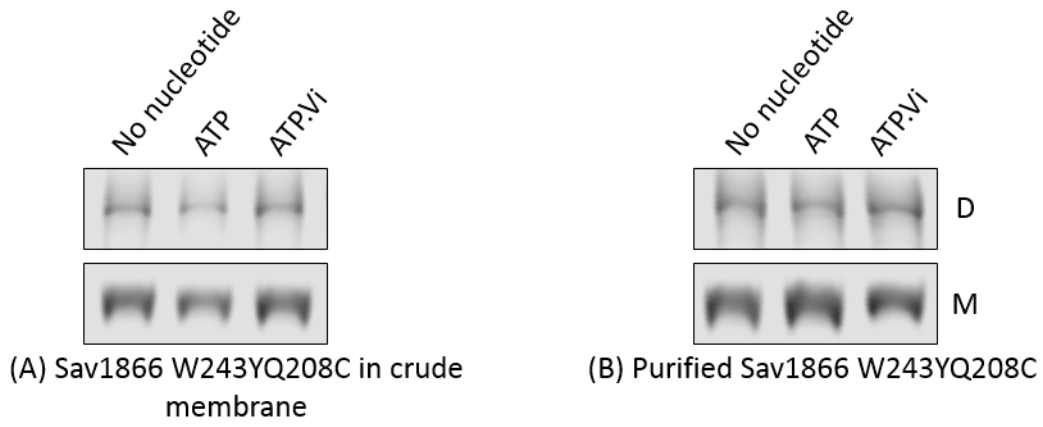

Figure 4.24 Crosslinking of Sav1866 W243YQ208C in crude membrane (A, 80 µg) and purified Sav1866 W243YQ208C (B, 2 µg) under different nucleotide conditions. Anti-His antibody was used to detect Sav1866 on the western blot. The lower panel shows the monomer (M, MW of 67.6 kDa) and the top panel shows the crosslinked dimer (D, MW of 135 kDa) of the protein. 0.5 mM copper phenanthroline was used for the crosslinking reaction as an oxidising agent. Experiments were repeated three times with similar results.

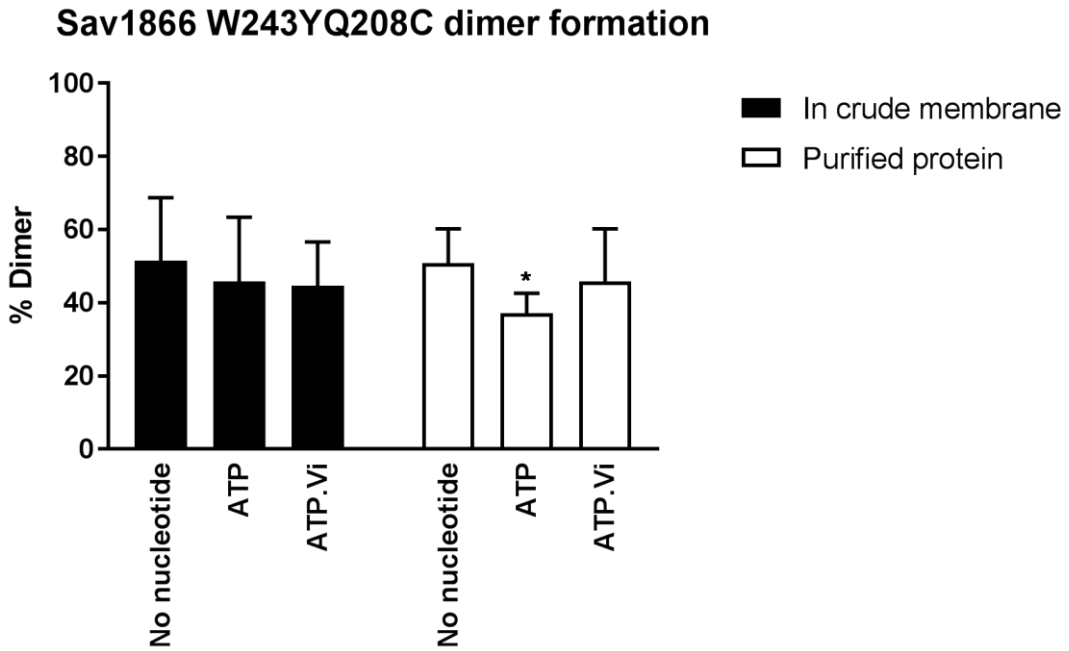

Figure 4.25 Densitometry analysis of crosslinked Sav1866 W243YQ208C in crude membrane (black bars) and purified protein (open bars) under different nucleotide conditions. The values are presented as a mean of dimer % with respect to the total Sav1866 W243YQ208C protein and error bars represent S.E (n=3). The statistical analysis was performed using a paired t-test. Asterisk indicates statistically different values between the basal and the nucleotide-induced conditions (*$P < 0.05$). ImageJ software was used for the densitometry analysis of the protein bands.

From densitometry analysis in Figure 4.23, 11% of Sav1866 W243YA281C in crude membrane forms crosslinked dimers. Addition of ATP lowers the crosslinked dimers to 3% but ATP.Vi increases the levels significantly to 44%. Both nucleotide conditions were significantly different from the basal condition.

For purified Sav1866 W243YA281C the levels of crosslinked dimers formed under various nucleotide conditions are fairly constant at ~30%.

From Figure 4.24 and Figure 4.25, Sav1866 W243YQ208C in crude membrane maintained similar levels of crosslinked dimers in the presence or absence of nucleotides. When no nucleotides were present ~50% crosslinked dimers were formed. The addition of ATP or ATP.Vi lowered the levels slightly ~45%.

For purified Sav1866 W87YQ208C, the presence of ATP significantly lowered the levels of crosslinked dimers ~37% compared to 50% under nucleotide-free condition. When ATP.Vi was added the levels were increased slightly to 46% but still not as high as for lack of nucleotides.

4.3.1.1.6 Formation of intermediate products

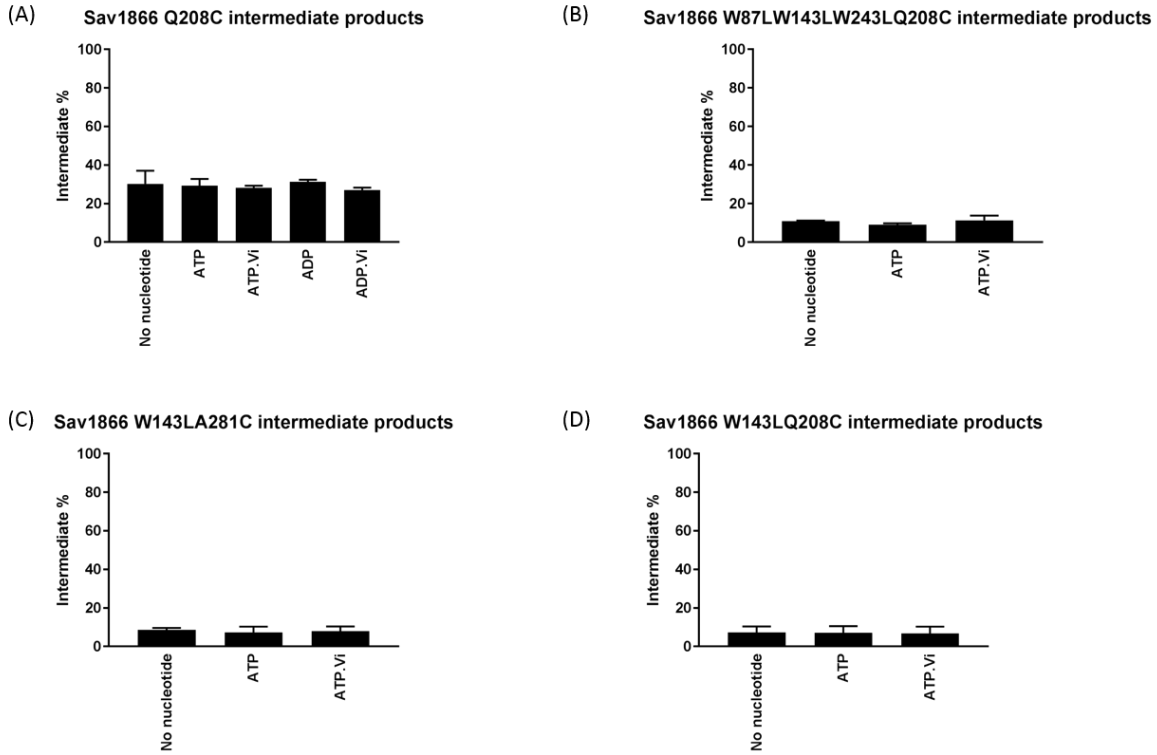

Figure 4.26 Densitometry analysis of the intermediate products formed through the crosslinking of Sav1866 mutants under different nucleotide conditions. (A) Sav1866 Q208C purified protein; (B) Sav1866 W87LW143LW243LQ208C purified protein; (C) Sav1866 W143LA281C purified protein; (D) Sav1866 W143LQ208C. The values are presented as a mean of dimer % with respect to the total Sav1866 W243YQ208C protein and error bars represent S.E (n=3). The statistical analysis was performed using a paired t-test. ImageJ software was used for the densitometry analysis of the protein bands.

Following crosslinking using copper phenanthroline of Sav1866 cysteine mutants, some of the detergent purified mutants produced an intermediate product (I) in addition to the crosslinked dimers. The levels of these intermediate products have been quantified using densitometry and are shown in Figure 4.26. For Sav1866 Q208C, the level of intermediate products were ~ 30% under all nucleotide conditions (ATP and ATP.Vi). The levels were slightly lower for Sav1866 W87LW143LW243LQ208C, Sav1866 W143LA281C and Sav1866 W143LQ208C at ~10%, 8% and 7% respectively.

4.3.2 Effect of anionic vs neutral phospholipids on the crosslinking of Sav1866

To study the impact of anionic and neutral lipid reconstitution on the conformation of Sav1866, detergent purified Sav1866 proteins (see General Materials and Methods 2.2.4) were reconstituted in DOPG and DOPC (see 4.2.5 for methods) respectively. The proteoliposomes were then treated to crosslinking using copper phenanthroline as an oxidising agent following the protocol described in 4.2.6. The following nucleotide conditions were tested.

i. Nucleotide-free
ii. ATP
iii. ATP and vanadate (ATP.Vi)
iv. ADP
v. ADP and vanadate (ADP.Vi)

The following figures show SDS-PAGE gels and western blot images of Sav1866 proteoliposomes in the presence and absence of nucleotides. In cases where the protein concentration was too low to visualise on an SDS-PAGE gel using Instant Blue, the SDS-PAGE gel was transferred to a nitrocellulose membrane, and anti-His antibody was used for detection.

4.3.2.1 Sav1866 A281C and Q208C

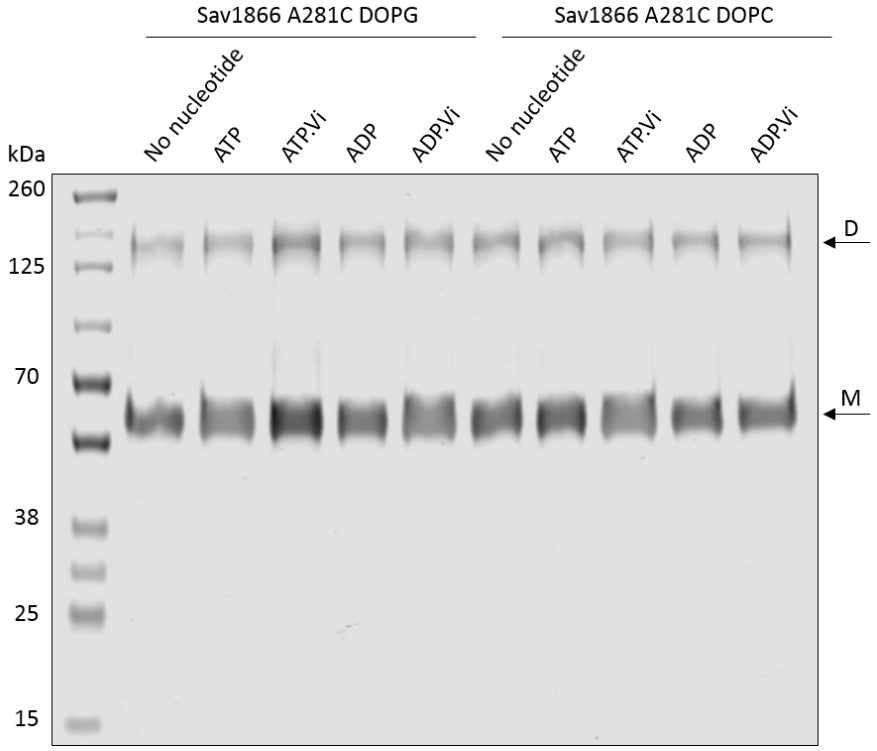

Figure 4.27 Crosslinking of Sav1866 A281C (2 µg) reconstituted in DOPG and DOPC under different nucleotide conditions. InstantBlue Protein stain was used to visualise Sav1866 on the SDS-PAGE gel. The arrows indicate the monomer (M, MW of 67.6 kDa) and the crosslinked dimer (D, MW of 135 kDa) of the protein. 0.5 mM copper phenanthroline was used for the crosslinking reaction as an oxidising agent. The molecular marker is on the left lane in kDa. Experiments were repeated three times with similar results.

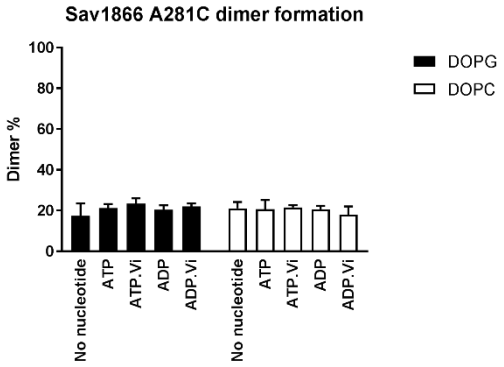

Figure 4.28 Densitometry analysis of crosslinked Sav1866 A281C reconstituted in DOPG (black bars) and DOPC (open bars) under different nucleotide conditions. The values are presented as a mean of dimer % with respect to the total Sav1866 A281C protein and error bars represent S.E (n=3). The statistical analysis was performed using a paired t-test. ImageJ software was used for the densitometry analysis of the protein bands.

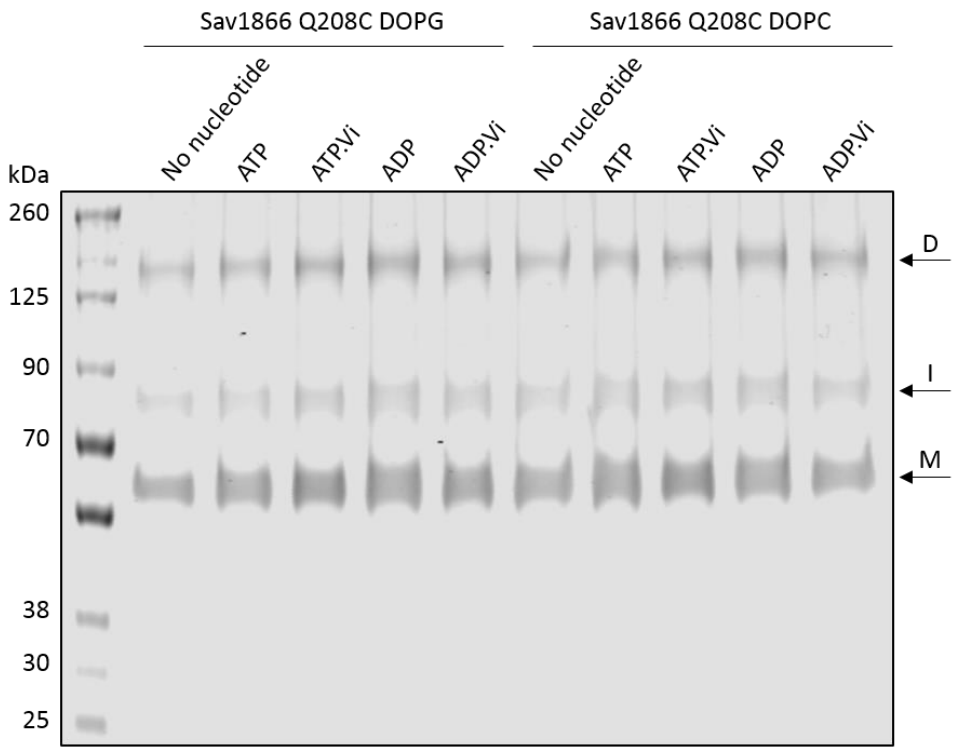

Figure 4.29 Crosslinking of Sav1866 Q208C (2 µg) reconstituted in DOPG and DOPC under different nucleotide conditions. InstantBlue Protein stain was used to visualise Sav1866 on the SDS-PAGE gel. The arrows indicate the monomer (M, MW of 67.6 kDa) and the crosslinked dimer (D, MW of 135 kDa) of the protein. 0.5 mM copper phenanthroline was used for the crosslinking reaction as an oxidising agent. The molecular marker is on the left lane in kDa. Experiments were repeated three times with similar results.

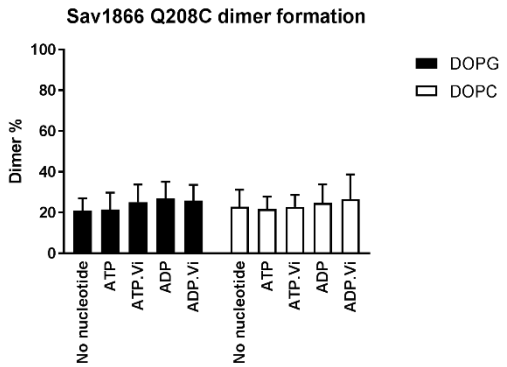

Figure 4.30 Densitometry analysis of crosslinked Sav1866 Q208C reconstituted in DOPG (black bars) and DOPC (open bars) under different nucleotide conditions. The values are presented as a mean of dimer % with respect to the total Sav1866 Q208C protein and error bars represent S.E (n=3). The statistical analysis was performed using a paired t-test. ImageJ software was used for the densitometry analysis of the protein bands.

From Figure 4.27 and Figure 4.28, Sav1866 A281C reconstituted in DOPG and DOPC showed ~20% of crosslinked dimers in the absence of nucleotide. When co-incubated with nucleotides ATP, ATP.Vi, ADP and ADP.Vi, there were no significant changes in the levels of dimers formed.

Sav1866 Q208C reconstituted in DOPG and DOPC behaved in a similar manner to Sav1866 A281C (Figure 4.29 and Figure 4.30) with no significant changes in the levels of crosslinked dimers upon addition of nucleotides compared to the nucleotide-free condition (~24%). However, Sav1866 Q208C crosslinking produced intermediate products that ran between the dimer and monomer bands just under 90 kDa shown in Figure 4.29. The quantification of the intermediate products is discussed in 4.3.2.6.

4.3.2.2 Sav1866 W87LW143LW243LA281C and W87LW143LW243LQ208C

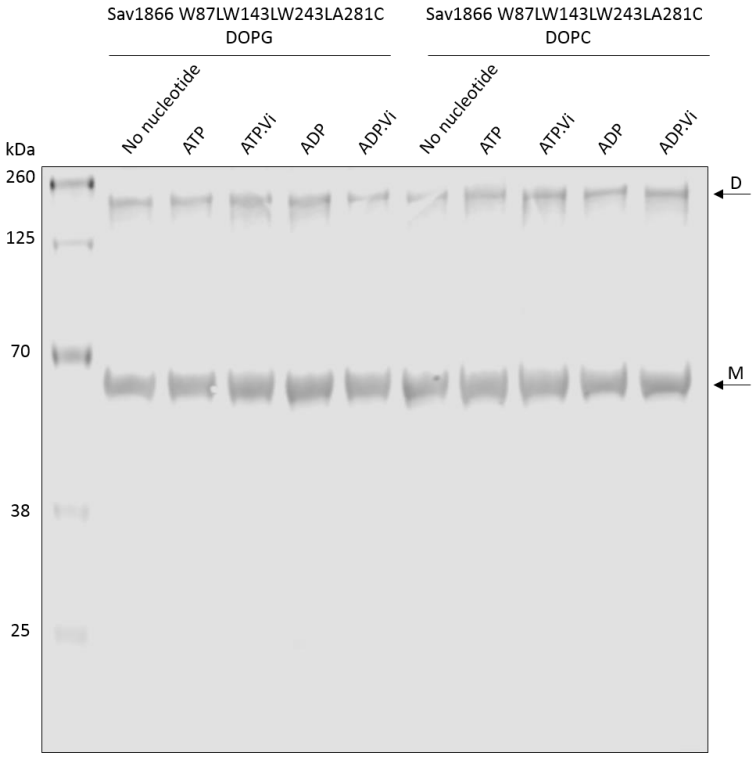

Figure 4.31 Crosslinking of Sav1866 W87LW143LW243LA281C (2 µg) reconstituted in DOPG and DOPC under different nucleotide conditions. Anti-His antibody was used to detect Sav1866 on the western blot. The arrows indicate the monomer (M, MW of 67.6 kDa) and the crosslinked dimer (D, MW of 135 kDa) of the protein. 0.5 mM copper phenanthroline was used for the crosslinking reaction as an oxidising agent. The molecular marker is on the left lane in kDa. Experiments were repeated three times with similar results.

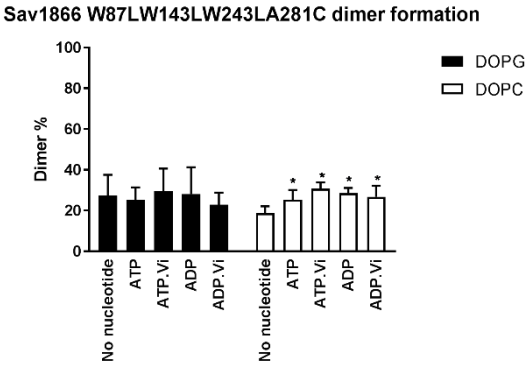

Figure 4.32 Densitometry analysis of crosslinked Sav1866 W87LW143LW243LA281C reconstituted in DOPG (black bars) and DOPC (open bars) under different nucleotide conditions. The values are presented as a mean of dimer % with respect to the total Sav1866 W87LW143LW243LA281C protein and error bars represent S.E (n=3). The statistical analysis was performed using a paired t-test. Asterisk indicates statistically different values between the basal and the nucleotide-induced conditions (*P < 0.05). ImageJ software was used for the densitometry analysis of the protein bands.

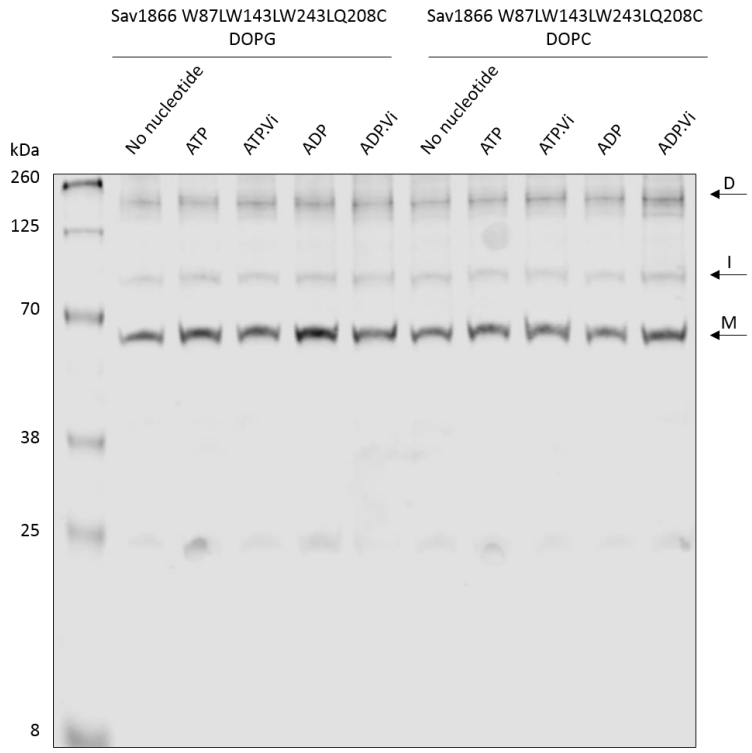

Figure 4.33 Crosslinking of Sav1866 W87LW143LW243LQ208C (2 µg) reconstituted in DOPG and DOPC under different nucleotide conditions. Anti-His antibody was used to detect Sav1866 on the western blot. The arrows indicate the monomer (M, MW of 67.6 kDa), intermediate product (I, Mr of ~90kDa) and the crosslinked dimer (D, MW of 135 kDa) of the protein. 0.5 mM copper phenanthroline was used for the crosslinking reaction as an oxidising agent. The molecular marker is on the left lane in kDa. Experiments were repeated three times with similar results.

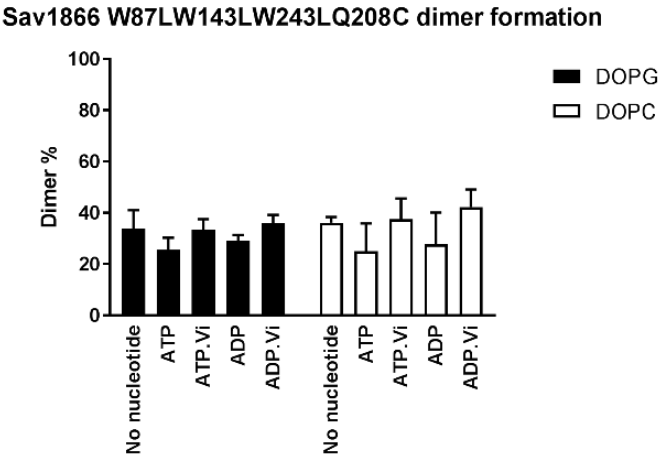

Figure 4.34 Densitometry analysis of crosslinked Sav1866 W87LW143LW243LQ208C reconstituted in DOPG (black bars) and DOPC (open bars) under different nucleotide conditions. The values are presented as a mean of dimer % with respect to the total Sav1866 W87LW143LW243LQ208C protein and error bars represent S.E (n=3). The statistical analysis was performed using a paired t-test. ImageJ software was used for the densitometry analysis of the protein bands.

Sav1866 W87LW143LW243LA281C reconstituted in DOPG showed a slight increase in crosslinked dimers when co-incubated with ATP.Vi (30%) and ADP (28%), but a decrease with ATP (25%) or ADP.Vi (23%) compared to the nucleotide-free condition (27%), as shown in Figure 4.32.

The nucleotide-free condition for Sav1866 W87LW143LW243LA281C reconstituted in DOPC produced 19% of dimers. This was increased significantly to 25% by ATP, 31% by ATP.Vi, 29% by ADP and 27% by ADP.Vi.

In Figure 4.34, co-incubation with ATP or ADP decreased the levels of dimers formed by ~4%, but ATP.Vi and ADP.Vi did not change the levels of dimers compared to the nucleotide-free condition (34%) for Sav1866 W87LW143LW243LQ208C reconstituted in DOPG.

For Sav1866 W87LW143LW243LQ208C reconstituted in DOPC, co-incubation with ATP and ADP decreased the crosslinked dimers formed by ~10% compared to the nucleotide-free condition, while ATP.Vi and ADP.Vi did not change the level of the crosslinked dimers. Sav1866 W87LW143LW243LQ208C also formed intermediate products in a similar way to Sav1866 Q208C, which is discussed in 4.3.2.6.

4.3.2.3 Sav1866 W87YA281C and W87YQ208C

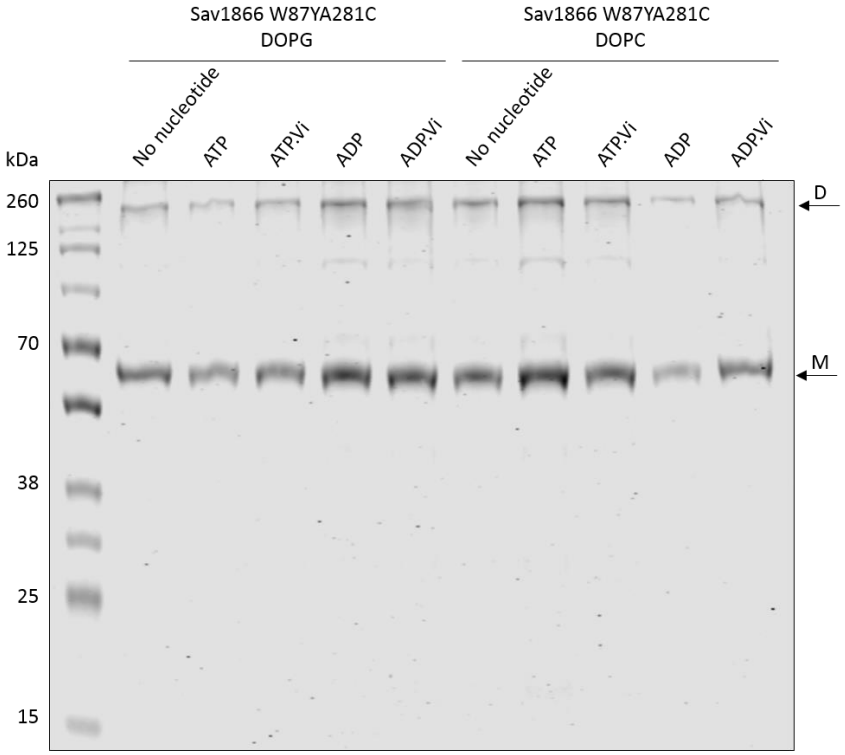

Figure 4.35 Crosslinking of Sav1866 W87YA281C (2 µg) reconstituted in DOPG and DOPC under different nucleotide conditions. InstantBlue Protein stain was used to visualise Sav1866 on the SDS-PAGE gel. The arrows indicate the monomer (M, MW of 67.6 kDa) and the crosslinked dimer (D, MW of 135 kDa) of the protein. 0.5 mM copper phenanthroline was used for the crosslinking reaction as an oxidising agent. The molecular marker is on the left lane in kDa. Experiments were repeated three times with similar results.

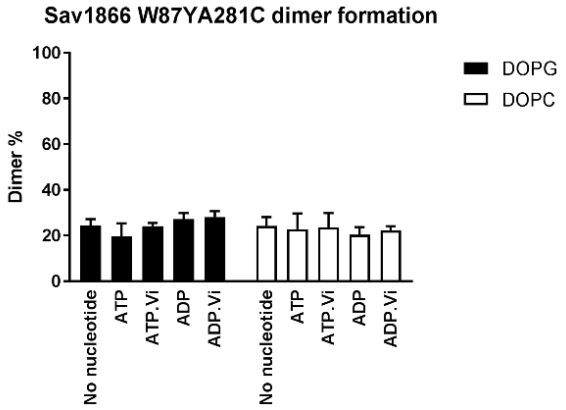

Figure 4.36 Densitometry analysis of crosslinked Sav1866 W87YA281C reconstituted in DOPG (black bars) and DOPC (open bars) under different nucleotide conditions. The values are presented as a mean of dimer % with respect to the total Sav1866 W87YA281C protein and error bars represent S.E (n=3). The statistical analysis was performed using a paired t-test. ImageJ software was used for the densitometry analysis of the protein bands.

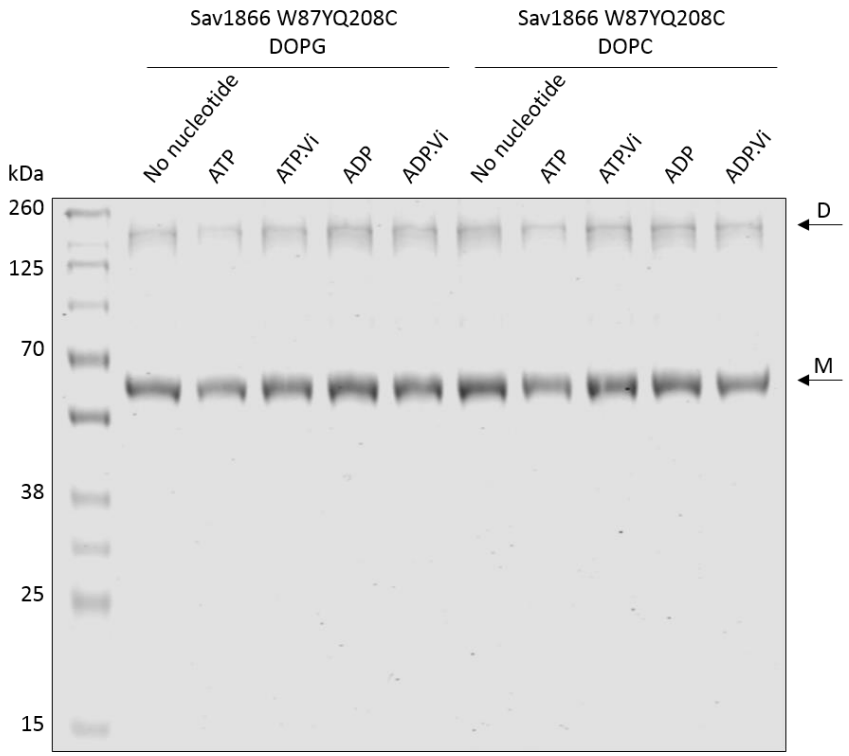

Figure 4.37 Crosslinking of Sav1866 W87YQ208C (2 µg) reconstituted in DOPG and DOPC under different nucleotide conditions. InstantBlue Protein stain was used to visualise Sav1866 on the SDS-PAGE gel. The arrows indicate the monomer (M, MW of 67.6 kDa) and the crosslinked dimer (D, MW of 135 kDa) of the protein. 0.5 mM copper phenanthroline was used for the crosslinking reaction as an oxidising agent. The molecular marker is on the left lane in kDa. Experiments were repeated three times with similar results.

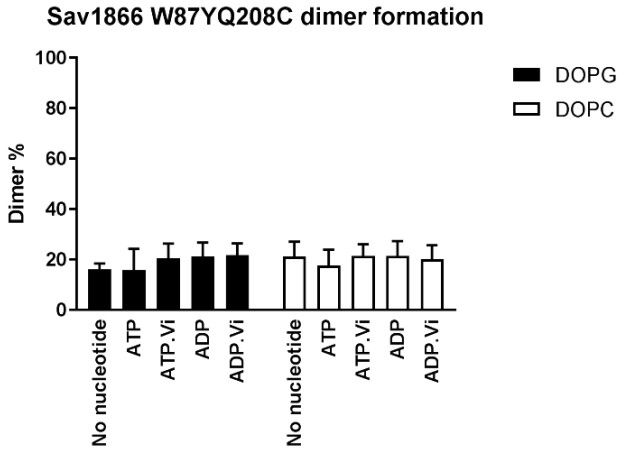

Figure 4.38 Densitometry analysis of crosslinked Sav1866 W87YQ208C reconstituted in DOPG (black bars) and DOPC (open bars) under different nucleotide conditions. The values are presented as a mean of dimer % with respect to the total Sav1866 W87YQ208C protein and error bars represent S.E (n=3). The statistical analysis was performed using a paired t-test. ImageJ software was used for the densitometry analysis of the protein bands.

Figure 4.35 shows crosslinked Sav1866 W87YA281C reconstituted in DOPG and DOPC. In the absence of nucleotides, Sav1866 W87YA281C reconstituted in both DOPG and DOPC form ~24% of dimers. The level of crosslinked dimers is not affected drastically by the addition of nucleotides (ATP, ATP.Vi, ADP or ADP.Vi) as the changes in the levels are less than 5%.

Sav1866 W87YQ208C reconstituted in both DOPG and DOPC did not show significant changes in crosslinked dimers upon addition of nucleotides as shown in Figure 4.37 with changes less than 5% compared to the nucleotide-free condition.

4.3.2.4 Sav1866 W143LA281C and W143LQ208C

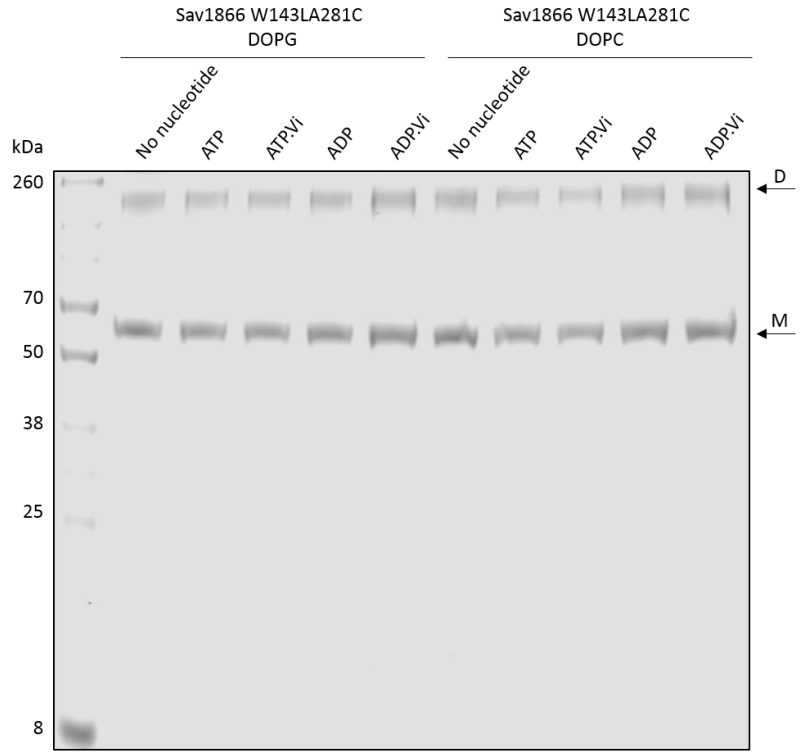

Figure 4.39 Crosslinking of Sav1866 W143LA281C (2 µg) reconstituted in DOPG and DOPC under different nucleotide conditions. InstantBlue Protein stain was used to visualise Sav1866 on the SDS-PAGE gel. The arrows indicate the monomer (M, MW of 67.6 kDa) and the crosslinked dimer (D, MW of 135 kDa) of the protein. 0.5 mM copper phenanthroline was used for the crosslinking reaction as an oxidising agent. The molecular marker is on the left lane in kDa. Experiments were repeated three times with similar results.

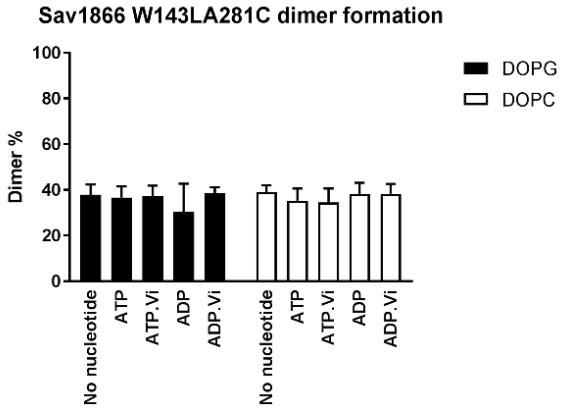

Figure 4.40 Densitometry analysis of crosslinked Sav1866 W143LA281C reconstituted in DOPG (black bars) and DOPC (open bars) under different nucleotide conditions. The values are presented as a mean of dimer % with respect to the total Sav1866 W143LA281C protein and error bars represent S.E (n=3). The statistical analysis was performed using a paired t-test. ImageJ software was used for the densitometry analysis of the protein bands.

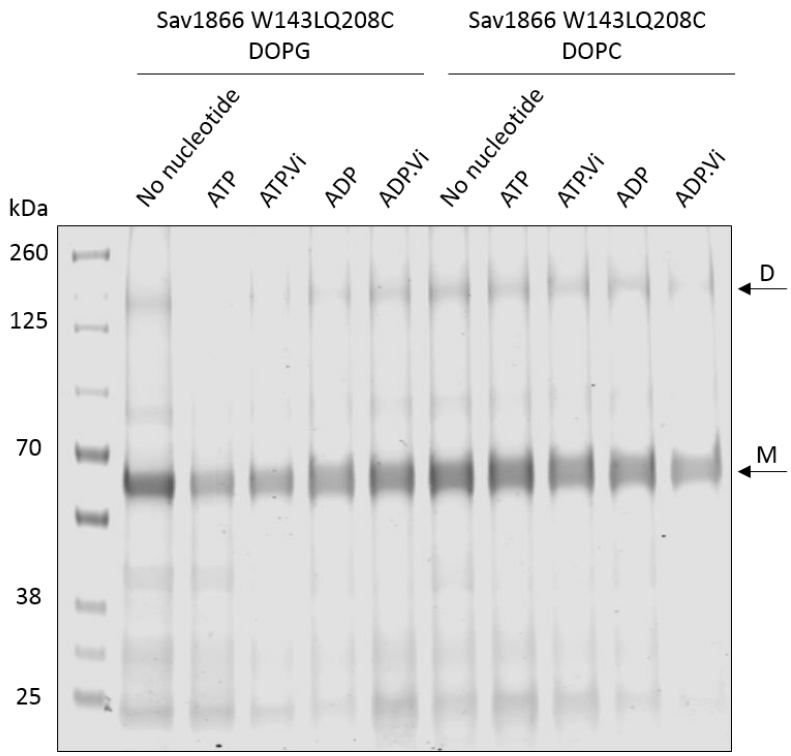

Figure 4.41 Crosslinking of Sav1866 W143LQ208C (2 µg) reconstituted in DOPG and DOPC under different nucleotide conditions. InstantBlue Protein stain was used to visualise Sav1866 on the SDS-PAGE gel. The arrows indicate the monomer (M, MW of 67.6 kDa) and the crosslinked dimer (D, MW of 135 kDa) of the protein. 0.5 mM copper phenanthroline was used for the crosslinking reaction as an oxidising agent. The molecular marker is on the left lane in kDa. Experiments were repeated three times with similar results.

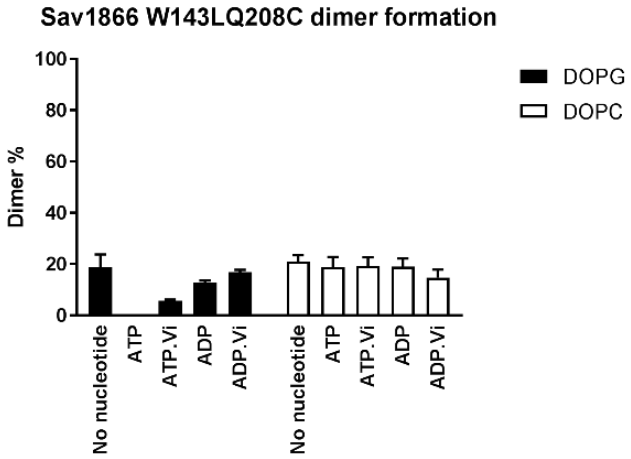

Figure 4.42 Densitometry analysis of crosslinked Sav1866 W143LQ208C reconstituted in DOPG (black bars) and DOPC (open bars) under different nucleotide conditions. The values are presented as a mean of dimer % with respect to the total Sav1866 W143LQ208C protein and error bars represent S.E (n=3). The statistical analysis was performed using a paired t-test. ImageJ software was used for the densitometry analysis of the protein bands.

From Figure 4.39, it is clear that the addition of ATP, ATP.Vi or ADP.Vi did not bring significant changes to the levels of dimers formed (37%) for Sav1866 W143LA281C reconstituted in DOPG, while co-incubation with ADP decreased the level of crosslinked dimers by 7%.

For Sav1866 W143LA281C reconstituted in DOPC, in relation to the nucleotide-free condition (39%), ATP and ATP.Vi decreased the level of dimers formed by 4%, while ADP and ADP.Vi did not change the levels of dimers formed.

From Figure 4.41 and Figure 4.42, Sav1866 W143LQ208C reconstituted in DOPG forms 19% of crosslinked dimers in the absence of nucleotides. Adding ATP does not let the protein form any dimers while ATP.Vi allows ~6% crosslinked dimer formation. ADP and ADP.Vi have a higher % of dimers formed at 13% and 17% respectively.

For Sav1866 W143LQ208C reconstituted in DOPC, the effect of the nucleotides is not significant. Co-incubation with ADP.Vi reduces the level of dimers by 6%, while the changes in levels of dimers caused by ATP, ATP.Vi and ADP is less than 3% compared to the nucleotide-free condition.

4.3.2.5 Sav1866 W243YA281C and Sav1866 W243YQ208C

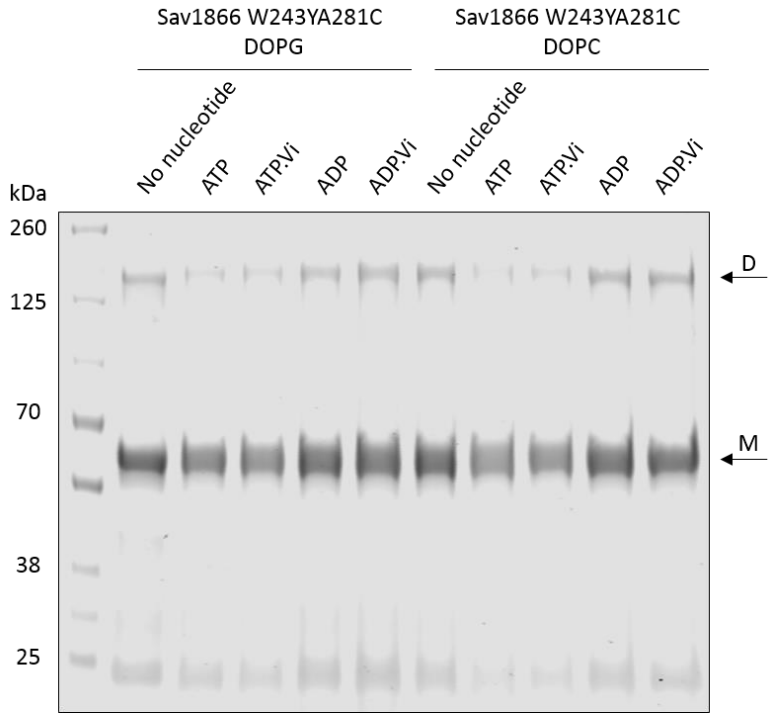

Figure 4.43 Crosslinking of Sav1866 W243YA281C (2 µg) reconstituted in DOPG and DOPC under different nucleotide conditions. InstantBlue Protein stain was used to visualise Sav1866 on the SDS-PAGE gel. The arrows indicate the monomer (M, MW of 67.6 kDa) and the crosslinked dimer (D, MW of 135 kDa) of the protein. 0.5 mM copper phenanthroline was used for the crosslinking reaction as an oxidising agent. The molecular marker is on the left lane in kDa. Experiments were repeated three times with similar results.

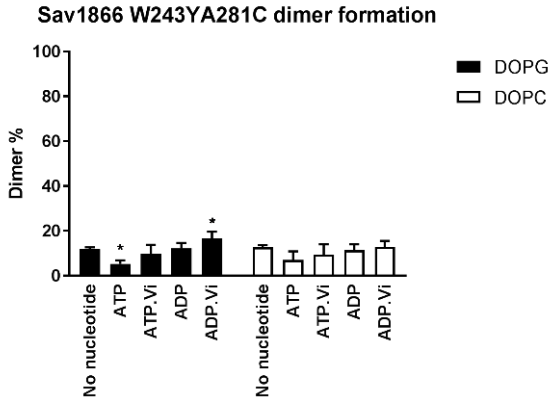

Figure 4.44 Densitometry analysis of crosslinked Sav1866 W243YA281C reconstituted in DOPG (black bars) and DOPC (open bars) under different nucleotide conditions. The values are presented as a mean of dimer % with respect to the total Sav1866 W243YA281C protein and error bars represent S.E (n=3). The statistical analysis was performed using a paired t-test. Asterisk indicates statistically different values between the basal and the nucleotide-induced conditions (*P < 0.05). ImageJ software was used for the densitometry analysis of the protein bands.

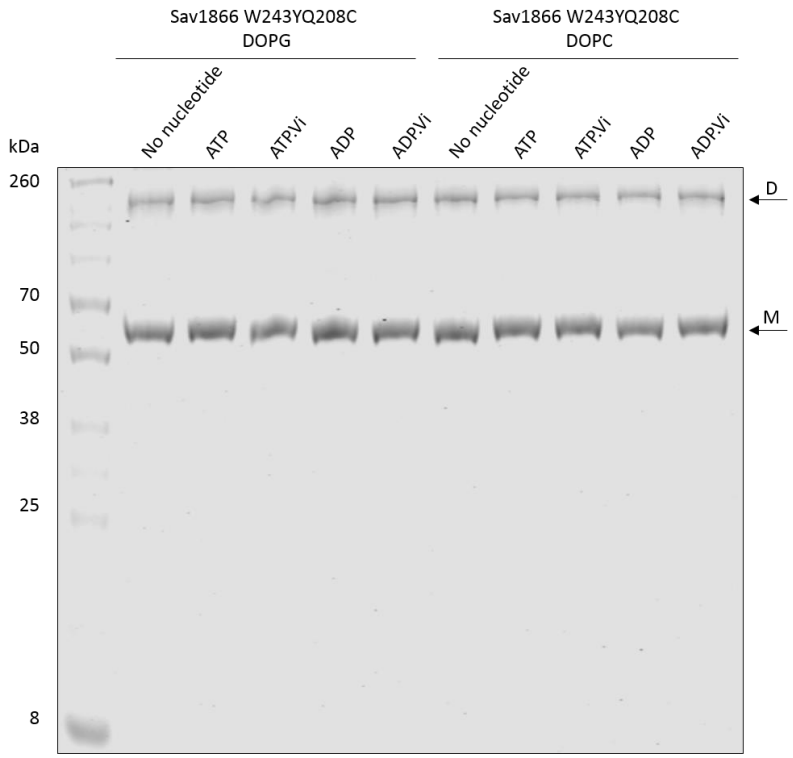

Figure 4.45 Crosslinking of Sav1866 W243YQ208C (2 µg) reconstituted in DOPG and DOPC under different nucleotide conditions. InstantBlue Protein stain was used to visualise Sav1866 on the SDS-PAGE gel. The arrows indicate the monomer (M, MW of 67.6 kDa) and the crosslinked dimer (D, MW of 135 kDa) of the protein. 0.5 mM copper phenanthroline was used for the crosslinking reaction as an oxidising agent. The molecular marker is on the left lane in kDa. Experiments were repeated three times with similar results.

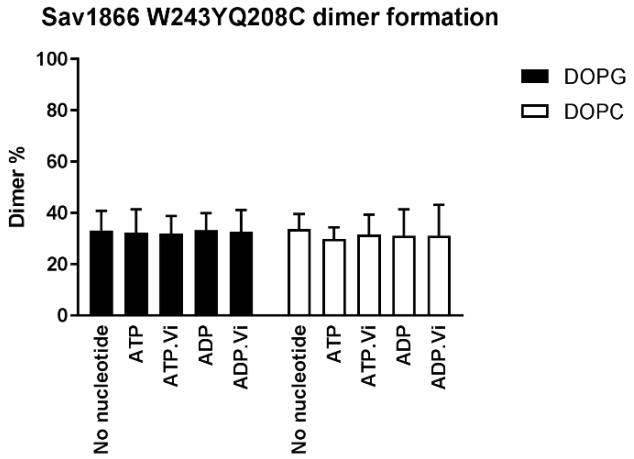

Figure 4.46 Densitometry analysis of crosslinked Sav1866 W243YQ208C reconstituted in DOPG (black bars) and DOPC (open bars) under different nucleotide conditions. The values are presented as a mean of dimer % with respect to the total Sav1866 W243YQ208C protein and error bars represent S.E (n=3). The statistical analysis was performed using a paired t-test. ImageJ software was used for the densitometry analysis of the protein bands.

Sav1866 W243YA281C reconstituted in both DOPG and DOPC form 12% of crosslinked dimers in the absence of nucleotide. Co-incubation with ADP.Vi increases the level to 17% for Sav1866 W243YA281C reconstituted in DOPG, while co-incubation with ATP decreases the dimer level to 5% significantly. Co-incubation with ATP.Vi and ADP have fairly similar levels to nucleotide-free conditions from Figure 4.43 and Figure 4.44.

Sav1866 W243YA281C reconstituted in DOPC did not show significant changes in the presence of nucleotides compared to the nucleotide-free condition.

Sav1866 W243YQ208C reconstituted in both DOPG and DOPC show no response to the addition of nucleotides as no changes in the dimer formation is observed. The level of crosslinked dimers is reasonably constant at 32% as seen in Figure 4.45 and Figure 4.46.

4.3.2.6 Formation of intermediate products

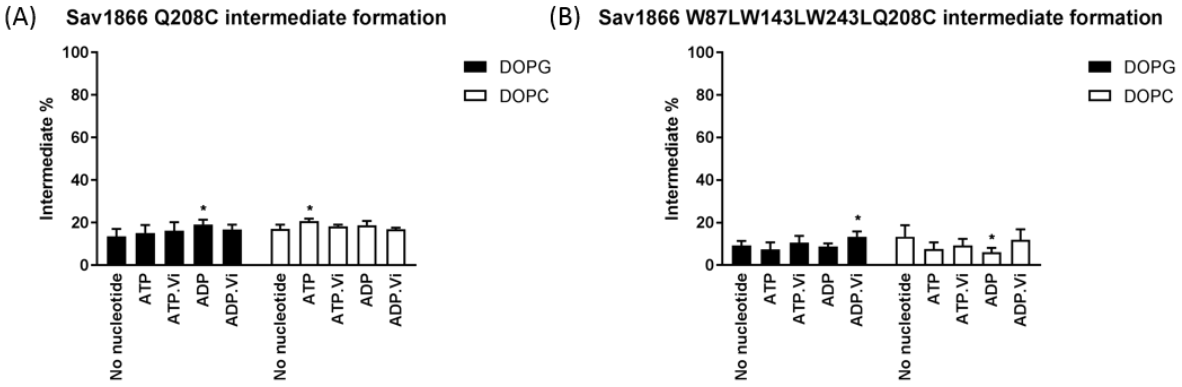

Figure 4.47 Densitometry analysis of the intermediate products formed through the crosslinking of Sav1866 mutants reconstituted in DOPG (black bars) and DOPC (open bars) under different nucleotide conditions. (A) Sav1866 Q208C; (B) Sav1866 W87LW143LW243LQ208C. The values are presented as a mean of dimer % with respect to the total Sav1866 W243YQ208C protein and error bars represent S.E (n=3). The statistical analysis was performed using a paired t-test. Asterisk indicates statistically different values between the basal and the nucleotide-induced conditions (*P < 0.05). ImageJ software was used for the densitometry analysis of the protein bands.

Sav1866 Q208C and W87LW143LW243LQ208C reconstituted in DOPG and DOPC produced intermediate products ~90 kDa in addition to the crosslinked dimers as observed in Figure 4.29 and Figure 4.33. The levels of intermediate formed remained fairly constant under all nucleotide conditions for Sav1866 Q208C reconstituted in DOPG and DOPC. For Sav1866 W87LW143LW243LQ208C reconstituted in DOPC, the addition of ATP and ADP almost halved the levels of intermediate products while ATP.Vi and ADP.Vi showed 4% and 1% decrease respectively. For Sav1866 W87LW143LW243LQ208C reconstituted in DOPG no major changes in the levels of intermediate products were observed upon addition of nucleotides.

4.4 Discussion

The mechanism behind the transport of substrate by ABC transporters and the conformational changes of the protein involved during the process is still an open question. Although crystal structures are available for ABC proteins portraying inward (Hollenstein, Frei, & Locher, 2007; Pinkett et al., 2007) and outward-facing (Dawson & Locher, 2006; Velamakanni et al., 2008) conformations, these structures lack the presence of either substrates or nucleotides, which makes it difficult to have a complete view of the ATPase cycle (Davidson & Maloney, 2007). In addition, the use of detergents to solubilise the proteins and remove the native lipids may have an impact on the protein's conformation (Dawson & Locher, 2006; Pinkett et al., 2007).

To elucidate the mechanism behind the conformational changes, crosslinking experiments using copper phenanthroline as an oxidising agent to oxidise cysteine residues to form disulphide bridges were performed. The cysteine at position 208 at the end of helix four is adjacent to the periplasmic space, so crosslinking at this site would represent an outward-facing dimer. On the contrary, the cysteine at 281 on top of helix 6 is located on the opposite end of the protein closer to the extracellular side of the protein. Therefore, crosslinking at position 281 would represent an inward-facing conformation. Cysteines were introduced to wild-type, single and triple Trp Sav1866 mutants that had varying ATPase activity rates.

The checkpoints of the ATPase cycle, i.e. nucleotide-free, ATP bound, ADP. Pi bound (post ATP hydrolysis), and ADP bound (post ATP hydrolysis and Pi release) (Doshi, Woebking, & van Veen, 2010) were used to check the conformation of Sav1866 at each stage. Vanadate (Vi) is an analogue of inorganic phosphate (Sharma & Davidson, 2000) used to trap ATPase proteins in a post ATP hydrolysis transition state.

4.4.1 Effect of detergents on the crosslinking of Sav1866

Sav1866 in crude membrane, detergent purified and lipid reconstituted Sav1866 were subjected to crosslinking in the presence of nucleotides. Although crude membrane represents a native environment, Sav1866 was expressed in *E.coli.* This meant that Sav1866 was surrounded by lipids that were native to *E.coli* as opposed to *S. aureus*. Despite the difference in lipid composition between the two species, Sav1866 in crude membrane was not exposed to detergents meaning Sav1866 was still left undisturbed in the membrane bilayer.

For Sav1866 in crude membrane, nucleotide-free and ATP binding showed crosslinking signals at Q208C indicating that the two cysteines at 208 are close enough to form a cysteine disulphide

bridge bringing the two NBDs close together. The lack of crosslinking signals (or very little) at position A281C (closer to the periplasmic space) suggests an opening on the periplasmic side between the TMDs and closed NBDs on the cytoplasmic side, forming a V shape, i.e. outward conformation. Such observation agrees with the switch model where the two NBDs come close when ATP molecules bind at the dimer interface forming an outward-facing conformation (Higgins & Linton, 2004).

Conditions representing post ATP hydrolysis, i.e. ATP.Vi, ADP and ADP.Vi binding produced dimeric signals at both positions A281C and Q208C in crude membrane. Previous crystal structures of vitamin B_{12} uptake protein, BtuCD (Korkhov, Mireku, & Locher, 2012) and antimicrobial peptide MccJ25 exporter McjD in the presence of nucleotides have demonstrated an occluded state protein with a cavity in the TMD closed off at the two periplasmic and cytoplasmic ends (Choudhury et al., 2014).

The crosslinking at both periplasmic and cytoplasmic ends at A281C and Q208C respectively in the presence of ATP.Vi, ADP and ADP.Vi suggests a closed structure on either side of the protein. This does not agree with the second part of the ATP switch model; where following ATP hydrolysis, the protein adopts an inward-facing conformation with the separated NBDs creating an open dimer interface (Higgins & Linton, 2004). In this case, the levels of dimers formed for Sav1866 Q208C were higher than for A281C in crude membrane, suggesting that Sav1866 is more likely to adopt an outward-facing conformation than an inward-facing conformation. As a result, Sav1866 in crude membrane maintained a close proximity between the two NBDs throughout the ATPase cycle. Therefore, the crosslinking results suggest a constant contact model.

There is a stark difference between the dimer formations of Sav1866 in crude membrane and purified Sav1866. The levels of dimer formation for purified Sav1866 A281C were higher than for Sav1866 A281C in crude membrane under all nucleotide conditions. On the contrary, purified Sav1866 Q208C had lower levels of dimers formed compared to Sav1866 Q208C in crude membrane. This suggests that the presence of detergents alters the native conformation of the protein in the lipid bilayer. In this case, the presence of detergents has increased the levels of dimers formed for Sav1866 A281C compared to Sav1866 Q208C. Therefore, the protein is more likely to adopt an inward-facing conformation as opposed to the outward-facing conformation observed with Sav1866 in crude membrane. Perhaps, the detergents narrow the gap between TMDs in the periplasmic side, bringing the cysteines at position 281 close enough to form crosslinks.

In the literature, the crystal structures of Sav1866 in the presence of ADP (Dawson & Locher, 2006) and AMP-PNP (Dawson & Locher, 2007), a non-hydrolysable analogue of ATP, showed an outward-facing conformation. Because ADP binding was sufficient for Sav1866 to undertake an ATP bound conformation, i.e. outward-facing, the authors proposed the possible effect of detergents on the equilibrium shift of Sav1866 from inward-facing to outward-facing (Dawson & Locher, 2006, 2007). Moreover, in the presence of lipids, it was suggested that only ATP would create an outward-facing conformation (Dawson & Locher, 2007).

In addition to the differences in crosslinking between crude membrane and purified Sav1866, the outward-facing conformation in the presence of ATP analogue, AMP-PNP, seen in the crystal structure (Dawson & Locher, 2007) could not be replicated with the purified Sav1866 crosslinking. This could be due to the different detergents used for purification affecting the structural features of Sav1866 in different ways. Polyoxyethylene(8)dodecyl Ether ($C_{12}E_8$) was used for purification of the crystallised Sav1866 protein (Dawson & Locher, 2007), and n-Dodecyl-β-D-maltopyranoside (DDM) was used for the crosslinking studies presented here.

Intermediate products were observed in addition to the dimers and monomers for Sav1866 Q208C, W87LW143LW243LQ208C, W143LA281C and W143LQ208C purified proteins. These intermediate products were not present in crude membrane conditions indicating that significant proteolytic products were to be found in purified Sav1866 that could then assemble to form intermediate products.

4.4.2 Effect of anionic vs neutral phospholipids on the crosslinking of Sav1866

ATPase activity rates varied when Sav1866 was reconstituted in anionic and neutral lipids (discussed in Chapter 5). However, there was no apparent difference in crosslinks formed between Sav1866 mutants reconstituted in DOPC and DOPG. This suggests that the difference in the lipid head group does not necessarily affect the conformation of the protein. Hence, it is unlikely that the difference in the ATPase activity of Sav1866 reconstituted in lipids is due to the lipid influencing the conformation of the protein. Alternatively, the crosslinking method is not sensitive enough to observe the conformational changes when Sav1866 is reconstituted in lipid bilayers.

The levels of dimers formed for both Sav1866 A281C and Q208C in DOPC and DOPG were comparable in the presence and absence of nucleotides. It is not clear whether the protein adopts an outward-facing or an inward-facing conformation. There may be the possibility that the protein

is more likely to adopt an occluded state (closed on the periplasmic and cytoplasmic side) in the presence and absence of nucleotides.

The likelihood of Sav1866 to adopt an outward-facing conformation when in crude membrane (as discussed earlier) was not reflected by Sav1866 reconstituted in either DOPC or DOPG. This may be due to the difference in lipid composition between the *E.coli* membrane that contains 20% phosphatidylglycerol, 5% cardiolipin and 75% phosphatidylethanolamine (Huijbregts et al., 2000; Raetz, 1978) and the lipids used for reconstitution in this study. Alternatively, lipid reconstitution was not able to restore the native environment for the protein due to the detergent solubilisation in the purification process.

4.4.3 Monitoring the structural stability of Sav1866 mutants using crosslinking studies

Crosslinking reactions were performed on multiple Sav1866 Trp mutants with varying rates of ATPase activity (discussed in Chapter 3). Sav1866 W87Y and W243Y were active while Sav1866 W87LW143LW243L and W143L were inactive. Conditions that were tested included nucleotide-free and presence of ATP and ATP.Vi. For mutants with no ATPase activity, any conformational changes in response to the nucleotides would indicate correct folding of the mutant protein and a close resemblance to the native conformation of Sav1866.

4.4.3.1 Active Sav1866 mutants

The ATPase activity results of Sav1866 W87Y and W243Y from Chapter 3 suggest that the mutant proteins are folded correctly in order to hydrolyse ATP. In this section, crosslinking between cysteines at either 281 or 208 is used to elucidate the mechanism behind the difference in the ATPase rates between the wild-type Sav1866 and the mutants.

4.4.3.1.1 Sav1866 W87YA281C and Sav1866 W87YQ208C

For the active Sav1866 W87YA281C mutant in crude membrane in Figure 4.15, the levels of dimers formed in the presence and absence of nucleotides were slightly higher than for Sav1866 A281C (Figure 4.7). Similarly, Sav1866 W87YQ208C in crude membrane (Figure 4.17) had higher levels of dimers than Sav1866 Q208C (Figure 4.9). This suggests that despite the mutant retaining its ATPase activity, there are differences in the dimer formation compared to Sav1866 A281C and Q208C, which are the closest resemblances of the wild-type Sav1866.

As the levels of dimers formed for Sav1866 W87YQ208C are higher than for Sav1866 W87YA281C in crude membrane, it is possible that the mutant is more likely to form an outward-facing conformation under the nucleotide-free condition and in the presence of ATP and ATP.Vi.

For purified Sav1866 W87YA281C (Figure 4.15) and Sav1866 W87YQ208C (Figure 4.17), the levels of dimers formed are comparable. This suggests that the purified protein is likely to adopt an occluded state in the absence and presence of nucleotides.

There was no difference in the levels of dimers formed between DOPC and DOPG lipid reconstitution (Figure 4.36 and Figure 4.38) suggesting that the difference in the head groups did not have any significant changes to the protein's conformation. In addition, the levels of dimers formed during the lipid reconstitutions were less than in crude membrane and purified protein. This suggests that the lipid reconstitution inhibits the protein's ability to form dimers compared to purified proteins and protein in crude membrane.

Nevertheless, the significant increase in the level of dimers in the presence of ATP.Vi in Sav1866 A281C in crude membrane was also observed with Sav1866 W87YA281C in crude membrane (although the difference in dimer levels between the nucleotide-free condition and co-incubation with ATP.Vi was insignificant). This suggested that the Sav1866 W87YA281C mutant retained a native folding similar to the wild-type.

4.4.3.1.2 Sav1866 W243YA281C and Sav1866 W243YQ208C

For the active Sav1866 W243Y mutant in crude membrane, in the absence of nucleotides and ATP bound state, the protein is likely to adopt an outward-facing conformation due to high levels of crosslinking at Sav1866 W243YQ208C (Figure 4.25), correlating with the ATP switch model (Higgins & Linton, 2004). However, post ATP hydrolysis, both Sav1866 W243YA281C (Figure 4.23) and Sav1866 W243YQ208C showed similar levels of crosslinks, suggesting an occluded state conformation.

For purified Sav1866 W243Y (Figure 4.23 and Figure 4.25), higher levels of dimers were observed for Sav1866 W243YQ208C, suggesting an outward-facing conformation under the nucleotide-free condition and in the presence of ATP and ATP.Vi.

Lipid reconstitution of Sav1866 W243Y (Figure 4.44 and Figure 4.46) produced similar levels of dimers between DOPC and DOPG reconstituted proteins suggesting no direct influence of the lipid head groups on the conformation of the protein. However, higher levels of dimers formed for

Sav1866 W243YQ208C suggest an outward-facing conformation under the presence and absence of nucleotides.

The significant increase in the level of dimers in the presence of ATP.Vi in Sav1866 A281C compared to the nucleotide-free condition in crude membrane was also observed with Sav1866 W243YA281C in crude membrane, which suggests that the mutant retained a native folding similar to the wild-type.

4.4.3.2 Inactive Sav1866 mutants

Sav1866 W143L and W87LW143LW243L lost their ATPase activity as discussed in Chapter 3. Using crosslinking studies, the conformational changes of the mutants in response to nucleotides would indicate correct folding of the mutants. Therefore, despite losing the ability to hydrolyse ATP, crosslinked dimers of the mutants suggest that they still retain native structure in order for the cysteines to be in close proximity to form dimers.

4.4.3.2.1 Sav1866 W143LA281C and Sav1866 W143LQ208C

For the inactive mutant, Sav1866 W143L (Figure 4.19 and Figure 4.21), nucleotide-free condition and ATP binding caused the protein to adopt an outward conformation in crude membrane. In the presence of ATP.Vi, however, the protein formed crosslinks at 281 cysteines, albeit, the level was approximately half of crosslinks at 208 cysteines. Therefore, it is not clear whether the mutant forms an outward-facing conformation or adopts and occluded state conformation in the presence of ATP.Vi. The changes in the conformation observed in response to ATP.Vi suggests that the protein still retains its native conformation despite losing its ability to hydrolyse ATP. This is due to a similar effect seen in the Sav1866 A281C in the presence of ATP.Vi as discussed previously.

For purified Sav1866 W143L (Figure 4.19 and Figure 4.21), similar levels of crosslinks at either side of the protein suggest that the protein adopted an occluded state conformation in the absence of nucleotides, ATP and ATP.Vi bound conditions. The lack of changes in the conformation for purified Sav1866 W143L would suggest that the protein is no longer able to respond to the presence of nucleotides as observed with when in crude membrane. This could suggest that the protein is locked in its occluded state conformation and so, cannot alter its conformation possibly due to the presence of detergents.

Lipid reconstitutions did not have any distinct effects on the dimer formation except for Sav1866 W143LQ208C (Figure 4.42) in the presence of ATP, where no dimers were formed when reconstituted in DOPG compared to 20% for when in DOPC. Presence of ATP.Vi and ADP also

produced less dimers for Sav1866 W143LQ208C in DOPG than in DOPC. Overall, the levels of dimers formed were higher for Sav1866 W143LA281C (Figure 4.40) in both DOPC and DOPG, suggesting that the mutant is more like to form an inward-facing conformation when reconstituted in lipids.

The difference in the levels of dimers formed for Sav1866 W143L in crude membrane, purified and reconstituted conditions highlights the variable effects of detergents, native lipids and synthetic lipids on the protein.

4.4.3.2.2 Sav1866 W87LW143LW243LA281C and Sav1866 W87LW143LW243LQ208C

For the second inactive mutant, Sav1866 W87LW143LW243L (Figure 4.11 and Figure 4.13), in the absence of nucleotides and ATP bound, the mutant adopted an outward conformation in crude membrane due to the crosslinks formed at Q208C. In the presence of ATP.Vi the mutant is likely to adopt an occluded state due to the crosslinks at either side of the mutant. There was a significant difference between the nucleotide-free condition and the presence of ATP, suggesting that the protein is able to undergo conformational changes in response to ATP. In addition, an increase in the level of dimers in the presence of ATP.Vi compared to the nucleotide-free condition indicates a native folding for the mutant due to a similar effect observed for the wild-type.

For purified Sav1866 W87LW143LW243L (Figure 4.11 and Figure 4.13), crosslinking at both A281C and Q208C sites suggested an occluded state conformation. The difference in crosslinks between the nucleotide-free condition and the presence of ATP or ATP.Vi observed for the mutant in crude membrane was not seen for purified Sav1866 W87LW143LW243L, suggesting that the protein lost the ability to change conformations in response to the nucleotides probably due to the detergents. This may be due to the protein being in a locked conformation preventing it from undertaking either inward-facing or outward-facing conformation.

The effect of lipid reconstitution showed comparable results between DOPC and DOPG. Similar levels of dimers were formed between Sav1866 W87LW143LW243LA281C (Figure 4.32) and Sav1866 W87LW143LW243LQ208C (Figure 4.34), suggesting an occluded state when reconstituted into lipids.

4.5 Conclusion

The crosslinking study was adopted as a method to investigate the folding of the inactive mutants by comparing them to the wild-type Sav1866. The increase in the crosslinked dimers in the presence of ATP.Vi compared to the nucleotide-free condition in Sav1866 A281C (representing the wild-type) in crude membrane was observed for the active and inactive mutants too. This suggests that the protein's inability to hydrolyse ATP does not necessarily mean that it is incapable of binding to ATP and can undergo a conformational change as a consequence.

The results obtained from my crosslinking data has shed some light into the conformation of Sav1866 at various stages of the ATPase cycle. Under the nucleotide-free condition and the binding of ATP, Sav1866 has an outward-facing conformation in crude membrane. Upon ATP hydrolysis, i.e. ATP.Vi, ADP and ADP.Vi bound state, the protein is likely to shift to an occluded conformation, suggesting a constant contact model.

Use of detergents to solubilise Sav1866 and purify the protein had a profound effect on the conformation of the protein. The crosslinking data obtained from the purified Sav1866 protein suggested an inward facing conformation or possibly an occluded state under the nucleotide-free condition and in the presence of nucleotides. The difference in the results suggested the role of detergents in changing the state of conformation of Sav1866. In addition, the disparity in conformation between the published crystal structure of Sav1866 (Dawson & Locher, 2007) and the crosslinking data obtained here demonstrates the variable effects of different detergents.

The crosslinking data highlights the difference in conformation between Sav1866 in native environment and Sav1866 reconstituted in lipids. This suggests that the use of detergents and the following reconstitution of the protein into defined lipid composition do not reflect native conditions. In addition, the difference in the lipid head group did not have any major effect on the conformation of the protein. Therefore, the variation in the ATPase activity of Sav1866 reconstituted in neutral and anionic phospholipids is possibly not due to the change in conformation of the protein.

Crosslinking is a useful technique to study a protein's conformation under various conditions. Due to the lack of any ligands in the reaction, the crosslinking data presented here corresponds to a futile ATPase cycle, i.e. ATPase activity in the absence of ligands. There is a possibility that in the presence of ligands, Sav1866 conformation would be different to a ligand-free system.

Chapter 5 Effect of lipid head groups on ABC transporters

5.1 Introduction

The evidence for the influence of membrane lipid composition on the orientation and function of membrane proteins is compelling (Lange et al., 2001; A. M. Powl et al., 2005; W. Zhang et al., 2005). However, it remains to be investigated whether the modulatory influence of certain lipids on membrane protein function is widespread or confined to a few notable examples. There is evidence that the ABC transporter, P-glycoprotein, which contributes towards drug resistance in cancer treatment, is modulated by lipid distribution in the plasma membrane (Elliott et al., 2005). Therefore, it is of interest to examine the relationship between ABC transporter and lipids and analyse potential lipid binding sites on these proteins. This could be of value in identifying druggable targets on P-glycoprotein, to inhibit their activity.

Membrane lipids and proteins must have co-evolved to support membrane protein function and stability (A. G. Lee, 2003). Much of our understanding on lipid-protein interactions have come from structural studies of membrane proteins that include lipid molecules bound to the protein (McAuley et al., 1999; Zhou, Morais-Cabral, Kaufman, & MacKinnon, 2001). A recent example was the high-resolution structure of an antibacterial peptide ABC transporter, McjD with a bound lipid molecule (Mehmood et al., 2016). The refined lipid structure was modelled as a phosphatidylglycerol (PG) molecule between transmembrane domains 3 and 4. However, because a phosphatidylethanolamine (PE) molecule can also be refined within the electron density, there is a possibility that the lipid molecule could be a PE (Mehmood et al., 2016). In this study, the lipid binding site on McjD is studied using a fluorescence quenching method previously described in (East & Lee, 1982). The binding site predicted from the crystal structure (Choudhury et al., 2014; Mehmood et al., 2016) is accommodated by a cluster of positively charged residues containing arginine residues at positions 186 and 311 on the cytoplasmic side of McjD (Figure 5.1). Therefore, an anionic lipid binding is predicted for the site.

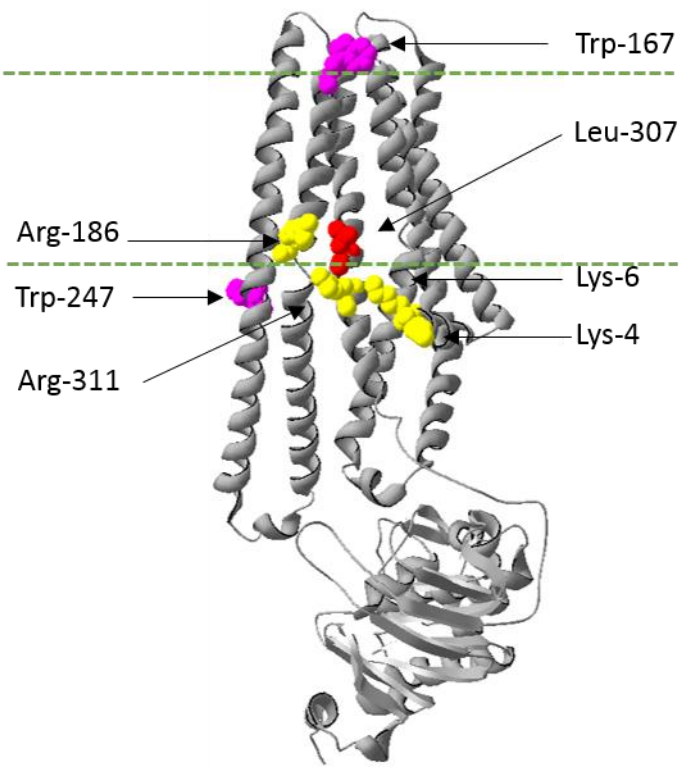

Figure 5.1 Schematic representation of McjD monomer (PDB: 5EG1). The endogenous Trp-167 (periplasmic side) and Trp-247 (cytoplasmic side), a positive cluster of Arg-186, Arg-311, Lys-6 and Lys-4 residues, and Leu-307, which was mutated to a reporter Trp-307 are shown. The dotted lines represent the extent of the lipid bilayer of the cell membrane. Figure is edited using Swiss-PdbViewer software (4.1.0).

Anionic lipid binding on Sav1866 was investigated using the fluorescence quenching technique. However, no specific binding for anionic lipids was observed for the protein (data not shown). The biological membrane of *S. aureus* contains 57% lysyl phosphatidylglycerol (Pasupuleti et al., 2012), which is a positively charged (cationic) phospholipid, not found in eukaryotic membranes. In addition, *S. aureus* membranes contain virtually no neutral lipids. Alternatively, McjD from *E.coli*, which has a membrane lipid composition (20% PG, 5% cardiolipin (CL) and 75% PE (Huijbregts et al., 2000; Raetz, 1978)) similar to eukaryotic membranes in terms of neutral and anionic lipids (Van Meer et al., 2008), was studied.

5.1.1 Alternative methods of membrane protein purification using styrene maleic acid (SMA)

Over 50% of available drugs in the market target membrane proteins (Saeui, Mathew, Liu, Urias, & Yarema, 2015), which are encoded by over 20% of human and *E.coli* genome code (Almén, Nordström, Fredriksson, & Schiöth, 2009; Lander et al., 2001). Due to the difficulties associated

with the purification process, less than 1% of the available structures in the protein data bank is of membrane proteins (Berman et al., 2000). Detergents have been commonly used for purifying membrane proteins; they disrupt the membrane at concentrations above their critical micelle concentration (CMC). Their amphipathic nature allows them to form soluble micelles with proteins shielded by the detergents' hydrophobic tails (le Maire, Champeil, & Moller, 2000). Detergent solubilisation of membrane proteins often affects their structure or function depending on the type of detergent. Generally, non-ionic detergents are milder than ionic detergents but are less efficient at solubilising proteins. Similarly, other types of detergents (zwitterionic, bile acid salts) have their strengths and weaknesses (Seddon, Curnow, & Booth, 2004). As there is not a single universal detergent that can solubilise the variety of membrane proteins efficiently, often a thorough screen is required for the best yield and purity (Arachea et al., 2012). This is both time consuming and often quite costly. Moreover, detergents strip off most of the native lipids attached to the protein, which has a serious impact on the conformation and the function of the protein (Bordag & Keller, 2010).

More recently a radically different mechanism involving styrene maleic acid (SMA) for isolating membrane proteins from their native membrane while retaining contacts with adjacent lipids has been developed (Knowles et al., 2009). SMA is a synthetic copolymer with hydrophilic maleic acid and hydrophobic styrene moieties. The radical polymerisation of maleic anhydride and styrene forms styrene maleic anhydride, which is hydrolysed to its acidic form, styrene maleic acid (Dörr et al., 2016). The distribution of the monomer is not always alternating as styrene radical tends to react with another styrene or maleic anhydride, whereas maleic anhydride radical can only react with another styrene molecule (Hill, O'Donnell, & O'Sullivan, 1985). Therefore, the end product is not all of the same length or heterogeneity.

The amphipathic nature of SMA destabilises lipid bilayers and extracts membrane proteins forming SMA lipid particles (SMALPs) (Tonge & Tighe, 2001). Since SMA does not strip any lipids associated with the protein, it preserves the native annular lipids surrounding the protein (Xue, Cheng, Faustino, Guo, & Marrink, 2018) providing potential insight into the nature of the roles these special lipids.

Purification of membrane proteins using SMA has been very successful with a wide variety of proteins such as G protein-coupled receptors (Wheatley et al., 2016), AcrB (Postis et al., 2015) and potassium channels (Dörr et al., 2014). The biggest protein complex (464 kDa) purified using SMA is complex III of the electron transport chain (Sun et al., 2018). SMA also supports a variety of biochemical techniques such as circular dichroism, analytical ultracentrifugation (Knowles et al.,

2009), nuclear magnetic resonance (Bersch, Dorr, Hessel, Killian, & Schanda, 2017; Puthenveetil, Nguyen, & Vinogradova, 2017), crystallography (Broecker, Eger, & Ernst, 2017) and cryo-electron microscopy (Parmar et al., 2018). However, SMA has its limitations. SMA is only functional above pH 6.5 and does not tolerate millimolar concentrations of divalent cations such as magnesium and calcium. The latter can be problematic for biochemical assays such as the ATPase activity assay that requires magnesium ions (Rule, Patrick, & Sandkvist, 2016). The encapsulation of proteins in its lipid shell by SMA may also restrict changes in conformation (Stroud, Hall, & Dafforn, 2018).

Among the commercially available SMA polymers, SMA 2000, which is a 2:1 styrene to maleic acid ratio, has been shown to be most effective in terms of solubilisation, purification yield and purity (Morrison et al., 2016).

In this chapter, Sav1866 and McjD are purified using SMA and the benefits and disadvantages of the approach over the use of detergents are discussed.

5.2 Methods

5.2.1 Construction of plasmids

The construction of plasmid vectors with *mcjD* gene has been described in section 2.2.2. Site-directed mutagenesis was used to introduce mutations in *mcjD*. All the mutagenic oligonucleotides have been listed in Table 5.1, and the mutated site has been underlined.

Mutation		**Primer sequence 5'-3'**
W167Y	Forward	ATCTACGAAGGACTACTTTTCTGCCGGTGTGTTTTTTCTC
	Reverse	AAAACACACCGGCAGAAAAGTAGTCCTTCGTAGATAAAAC
W247Y	Forward	AATGCTCAGAAAAAATACTACTTACTCAGTTCTAAAGTTC
	Reverse	AGAACTGAGTAAGTAGTATTTTTTCTGAGCATTGTTTTCC
L307W	Forward	GTGGAAAATATAGGGGCATTGTGGAGTGAGATCAGGCAGTCAATG
	Reverse	CATTGACTGCCTGATCTCACTCCACAATGCCCCTATATTTTCCAC
R186Q	Forward	TTGTAATTTTTAACACCCAACTGACTGGCAGTTTAGCGTC
	Reverse	AGTCAGTTGGGTGTTAAAAATTACAAATACCAGAATATAG
R311Q	Forward	GGGCATTGTGGAGTGAGATTCAGCAGTCAATGTCTAGCCTGGCAG
	Reverse	AGACATTGACTGCTGAATCTCACTCCACAATGCCCCTATATTTTC

Table 5.1 Synthetic oligonucleotides used for QuickChange™ site-directed mutagenesis The sites used to create mutations in *mcjD* are underlined.

5.2.2 Transformation of DH5α cells and BL21 (λDE3) pLysS cells

The protocol for transformation of DH5α cells and BL21 (λDE3) pLysS cells is described in the General materials and methods section 2.2.3.

5.2.3 Protein expression and purification

The protocol for the purification of McjD has been outlined in the General Materials and Methods section 2.2.5.

For the purification of Sav1866 protein, the buffer contained phosphate buffered saline, PBS (137 mM sodium chloride, 2.7 mM potassium chloride and 11.9 mM phosphate). The protocol for the purification is described in 2.2.5.

5.2.3.1 Removal of GFP tag from pWaldo-GFPd-McjD

Following the elution of His-tagged McjD from the His-Trap column, the protein eluate was dialysed in 3L of dialysis buffer (20 mM Tris, 150 mM NaCl, 0.03% DDM) containing 30 µl of TEV protease (10 KU/ml) overnight in the cold room at 4˚C.

5.2.4 Preparation of styrene maleic acid copolymer from styrene maleic anhydride copolymer

25 g of styrene maleic anhydride copolymer was weighed and transferred to a 500 ml round-bottom flask in the fume hood. 250 ml of 1 M NaOH was added to the round-bottom flask with 0.5 g of anti-bumping granules. The round-bottom flask was connected to a condenser coil, with water flowing through and heated using a heating mantle. The solution was maintained at a steady boil for two hours. The refluxed solution was allowed to cool down at room temperature with the water flowing through the condenser before being divided into two aliquots in 500 ml centrifuge bottles. The polymer was precipitated using concentrated HCl until the pH was less than 5. MilliQ water was added to the precipitated polymer to fill the centrifuge bottle to its maximum volume. The polymer was then centrifuged at 11,000 g at room temperature for 15 minutes. The supernatant was removed, and the pellet was resuspended in MilliQ water by vigorously shaking the centrifuge bottle. The polymer was recentrifuged at 11,000 g at room temperature for 15 minutes. The supernatant was removed, and the pellet was resuspended in MiliQ water, which was then centrifuged at the same speed. This step was repeated two times. 125 ml of 0.6 M NaOH was added to the pellet and incubated at 37˚C at 180 rpm until the pellet was dissolved completely. Once the pellet was dissolved, the polymer was precipitated using concentrated HCl as earlier and the following steps were repeated. After the second dissolving of the pellet in 0.6 M NaOH, the pH was adjusted to ~8.0 using concentrated HCl or NaOH. Finally, the solution was transferred to a 1 L round-bottom flask and frozen at -20˚C for 18 hours. The flask was covered with poly-net and allowed to freeze dry until the polymer was dried to a powder. The polymer was stored at room temperature.

5.2.5 Protein extraction and purification using styrene maleic acid (SMA)

Following the same protocol as described above in section 2.2.5.1 for protein expression, the cell pellet was resuspended in homogenisation buffer (50 mM Tris pH 8.0, 500 mM NaCl, 0.5 mM

EDTA and SigmaFast Protease Inhibitor Tablets) using 10 ml of homogenisation per 1 g of cell pellet. The homogenised solution was passed through the C3 lysis device at 35 kPa, 3 times at 4˚C to break open the cells. Then, unbroken cells and organelles were removed from the lysate by centrifugation at 12,000 g for 20 minutes at 4˚C. The supernatant was then recentrifuged at 100,000 g for 45 minutes to isolate the crude membranes. The membrane pellet was then re-suspended in 20 mM Tris, 150 mM NaCl, 2.5 % SMA (kind gift of Prof Dafforn, University of Birmingham), using 1 ml of buffer per 40 mg of membrane. The mixture was incubated at room temperature for 90 minutes on a rocking platform.

5.2.5.1 His-tag affinity chromatography

After the resuspension of the membrane in SMA buffer, the mixture was centrifuged at 100,000 g at 4˚C for 25 minutes. The SMA soluble material (supernatant) was passed through a His-Trap column overnight at 4˚C. The following day, the column was washed with 10 CV wash buffer (20 mM Tris pH 8, 150 mM NaCl) followed by further 5 CV of wash buffer with 20 mM imidazole. Finally, the protein was eluted using 500 mM imidazole.

5.2.5.2 Size exclusion chromatography

The eluted protein was further purified by size exclusion chromatography (SEC) using a Superdex increase 10/300 column (GE Healthcare) at 1 ml/min. The equilibration buffer (filtered and degassed prior to use) was the same as the wash buffer without the imidazole.

5.2.6 ATPase activity assay

See 2.2.10 under General Materials and Methods section.

5.2.7 Lipid preparation

Preparation of synthetic lipids has been described in section 2.2.11.

To prepare a brominated lipid, bromine was added drop-wise to the lipid suspended in chloroform until the suspension turned a pale yellow colour. The solvent was dried under nitrogen first followed by a vacuum desiccator overnight. The brominated lipid was then adjusted to a 20 mg/ml solution, sealed under nitrogen and stored at -20˚C.

5.2.8 Lipid reconstitution

See 2.2.12 for the protocol.

5.2.9 Fluorescence quenching assay

50 µl of protein-lipid sample prepared using the protocol described in section 2.2.12 was added to 2.95 ml of 20mM Hepes (pH 7.2), 1 mM EGTA buffer (final protein concentration 0.2 µM). Fluorescence measurements were observed using an SLM 8000C fluorimeter with excitation at 295 nm at 25˚C.

Fluorescence quenching analysis was based on the lattice model of quenching, where the level of quenching is proportional to the probability of a brominated lipid to occupy a lattice close to the site of tryptophan (Trp) residue (O'Keeffe, East, & Lee, 2000).

In a mixture of lipids, the mole fraction of brominated lipids is represented by x_{Br}. Therefore, the probability for any sites on the protein not to be occupied by a brominated lipid is given by 1 - $x_{Br.}$

The probability that a Trp residue will fluoresce is proportional to the probability that the lattice sites are not occupied by brominated lipid to quench its fluorescence. This is described in equation 1 below.

$$F = F_{min} + (F_0 - F_{min}) * (1 - x_{Br})^n \qquad \text{Equation 1}$$

F_0 = Fluorescence intensity of protein in non-brominated lipid

F_{min} = Fluorescence intensity of protein in brominated lipid

F = Fluorescence intensity of protein in the lipid mixture

The lattice model can be further explained by the equilibrium equation below, where P is the protein and L and Q are non-brominated and brominated lipids respectively with different affinities of binding to P.

$$\mathrm{PL} + \mathrm{Q} = \mathrm{PQ} + \mathrm{L}$$

The equilibrium constant K for the equilibrium can be written as

$$K = \frac{[PQ] * [L]}{[PL] * [Q]} \qquad \text{Equation 2}$$

Where K is the binding constant for the brominated lipid Q in relation to the non-brominated lipid L. Now, the fluorescence quenching equation can be fitted to equation 3.

$$F = F_{min} + (F_0 - F_{min}) * (1 - f_{Br})^n$$ Equation 3

f_{Br} = fraction of sites at the lipid-protein interface that is occupied by brominated lipid. f_{Br} can be related to x_{Br} by the following equation.

$$f_{Br} = \frac{K x_{Br}}{K x_{Br} + [1 - x_{Br}]}$$ Equation 4

5.3 Results

5.3.1 Expression and purification of McjD

The original construct of McjD contained a GFP-octahistidine affinity tag at the C terminus with a TEV cleavage site prior to the GFP tag. Expression and purification of this construct produced a low yield of McjD protein (data not shown). Besides, it was challenging to remove the GFP tag using the TEV protease to cleave at the TEV cleavage site (data not shown). Therefore, the GFP tag was removed from the DNA construct using the method described in 2.2.2.2. The new construct of McjD without the GFP tag improved the expression and purification of the protein.

A new reporter Trp at position 307 (McjD W167Y:W247Y:L307W) was placed close to the phospholipid binding site on McjD, predicted from the crystal structure (Choudhury et al., 2014; Mehmood et al., 2016) as shown in Figure 5.1. Prior to this, the two endogenous Trps at positions 167 and 247 were removed and replaced with tyrosines (Tyr). An alternative reporter Trp, within the same binding site vicinity, was placed at position 182 (McjD W167Y:W247Y:I182W) in a similar manner. The positive arginine residues were later mutated individually to neutral glutamine (McjD W167Y:W247Y:L307W:R186Q and McjD W167Y:W247Y:L307W:R311Q) to study any alterations in the binding of anionic phospholipids on McjD.

5.3.2 Reconstitution of Sav1866 and McjD into defined lipid bilayers

Following purification of Sav1866 and McjD using detergents as described in 5.2.3, they were reconstituted into bilayers of defined lipid composition. An excess amount of lipids in buffer with cholate was added to the protein in 100:1 molar ratio of phospholipid to protein monomer, which was further diluted in more buffer (20 fold) to reduce the concentration of cholate below its CMC level. This allowed the formation of unsealed membrane fragments (Williamson, Alvis, East, & Lee, 2002).

The lack of any significant alteration in the maximum emission wavelength for the Trp residues in the McjD mutants (discussed in 5.3.5.2) suggested that the mutations did not cause any major disruption to the conformation of McjD, and that the proteins had reconstituted into the lipid bilayers successfully.

Previous membrane protein studies with Ca^{2+}ATPase (Caffrey & Feigenson, 1981; East & Lee, 1982; Starling, East, & Lee, 1993), Na^{+}, K^{+} ATPase (Cornelius, 2001) and rhodopsin (Baldwin & Hubbell, 1985) all showed highest level of activities in bilayers containing phospholipids with 18 carbon fatty acyl chains. Therefore, in this study, phospholipids with 18 carbon chains were used.

5.3.3 Basal ATPase activity of Sav1866 reconstituted in phospholipid bilayers

The effect of phospholipids with different head groups and charges on the basal ATPase activity of Sav1866 was examined by reconstituting the protein into defined lipid composition. The basal ATPase activity was tested using a coupled enzyme reaction where the absorbance of NADH was measured at 340 nm, which correlated to the hydrolysis of ATP by the protein (Technikova-Dobrova, Sardanelli, & Papa, 1991). Sav1866 was reconstituted in the following phospholipids to measure the ATPase activity.

- Anionic phospholipids
    - 1,2-dioleoyl-sn-glycero-3-phosphate (di(C18:1) PA)
    - 1,2-dioleoyl-sn-glycero-3-phospho-(1'-rac-glycerol) (di(C18:1) PG)
    - 1',3'-bis[1,2-dioleoyl-sn-glycero-3-phospho] -glycerol (tetra(C18:1) CL)
- Neutral phospholipids
    - 1,2-dioleoyl-sn-glycero-3-phosphoethanolamine (di(C18:1) PE)
    - 1,2-dioleoyl-sn-glycero-3-phosphocholine (di(C18:1) PC)
- Cationic phospholipids
    - 1,2-dioleoyl-sn-glycero-3-ethylphosphocholine (di(C18:1)EPC)
    - 1,2-dioleoyl-sn-glycero-3-[phospho-rac-(3-lysyl(1-glycerol))] (di(C18:1)lysyl PG)

Figure 5.2 shows that the basal ATPase activity of Sav1866 reconstituted in phosphatidylcholine (PC) was the highest at 1.49 ± 0.03 µmol ATP/mg/min. Reconstituting Sav1866 in a phospholipid mix containing 0.25 mole fraction of anionic phospholipids mixed with PC caused a significant reduction in its ATPase activity lowering the rate to 0.38 ± 0.01 µmol ATP/mg/min by cardiolipin (CL), 0.68 ± 0.01 µmol ATP/mg/min by phosphatidylglycerol (PG) and 0.82 ± 0.02 µmol ATP/mg/min by phosphatidic acid (PA). The activity rate was reduced further at higher mole fractions of anionic phospholipids with the lowest rate of 0.04 ± 0.02 µmol ATP/mg/min by 100% PG.

The rate of ATP hydrolysis for Sav1866 reconstituted in cationic lipids, ethyl phosphocholine (EPC) and lysyl PG was 40% less than in PC. In mixtures of EPC and PC, there was little variation in the ATPase rate. However, in mixtures of lysyl PG and PC, the ATPase rate decreased with respect to increase in lysyl PG up to 0.75 mole fraction. Reconstitution in neutral phosphatidylethanolamine (PE) caused a 76% decline in activity compared to in PC. In mixtures of PE and PC, the ATPase rate decreased uniformly with an increase in PE content.

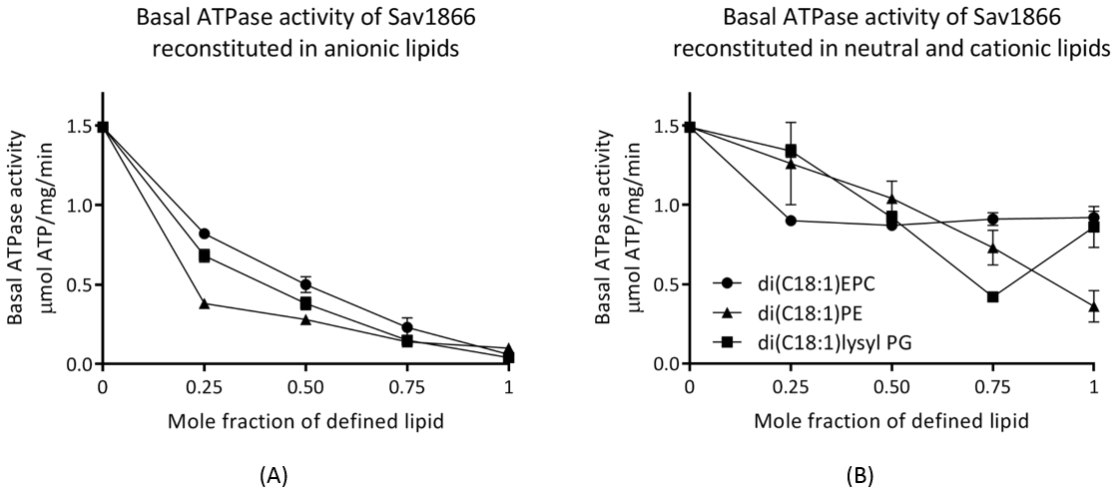

Figure 5.2 Basal ATPase activity of Sav1866 reconstituted in bilayers of defined lipid composition. Sav1866 (100 µg) was reconstituted into bilayer mixtures containing 0.6 µmol of di(C18:1)PC and increasing mole fractions of the defined phospholipids; (A) anionic (●) di(C18:1)PA, (■) di(C18:1)PG, (▲) tetra(C18:1)CL; (B) neutral and cationic (●) di(C18:1)EPC, (■) di(C18:1)lysyl PG, (▲) di(C18:1)PE. The ATPase activity was monitored quantitatively using the oxidation of NADH to NAD^+ measured at 340nm, which was coupled to the hydrolysis of ATP by Sav1866 in an enzyme coupled reaction. Data points represent an average of at least three independent experiments, and the error bars show the standard deviation.

5.3.4 Basal ATPase activity of McjD wild-type and mutants reconstituted in anionic and neutral phospholipid bilayers

The inhibitory effect of anionic phospholipids on Sav1866 prompted a wider investigation of other ABC transporters. McjD protein was a good candidate for this study as previous research had shed some light on the regulatory effects of anionic phospholipids on McjD (Mehmood et al., 2016). Basal ATPase activity of McjD wild-type (WT) and the mutants were tested when reconstituted in respective anionic phospholipids PA, CL and PG and neutral PE as shown in Figure 5.3.

In Figure 5.3 (A), the basal ATPase activity of McjD WT reconstituted in PC was the highest at 0.13 ± 0.01 µmol ATP/mg/min while anionic phospholipids caused a marked reduction in the ATPase activity. Reconstitution in mixtures of anionic phospholipids and PC decreased the ATPase activity with increasing anionic phospholipid content. However, the degree of inhibition by PG was less than with CL and PA. Nevertheless, the ATPase activity was decreased by 33 % by PG, 87 % by PA and 92 % by CL. McjD WT reconstituted in PE had slightly higher activity than in PC, though not significantly. When reconstituted in mixtures of PC and PE, there was no significant difference in the ATPase activity at any point.

The basal ATPase activity of McjD W167Y:W247Y:L307W (Figure 5.3 (B)) reconstituted in PC was 0.15 ± 0.03 µmol ATP/mg/min, which was slightly higher than the WT. Reconstituting McjD W167Y:W247Y:L307W in anionic phospholipids, PA, PG and CL caused an 82% decrease in the ATPase activity compared to in PC. In mixtures of PC with increasing amounts of PA and CL, the ATPase activity did not change significantly. However, it was a different case for PG. Reconstituting in 0.25 mole fraction PG had the same ATPase rate as in PC, but subsequent addition of PG decreased the ATPase activity.

The ATPase activities of McjD W167Y:W247Y:L307W:R186Q (Figure 5.3 (C))and McjD W167Y:W247Y:L307W:R311Q (Figure 5.3 (D)) reconstituted in PC as shown in Figure 5.3 were 0.06 ± 0.02 µmol ATP/mg/min and 0.05 ± 0.0 µmol ATP/mg/min respectively. Addition of anionic phospholipids had a decreasing effect on their ATPase activities, lowering the rate by 74%. There was no distinction in the ATPase activity profile between PG, PA and CL as seen previously with McjD WT and McjD W167Y:W247Y:L307W. The inhibitory effect of PG was stronger for McjD W167Y:W247Y:L307W:R186Q and McjD W167Y:W247Y:L307W:R311Q as opposed to what was observed for the WT and McjD W167Y:W247Y:L307W.

McjD W167Y:W247Y:I182W in Figure 5.4 had the highest level of ATPase activity when reconstituted in PC (0.21 ± 0.05 µmol ATP/mg/min), which was higher than the WT and McjD W167Y:W247Y:L307W. Reconstitution in PG and PE reduced the ATPase activity by approximately 50% and 30% respectively compared to in PC. In mixtures of PC with PG and PC with PE, the ATPase rate did not vary significantly as shown in Figure 5.4.

The ATPase activity data of McjD mutants showed that the mutants are structurally stable and functional as they were all able to hydrolyse ATP. This assures that the mutants are folded correctly for the fluorescence quenching assays. The ATPase activity profiles of McjD WT and McjD W167Y:W247Y:L307W are similar, but the introduction of the additional mutants experienced greater inhibition of ATPase activity. In addition, the ATPase activity of the protein was dependent on the difference in the charge of the phospholipid head.

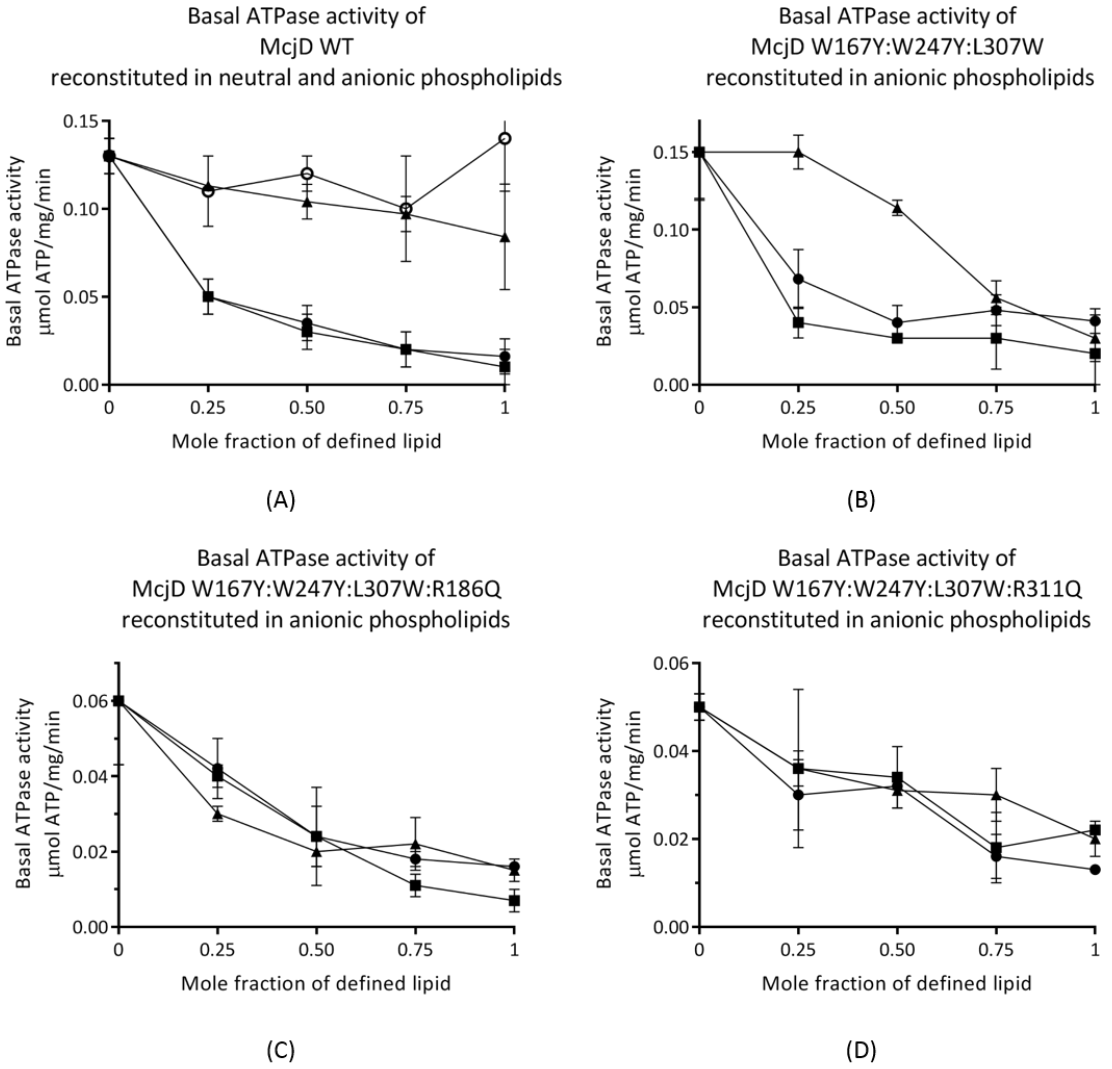

Figure 5.3 Basal ATPase activity of McjD WT (A) and mutants (B-D) reconstituted in bilayers of defined lipid composition. McjD (100 µg) was reconstituted into bilayer mixtures containing 0.6 µmol of di(C18:1)PC and increasing mole fractions of defined phospholipids; (▲) di(C18:1)PG, (●)di(C18:1)PA, (■) tetra(C18:1)CL, (O) di(C18:1)PE. The ATPase activity was monitored quantitatively using the oxidation of NADH to NAD^+ measured at 340nm, which was coupled to the hydrolysis of ATP by Sav1866 in an enzyme coupled reaction. Data points represent an average of at least three independent experiments, and the error bars show the standard deviation.

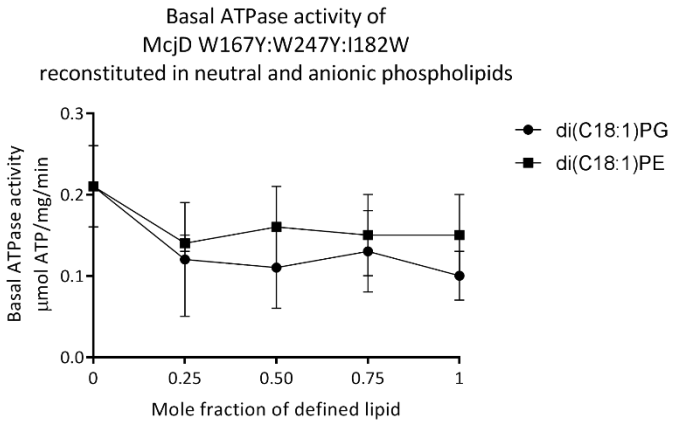

Figure 5.4 Basal ATPase activity of McjD W167Y:W247Y:I182W reconstituted in bilayers of defined lipid composition. McjD was reconstituted into bilayer mixtures containing 0.6 µmol of di(C18:1)PC and increasing mole fractions of defined phospholipids; anionic (●) di(C18:1)PG and neutral (■) di(C18:1)PE. The ATPase activity was monitored quantitatively using the oxidation of NADH to NAD^+ measured at 340nm, which was coupled to the hydrolysis of ATP by Sav1866 in an enzyme coupled reaction. Data points represent an average of at least three independent experiments, and the error bars show the standard deviation.

5.3.5 Fluorescence spectroscopy

Fluorescence quenching of a strategically placed Trp on McjD protein by brominated phospholipids was used to study lipid interactions with McjD. Fluorescence quenching data for McjD mutants reconstituted in mixtures of brominated phospholipids and their corresponding non-brominated phospholipids were fitted to Equation 1 to generate the number of binding sites, n. The n value is the apparent number of sites from which the fluorescence of the reporter Trp of McjD can be quenched by the brominated phospholipids. The fluorescence intensity was plotted as a fraction of fluorescence quenching, F/F_0, where F is the fluorescence of McjD at intermediate fractions of brominated lipid and F_0 is the fluorescence of McjD with non-brominated lipid. Fluorescence quenching data for McjD mutants reconstituted in mixtures of brominated anionic phospholipids and non-brominated PC were fitted to Equation 3 to determine the binding constants for the anionic phospholipids with respect to PC. Fluorescence quenching data of McjD reconstituted into mixtures of brominated PC and non-brominated anionic phospholipids would provide the binding constant for PC relative to anionic phospholipids. The relative constants of anionic phospholipids were compared with PC due to its neutral charge and bilayer forming properties (Dowhan William, 2002).

The number of binding sites and relative binding constants for phospholipids were determined for:

i. McjD W167Y:W247Y:L307W
ii. McjD W167Y:W247Y:L307W:R186Q
iii. McjD W167Y:W247Y:L307W:R311Q
iv. McjD W247Y

5.3.5.1 Tryptophan and tyrosine fluorescence analysis

As McjD has 29 endogenous Tyr residues, the fluorescence emission of 29 µM of Tyr was compared to 1 µM of Trp. The fluorescence intensity of Trp and Tyr in an aqueous buffer was measured when excited at 280 nm and 295 nm. From Figure 5.5 it is evident that the fluorescence intensity of Trp is virtually unchanged when excited at either 280 nm or 295 nm. However, exciting 29 µM of Tyr at 280 nm had a significant effect on the fluorescence emission and the emission of Tyr is significantly low when excited at 295 nm. This experiment was conducted in order to test the optimum excitation wavelength for McjD. Therefore, 295 nm was chosen as the excitation wavelength for the following fluorescence quenching experiments.

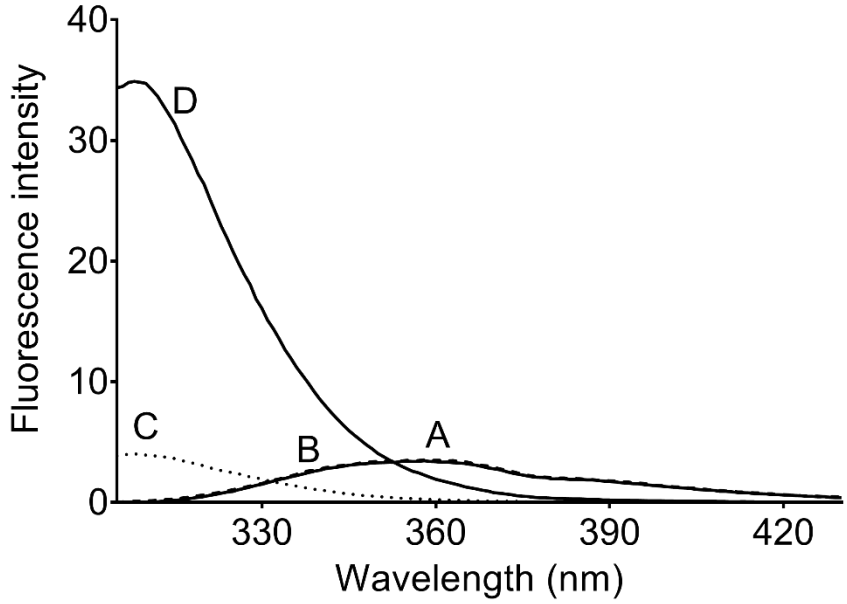

Figure 5.5 Corrected fluorescence intensity spectra of tryptophan (Trp) and tyrosine (Tyr) in aqueous buffer. (A) The emission spectrum of 1 µM Trp in buffer when excited at 280 nm wavelength. (B) The emission spectrum of 1 µM Trp in buffer when excited at 295 nm wavelength. (C) The emission spectrum of 29 µM Tyr in buffer when excited at 295 nm wavelength. (D) The emission spectrum of 29 µM Tyr in buffer when excited at 280 nm wavelength. The buffer was 20 mM Hepes, 1 mM EGTA, pH 7.2.

5.3.5.2 Fluorescence quenching of McjD by brominated phospholipids

McjD WT and McjD W167Y:W247Y were reconstituted into bilayers of di(C18:1)PC and di(Br_2C18:1)PC in 100:1 phospholipid to McjD monomer ratio and excited at 295 nm to produce intensity corrected emission spectra shown in Figure 5.6. The level of fluorescence intensity for McjD WT reconstituted in di(C18:1)PC was expectedly higher due to the presence of two Trp residues compared to McjD W167Y:W247Y, with no Trps, reconstituted in di(C18:1)PC. di(Br_2C18:1)PC quenched 41% of McjD WT fluorescence intensity and 35% of McjD W167Y:W247Y fluorescence intensity.

McjD W167Y:W247Y:L307W, McjD W167Y:W247Y:L307W:R311Q and McjD W167Y:W247Y:L307W:R186Q were reconstituted in di(C18:1)PC in 100:1 molar ratio of phospholipid to McjD monomer and excited at 295 nm. The maximum emission wavelengths (λ_{max}) were determined as 335 nm, 337 nm and 336 nm for McjD W167Y:W247Y:L307W, McjD W167Y:W247Y:L307W:R311Q and McjD W167Y:W247Y:L307W:R186Q respectively. Subsequent fluorescence intensity values were recorded at the respective maximum emission wavelengths.

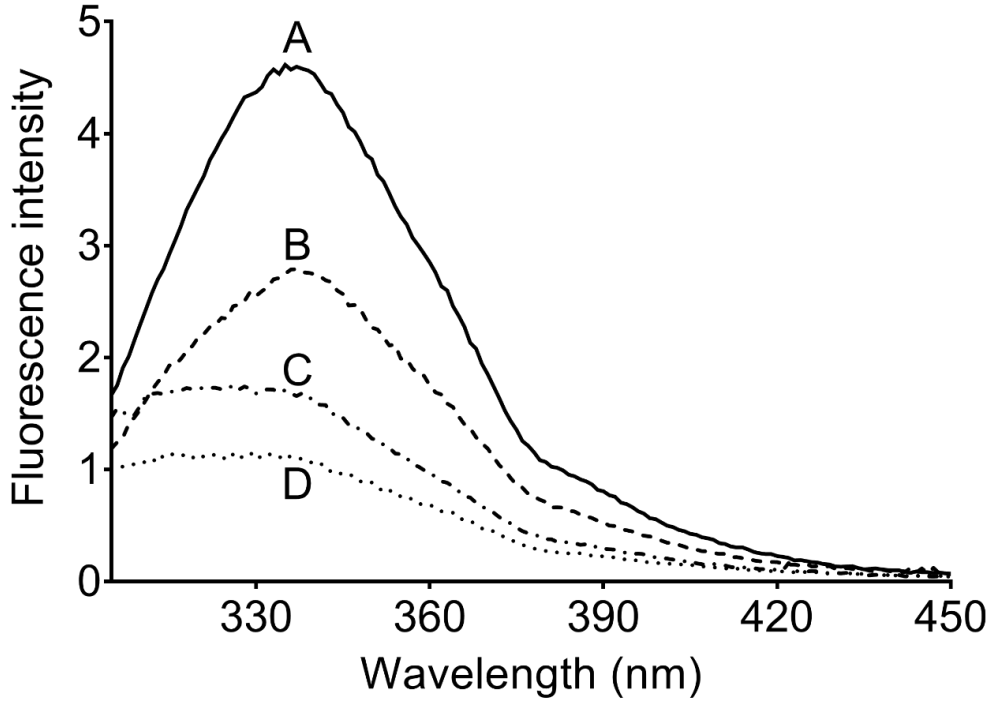

Figure 5.6 Intensity corrected fluorescence spectra of McjD WT and W167YW247Y. Fluorescence spectra are shown for (A) McjD WT and (C) McjD W167YW247Y reconstituted into bilayers of di(C18:1)PC and (B) McjD WT and (D) McjD W167YW247Y reconstituted into bilayers of di(Br_2C18:1)PC. 0.2 μM of McjD was reconstituted in 100:1 lipid to McjD molar ratio and excited at 295 nm wavelength. The buffer was 20 mM Hepes, 1 mM EGTA, pH 7.2.

5.3.5.3 Determining the number of binding sites and the relative binding constant of phospholipids for McjD W167Y:W247Y:L307W

A Trp residue introduced at position 307 on helix 6 acted as a reporter for phospholipid binding site adjacent to the residues arginine 186 (helix 4) and 311 (helix 6) on the cytoplasmic face of McjD (see Figure 5.1).

The level of fluorescence quenching (F/F_0) was similar for all phospholipids as shown in Table 5.2. F and F_0 are the fluorescence of McjD reconstituted in brominated and non-brominated phospholipids respectively. From Figure 5.7, the fluorescence intensity is decreased with respect to the increase in mole fraction of brominated lipids.

The number of binding sites, n, from which the brominated phospholipids could quench the Trp's fluorescence was derived by fitting the fluorescence quenching data of McjD W167Y:W247Y:L307W reconstituted into mixtures of brominated and corresponding non-brominated phospholipids to Equation 1 (n values listed in Table 5.2).

The number of binding sites was unusually high for phosphatidylcholine (3.06 ± 0.18) compared to the anionic phospholipids. Phosphatidylglycerol and phosphatidic acid had similar number of binding sites of 1.85 ± 0.09 and 1.90 ± 0.07 respectively, but cardiolipin had half the number of binding sites of 0.92 ± 0.07. The half n value is compensated by the fact that cardiolipin has four lipid tails as opposed to two for other phospholipids.

Fluorescence quenching data of McjD W167Y:W247Y:L307W reconstituted into mixtures of brominated and non-brominated phospholipids were fitted to Equation 3 to determine the relative binding constant, k (k values listed in Table 5.3).

The binding constants for anionic phospholipids were higher than for phosphatidylcholines as shown in Table 5.3. The binding constant for phosphatidylglycerol derived from fluorescence quenching data of McjD W167Y:W247Y:L307W reconstituted into mixtures of di(Br_2C18:1)PG and di(C18:1)PC was 1.53 ± 0.21 relative to phosphatidylcholine and the binding constant for phosphatidylcholine derived from fluorescence quenching data of McjD W167Y:W247Y:L307W reconstituted into mixtures of di(Br_2C18:1)PC and di(C18:1)PG was 0.73 ± 0.08 relative to phosphatidylglycerol. This suggested that the positive clustered binding site near Trp 307 has a higher binding affinity for phosphatidylglycerol than for phosphatidylcholine.

Fluorescence quenching data of McjD W167Y:W247Y:L307W reconstituted into mixtures of di(Br_2C18:1)PA and di(C18:1)PC generated a higher binding constant (2.02 ± 0.29) for phosphatidic

acid than phosphatidylcholine (0.87 ± 0.15), which was derived from fluorescence quenching data of McjD W167Y:W247Y:L307W reconstituted into mixtures of di(Br_2C18:1)PC and di(C18:1)PA.

Cardiolipin had the binding constant value of 0.82 ± 0.17, which was derived from fluorescence quenching data of McjD W167Y:W247Y:L307W reconstituted into mixtures of tetra(Br_2C18:1)CL and di(C18:1)PC. The binding constant for phosphatidylcholine was lower than of cardiolipin, 0.37 ± 0.06, which was derived from fluorescence quenching data of McjD W167Y:W247Y:L307W reconstituted into mixtures of di(Br_2C18:1)PC and tetra(C18:1)CL. It is difficult to interpret the binding constant values for cardiolipin due to its four-chain structure compared to two for phosphatidylcholine.

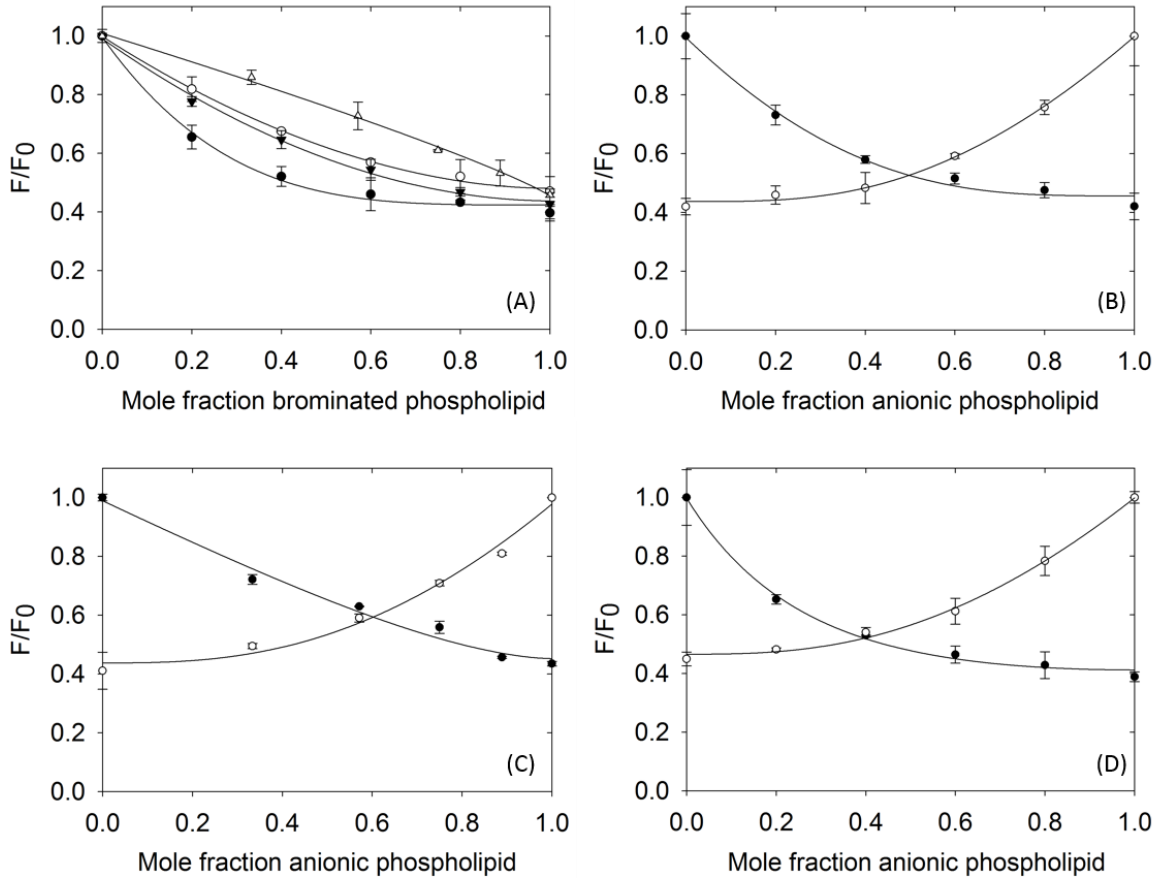

Figure 5.7 Fluorescence quenching of McjD W167Y:W247Y:L30W by brominated phospholipids. (A) McjD W167Y:W247Y:L30W was reconstituted into mixtures of brominated and corresponding non-brominated lipids: (●)di(C18:1)PC, (o) di(C18:1)PG, (▼)di(C18:1)PA, (△) tetra(C18:1)CL. Two replicates were averaged for each reading, and the data were fitted to Equation 1 to generate the number of binding sites, n listed in Table 5.2. McjD W167Y:W247Y:L30W was reconstituted into mixtures of brominated anionic lipids and non-brominated di(C18:1)PC (filled circles) and brominated di(Br_2C18:1)PC and non-brominated anionic lipids (open circles): (B) di(C18:1)PG, (C) tetra(C18:1)CL and (D) di(C18:1)PA. Two replicates were averaged for each reading, and the data were fitted to Equation 3 to generate a relative binding constant, k, listed in Table 5.3. The mole fraction of phospholipids is based on the number of lipid chains.

Phospholipid	n	F/F_0
di(C18:1)PC	3.06 ± 0.18	0.42 ± 0.02
di(C18:1)PG	1.85 ± 0.09	0.46 ± 0.02
tetra(C18:1)CL	0.92 ± 0.07	0.44 ± 0.03
di(C18:1)PA	1.90 ± 0.07	0.43 ± 0.00

Table 5.2 Number of lipid binding sites, n, and the ratio of fluorescence intensities of McjD W167Y:W247Y:L30W reconstituted in mixtures of brominated phospholipids and their corresponding non-brominated phospholipids. Fluorescence quenching of McjD W167Y:W247Y:L30W by brominated phospholipids shown in Figure 5.7 (A) was fitted to Equation 1 to derive their number of binding sites, n, on McjD. The values represent an average of three or more independent repeats and their standard deviation. F and F_0 are the fluorescence intensities of McjD W167Y:W247Y:L30W reconstituted in brominated phospholipids and their corresponding non-brominated phospholipids respectively.

Phospholipid	Binding constant of brominated anionic phospholipids relative to phosphatidylcholine	Binding constant of brominated phosphatidylcholine relative to anionic phospholipids
di(C18:1)PG	1.53 ± 0.21	0.73 ± 0.08
tetra(C18:1)CL	0.82 ± 0.17	0.37 ± 0.06
di(C18:1)PA	2.02 ± 0.29	0.87 ± 0.15

Table 5.3 Relative lipid binding constant, k, of phospholipids for McjD W167Y:W247Y:L30W. Fluorescence quenching of McjD W167Y:W247Y:L30W in mixtures of brominated anionic lipids and non-brominated PC or brominated PC and non-brominated anionic lipids was fitted to Equation 3 and plotted in Figure 5.7 (B-D). The n values from Table 5.2 were used to determine the relative binding constant, k, for the respective phospholipids.

5.3.5.4 Determining the number of binding sites and the relative binding constant of phospholipids for McjD W167Y:W247Y:L307W:R186Q and McjD W167Y:W247Y:L307W:R311Q

The predicted binding site for anionic phospholipids on the cytoplasmic face of McjD consisted of positively charged residues arginine 186 (helix 4) and arginine 311 (helix 6). The positive arginine residues were mutated to neutral glutamine residues individually creating McjD W167Y:W247Y:L307W:R186Q and McjD W167Y:W247Y:L307W:R311Q, to investigate their role in creating a high affinity site for anionic lipids.

The level of fluorescence quenching (F/F_0) was similar for all phospholipids as shown in Table 5.4 and Table 5.6. F and F_0 are the fluorescence of McjD reconstituted in brominated and non-brominated phospholipids respectively. From Figure 5.8 and Figure 5.9, the fluorescence intensity is decreased with respect to the increase in mole fraction of brominate lipids.

McjD W167Y:W247Y:L307W:R186Q and McjD W167Y:W247Y:L307W:R311Q were reconstituted into mixtures of brominated and their corresponding non-brominated phospholipids and the fluorescence quenching data were fitted to Equation 1 to generate the number of binding sites of phospholipids, n, on McjD (n values listed in Table 5.4 and Table 5.6).

The number of binding sites for phosphatidylcholine was higher than for anionic phospholipids for both McjD W167Y:W247Y:L307W:R186Q (2.81 ± 0.77) and McjD W167Y:W247Y:L307W:R311Q (2.71 ± 0.49). The n values for anionic phospholipids were similar for both mutants as shown in Table 5.4 and Table 5.6. The n value for phosphatidylglycerol was approximately 2 and for phosphatidic acid was slightly less than 2 (1.75 ± 0.19 for McjD W167Y:W247Y:L307W:R186Q; 1.62 ± 0.35 for McjD W167Y:W247Y:L307W:R311Q). Cardiolipin had the lowest n number (0.90 ± 0.22 for McjD W167Y:W247Y:L307W:R186Q; 0.82 ± 0.09 for McjD W167Y:W247Y:L307W:R311Q) for reasons discussed previously.

McjD W167Y:W247Y:L307W:R186Q and McjD W167Y:W247Y:L307W:R311Q were reconstituted into mixtures of brominated anionic phospholipids and non-brominated phosphatidylcholine or brominated phosphatidylcholine and non-brominated anionic phospholipids. The fluorescence quenching data from such reconstitutions were fitted to Equation 3 to generate the relative binding constants for the phospholipids (k values listed in Table 5.5 and Table 5.7).

Fluorescence quenching curves of McjD W167Y:W247Y:L307W:R186Q in mixtures of di(Br_2C18:1)PC and anionic phospholipids or brominated anionic phospholipids and di(C18:1)PC

are shown in Figure 5.8. The binding constants calculated from the fluorescence quenching data from both mixtures are reasonably close to 1, suggesting an equal affinity between phosphatidylcholine and anionic phospholipids towards the binding site on McjD. Similar observations were made from fluorescence quenching curves of McjD W167Y:W247Y:L307W:R311Q in Figure 5.9 except for phosphatidic acid. The binding constant derived from the brominated phosphatidylcholine and non-brominated phosphatidic acid fluorescence quenching data suggested that phosphatidylcholine was binding with the same affinity as phosphatidic acid. However, according to the brominated phosphatidic acid and non-brominated phosphatidylcholine fluorescence quenching data, phosphatidic acid was binding more strongly to McjD than phosphatidylcholine.

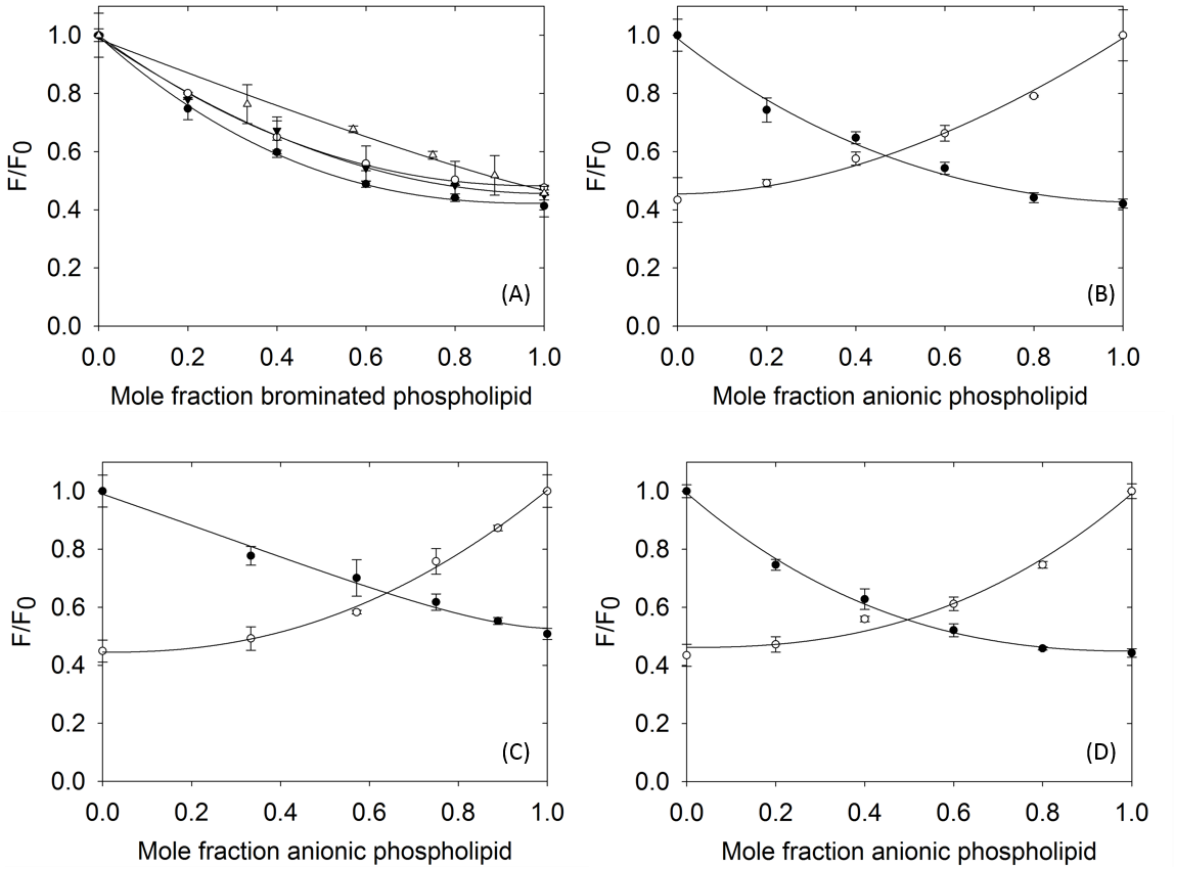

Figure 5.8 Fluorescence quenching of McjD W167Y:W247Y:L30W:R186Q by brominated phospholipids. (A) McjD W167Y:W247Y:L30W:R186Q was reconstituted into mixtures of brominated and corresponding non-brominated lipids: (●)di(C18:1)PC, (o) di(C18:1)PG, (▼)di(C18:1)PA, (△) tetra(C18:1)CL. Two replicates were averaged for each reading, and the data were fitted to Equation 1 to generate the number of binding sites, n listed in Table 5.4. McjD W167Y:W247Y:L30W:R186Q was reconstituted into mixtures of brominated anionic lipids and non-brominated di(C18:1)PC (filled circles) and brominated di(Br_2C18:1)PC and non-brominated anionic lipids (open circles): (B) di(C18:1)PG, (C) tetra(C18:1)CL and (D) di(C18:1)PA. Two replicates were averaged for each reading, and the data were fitted to Equation 3 to generate a relative binding constant, k, listed in Table 5.5 and Table 5.7. The mole fraction of phospholipids is based on the number of lipid chains.

Phospholipid	n	F/F_0
di(C18:1)PC	2.81 ± 0.77	0.42 ± 0.02
di(C18:1)PG	2.19 ± 0.05	0.46 ± 0.02
tetra(C18:1)CL	0.90 ± 0.22	0.49 ± 0.03
di(C18:1)PA	1.75 ± 0.19	0.45 ± 0.01

Table 5.4 Number of lipid binding sites, n, and the ratio of fluorescence intensities of McjD W167Y:W247Y:L30W:R186Q reconstituted in mixtures of brominated phospholipids and their corresponding non-brominated phospholipids. Fluorescence quenching of W167Y:W247Y:L30W:R186Q by brominated phospholipids shown in Figure 5.8 (A) was fitted to Equation 1 to derive their number of binding sites, n, on McjD. The values represent an average of three or more independent repeats and their standard deviation. F and F_0 are the fluorescence intensities of McjD W167Y:W247Y:L30W:R186Q reconstituted in brominated phospholipids and their corresponding non-brominated phospholipids respectively.

Phospholipid	Binding constant of brominated anionic phospholipids relative to phosphatidylcholine	Binding constant of brominated phosphatidylcholine relative to anionic phospholipids
di(C18:1)PG	0.97 ± 0.15	0.96 ± 0.26
tetra(C18:1)CL	0.95 ± 0.27	0.60 ± 0.13
di(C18:1)PA	1.19 ± 0.39	0.92 ± 0.13

Table 5.5 Relative lipid binding constant, k, of phospholipids for McjD W167Y:W247Y:L30W:R186Q reconstituted in mixtures of brominated anionic lipids and non-brominated PC or brominated PC and non-brominated anionic lipids. Fluorescence quenching of McjD W167Y:W247Y:L30W:R186Q in mixtures of brominated anionic lipids and non-brominated PC or brominated PC and non-brominated anionic lipids was fitted to Equation 3 and plotted in Figure 5.8 (B-D). The n values from Table 5.4 were used to determine the relative binding constant, k, for the respective phospholipids.

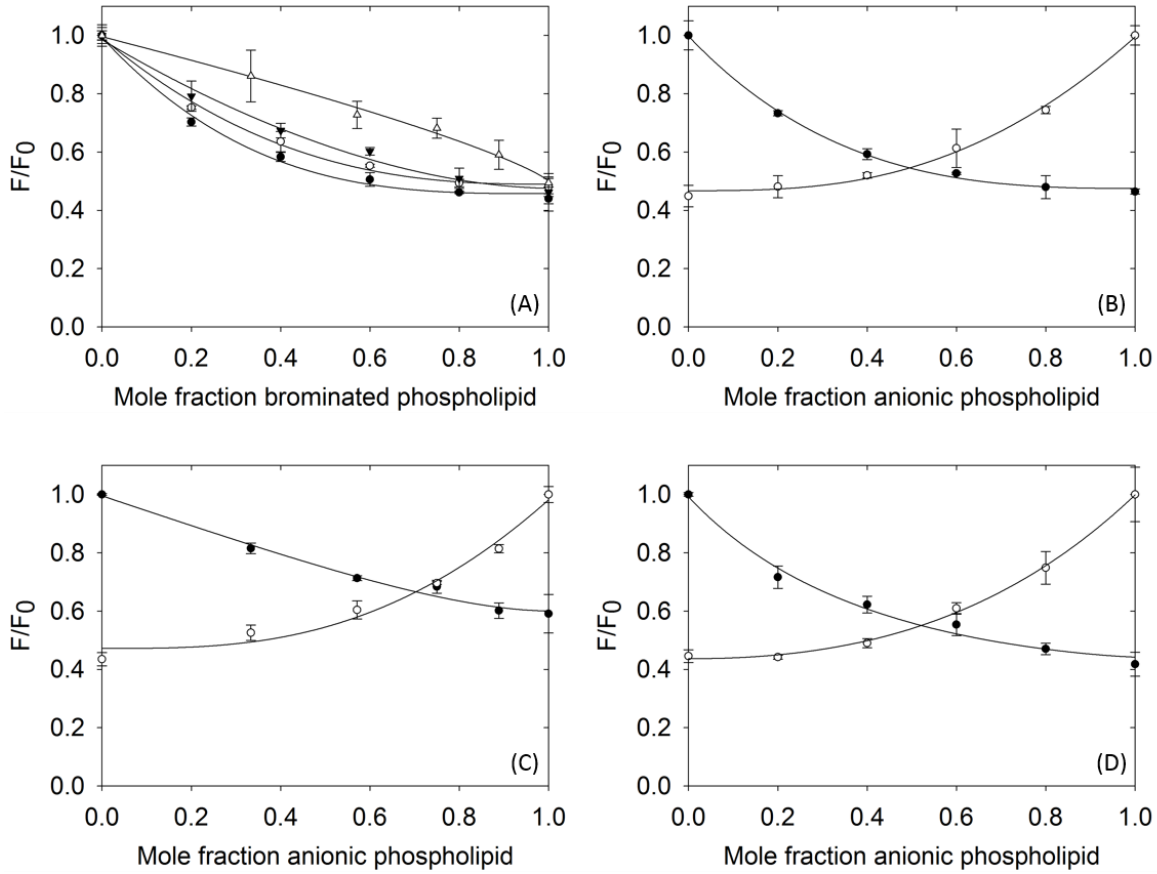

Figure 5.9 Fluorescence quenching of McjD W167Y:W247Y:L30W:R311Q by brominated phospholipids. (A) McjD W167Y:W247Y:L30W:R311Q was reconstituted into mixtures of brominated and corresponding non-brominated lipids: (●)di(C18:1)PC, (o) di(C18:1)PG, (▼)di(C18:1)PA, (△) tetra(C18:1)CL. Two replicates were averaged for each reading, and the data were fitted to Equation 1 to generate the number of binding sites, n listed in Table 5.6. McjD W167Y:W247Y:L30W:R311Q was reconstituted into mixtures of brominated anionic lipids and non-brominated di(C18:1)PC (filled circles) and brominated di(Br_2C18:1)PC and non-brominated anionic lipids (open circles): (B) di(C18:1)PG, (C) tetra(C18:1)CL and (D) di(C18:1)PA. Two replicates were averaged for each reading, and the data were fitted to Equation 3 to generate a relative binding constant, k, listed in Table 5.7. The mole fraction of phospholipids is based on the number of lipid chains.

Phospholipid	n	F/F_0
di(C18:1)PC	2.71 ± 0.49	0.45 ± 0.01
di(C18:1)PG	2.24 ± 0.23	0.47 ± 0.02
tetra(C18:1)CL	0.82 ± 0.09	0.42 ± 0.01
di(C18:1)PA	1.62 ± 0.35	0.49 ± 0.04

Table 5.6 Number of lipid binding sites, n, and the ratio of fluorescence intensities of McjD W167Y:W247Y:L30W:R311Q reconstituted in mixtures of brominated phospholipids and their corresponding non-brominated phospholipids. Fluorescence quenching of W167Y:W247Y:L30W:R311Q by brominated phospholipids shown in Figure 5.9 (A) was fitted to Equation 1 to derive their number of binding sites, n, on McjD. The values represent an average of three or more independent repeats and their standard deviation. F and F_0 are the fluorescence intensities of McjD W167Y:W247Y:L30W:R311Q reconstituted in brominated phospholipids and their corresponding non-brominated phospholipids respectively.

Phospholipid	Binding constant of brominated anionic phospholipids relative to phosphatidylcholine	Binding constant of brominated phosphatidylcholine relative to anionic phospholipids
di(C18:1)PG	1.26 ± 0.05	1.03 ± 0.17
tetra(C18:1)CL	0.84 ± 0.10	0.65 ± 0.21
di(C18:1)PA	1.82 ± 0.41	1.03 ± 0.15

Table 5.7 Relative lipid binding constant, k, of phospholipids for McjD W167Y:W247Y:L30W:R311Q reconstituted in mixtures of brominated anionic lipids and non-brominated PC or brominated PC and non-brominated anionic lipids. Fluorescence quenching of McjD W167Y:W247Y:L30W:R311Q in mixtures of brominated anionic lipids and non-brominated PC or brominated PC and non-brominated anionic lipids was fitted to Equation 3 and plotted in Figure 5.9 (B-D). The n values from Table 5.6 were used to determine the relative binding constant, k, for the respective phospholipids.

5.3.5.5 Determining the number of binding sites and relative binding constant of phospholipids for McjD W247Y

McjD has two endogenous Trp residues at position 167 and 247. Trp 167 is located at the periplasmic side of McjD with no apparent cluster of positively charged residues. Therefore, removing the Trp at 247 provided a negative control for the McjD W167Y:W247Y:L307W reporter binding site.

The level of fluorescence quenching (F/F_0) was similar for all phospholipids as shown in Table 5.8. F and F_0 are the fluorescence of McjD reconstituted in brominated and non-brominated phospholipids respectively. From Figure 5.10, the fluorescence intensity is decreased with respect to the increase in mole fraction of brominate lipids.

McjD W247Y was reconstituted into mixtures of brominated phospholipids and their corresponding non-brominated phospholipids. The fluorescence quenching data obtained from such mixes were fitted to Equation 1 to derive the number of binding sites for phospholipids close to Trp 167 (n values listed in Table 5.8). Fluorescence quenching data of phosphatidylcholine showed the highest n value (2.64 ± 0.38) compared to the anionic phospholipids. Phosphatidylglycerol and phosphatidic acid had similar n values of 1.86 ± 0.22 and 1.72 ± 0.23 respectively while cardiolipin had approximately half the n value of 1.35 ± 0.26, for reasons discussed previously.

The relative binding constants (Table 5.9) derived from brominated anionic phospholipids and non-brominated phosphatidylcholine or brominated phosphatidylcholine and non-brominated anionic phospholipids were fairly similar to 1. This suggested that there was no difference in affinity between phosphatidylcholine and the anionic phospholipids at the site where no positively charged residues are present.

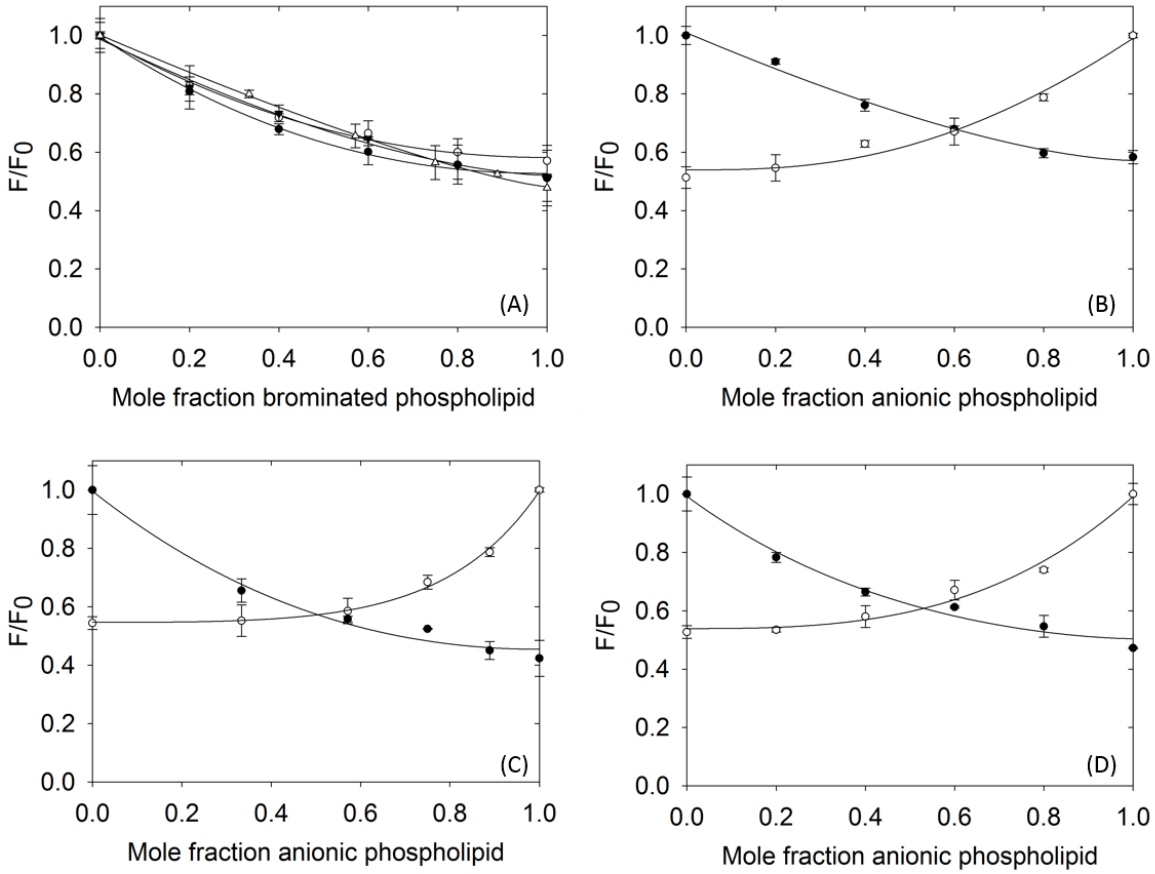

Figure 5.10 Fluorescence quenching of McjD W247Y by brominated phospholipids. (A) McjD W247Y was reconstituted into mixtures of brominated and corresponding non-brominated lipids: (●)di(C18:1)PC, (o) di(C18:1)PG, (▼)di(C18:1)PA, (△) tetra(C18:1)CL. Two replicates were averaged for each reading, and the data were fitted to Equation 1 to generate the number of binding sites, n listed inTable 5.8. McjD W247Y was reconstituted into mixtures of brominated anionic lipids and non-brominated di(C18:1)PC (filled circles) and brominated di(Br_2C18:1)PC and non-brominated anionic lipids (open circles): (B) di(C18:1)PG, (C) tetra(C18:1)CL and (D) di(C18:1)PA. Two replicates were averaged for each reading, and the data were fitted to Equation 3 to generate a relative binding constant, k, listed in Table 5.9. The mole fraction of phospholipids is based on the number of lipid chains.

Phospholipid	n	F/F_0
di(C18:1)PC	2.64 ± 0.38	0.46 ± 0.05
di(C18:1)PG	1.86 ± 0.22	0.58 ± 0.02
tetra(C18:1)CL	1.35 ± 0.26	0.51 ± 0.04
di(C18:1)PA	1.72 ± 0.23	0.53 ± 0.01

Table 5.8 Number of lipid binding sites, n, and the ratio of fluorescence intensities of McjD W247Y reconstituted in mixtures of brominated phospholipids and their corresponding non-brominated phospholipids. Fluorescence quenching of W247Y by brominated phospholipids shown in Figure 5.10 (A) was fitted to Equation 1 to derive their number of binding sites, n, on McjD. The values represent an average of three or more independent repeats and their standard deviation. F and F_0 are the fluorescence intensities of McjD W247Y reconstituted in brominated phospholipids and their corresponding non-brominated phospholipids respectively.

Phospholipid	Binding constant of brominated anionic phospholipids relative to phosphatidylcholine	Binding constant of brominated phosphatidylcholine relative to anionic phospholipids
di(C18:1)PG	0.91 ± 0.07	1.18 ± 0.55
tetra(C18:1)CL	0.93 ± 0.22	0.81 ± 0.17
di(C18:1)PA	1.12 ± 0.28	1.02 ± 0.10

Table 5.9 Relative lipid binding constant, k, of phospholipids for McjD W247Y reconstituted in mixtures of brominated anionic lipids and non-brominated PC or brominated PC and non-brominated anionic lipids. Fluorescence quenching of McjD W247Y in mixtures of brominated anionic lipids and non-brominated PC or brominated PC and non-brominated anionic lipids was fitted to Equation 3 and plotted in Figure 5.10 (B-D). The n values from Table 5.8 were used to determine the relative binding constant, k, for the respective phospholipids.

5.3.6 Styrene Maleic Acid (SMA) purification of membrane proteins

Following extraction of Sav1866 from the membrane using styrene maleic acid (SMA) as described in 5.2.5 and subsequent purification, 10 µl of eluted fractions (labelled 1-10) were run on an SDS-PAGE gel and visualised using InstantBlue Protein Stain (see Figure 5.11). The band between 78

kDa and 51 kDa corresponds to the Sav1866 monomer. A faint band close to 120 kDa could represent the Sav1866 dimer. The smaller bands at 25 kDa may be unspecifically bound proteins.

The eluted fractions were pooled together and further purified by size exclusion chromatography (SEC). 10 µl of the fractions collected (labelled 1-11) from SEC was loaded on an SDS-PAGE gel as shown in Figure 5.11. The smaller proteins at 25 kDa were removed after SEC.

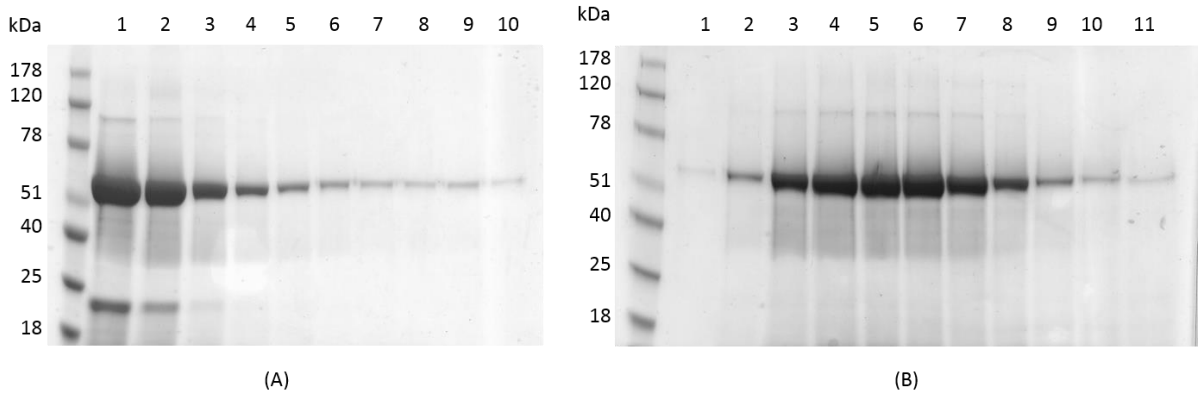

Figure 5.11 Purification of Sav1866 using SMA. 10 µl of 1 ml eluted fractions using 500 mM imidazole was loaded onto an SDS-PAGE gel in (A). The eluted fractions were pooled together for further purificaton using size exclusion chromatography (SEC). 10 µl of 1 ml fractions collected from the SEC were loaded onto an SDS-PAGE gel in (B). The band for Sav1866 lies between 51 kD and 78 kD. InstantBlue protein stain was used to visualise the bands on the gel. The molecular markers are shown on the left.

McjD was purified in a similar manner to Sav1866 but did not undergo SEC. Individual fractions from the wash and elution steps were loaded onto an SDS-PAGE gel and visualised using InstantBlue Protein Stain in Figure 5.12. McjD monomer was purified and can be seen between 70 kDa and 50 kDa on the SDS-PAGE and western blot images. Some amount of the protein is washed off the His-trap column during the wash steps. There is also a band for McjD at the insoluble step indicating that SMA solubilisation was not 100% efficient.

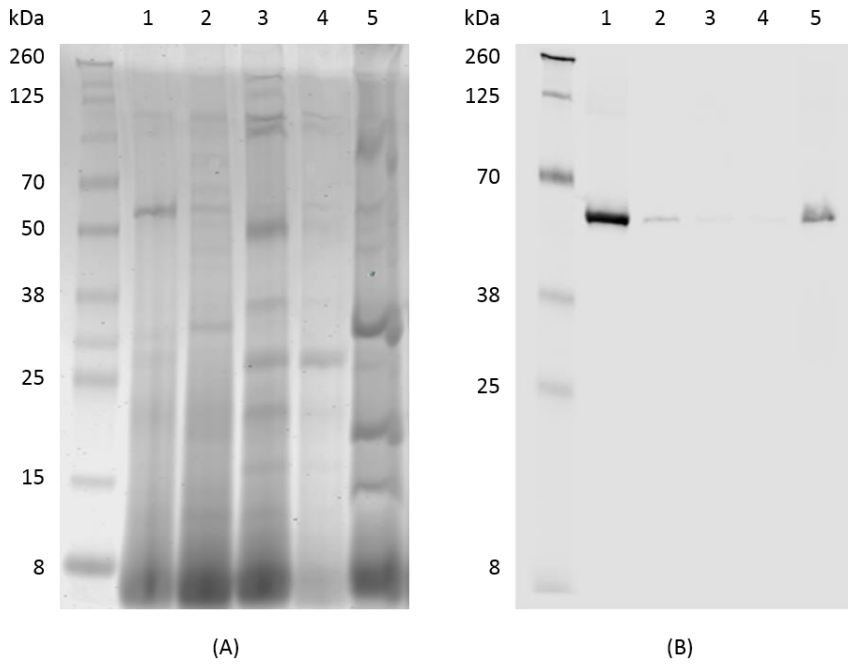

Figure 5.12 Purification of McjD using SMA. Lane 1 shows purified (5 µg) McjD eluted using 500 mM imidazole, lane 2 shows wash step without imidazole followed a by wash step with 20 mM imidazole in lane 3 and 50 mM imidazole wash in lane 4. Lane 5 shows the insoluble fraction after solubilisation with SMA in each (A) SDS-PAGE and (B) western blot image. The band for McjD lies between 50 kD and 70 kD. InstantBlue protein stain was used to visualise the bands on the SDS-PAGE gel. Anti-His antibody was used to detect the protein bands on the western blot. The molecular markers are shown on the left.

5.3.6.1 ATPase activity of SMA purified Sav1866 and McjD

The stability of SMA purified protein in the presence of magnesium was tested using a simple experiment where SMA purified Sav1866 was treated with a range of $MgCl_2$ concentrations (0-10 mM). After incubation at room temperature for 5 minutes, the sample was centrifuged at 13,000 g, and the supernatant was separated from the pellet. The presence of protein in the supernatant would indicate a stable SMA lipid particle (SMALP) protein and any protein deposited in the pellet would indicate precipitation of the SMALP. Figure 5.13 demonstrates the respective supernatant and pellet fractions for SMALP Sav1866 treated with 0-10 mM $MgCl_2$. It is evident that increasing the concentration of $MgCl_2$ precipitates more SMALP Sav1866 due to the presence of stronger bands for pellet fractions than supernatant fractions.

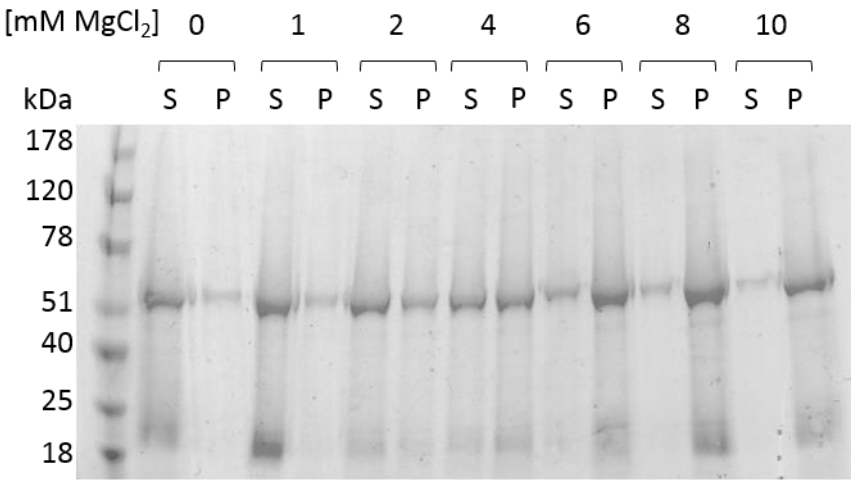

Figure 5.13 Effect of $MgCl_2$ on the stability of SMA. SMA purified Sav1866 was treated with 0-10 mM $MgCl_2$ to test the stability of SMA. Following the treatment with $MgCl_2$, the sample was centrifuged at 13,000 rpm. The supernatant (S) and the pellet (P) were separated and loaded onto the SDS-PAGE gel. Instant Blue protein stain was used to visualise the bands on the SDS-PAGE gel. The molecular marker is shown on the left.

For the ATPase assay since magnesium is essential for ATP hydrolysis, 1.3 mM $MgSO_4$ was chosen to compensate for the stability of the SMA. SMA purified proteins showed no ATPase activity compared to their respective n-Dodecyl-β-D-maltopyranoside (DDM) purified proteins for both Sav1866 and McjD.

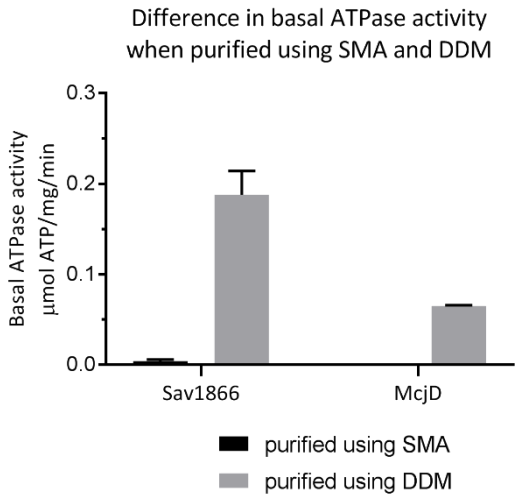

Figure 5.14 Basal ATPase activity of Sav1866 and McjD purified using SMA and DDM. The ATPase activity was monitored quantitatively using the oxidation of NADH to NAD^+ measured at 340nm, which was coupled to the hydrolysis of ATP by Sav1866 in an enzyme coupled reaction. Data represent an average of at least three independent experiments, and the error bars show the standard deviation.

5.4 Discussion

There have been numerous examples where anionic lipids have shown regulatory effects on the activity, translocation and conformation of membrane proteins (Elliott et al., 2005; Marius et al., 2008; Valiyaveetil et al., 2002; Van Klompenburg et al., 1997). Regulating membrane proteins, especially ABC transporters that are involved in multidrug resistance in infection control, diseases such as cancer, and agriculture, is crucial and yet challenging. Therefore, characterising the regulatory effects of lipids on the activity of those proteins might identify alternative methods to modulate their activity.

5.4.1 Regulating effects of phospholipids on the ATPase activity of Sav1866

Phosphatidylserine (PS) is translocated from the inner leaflet to the outer leaflet of the membrane to maintain its asymmetry by a phospholipid scramblase, TMEM16F (Elliott et al., 2005; Schmidt et al., 2015). Research has shown that this loss of PS asymmetry has an inhibitory effect on the P-glycoprotein function. On restoration of PS to the inner leaflet, the activity of the P-glycoprotein is re-established (Elliott et al., 2005). Therefore, changes in membrane lipid symmetry could provide a mechanism for modulating membrane protein activity. In this particular case, P-glycoprotein may have been rendered inactive due to the loss of a particular lipid-protein interaction or change in lipid composition (Elliott et al., 2005).

Sav1866, a bacterial homologue of P- glycoprotein (Dawson & Locher, 2006), was reconstituted into anionic, cationic and neutral phospholipids to study the effects of the phospholipids on its ATPase activity.

5.4.1.1 Effects of neutral lipids on Sav1866

Sav1866 had the highest ATPase activity when reconstituted in PC, possibly due to its neutral head group. However, reconstituting Sav1866 in PE, another neutral lipid, inhibited the ATPase activity significantly. This suggested that the bilayer forming property of PC was vital for Sav1866's ATPase activity as the non-bilayer forming properties of PE, leading to a cone-shaped membrane fragment (Cullis & De Kruijff, 1978), inhibited the protein's activity. Similar inhibition by PE was observed with Ca^{2+} ATPase due to its hexagonal H_{II} phase forming property (Starling et al., 1993).

5.4.1.2 Effects of anionic lipids on Sav1866

Similar to what was observed for P-gp (Elliott et al., 2005), anionic phospholipids had a significant effect on the ATPase activity of Sav1866 reducing its activity markedly compared to when

reconstituted in PC. CL had the largest inhibitory effect possibly due to the presence of two negatively charged head groups, followed closely by PG and PA.

5.4.1.3 Effects of cationic lipids on Sav1866

Cationic phospholipids, EPC did not have a major effect on Sav1866's ATPase activity albeit, the activity was lower than when reconstituted in PC. Lysyl PG, on the other hand, decreased the activity slightly but not as markedly as observed with the anionic phospholipids. This suggested that not all cationic phospholipids have the same effect on Sav1866. EPC is a synthetic cationic phospholipid whereas lysyl PG is found in the native membrane of *S. aureus* (Pasupuleti et al., 2012). Perhaps alterations in the balance of anionic and cationic lipids may modulate the activity of Sav1866 in a similar manner to the way in which phosphatidylserine modulates the activity of P-gp (Elliott et al., 2005).

5.4.2 Regulating effects of anionic and neutral phospholipids on the ATPase activity of McjD

The importance of lipids for the ATPase activity of McjD was demonstrated previously when the removal of lipids using octyl glucose neopentyl glycol (OGNG) caused the protein to aggregate and lose its ATPase activity. Following the reconstitution of the protein into PE vesicles, the ATPase activity was restored. However, reconstitution into PG vesicles failed to restore the ATPase activity to the basal level (Mehmood et al., 2016). The authors suggested the role of zwitterionic lipids (PE) in providing a hydrophobic environment for McjD for optimal ATP hydrolysis and PG molecule acting as a stabiliser for the protein to retain an outward occluded state (Mehmood et al., 2016).

The effects of cationic lipids on the ATPase activity of McjD was not tested here as the *E.coli* membrane does not contain any cationic lipids (Huijbregts et al., 2000; Raetz, 1978).

5.4.2.1 Effects of neutral lipids on McjD

In this study, the highest ATPase activity for McjD WT and McjD W167Y:W247Y:I182W was observed when it was reconstituted in PC or PE. The inhibitory effect of PE seen with Sav1866 possibly due to the lipid's non-bilayer forming properties (Cullis & De Kruijff, 1978) did not apply to McjD. PE is found in the *E.coli* membrane (Huijbregts et al., 2000; Raetz, 1978) but not in the *S.aureus* membrane. As Sav1866 is originally from *S.aureus*, there is a possibility that it did not evolve to be compatible with PE. McjD mutants, McjD W167Y:W247Y:L307W, McjD W167Y:W247Y:L307W:R186Q and McjD W167Y:W247Y:L307W:R311Q too had the highest

ATPase activity when reconstituted in PC. Nevertheless, McjD W167Y:W247Y:L307W:R186Q and McjD W167Y:W247Y:L307W:R311Q lost over 50% of activity when reconstituted in PC compared to the WT, which highlights the possible role of the positive residues on the protein's activity.

5.4.2.2 Effects of anionic lipids on McjD

The reconstitution of McjD in anionic lipids (PG, PA and CL) inhibited its ATPase activity, similar to what was observed for Sav1866. The effect of PG on the ATPase activity of McjD WT was less inhibitory than CL and PA suggesting a distinct role for PG. Such distinction between anionic phospholipids was not observed with Sav1866, highlighting the variable effects of PG on different ABC proteins. Similar to McjD WT, McjD W167Y:W247Y:I182W did not experience a strong inhibition by PG reconstitution. On the other hand, the ATPase activity of McjD W167Y:W247Y:L307W was strongly inhibited when reconstituted in over 0.25 mole fraction of PG. This suggests that replacing the leucine at position 307 with a Trp allows PG to inhibit the mutant's ATPase activity more strongly compared to WT.

The inhibitory effect of PG was stronger when the positive residues, Arg-186 and Arg-311, were removed and replaced with Gln. From the fluorescence quenching data, the removal of the positive residues created a lower affinity binding site for PG, resulting in PG not binding strongly to the site. There is a possibility that PG binding specifically at the positive clustered site on McjD is essential for its ATPase activity while PG binding at annular, non-specific site inhibits the protein's ATPase activity.

5.4.3 Identifying a specific binding site for anionic phospholipids on McjD

Fluorescence quenching of Trp residue by brominated phospholipids is a powerful tool to understand lipid-protein interaction. The bromine atoms on the lipid tails have to be in close contact with the Trp in order for them to quench the fluorescence. The brominated fatty acyl chains behave similarly to unsaturated fatty acyl chains as the bulky bromine atoms have similar lipid packing effects as the cis double bond (East & Lee, 1982).

The mechanism of quenching by the bromine atoms is thought to be due to intersystem crossing (Lakowicz, 2006). When the fluorophore is excited to the singlet state, it comes in contact with bromine atoms (quencher), which causes the singlet state to become an excited triplet state. Since emission from the excited triplet state is slow, it is then quenched to the ground state by the bromine atoms (Lakowicz, 2006).

In this study, Trp residues were introduced to study the lipid binding affinity on the cytoplasmic and periplasmic side of the protein. The McjD mutants were reconstituted into mixtures of brominated and non-brominated phospholipids. The successful reconstitution was verified by the decrease in fluorescence intensity when reconstituted into brominated phospholipids compared to reconstitution in non-brominated phospholipids.

The number of sites, n from which the fluorescence of the Trp residue can be quenched by brominated phospholipid was calculated for each McjD mutant. The n values remained fairly constant for all mutants suggesting that the mutation did not affect the number of binding sites for the lipids. The number of binding sites for PC was higher than for anionic phospholipids. This difference in the number of binding sites can be explained by the neutral charge of the PC head groups, which allows for close alignment of the PC. On the contrary, the negative charges on the anionic phospholipid head groups would cause repulsion to allow more than two lipids on the site. For CL, the n value was half compared to other anionic phospholipids because of its unique four lipid tail structure.

5.4.3.1 Lipid binding at the periplasmic interface

The periplasmic side was probed using one of the endogenous Trps, Trp-167 (McjD W247Y). Since there is no obvious cluster of positively charged residues on this side of McjD, no specific binding of anionic phospholipids was expected. The fluorescence quenching data of Trp-167 in Table 5.8 show equal binding affinities towards anionic phospholipids and PC as the binding constants are close to 1. This suggested that there is no selectivity between anionic phospholipids and PC in binding to the site close to Trp-167 consistent with the fact that there is no cluster of positively charged residues close to that site.

5.4.3.2 Lipid binding at the cytoplasmic interface

On the cytoplasmic face of McjD, a positive clustered site containing residues Arg-186 and Arg-311 was predicted to provide a high-affinity binding site for the negative head groups of anionic phospholipids. The site was probed using the reporter Trp-307. The fluorescence quenching data suggest a higher binding affinity towards anionic phospholipids than PC. The binding constants for anionic phospholipids relative to PC are double or more than for PC relative to anionic phospholipids as shown in Figure 5.2. This suggested that the site close to Trp-307 favoured anionic phospholipids resulting in their higher binding affinity. Previous studies using mass spectrometry and crystallisation methods have revealed an anionic phospholipid, PG, bound close to the Trp-307 (Mehmood et al., 2016). It was suggested that the presence of positively charged

residues, Lys-4, Lys-6, Arg-186 and Arg-311 could help attract the negatively charged head groups for selective binding. In addition, following the removal of lipids associated with McjD using octyl glucose neopentyl glycol (OGNG), PG molecules were still retained by the protein, suggesting a strong binding for PG (Mehmood et al., 2016).

However, the same study had speculated an alternative PE binding at the site instead of PG, as a PE head group could also be refined in the electron density (Mehmood et al., 2016). Unfortunately, the binding of PE could not be studied using fluorescence quenching method due to insufficient quenching by brominated PE.

5.4.4 The influence of positive residues on the binding affinity for anionic phospholipids

Mutating the positive residues adjacent to Trp-307 to neutral glutamine caused significant changes to the relative binding constants of anionic phospholipids as shown in Figure 5.4 and Figure 5.6. The binding constants for anionic phospholipids relative to PC were close to 1 suggesting no selectivity in binding between the two phospholipids. These positive residues are vital for creating a high-affinity binding site for anionic phospholipids. The exception was for McjD W167Y:W247Y:L30W:R311Q, where PA showed higher binding constant than PC (but lower than McjD W167Y:W247Y:L30W), which could mean that Arg-311 was less competent than Arg-186 in binding PG.

The findings here suggest that PG binds more tightly to the proposed anionic lipid binding site in McjD than neutral PC. Furthermore, mutating the two positive arginine residues associated with this site leads to the loss of PG binding, which is strong evidence for the lipid seen in McjD crystals (Mehmood et al., 2016) is PG.

5.4.5 Purification of membrane proteins using SMA

Sav1866 and McjD were both successfully purified using SMA. The tolerance of SMA regarding divalent cation, magnesium showed that SMA precipitated significantly when the magnesium chloride concentrations were higher than 2 mM. Due to this low tolerance, 1.3 mM magnesium chloride was used for the ATPase activity assay. However, neither Sav1866 nor McjD had ATPase activity unlike the DDM purified proteins. SMA purification results in the protein being surrounded by the lipids in the native membrane (Stroud et al., 2018). In this case, as *E.coli* was used to express the proteins, the proteins are likely to be surrounded by CL, PG and PE, which are native to *E.coli* (Huijbregts et al., 2000; Raetz, 1978). Anionic phospholipids inhibited the activity of Sav1866 and McjD as discussed earlier in this chapter. Therefore, it is likely that the lack of

ATPase activity of SMA purified Sav1866 and McjD may is due to the protein being surrounded by the anionic phospholipids in its near native environment encapsulated within the SMA. Alternatively, the SMA could restrict conformational changes of the protein by the tight packing of lipids within the SMALP (Stroud et al., 2018). As a result, the protein may be incapable of hydrolysing ATP.

5.5 Conclusion

The effects of anionic phospholipids on ABC transporters have been studied by measuring the ATPase activity of Sav1866 and McjD reconstituted into defined lipid bilayers. Despite the similarity in the head group charges of the phospholipids, variable effects were demonstrated on ABC proteins. For example, while reconstitution of Sav1866 in neutral phospholipid, PC produced the highest level of ATPase activity, reconstitution into PE did not produce the same results possibly due to the non-bilayer forming properties of PE (Cullis & De Kruijff, 1978). On the contrary, reconstitution of McjD into PE had a similar level of activity compared to PC.

The ATPase activity of Sav1866 reconstituted into cationic phospholipids was not as high as when reconstituted into PC but was not as inhibitory as the anionic phospholipids.

Anionic phospholipids such as CL, PG and PA inhibited the ATPase activity of Sav1866 and McjD. However, the level of inhibition caused by PG on McjD was significantly smaller than the other anionic phospholipids. In the absence of the positive residues, the level of inhibition caused by PG increased significantly indicating that binding to the specific PG site might enhance ATPase activity, whereas binding to non-specific sites might inhibit ATPase activity.

The distinctive effect of PG on McjD was further investigated using a fluorescence quenching technique, which suggested that the positive amino acid residues clustered on the cytoplasmic site of McjD was a high-affinity binding site for anionic phospholipids. Upon mutating the positively charged residues to neutral glutamines, the binding affinity for anionic phospholipids was indistinguishable from that of neutral PC, suggesting that the positively charged residues were responsible for creating the high affinity binding site for anionic phospholipids. Such binding sites could be crucial in inhibiting the activity of multidrug resistance proteins such as P-glycoprotein (Elliott et al., 2005; Sharom, 2011).

Lastly, SMA purification of membrane proteins is a relatively simple technique that conserves the near native environment of the protein with its surrounding lipids. The purification of Sav1866 and McjD using SMA led to inactive proteins. This may be due to the presence of anionic phospholipids in the SMALPs as they were encapsulated from the *E.coli* membrane that contains 20% PG, 5% CL and 75% PE (Huijbregts et al., 2000; Raetz, 1978). Alternatively, the SMA could create a sub-optimal environment for the protein preventing conformational flexibility within the SMALPs (Stroud et al., 2018).

Chapter 6 Expression and purification of eukaryotic ABC transporter, Mdl1

6.1 Introduction

Following the review of bacterial ABC transporters, Sav1866 and McjD in the previous chapters, this chapter focuses on a eukaryotic ABC transporter, Mdl1. The work was undertaken in the laboratory of the CASE studentship sponsor, Syngenta, at Jealott's Hill.

Mdl1 is a half ABC transporter that resides in the inner membrane of the mitochondria in yeast (Dean et al., 1994; Kuchler, Goransson, Viswanathan, & Thorner, 1992; Young, Leonhard, Tatsuta, Trowsdale, & Langer, 2001). Peptides with molecular masses between 600 and 2100 Daltons that are degraded by m-AAA protease in the mitochondrial matrix were proposed to be transported by Mdl1 across the inner membrane (Young et al., 2001). However, transport assays failed to show any evidence for the transport of the peptides by Mdl1 in liposomes (Hofacker et al., 2007).

A recent study has exploited whole-genome sequencing and reverse genetics to elucidate resistance mechanisms towards anilinopyrimidine fungicides in *B. cinerea*. Nine resistant genes were identified in laboratory generated and field isolate mutant resistant strains, all of them encoding mitochondrial proteins, indicating that mitochondria are the likely target of this family of fungicides (Mosbach et al., 2017). Mdl1 is one of these proteins, and interestingly is the major contributor to resistance seen in the field (Mosbach et al., 2017).

6.1.1 The role of Mdl1 in anilinopyrimidine fungicide resistance

Anilinopyrimidine (AP) fungicides is a group of fungicides comprising of cyprodinil (Heye et al., 1994), pyrimethanil (Neumann, Winter, & Pittis, 1992) and mepanipyrim (Maeno, Miura, Masuda, & Nagata, 1990). They are used to treat a range of plant pathogens, but a major target is the mould, *Botrytis cinerea*, that is responsible for damaging crops such as grapes and vegetables.

Although the mechanism of resistance is not established, mutations of the protein that caused resistance have been located within the transmembrane helices of Mdl1, which are predicted to form a part of the substrate binding cavity (T. A. Schaedler et al., 2015). Thus, the mutations could affect substrate preference or change the kinetics of substrate transport (Mosbach et al., 2017).

Changes in nuclear gene expression have been reported in the absence of i-AAA protease and Mdl1 in yeast cells suggesting a role for Mdl1 in mitochondria to nucleus signalling (Arnold, Wagner-Ecker, Ansorge, & Langer, 2006). Although such signalling pathway has not been observed in *B. cinerea*, the mutations of *mdl1* could interfere with the transport of possible peptides that can act as signalling molecules (Mosbach et al., 2017). In addition, Mdl1 appears to play a role in regulating resistance to oxidative stress; it reduces hydrogen peroxide sensitivity in Atm1 deficient yeast. Atm1 is an ABC transporter involved in iron homeostasis (Chloupkova, LeBard, & Koeller, 2003).

Given the link between Mdl1 and anilinopyrimidine resistance, and the fact that Syngenta produces the AP fungicide cyprodinil, the expression and preliminary characterisation of the activity of *B. cinerea* Mdl1 and the resistance mutants BcMdl1^{E407K}, BcMdl1^{G422R} and BcMdl1^{S466R} as well as the homologous proteins in *S. cerevisiae* was undertaken. This is a preliminary investigation *en route* to identifying the substrate(s) for Mdl1 and the role of Mdl1 in AP resistance.

6.2 Materials and Methods

Anatrace

- n-Dodecyl-β-D-maltopyranoside (DDM)

Biolabs

- NEB 5-alpha competent *E.coli*
- Super Optimal broth with Catabolite repression (SOC) outgrowth medium

Clonetech

- Amino acids supplement without uracil
- Yeast minimal SD base with galactose and raffinose
- Yeast minimal synthetic defined base media/agar

GE Healthcare

- HiTrap FF histidine-tagged protein purification column

Generon

- Vivaspin 20 100,000 molecular weight cut off
- Quick Coomassie protein stain

Merck

- Digitonin

MP Biomedicals

- Zymolyase-20T from *Arthrobacter luteus*

Roche

- EDTA- free complete protease inhibitor mixture

Sigma

- Agar
- Amersham ECL Rainbow Marker – Full range
- Ampicillin
- BSA
- Dithiothreitol (DTT)
- EDTA
- Glucose
- Imidazole
- Lithium acetate
- MOPS
- Peptone
- Polyethylene glycol (PEG) 3500

- Potassium phosphate
- Single-Stranded carrier DNA
- Sodium chloride
- Sorbitol
- Sucrose
- Tris
- Yeast extract

6.2.1 Construction of plasmids

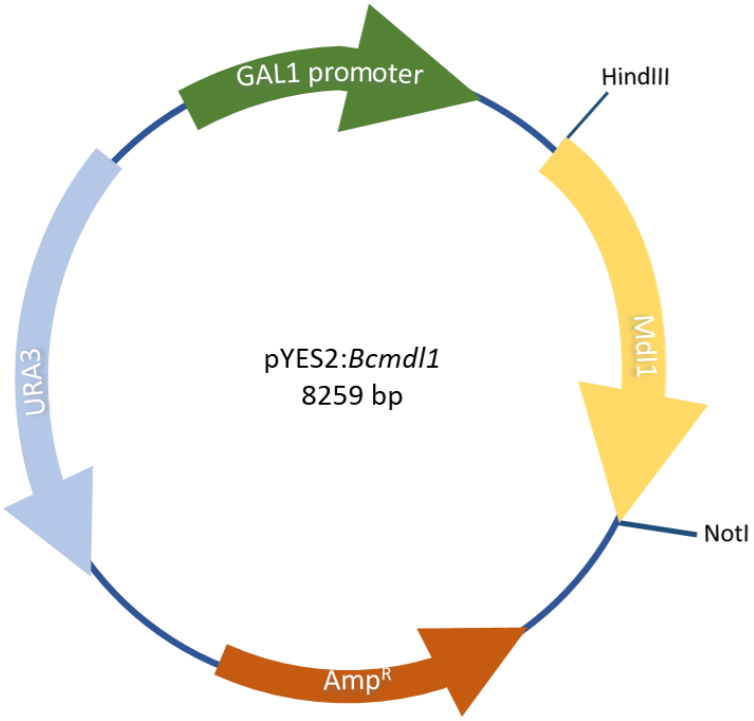

Figure 6.1 Circular representation of pYES2: *Bcmdl1* vector. The *mdl1* gene with a C-terminal octa-Histidine tag was inserted into a pYES2 vector (8259 bp) (Invitrogen) using HindIII and NotI multiple cloning sites. GAL1 promoter allows inducible expression of the *mdl1* gene. The vector provides ampicillin resistance, useful for selecting *E.coli* transformants while *URA3* allows selection of transformed yeast in the uracil-deficient medium.

The *mdl1* gene was introduced into a pYES2 vector (ThermoFisher Scientific) between HindIII and NotI multiple cloning sites by GENEWIZ (Figure 6.1). The recombinant protein contains a *GAL1* promoter for expression, which is highly induced by galactose and repressed by glucose. An octahistidine affinity tag at the C terminus on the vector is for nickel affinity chromatography purification. pYES2 vector provides ampicillin resistance and *URA3* gene for selection.

6.2.2 Transformation of E.coli NEB 5-alpha competent cells

Competent *E.coli* NEB 5-alpha cells were thawed on ice. 1µl of DNA was added to 10µl of NEB 5-alpha cells and mixed gently. The NEB 5-alpha cells were then placed on ice for 10 minutes, and heat shocked at 42˚C for 60 seconds. The cells were placed back on ice for 2 minutes, and 100 µl of SOC outgrowth media (2% vegetable peptone, 0.5% yeast extract, 10 mM NaCl, 2.5 mM KCl, 10 mM $MgCl_2$, 10 mM $MgSO_4$, 20 mM glucose) was added to the mixture. After 60 minutes of incubation at 37˚C, shaking at 200 rpm, the NEB 5-alpha cells were plated onto LB plates containing ampicillin.

6.2.3 Small-scale purification of plasmid DNA

GeneJet Plasmid Miniprep kit from ThermoFisher Scientific was used, and the protocol described in 2.2.2.6 was followed for plasmid DNA purification.

6.2.4 Transformation of *S. cerevisiae* BY4743 competent cells

This transformation protocol is based on the method described in (Daniel Gietz & Woods, 2002). *S. cerevisiae* BY4743 competent cells were streaked onto a YPD agar plate (1% yeast extract, 2% peptone, 2% dextrose, 2% agar). After 3-5 days of incubation at 30˚C, a single colony was used to inoculate 5 ml of YPD media (1% yeast extract, 2% peptone, 2% dextrose) and incubated at the same temperature overnight. 3 ml of the overnight culture was used to inoculate 50 ml of YPD media for 5 hours at 30˚C shaking at 200 rpm. The cells were then harvested by centrifuging at 3000 g for 5 minutes at room temperature. The cells were washed with sterile distilled water and centrifuged at 3000 g for another 5 minutes. Next, the cells were resuspended in 1 ml of 100 mM lithium acetate (LiAc) to give a cell concentration of $1x10^9$. 100 µl of the cell suspension was transferred to a 1.5 ml centrifuge tube and centrifuged for 30 seconds. The supernatant was removed, and the cell pellet was resuspended in the transformation mix (Polyethylene glycol (PEG) 3500 50% (w/v), 1 M LiAc, single-stranded carrier DNA (200 mg of salmon sperm DNA in 100 ml of TE buffer (10mM Tris-HCl, 1 mM Na2EDTA, pH 9.0) pre-boiled for 5 minutes) and plasmid DNA) followed by incubation at 30 ˚C for 30 minutes and 42˚C for 20 minutes. The tube was centrifuged for another 30 seconds, and the supernatant was removed. The cells were resuspended in 300 µl of sterile distilled water by vortexing and plated onto yeast minimal synthetic defined (SD) base agar (Clonetech) supplemented with 2% glucose and amino acids without uracil. The plates were incubated for 5 days at 30˚C.

6.2.5 Mdl1 protein expression and purification

6.2.5.1 Growth of *S.cerevisiae* BY4743 cells

A fresh colony was used to inoculate 10 ml of yeast minimal SD base media (Clonetech) supplemented with 2% glucose (sterile filtered) and amino acids without uracil. The culture was incubated at 30˚C for 24 hours with shaking at 200 rpm. Next, the 10 ml culture was used to inoculate 1 L of yeast minimal SD base media supplemented with 2% glucose and amino acids without uracil and incubated at 30˚C for 24 hours with shaking at 200 rpm.

6.2.5.2 Mdl1 protein expression

For induction, the cells were harvested by centrifuging at 8000 g at 4˚C for 20 minutes and resuspended in induction media (yeast minimal SD base with galactose and raffinose supplemented with amino acids without uracil) with final OD of 0.4. The induction period was for 8 hours at 30˚C with shaking at 200 rpm. Following induction, the cells were harvested as earlier and stored at -20˚C.

6.2.5.3 Isolation of crude mitochondria

The pelleted cells were first washed with distilled water and centrifuged for 5 minutes at 3000 g at room temperature. This step was repeated before the cells were resuspended in DTT buffer (100 mM Tris/H_2SO_4 pH 9.4, 10 mM dithiothreitol) in 2 ml of buffer per gram of weight cells ratio. The cell suspension was transferred to a 50 ml Falcon plastic tube and incubated at 30˚C for 20 minutes at 70 rpm in a shaker. The cells were then pelleted by centrifugation at 3000 g for 5 minutes at room temperature. The pelleted cells were resuspended in Zymolyase buffer (20 mM potassium phosphate pH 7.4, 1.2 M sorbitol) without the Zymolyase-20T in 7 ml of buffer per gram of wet cells ratio. The cells were then pelleted by centrifugation at 3000 g for 5 minutes at room temperature. After centrifugation, the cells were resuspended in Zymolyase buffer without the Zymolyase in 7 ml of buffer per gram of wet cells ratio and transferred to a glass flask. Powder of Zymolyase-20T was added to the glass flask in 5 mg of Zymolyase-20T per gram of wet cells ratio. The flask was incubated shaking at 70 rpm at 30˚C for 30 minutes in a shaker. Following incubation with Zymolyase-20T, the cell wall was digested, and spheroplasts were formed. The spheroplasts were centrifuged at 2200 g for 8 minutes at 4˚C, and the pelleted spheroplasts were resuspended in ice-cold homogenization buffer (10 mM Tris/HCl pH 7.4, 0.6M sorbitol, 1 mM EDTA, 0.2% (w/v) BSA) in 6.5 ml of buffer per gram of weight cells ratio. The spheroplasts were re-pelleted by centrifugation at 2200 g for 8 minutes at 4˚C and resuspended in ice-cold homogenization buffer as before. Next, using a pre-chilled glass homogeniser, the spheroplasts

were homogenised with 15 strokes of the pestle and diluted with 1 volume of ice-cold homogenization buffer. The homogenised spheroplasts were centrifuged at 1500 g for 5 minutes at 4˚C to pellet unbroken cells, nuclei and any large debris. The supernatant was then centrifuged at 3000 g for 5 minutes at 4˚C. The resulting supernatant was centrifuged at 12,000 g for 15 minutes at 4˚C. The pellet was resuspended in ice-cold homogenization buffer as before and centrifuged at 3000 g for 5 minutes at 4˚C. The resulting supernatant was centrifuged again at 12,000 g for 15 minutes at 4˚C. The pellet contained crude mitochondria with other contaminants such as endoplasmic reticulum, Golgi and vacuoles.

6.2.5.4 Purification of pure mitochondria using sucrose density gradient

Crude mitochondria were resuspended in 3.5 ml of SEM buffer (10 mM MOPS/KOH pH 7.2, 250 mM sucrose, 1 mM EDTA). To set up a sucrose gradient, 1.5 ml of ice-cold 60% (w/v) sucrose in EM buffer (10 mM MOPS/KOH pH 7.2, 1 mM EDTA) was placed at the bottom of a Beckman Ultra-Clear centrifuge tube. Next, 60% sucrose layer was overlaid with 4 ml of 32%, 1.5 ml of 23% and 1.5 ml of 15% all in EM buffer. Finally, the crude mitochondria fraction was placed on top of the 15% sucrose layer. The tubes were centrifuged in a Beckman SW41 Ti swinging-bucket rotor for 1 hour at 134,000 g at 4˚C. The mitochondria formed a band at the 60%/32% sucrose interface and were carefully removed from the sucrose gradient using a Pasteur pipette and diluted with 2 volume of SEM buffer. To pellet the mitochondria, the diluted mitochondria fraction was centrifuged at 10,000 g for 30 minutes at 4˚C in a TLC-100 rotor.

6.2.5.5 Protein purification

Following the isolation of mitochondria, protein was solubilised in Buffer A (50 mM Tris-HCl, 150 mM NaCl, 15% (v/v) glycerol, 2 mM imidazole, pH 7.5) supplemented with 1% n-Dodecyl-β-D-maltopyranoside (DDM) and EDTA- free complete protease inhibitor mixture in 1 ml for every 5 mg of wet mitochondria ratio. After the solubilising of the membrane for 1 hour at 4˚C, the solution was centrifuged at 100,000 g at 4˚C for 30 minutes. Any insoluble protein and larger protein complexes were pelleted in this step. The supernatant was then applied to a His-trap column to allow the His-tagged protein to bind to the nickel. The column was washed with 5 column volume of Buffer A supplemented with 0.1% DDM and 60 mM imidazole followed by 120 mM imidazole. The bound protein was eluted with 5 column volume of Buffer A supplemented with 0.1% DDM and 200 mM imidazole. The eluted protein was concentrated using a Vivaspin protein concentrator with 100 kDa molecular weight cut off.

6.2.6 SDS-PAGE gel

Pre-cast Bolt 4-12% Bis-Tris Plus protein gel (Thermo Fisher Scientific) was used to separate proteins. Samples were prepared using LDS sample buffer and Bolt sample reducing agent. The gel tank was filled with Bolt MES SDS running buffer, and a constant 200 V was applied for 26 minutes.

6.2.7 Western Blot

The SDS-PAGE gel was transferred onto a PVDF membrane using a Trans-Blot Turbo (Bio-Rad). The bottom ion reservoir stack was placed on the anode cassette electrode followed by the blotting membrane and the gel. The top ion reservoir stack was then placed on top of the gel, and a blot roller was used to remove trapped air bubbles. Once the cathode cassette electrode was placed on the top ion reservoir stack, the cassette lid was locked. The gel was transferred onto the membrane at constant 2.5 A for 7 minutes at room temperature.

Following the transfer, an iBind Flex western Device (Thermo Fisher Scientific), which uses a sequential lateral flow technology was used to block the membrane and incubated with mouse monoclonal anti-His6-peroxidase conjugated primary antibody (diluted 1:1000). The iBind Flex solution (prepared using 10 ml of iBind Flex 5X buffer, 500 µl of iBind Flex 100X Additive and 39.5 ml of distilled water) acts as a blocking, washing and diluting reagent. Once the membrane is placed on a wet (with iBind Flex solution) iBind Flex Card, the primary antibody along with iBind Flex solution are added to the respective wells and allowed to flow towards the membrane. The glass fibre matrix of the iBind Card allows a consistent flow of the solutions to the membrane. After 2.5 hours incubation, the membrane was incubated with 1-Step Ultra TMB (3, 3', 5, 5' – tetramethylbenzidine) -Blotting Solution (Thermo Fisher Scientific), which is a horseradish peroxidase (HRP) substrate and produces an insoluble dark blue precipitate.

6.2.8 Gel and western blot analysis

SDS-PAGE gels were stained using Quick Coomassie protein stain. Protein gels and western blots were scanned using a BIO-RAD Chemidoc MP scanner.

6.2.9 ATPase assay

The ATPase activity was measured using the ATPase activity assay kit (MAK113) from Sigma. Free phosphates liberated during hydrolysis of ATP by the protein was quantified using malachite green reagent, which formed a stable dark green colour measured at 620 nm using a Spectra Flour plus Tecan plate reader. Phosphate standards were prepared for colourimetric detection

from 0 to 50 µM phosphate concentration to determine the concentration of free phosphate liberated by the protein. The reaction was conducted in a 96 well flat-bottom plate and contained 10 µl of 4 mM ATP, 10 µl of 4 mM pyridine nucleotide, 10 µl of protein and assay buffer (40 mM Tris, 80 mM NaCl, 8 mM $MgAc_2$, and 1 mM EDTA, pH 7.5) to make up to 40 µl. After 30 minutes of incubation at room temperature, 200 µl of malachite green reagent was added and incubated for another 30 minutes followed by colourimetric detection using a FLUOstar OPTIMA plate reader. The ATPase activity rate (µmole/min/µg) was calculated using the formula below.

$$ATPase\ activity\ rate = \frac{Sa\ \times Rv}{Sv\ \times T}$$

Where, Sa = concentration of free phosphate (µM); Rv = reaction volume (µl); Sv = sample volume (µl) or sample mass (µg); T = reaction time (min)

6.3 Results

6.3.1 Protein sequence alignment of *S.cerevisiae* Mdl1 and *B.cinerea* Mdl1

There is 51% similarity in sequence between *S.cerevisiae* Mdl1 (Scmdl1) and *B.cinerea* Mdl1 (Bcmdl1) (Papadopoulos & Agarwala, 2007). Bcmdl1 mutations that cause resistance to AP fungicides, E407K, G422R and S466R correspond to Scmdl1 E332, G348 and S391, which are highlighted in Figure 6.2.

```
Scmdl1   1  MIVRMIRL---------C---------------------KGPKLLRSQFAS---------ASALYSTKSLFKPPMYQKAE  41
Bcmdl1   1  -MRRTLTLGNGWGGASICDVAFKQVSKPISAPAAARWTPSGPSLVAKRFSSGFKNSPSPLSPASKPTPQLSTSRLLQQTR  79

Scmdl1  42  INLIIP------------------------HRKHFLLR-----------SIRLQSDIAQGKKSTKPTLKLSNANSKSSG-  85
Bcmdl1  80  IGLSSPWRPAVSQLRPFNSASPLQNSPKGSDRQDHITRERQRREEEEEDNIDEQGDFARSEKASKATQVNLSARLQSSGK  159

Scmdl1  86  -------FKDIKRLFVLSKPESKYIGLALLLILISSSVSMAVPSVIGKLLDLASESDGEDEEGSKSNKLYGFTKKQFFTA  158
Bcmdl1 160  KQGNTAAFGEIWRLLKIARPEAKWLGLAFVFLLISSSITMSIPFSIGKILDLATKDPSEGE------KLFGLDISQFFIA  233

Scmdl1 159  LGAVFIIGAVANASRIIILKVTGERLVARLRTRTMKAALDQDATFLDTNRVGDLISRLSSDASIVAKSVTQNVSDGTRAI  238
Bcmdl1 234  LACVLTMGAAANYGRIIILRIVGERIVARLRSQLYRRTYVQNAEFFDANRVGDLISRLSSDTVIVGKSITQNLSDGLRAI  313

Scmdl1 239  IQGFVGFGMMSFLSWKLTCVMMILAPPLGAMALIYGRKIRNLSRQLQTSVGGLTKVAEEQLNATRTIQAYGGEKNEVRRY  318
Bcmdl1 314  VSGGAGFTAMAWVSLKLTSILCLMFPPVAIGAFFYGRAIRNLSRKIQRNLGTLTKIAEERLGNVRTSQAFAGETQEVGRY  393

Scmdl1 319  AKEVRNVFHIGLKEAVTSGLFFGSTGLVGNTAMLSLLLVGTSMIQSGSMTVGELSSFMMYAVYTGSSLFGLSSFYSELMK  398
Bcmdl1 394  NQQIKKIFSLGKREALISATFFSSSGFFGNMTILALLYTGGSMVKNGMISIGELTSFLMYTAYAGSSLFGVSSFYSELMK  473

Scmdl1 399  GAGAAARVFELNDRKPLIRPTIGKDPVSLAQKPIVFKNVSFTYPTRPKHQIFKDLNITIKPGEHVCAVGPSGSGKSTIAS  478
Bcmdl1 474  GVGAASRLFELQDRKPTIPATVGTK-VKSAQGVIKFHNVSFAYPTRPAVTIFDGLDFEIPSGTNVAIVGPSGGGKSTIGS  552

Scmdl1 479  LLLRYYDVNSGSIEFGDEDIRNFNLRKYRRLIGYVQQEPLLFNGTILDNILYCIPPEIAEQDDRIRRAIGKANCTKFLAN  558
Bcmdl1 553  LLLRFYNPTEGKITINGQDITKMNGKSLRRRIGMVGQEPVLMSGSVAENIAYGKPHASRSE---IIAAARKANC-QFIGD  628

Scmdl1 559  FPDGLQTMVGARGAQLSGGQKQRIALARAFLLDPAVLILDEATSALDSQSEEIVAKNLQRRVERGFTTISIAHRLSTIKH  638
Bcmdl1 629  FPEGLDTQVGARGAQLSGGQKQRIAIARALLKNPDILILDEATSALDAESETLVNSALAALLRGHNTTISIAHRLSTIKR  708

Scmdl1 639  STRVIVLGKHGSVVETGSFRDLIAIPNSELNALLAEQ-------------------QDEEGKGGVIDLDNSVAREV----  695
Bcmdl1 709  SDHIIVLGNDGKVAETGTYNSLSNNPNSAFSKLMEWQMSGGDAADHRPVELEGHFTESEEISDDLSRLSDSDATEGEAIE  788

Scmdl1      -----------------
Bcmdl1  789  EKTKTEAVLEKTNTRTK  805
```

Figure 6.2 Protein sequence alignment of *S.cerevisiae* mdl1 (Scmdl1) and *B. cinerea* mdl1 (Bcmdl1). Red coloured amino acids are highly conserved, and the blue and grey amino acids are not conserved. Bcmdl1 mutations E407K, G422R and S466R (causing resistance to AP fungicides) that correspond to Scmdl1 E332, G348 and S391 are highlighted in the rectangles. Alignment performed using BLASTp (Papadopoulos & Agarwala, 2007).

6.3.2 Transformation of *E.coli* NEB 5-alpha competent cells

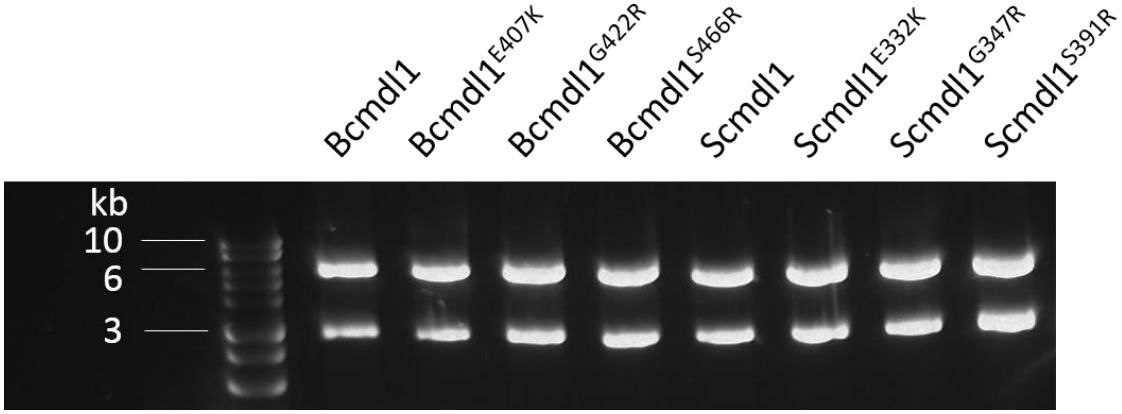

Figure 6.3 Restriction digest analysis of constructs of *Bcmdl1* and *Scmdl1*. 400 ng of plasmid DNA was digested with NdeI and HindIII yielding 5.3 kbp and 2.7 kb DNA fragments. The DNA fragments were separated on 1% agarose gel and visualised using Safeview (NBS-SV1) under the UV. 1 kb DNA ladder (Promega) is on the left.

Bcmdl1 and *Scmdl1* constructs obtained from GENEWIZ were used to transform *E.coli* NEB 5-alpha cells using the protocol described in 6.2.2. Transformed *E.coli* NEB 5-alpha cells containing the pYES2 vector with the *mdl1* gene were used to amplify the plasmid DNA for further *S. cerevisiae* BY4743 transformation. The purified plasmid DNA was digested using NdeI and HindIII restriction digest enzymes resulting in 5.3 kbp and 2.7 kbp DNA fragments as shown in the agarose gel in Figure 6.3.

6.3.3 Expression and purification of Mdl1

6.3.3.1 Isolation of mitochondria from *S. cerevisiae* BY4743 cells

Following the growth and induction of *S. cerevisiae* BY4743 cells (see methods 6.2.5), the cell pellet was frozen from which the mitochondria were isolated using the protocol described in 6.2.5.3. The pellet from each centrifugation step was resuspended in Buffer A (50 mM Tris-HCl, 150 mM NaCl, 15% (v/v) glycerol, 2 mM imidazole, pH 7.5) and loaded onto an SDS-PAGE gel and a western blot was performed as shown in Figure 6.4. The lack of Mdl1 protein observed during the purification process (lanes 1-3) indicates that the method provided a concentrated and pure mitochondria, which was ideal for the extraction of Mdl1 proteins.

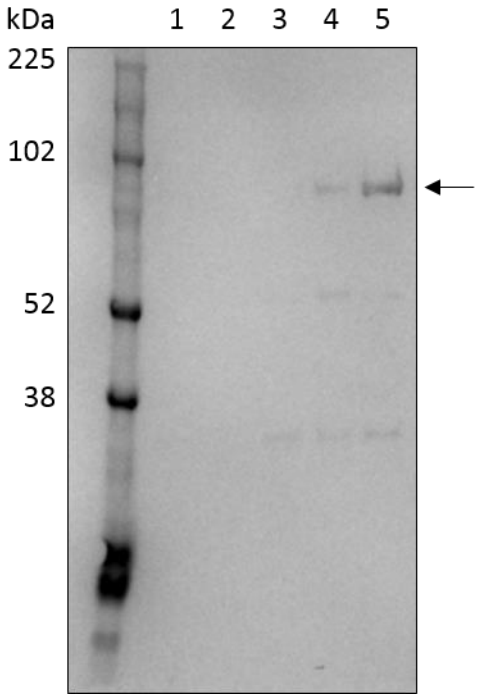

Figure 6.4 Extracts from the purification steps for the isolation of the mitochondria. Lane 1 shows cell debris pelleted at 1500 x g following Zymolyase lysis and homogenisation treatment. Lane 2 and 3 show subsequent pellets formed following 3000 x g centrifugation steps. Lane 4 shows 0.4 mg of crude mitochondria following 12000 x g centrifugation step. Lane 5 shows 2 mg of purified mitochondria following sucrose density gradient. The arrow shows BcMdl1^{E407K} (87 kDa) protein. 1:1000 mouse monoclonal anti-His6-peroxidase conjugated primary antibody and TMB solution were used for colourimetric detection of the protein on the western blot. The molecular marker is shown on the left.

6.3.3.2 Solubilisation of Mdl1

1% digitonin has previously been used for the solubilisation of the Mdl1 protein (Hofacker et al., 2007). The protein here was solubilised in Buffer A (50 mM Tris-HCl, 150 mM NaCl, 15% (v/v) glycerol, 2 mM imidazole, pH 7.5) supplemented with 1% digitonin and EDTA- free complete protease inhibitor mixture in 1 ml for every 5 mg of wet membrane for 1 hour at 4˚C. Any insoluble membrane was pelleted by centrifugation at 100,000 g at 4˚C for 30 minutes

Whole cell extract, soluble fraction and insoluble pellet were loaded onto an SDS-PAGE gel after resuspending in Buffer A (Figure 6.5). Digitonin was not effective at solubilising Mdl1. This is evident by the presence of the protein in the insoluble fraction rather than the soluble fraction in Figure 6.5.

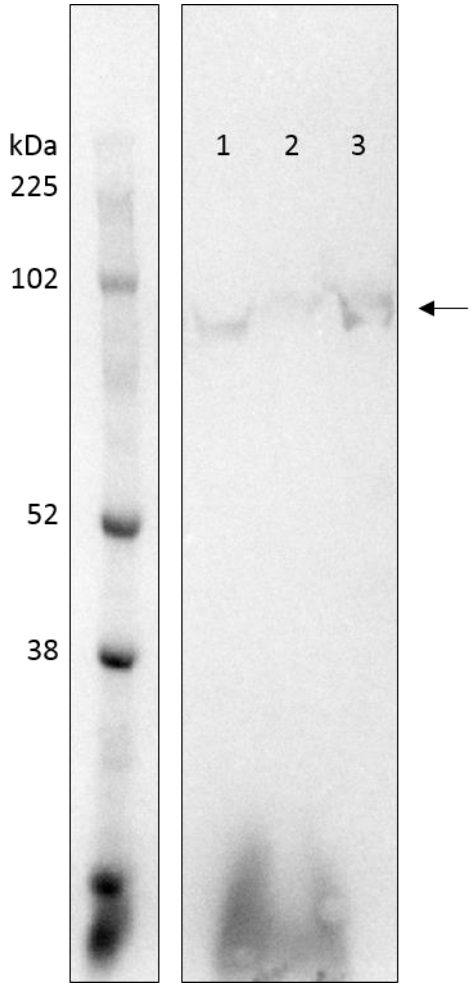

Figure 6.5 Solubilisation efficiency of 1% digitonin. Lane 1 shows total cell pellet. Lane 2 shows 1% digitonin solubilised fraction. Lane 3 shows the insoluble fraction of 1% digitonin solubilisation. The arrow indicates BcMdl1^{G422R} protein (87 kDa). 1:1000 mouse monoclonal anti-His6-peroxidase conjugated primary antibody and TMB solution were used for colourimetric detection of the protein on the western blot. The molecular marker is shown on the left.

DDM was the alternative choice for solubilisation, which gave better solubilisation of Mdl1 protein and was used successfully for further purification.

Due to the low expression of Mdl1 protein, the resulting yield of the protein was very low. Nevertheless, sufficient material was produced to demonstrate the purification of BcMdl1, ScMdl1 and ScMdl1^{E332K} as shown in Figure 6.6 and Figure 6.7.

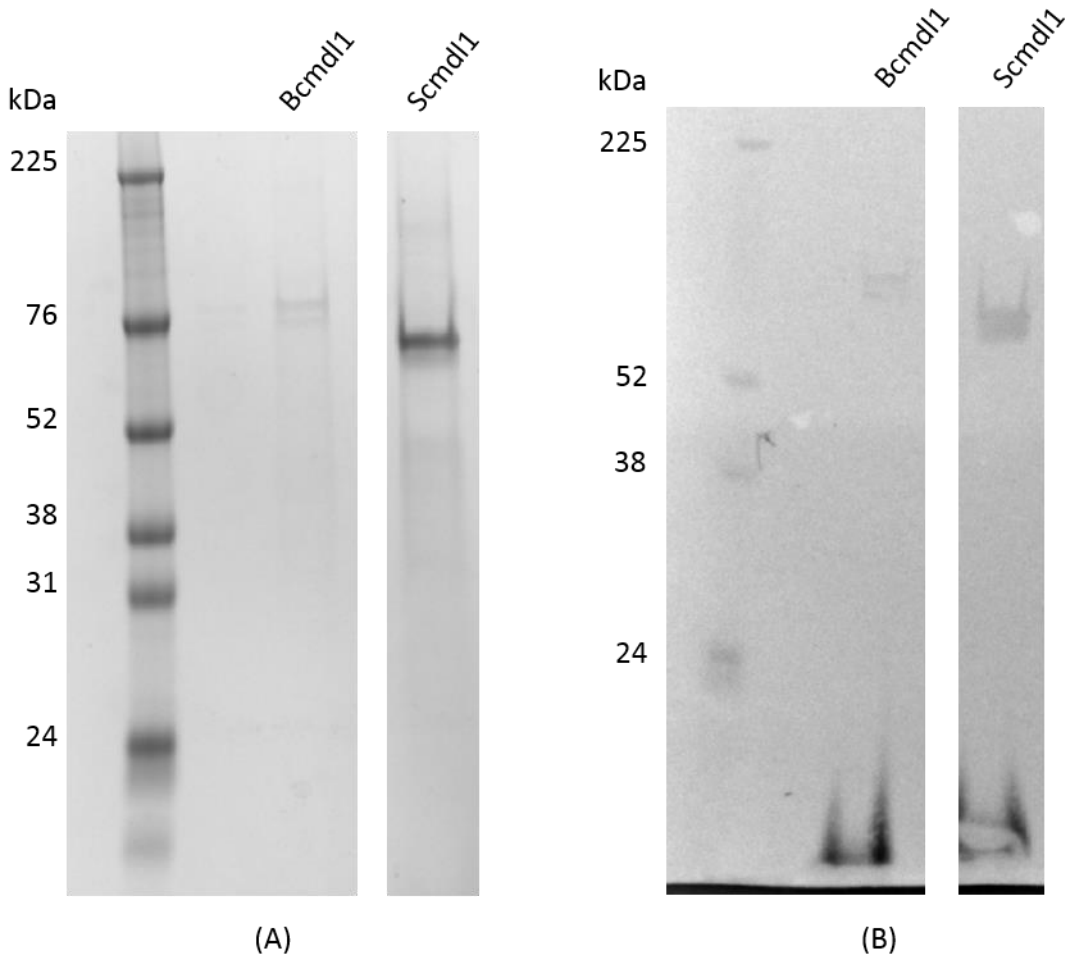

Figure 6.6 Purification of BcMdl1 (87 kDa) and ScMdl1 (76 kDa). Quick Coomassie protein stain was used to visualise proteins on the (A) SDS-PAGE gel. 1:1000 mouse monoclonal anti-His6-peroxidase conjugated primary antibody and TMB solution were used for colourimetric detection of the protein on the (B) western blot. The molecular markers are shown on the left.

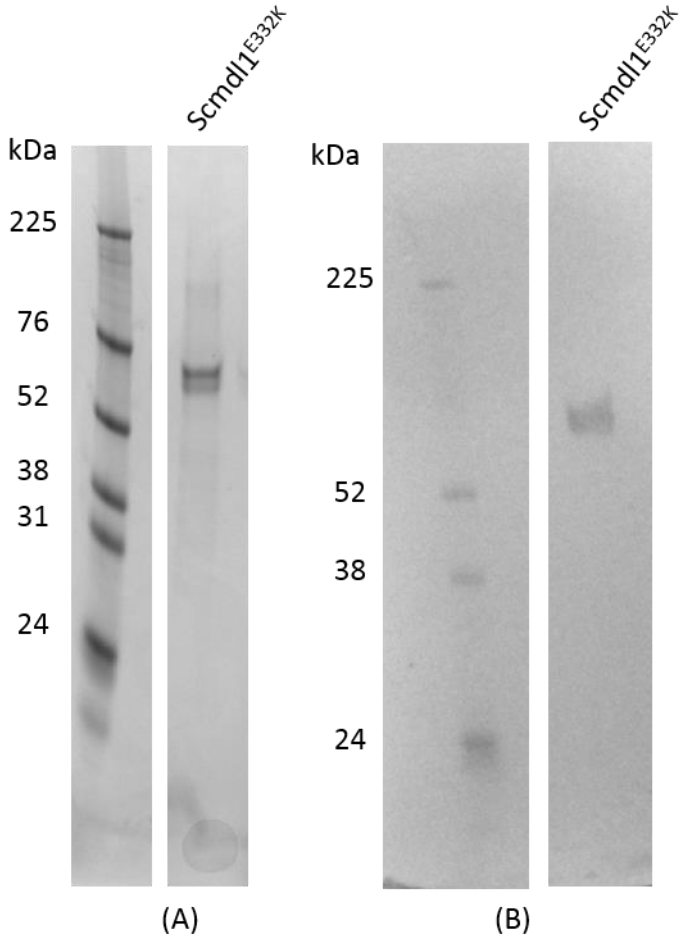

Figure 6.7 Purification of ScMdl1^{E332K} (76 kDa). Quick Coomassie protein stain was used to visualise proteins on the (A) SDS-PAGE gel. 1:1000 mouse monoclonal anti-His6-peroxidase conjugated primary antibody and TMB solution were used for colourimetric detection of the protein on the (B) western blot. The molecular markers are shown on the left.

6.3.3.3 Determination of protein concentration

There was insufficient material to perform a BCA protein assay, so the protein concentrations were estimated from the intensity of the Mdl1 proteins relative to the protein standards from the SDS-polyacrylamide gels. This provided a rough estimation of the concentration of the proteins. Due to the uncertainty in the concentration of the protein, the values calculated for the ATPase activity of the protein may not reflect true values.

6.3.4 ATPase activity of Mdl1

The ATPase activity assay was measured according to the protocol described in 6.2.9.

The absorbance of free phosphates ranging from 0 µM to 50 µM was measured to produce a standard curve (Figure 6.8). The basal ATPase activity rate of ScMdl1 and BcMdl1 was compared to when various pyridine nucleotides NAD^+, NADH, $NADP^+$ or NADPH were added. The rate of activity was calculated as described in 6.3.4.

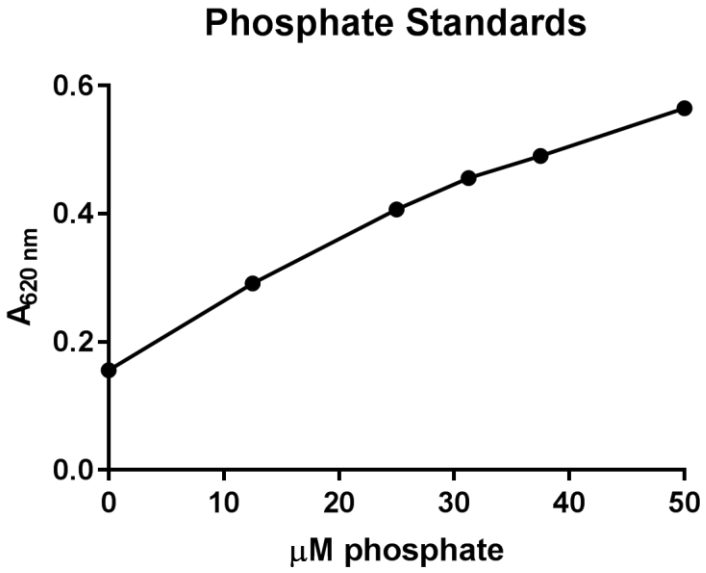

Figure 6.8 Absorbance curve of malachite green reagent reacting with free phosphates at 620nm. Free phosphate from 0 µM to 50 µM was diluted in ultrapure water to produce a standard curve. The absorbance was measured using a Spectra Flour plus Tecan plate reader in a 96 well flat-bottom plate.

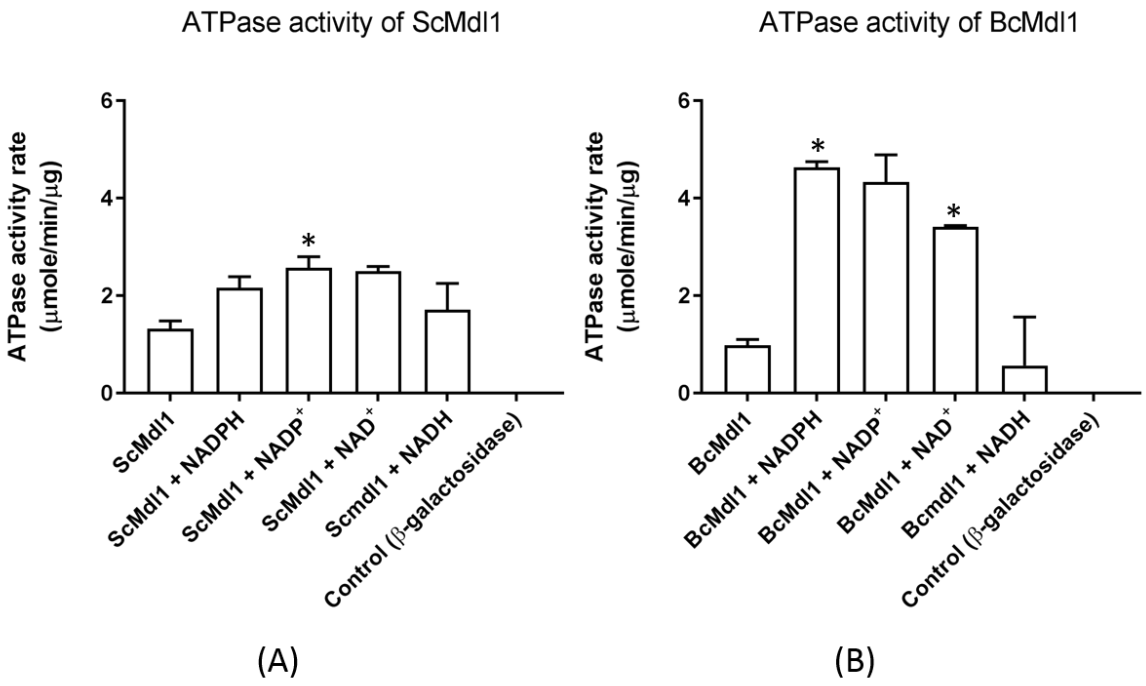

Figure 6.9 Basal and 1 mM pyridine nucleotides induced ATPase activity (μmole/min/μg) of (A) ScMdl1 and (B) BcMdl1. The absorbance of malachite green reagent reacting with the liberated phosphates was measured using a Spectra Flour plus Tecan plate reader in a 96 well flat-bottom plate at 620 nm. The experiment was performed once and the absorbance was measured in duplicates to generate the protein's ATPase activity. The statistical analysis was performed using a paired t-test. Asterisk indicates statistically different values between the basal and the pyridine nucleotide-induced conditions (*$P < 0.05$).

Following the elution of the protein from the His-trap column, the eluted sample was concentrated and used to measure the ATPase activity of Mdl1. A pYES2 vector containing the *lacZ* gene was used to express and purify β-galactosidase as a negative control and was treated the same way. An equal amount of Mdl1 protein was used for measuring the basal activity and when in the presence of pyridine nucleotides. Due to the low yield of the protein, the ATPase activity could only be done once in duplicates.

The basal activity of ScMdl1 was 1.3 μmole/min/μg. This was increased by almost two-fold when $NADP^+$ (2.6 μmole/min/μg) or NAD^+ (2.5 μmole/min/μg) was added. NADPH and NADH also increased the activity to 2.2 μmole/min/μg and 1.7 μmole/min/μg respectively.

The basal activity of BcMdl1 (1.0 μmole/min/μg) was increased almost 5 fold by NADPH (4.6 μmole/min/μg) and $NADP^+$ (4.3 μmole/min/μg). NADH decreased the activity slightly to 0.6 μmole/min/μg and NAD^+ increased it to 3.4 μmole/min/μg.

No ATPase activity was detected from the β-galactosidase sample, which served as the negative control.

Unfortunately, due to the low yield of ScMdl1^{E332K}, there was insufficient protein to measure its ATPase activity

6.4 Discussion

6.4.1 Anilinopyrimidine fungicide

Early studies on AP fungicides suggested the inhibition of methionine biosynthesis in the pathogen as their primary target. This was supported by the partial reversal of growth inhibition when sulphur containing amino acids such as methionine and homocysteine were added to the minimal culture media (Leroux, 1994; Masner, Muster, & Schmid, 1994). Further analysis of the metabolites in the methionine biosynthesis pathway using [^{35}S] disodium sulphate revealed an accumulation of [^{35}S] cystathione and a 3-fold reduction in [^{35}S] methionine in AP-treated *B. cinerea*, which suggested cystathione β-lyase as the primary target of inhibition (Rene Fritz, Lanen, Colas, & Leroux, 1997). However, upon examination of crude extract of cystathione β-lyase isolated from *Botrytis cinerea*, inhibition by AP was very low. Besides, there was no significant difference in inhibition of cystathione β-lyase extract from AP resistant and the sensitive strain, indicating that cystathione β-lyase was unlikely to be the primary target of AP fungicides (René Fritz, Lanen, Chapeland-Leclerc, & Leroux, 2003). Moreover, the addition of sulphur containing amino acids to AP treated *Penicillium digitatum* failed to reduce the toxicity of AP fungicides suggesting an alternative mode of action (Kanetis, Forster, Jones, Borkovich, & Adaskaveg, 2008).

AP fungicides have also been shown to inhibit the secretion of hydrolytic enzymes such as lipases, proteases, and cell wall degrading enzymes such as cutinase, pectinase and cellulase leading to their intracellular accumulation (Milling & Richardson, 1995; Miura, Kamakura, Maeno, Hayashi, & Yamaguchi, 1994). Due to the lack of direct inhibition of these enzymes or their synthesis in the host by AP fungicides, the target site was proposed to be in the post-translational secretory pathway (Milling & Richardson, 1995; Miura et al., 1994).

There is a possibility that the identified *mdl1* mutations within its substrate binding cavity (T. A. Schaedler et al., 2015) could allow the transport of APs as their substrates out of the mitochondria, supporting resistance towards AP fungicides.

6.4.2 Interactions between Anilinopyrimidine resistant mitochondrial proteins

A recent study on AP resistance-conferring mutations has highlighted nine mitochondrial proteins including Mdl1 as potential targets of AP fungicides in *B. cinerea* (Mosbach et al., 2017). The inter-link between the identified proteins was highlighted in this study, which is discussed below.

Pos5 was one of the genes identified by Mosbach et al. that caused resistance towards AP fungicides (Mosbach et al., 2017). Pos5 is an NAD(H) kinase and is located in the mitochondrial

matrix (Outten & Culotta, 2003). AP resistance-conferring *Botrytis cinerea* (Bc) *pos5* mutations corresponded to positions close to the NAD^+ ribose phosphorylation site in yeast *pos5* (Ando et al., 2011). This suggested that the mutations could cause changes in the catalysis of its substrate (Mosbach et al., 2017).

Iron-sulphur (Fe/S) clusters are vital cofactors for proteins involved in various cellular processes such as respiration, DNA repair and protein translation (Johnson, Dean, Smith, & Johnson, 2005). The precursors for the Fe/S clusters, mainly glutathione polysulfide derivatives (Theresia A. Schaedler et al., 2014) are transported from the mitochondria to the cytoplasm by Atm1, which is a mitochondrial inner membrane ABC protein (Kispal, Csere, Prohl, & Lill, 1999; Leighton & Schatz, 1995; Schueck, Woontner, & Koeller, 2001). The *atm1* mutation conferring resistance to AP in *B.cinerea* is predicted to affect the export of the Fe/S cluster precursors from the mitochondria (Mosbach et al., 2017) as the corresponding mutation in humans affects the maturation of cytosolic Fe/S cluster proteins (Bekri et al., 2000). NADPH plays a vital role in the Fe/S cluster biogenesis in the mitochondria (Pain, Balamurali, Dancis, & Pain, 2010). As Pos5 is the only enzyme that produces NADPH in the mitochondrial matrix (Outten & Culotta, 2003), there is a link between Pos5 and Atm1 (shown in Figure 6.10).

Loss of Atm1 can cause severe damage to the mitochondria as it results in up to 30-fold accumulation of iron in the mitochondria, oxidative damage to the mitochondrial DNA and loss of mitochondrial cytochromes (Kispal, Csere, Guiard, & Lill, 1997; Leighton & Schatz, 1995). However, such damage has been shown to be reversed by the overexpression of *mdl1* in Δ*atm1* cells in *S. cerevisiae*. As a result, there was a reduction of iron content in the mitochondria and decreased sensitivity to H_2O_2 to some degree (Chloupkova et al., 2003). Authors suggested that the overexpression of Mdl1 helped the cells cope with the high turnover of protein degradation caused by oxidative stress, which helped compensate for the lack of Atm1 (Chloupkova et al., 2003).

At low ATP levels, Mdl1 forms a complex with the F_1F_o-ATP synthase through the membrane-embedded F_o moiety of the synthase protein (Galluhn & Langer, 2004). The F_o moiety contains the oligomycin-sensitivity conferring subunit c (Atp9), where a mutation was found to cause AP resistance (Mosbach et al., 2017). The authors proposed the binding of Mdl1 to the F_1F_o-ATP synthase inactivated Mdl1 and upon its release from the complex was activated to export peptides degraded by m-AAA protease (Afg3) from the mitochondria. Moreover, the requirement of m-AAA protease for the assembly of F_1 and F_O of the ATP synthase is suggestive of a link between Mdl1, m-AAA protease and ATP synthase. (Galluhn & Langer, 2004).

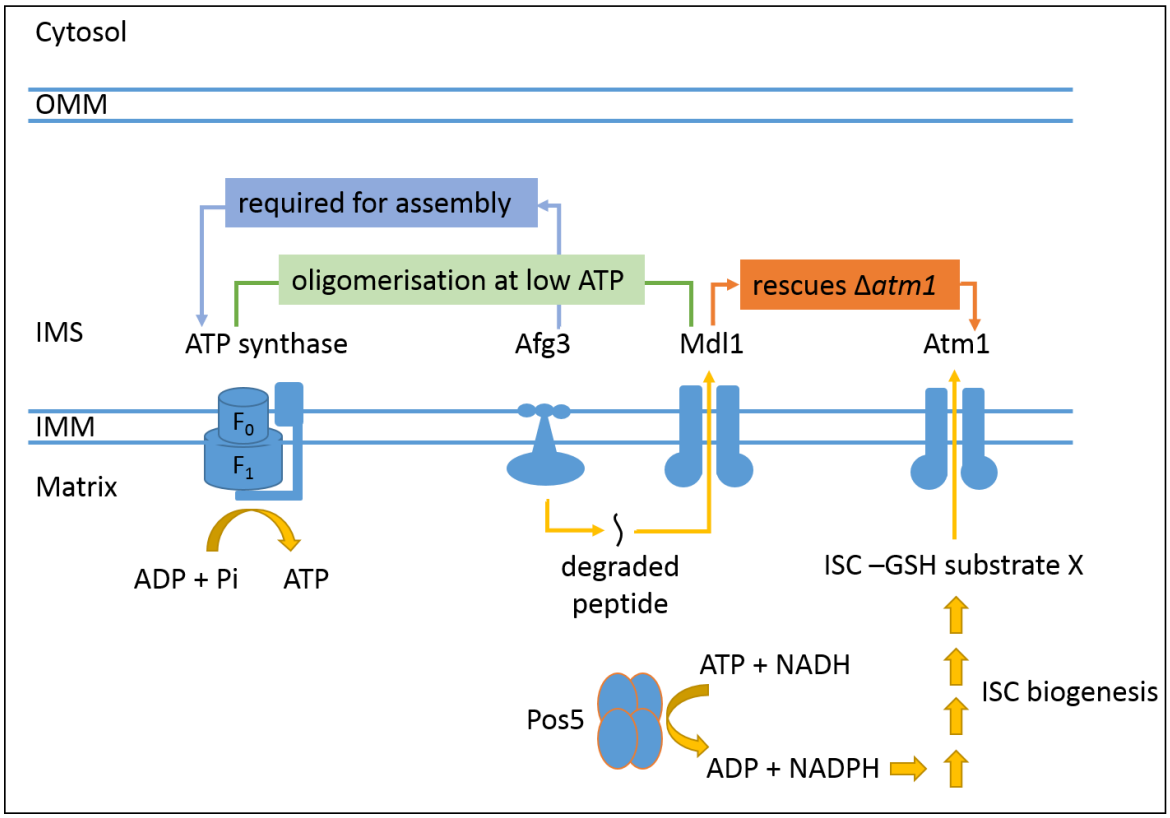

Figure 6.10 A representation of the inter-link between mitochondrial inner membrane (IMM) proteins. Mdl1 translocates peptides that are degraded by m-AAA protease (Afg3) across the inner membrane (Young et al., 2001). At low ATP levels, Mdl1 forms complexes with F_1Fo-ATP synthase (Galluhn & Langer, 2004). m-AAA protease (Afg3) is required for the assembly of F_1 and F_0 of the ATP synthase (Galluhn & Langer, 2004). Overexpression of Mdl1 suppresses the effects of oxidative stress in Δ*atm1* cells in S. cerevisiae (Chloupkova et al., 2003). Pos5 is an NADH kinase that produces NADPH, essential for protection from oxidative stress and biogenesis reactions (Bieganowski, Seidle, Wojcik, & Brenner, 2006; Miyagi, Kawai, & Murata, 2009; Outten & Culotta, 2003; Pain et al., 2010). The iron-sulphur cluster precursors from the biogenesis reactions aided by NADPH act as substrates for Atm1 (Kispal et al., 1999). [IMS- intermembrane space, OMS- outer membrane space; figure adapted from (Mosbach et al., 2017)

Among the lab generated AP resistance-conferring mutations, *mdl1* was the only mutant that caused AP resistance in the field isolates, making it a key player in AP resistance. The mutations in the rest of the resistance genes were considered inappropriate for the fitness of the host, *B. cinerea*, which would explain failure to observe the resistant alleles in the field population (Mosbach et al., 2017).

6.4.3 Overexpression and purification of Mdl1 proteins

The overexpression and purification of BcMdl1, ScMdl1 and ScMdl1^{E332K} were successful here. Unfortunately, due to the low yield of the proteins, repetition of the biochemical assays was not possible. Therefore, the results presented here are preliminary but demonstrate the feasibility of future studies to elucidate the mechanism behind AP resistance by Mdl1.

6.4.4 Identifying potential substrates for Mdl1

Mdl1 is proposed to be involved in the quality control of misassembled proteins by transporting a subset of 6-20 amino acids peptides that are degraded by m-AAA protease in the matrix of the mitochondria (Young et al., 2001). However, there was no evidence of transporting peptides in liposomes from transport assays. Moreover, no peptide stimulated ATPase activity was observed in Mdl1 (Hofacker et al., 2007). Perhaps the set of peptides transported by Mdl1 are specifically modified and was not included in the library of peptides that were tested (Hofacker et al., 2007).

The concentration of protein used to determine the ATPase activity was estimated from the intensity of the Mdl1 proteins relative to the protein standards from the SDS-polyacrylamide gels. As the concentration is a rough estimation, the values calculated for the ATPase activity of the protein may not reflect true values.

Nevertheless, the addition of pyridine nucleotides to ScMdl1 enhanced its ATPase activity (Figure 6.9). The highest increase (2 fold) was observed for $NADP^+$, which was closely followed by NAD^+. NAPDH increased the ATPase activity by approximately 40%. The basal ATPase activity of BcMdl1 was enhanced approximately fivefold by NADPH and $NADP^+$ while NAD^+ increased it by approximately 70%. The stimulation in the ATPase activity of Mdl1 in the presence of the pyridine nucleotides suggests that Mdl1 could potentially transport them as substrates. However, transport assays would be required to support such hypothesis further. The level of stimulation by the pyridine nucleotides was much greater for BcMdl1 than ScMdl1 suggesting that the pyridine nucleotides may be better substrates for the former. In addition, the effect of each pyridine nucleotide on ScMdl1 and BcMdl1 varied between the two proteins.

To reiterate our hypothesis, disruption of pyridine nucleotide balance in the mitochondria could possibly be a mode of action of AP fungicides, which is counteracted by the mobilisation of the pyridine nucleotides by Mdl1.

6.4.5 Potential role for Mdl1 in the transport of pyridine nucleotides in the mitochondria

If the pyridine nucleotides were potential substrates for Mdl1, the AP resistance conferring Mdl1 mutations could help reinstate the redox balance in the mitochondria and avoid deleterious consequences imposed by AP fungicides. The location of Mdl1 in the inner membrane of the mitochondria (Dean et al., 1994; Kuchler et al., 1992; Young et al., 2001) would suggest transport of the pyridine nucleotides from the mitochondrial matrix across the inner membrane under physiological conditions. This would be a novel mechanism of AP resistance in *B. cinerea*. However, additional transport assays are required to test whether pyridine nucleotides are the true substrates for Mdl1.

Pyridine nucleotides play crucial roles in metabolism, signalling and protection against oxidative damage (Pain et al., 2010).

The redox capability of NAD^+/NADH has made them key coenzymes in energy metabolism by regulating enzymes in glycolysis, TCA cycle and oxidative phosphorylation (reviewed by (Ying, 2006)). In addition to their redox properties, NAD^+ is involved in post-translational protein modifications such as ADP-ribosylation (Schreiber, Dantzer, Ame, & Murcia, 2006). NAD^+ can also be a precursor for second messenger molecules such as ADP-ribose in calcium mobilisation (Schuber & Lund, 2004).

NAD^+ is synthesised *de novo* using L-tryptophan or through salvage pathway using NAD^+ precursors (nicotinic acid, nicotinamide or nicotinamide riboside) as depicted in Figure 6.11 ((reviewed by (Foster & Moat, 1980; Houtkooper, Canto, Wanders, & Auwerx, 2010)). In yeast, as NAD^+ is not synthesised in the mitochondria, cytosolic NAD^+ is transported into the mitochondrial matrix by Ndt1p (Todisco, Agrimi, Castegna, & Palmieri, 2006). This would suggest that the transport of NAD^+ from the mitochondria by Mdl1 would be a futile process, despite what was suggested from the increase in ATPase activity of Mdl1 by NAD^+.

The oxidised phosphorylated $NADP^+$ is less abundant than its reduced form, NADPH, which is vital for protection against oxidative stress (Pollak, Dolle, & Ziegler, 2007). Anti-oxidation enzymes such as glutathione peroxidases require glutathione to function, which is regenerated with the help of NADPH (reviewed by (Agledal, Niere, & Ziegler, 2010)). NADPH is also involved in the reductive biosynthesis reactions of lipids, amino acids, and deoxyribonucleotides and is vital for the regeneration of cytochrome P-450 enzymes that help detoxify xenobiotics (Iyanagi, 2005). On

the other hand, $NADP^+$ maintains its role in calcium mobilisation by being converted into nicotinic acid adenine dinucleotide phosphate (NAADP) (Guse & Lee, 2008).

Three isoforms of NAD(H) kinase (NADK-1/2/3) are responsible for maintaining $NADP^+$ and NADPH pools. NADK-3 (Pos5p) is located in the mitochondrial matrix (Outten & Culotta, 2003) and NADK-1 (Utr1p) (Kawai, Suzuki, Mori, & Murata, 2001) and NADK-2 (Yef1p) (Shi, Kawai, Mori, Kono, & Murata, 2005) are found in the cytosol. The lack of efficient NAD^+/NADH kinase activity of Yef1p and the failure to rescue *pos5utr1* double mutation suggested that Pos5p and Utr1p are the main players in NAD^+/NADH kinase activity (Bieganowski et al., 2006). In the mitochondria, Pos5 can generate NADPH by phosphorylating NADH (Outten & Culotta, 2003). Alternatively, $NADP^+$ is reduced to NADPH by $NADP^+$ dependent acetaldehyde dehydrogenase (Ald4/Ald5) (Miyagi et al., 2009). In the cytosol, the $NADP^+$ is used by $NADP^+$ dehydrogenase (glucose-6-phosphate dehydrogenase (Zwf1p), acetaldehyde dehydrogenase (Ald6p) and isocitrate dehydrogenase (Idp2p)) to generate the majority of NADPH (Grabowska & Chelstowska, 2003).

The proposed hypothesis of AP fungicides causing disruption to the pyridine nucleotide balance in the mitochondria could be overcome by the mobilisation of pyridine nucleotides by Mdl1 in order to restore the redox state. Therefore, causing resistance towards AP fungicides. However, the compartmentalisation of NAD(H) kinases in the mitochondria and the cytosol (Kawai et al., 2001; Outten & Culotta, 2003; Shi et al., 2005) seems to make the need to transport pyridine nucleotides across the mitochondria redundant. In addition, NAD^+ is transported into the mitochondria by Ndt1p as it is synthesised in the cytosol (Todisco et al., 2006), it is difficult to understand why there would be a need to transport it out again.

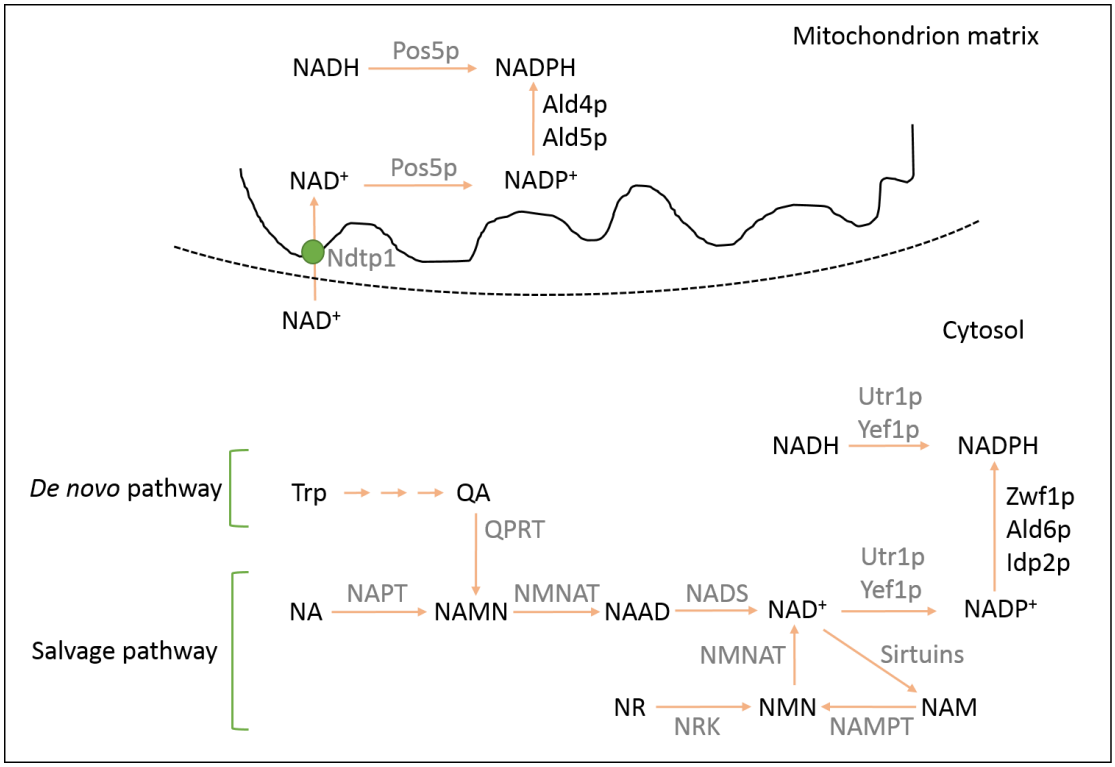

Figure 6.11 Schematic representation of the biosynthesis of pyridine nucleotides in the mitochondrial matrix and the cytosol. In the cytosol, the de novo pathway utilises L-tryptophan (Trp) to convert into quinolinic acid (QA) through a series of reactions. QA is converted to nicotinic acid mononucleotide (NAMN) by quinolinate phosphoribosyltransferase (QPRT), which is then catalysed by nicotinamide mononucleotide adenylyltransferase (NMNAT) to nicotinic acid adenine dinucleotide (NAAD). Finally, NAD^+ is synthesised by NAD synthase (NADS) using NAAD. In the salvage pathway, NAD^+ is synthesised from its precursors, nicotinic acid (NA), nicotinamide (NAM) and nicotinamide riboside (NR). NA is converted to NAMN by nicotinic acid phosphoribosyltransferase (NAPT) where it overlaps with the de novo pathway for the subsequent reactions. NAM and NR are both converted to nicotinamide mononucleotide (NMN) by nicotinamide phosphoriboysltransferase (NAMPT) and nicotinamide riboside kinase (NRK) respectively. Finally, NMN is converted to NAD^+ by NMNAT. Phosphorylation of NAD^+ and NADH are catalysed by NAD(H) kinases, Utr1p, Yef1p, Zwf1p, Ald6p and Idp2p to generate $NADP^+$ and NADPH respectively. Alternatively, NADPH is generated by $NADP^+$ dehydrogenase (glucose-6-phosphate dehydrogenase (Zwf1p), acetaldehyde dehydrogenase (Ald6p) and isocitrate dehydrogenase (Idp2p)) using $NADP^+$.In the mitochondrial matrix, NAD^+ is transported by Ndtp1 and subsequently phosphorylated by Pos5p to generate $NADP^+$, which can be reduced to NADPH by Ald4/5p. Pos5p can also phosphorylate NADH to generate NADPH. Figure adapted from (Pollak et al., 2007; Srivastava, 2016).

6.5 Conclusion

Mdl1 was identified as a major contributor to resistance towards anilinopyrimidine fungicides in *B. cinerea* (Mosbach et al., 2017). The hypothesis behind the mechanism of resistance was that the disruption of pyridine nucleotide balance in the mitochondria caused by anilinopyrimidine fungicides was counteracted by the mobilisation of the pyridine nucleotides by Mdl1.

ATPase activity assays conducted on *B. cinerea* and *S. cerevisiae* Mdl1 proteins show an increase in the basal activity by at least two-fold by $NADP^+$ and NAD^+ in ScMdl1 and almost fivefold by NADPH and $NADP^+$ in BcMdl1. Such effects suggest transport of pyridine nucleotides by Mdl1. However, further transport assays are required to validate that the pyridine nucleotides are true substrates of Mdl1.

The ATPase activity in the presence of NADH indicates that it is unlikely to be a potential substrate for Mdl1 as it decreased the activity for BcMdl1 and only causes a slight increase for ScMdl1.

The results presented in this report are preliminary. Further studies including transport assays of pyridine nucleotides by Mdl1 and the AP resistance-conferring Mdl1 mutants are necessary to carry the work forward. The identification of the substrates for Mdl1 will allow better understanding of their mechanism of resistance, and generate new inhibitors for the protein in order to modulate their resistance towards anilinopyrimidine fungicides.

Chapter 7 General Conclusions

This thesis has investigated an alternative method of tackling multidrug resistance (MDR) using ABC transporters, Sav1866, McjD and Mdl1 as model proteins. Previous studies have demonstrated regulatory effects of anionic lipids on membrane proteins (Marius et al., 2008; Andrew M. Powl et al., 2008; Valiyaveetil et al., 2002). The modulatory roles of the phospholipids can be exploited to control the activity of these drugs and chemicals-exporting ABC pumps.

Sav1866 and McjD were successfully extracted from the membrane of *E.coli* using DDM. The protein was purified further using nickel affinity chromatography. Following the reconstitution of Sav1866 and McjD into defined bilayers of phospholipids, it was evident that neutral and positively charged phospholipids favoured the protein's ATPase activity, while the anionic phospholipids had an inhibitory effect on the protein (5.3).

In order to investigate the mechanism behind the difference in ATPase activity of the protein between anionic, neutral and cationic phospholipids, fluorescence quenching technique was applied. Fluorescence quenching is a process by which the intensity of the fluorescence is decreased (Lakowicz, 2006). The quenching of intrinsic fluorescence of tryptophan by brominated phospholipids was used to determine the number of binding sites and relative binding affinities for phospholipids. Results from this study demonstrated a linkage between the protein's ATPase activity and its high affinity towards anionic phospholipids.

As Sav1866 has multiple native tryptophans, it was critical to replace them with non-fluorescent amino acids to avoid complexity in the fluorescent signals in Chapter 3 using site-directed mutagenesis. In Sav1866, tyrosine replacement was tolerated at positions 87 and 243, but not at 143. On the contrary, arginine replacement only worked for tryptophan at 143, but not 87 or 243. This suggested that the replacement was dependent on the position of the tryptophan on the protein. The single mutants retaining their ATPase activity were combined to create a tryptophan-less mutant, Sav1866 W87YW143RW243F. The tryptophan-less mutant could be used as a model protein to introduce a new tryptophan on the protein to study specific lipid binding site using fluorescence quenching assays, where the brominated phospholipids quench the fluorescence of the strategically placed new tryptophan.

The loss of ATPase activity of Sav1866 mutants when the native tryptophans were replaced with non-fluorescent amino acids in Chapter 3 was investigated further to understand the mechanism behind the inhibition. The mutant could have potentially lost its native conformation and become

inactive, or the mutant could have been locked in one conformation and been unable to hydrolyse ATP. In Chapter 4, the conformation of the mutants was studied using a crosslinking technique, where two cysteine residues were introduced separately at positions 281 and 208. Crosslinking of cysteines at 281 and 208 would indicate Sav1866 dimer in the inward-facing conformation and outward-facing conformation respectively. The crosslinking behaviour of the mutants was compared with the wild type protein in the presence and absence of nucleotides. The increase in the level of crosslinked dimers in the presence of ATP.Vi compared to the nucleotide-free condition at the inward-facing conformation was reflected in wild type and mutant Sav1866. This suggested that losing the ability to hydrolyse ATP does not necessarily mean that the mutants have lost their structure.

The crosslinking technique was also utilised to study the conformation of Sav1866 at various stages of the ATPase cycle. Under basal condition, Sav1866 adopted an outward-facing conformation, but post ATP hydrolysis, the protein was likely to adopt an occluded conformation. This suggested that Sav1866 adopted the proposed constant contact model.

The third element of Chapter 4 was understanding the effect of detergents and artificial lipid reconstitution on the conformation of the protein. From the crosslinking results, it was evident that the crosslinking behaviour of the protein changed when in detergents and reconstituted lipids compared to its native environment. In addition, the different lipid head groups of the phospholipids did not have any major effect on the protein's conformation despite changing its ATPase activity.

In Chapter 5, the tryptophan-less Sav1866 was used to introduce strategically placed new tryptophans at positions where lipid binding was anticipated to study lipid-protein interactions. However, there was no distinction between the bindings of anionic and neutral or cationic lipids suggesting no specificity. Therefore, McjD was used an alternative model protein. After replacing the 2 native tryptophans with tyrosines, a new reporter tryptophan was placed at position 307 instead of a leucine within the vicinity of a positively charged cluster of amino acids arginine 186 (helix 4) and 311 (helix 6) on the cytoplasmic face of McjD (see Figure 5.1). Phosphatidylcholine had 3 binding sites, whereas the anionic lipids had 2 binding sites near to the tryptophan at 307. It was suggested that the neutral head group of phosphatidylcholine allowed the molecules to group close together, whereas the negative charge on the anionic head groups would create repulsion between the head groups. The fluorescence quenching assay suggested that the positively charged cluster of amino acids provided a high-affinity binding site for anionic phospholipids. When those positive amino acids were replaced with neutral glutamines, the

binding affinity was lowered and equal to the binding affinity for neutral phospholipids, reconfirming that the positive residues were responsible for creating a high binding affinity for the anionic phospholipids.

SMA purification of membrane proteins was also reviewed in Chapter 5. The purpose of this method of purifying membrane protein was to conserve the near native environment of the protein with its surrounding lipids, which is often disrupted when using detergents during the purification process (le Maire et al., 2000). Unfortunately, the purification of Sav1866 and McjD using SMA led to inactive proteins, which was suggested to be caused due to the presence of anionic phospholipids in the SMALPs. Alternatively, the protein could be inhibited from conformational changes due to the SMA molecules (Stroud et al., 2018).

Chapter 6 reviewed the expression and purification of a eukaryotic ABC transporter, Mdl1, which was recently identified as a major contributor to resistance towards anilinopyrimidine fungicides (Mosbach et al., 2017). Mdl1 was expressed in *S. cerevisiae* and purified using DDM. The proposed mechanism of resistance through the mobilisation of pyridine nucleotides was investigated by testing the ATPase activity of the protein in the presence of the nucleotides. The resulting outcome was an enhanced ATPase activity by at least two-fold by $NADP^+$ and NAD^+ in ScMdl1 and almost fivefold by NADPH and $NADP^+$ in BcMdl1. This suggested that these nucleotides were transported by Mdl1. The results reported in this chapter were preliminary. Further studies should include transport assays with the pyridine nucleotides to clarify the mechanism of inhibition by Mdl1 in order to generate new inhibitors to modulate Mdl1's resistance towards anilinopyrimidine fungicides.

In conclusion, this thesis has explored a novel way of overcoming multidrug resistance of ABC transporter by using Sav1866, McjD and Mdl1 as model proteins. The apparent regulatory effect of anionic lipids on Sav1866 and McjD, and specific binding site shown on McjD can be essential in designing inhibitors to modulate the protein's activity. Further work can include investigating multidrug resistance proteins such as P-glycoprotein for lipid regulation and ultimately designing inhibitors to inhibit their activity (Elliott et al., 2005; Sharom, 2011).

References

Agledal, L., Niere, M., & Ziegler, M. (2010). The phosphate makes a difference: cellular functions of NADP. *Redox Rep, 15*(1), 2-10. doi:10.1179/174329210x12650506623122

Ahmed, M., Borsch, C. M., Neyfakh, A. A., & Schuldiner, S. (1993). Mutants of the Bacillus subtilis multidrug transporter Bmr with altered sensitivity to the antihypertensive alkaloid reserpine. *J Biol Chem, 268*(15), 11086-11089.

Albani, J. R. (2004). Chapter 4 - Fluorescence Quenching. In J. R. Albani (Ed.), *Structure and Dynamics of Macromolecules: Absorption and Fluorescence Studies* (pp. 141-192). Amsterdam: Elsevier Science.

Aller, S. G., Yu, J., Ward, A., Weng, Y., Chittaboina, S., Zhuo, R., . . . Chang, G. (2009). Structure of P-glycoprotein Reveals a Molecular Basis for Poly-Specific Drug Binding. *Science, 323*(5922), 1718-1722. doi:10.1126/science.1168750

Allhusen, J. S., & Conboy, J. C. (2016). The Ins and Outs of Lipid Flip-Flop. *Acc Chem Res*. doi:10.1021/acs.accounts.6b00435

Almén, M. S., Nordström, K. J. V., Fredriksson, R., & Schiöth, H. B. (2009). Mapping the human membrane proteome: a majority of the human membrane proteins can be classified according to function and evolutionary origin. *BMC Biology, 7*, 50-50. doi:10.1186/1741-7007-7-50

Amand, H. L., Fant, K., Norden, B., & Esbjorner, E. K. (2008). Stimulated endocytosis in penetratin uptake: effect of arginine and lysine. *Biochem Biophys Res Commun, 371*(4), 621-625. doi:10.1016/j.bbrc.2008.04.039

Ando, T., Ohashi, K., Ochiai, A., Mikami, B., Kawai, S., & Murata, K. (2011). Structural determinants of discrimination of NAD+ from NADH in yeast mitochondrial NADH kinase Pos5. *J Biol Chem, 286*(34), 29984-29992. doi:10.1074/jbc.M111.249011

Arachea, B. T., Sun, Z., Potente, N., Malik, R., Isailovic, D., & Viola, R. E. (2012). Detergent selection for enhanced extraction of membrane proteins. *Protein Expr Purif, 86*(1), 12-20. doi:10.1016/j.pep.2012.08.016

Arnold, I., Wagner-Ecker, M., Ansorge, W., & Langer, T. (2006). Evidence for a novel mitochondria-to-nucleus signalling pathway in respiring cells lacking i-AAA protease and the ABC-transporter Mdl1. *Gene, 367*, 74-88. doi:10.1016/j.gene.2005.09.044

Atkins, P. W., & De Paula, J. (2006). *Physical chemistry for the life sciences*: Oxford : Oxford University Press ; New York : W.H. Freeman, 2006.

Babakhani, A., Gorfe, A. A., Gullingsrud, J., Kim, J. E., & Andrew McCammon, J. (2007). Peptide insertion, positioning, and stabilization in a membrane: Insight from an all-atom molecular dynamics simulation. *Biopolymers, 85*(5‐6), 490-497. doi:doi:10.1002/bip.20698

Baldwin, P. A., & Hubbell, W. L. (1985). Effects of lipid environment on the light-induced conformational changes of rhodopsin. 2. Roles of lipid chain length, unsaturation, and phase state. *Biochemistry, 24*(11), 2633-2639.

Ball David W, H. J. W., Scott Rhonda J. (2012). *Introduction to Chemistry*.

Bassilana, M., & Wickner, W. (1993). Purified Escherichia coli preprotein translocase catalyzes multiple cycles of precursor protein translocation. *Biochemistry, 32*(10), 2626-2630.

Baugh, S., Ekanayaka, A. S., Piddock, L. J. V., & Webber, M. A. (2012). Loss of or inhibition of all multidrug resistance efflux pumps of Salmonella enterica serovar Typhimurium results in impaired ability to form a biofilm. *Journal of Antimicrobial Chemotherapy, 67*(10), 2409-2417. doi:10.1093/jac/dks228

Bekri, S., Kispal, G., Lange, H., Fitzsimons, E., Tolmie, J., Lill, R., & Bishop, D. F. (2000). Human ABC7 transporter: gene structure and mutation causing X-linked sideroblastic anemia with ataxia with disruption of cytosolic iron-sulfur protein maturation. *Blood, 96*(9), 3256-3264.

Berg, J. M., Tymoczko, J. L., & Stryer, L. (2002). *Biochemistry*. New York: W.H. Freeman.

Berman, H. M., Westbrook, J., Feng, Z., Gilliland, G., Bhat, T. N., Weissig, H., . . . Bourne, P. E. (2000). The Protein Data Bank. *Nucleic Acids Research, 28*(1), 235-242. doi:10.1093/nar/28.1.235

Bersch, B., Dorr, J. M., Hessel, A., Killian, J. A., & Schanda, P. (2017). Proton-Detected Solid-State NMR Spectroscopy of a Zinc Diffusion Facilitator Protein in Native Nanodiscs. *Angew Chem Int Ed Engl, 56*(9), 2508-2512. doi:10.1002/anie.201610441

Bevers, E. M., Comfurius, P., van Rijn, J. L., Hemker, H. C., & Zwaal, R. F. (1982). Generation of prothrombin-converting activity and the exposure of phosphatidylserine at the outer surface of platelets. *Eur J Biochem, 122*(2), 429-436.

Bieganowski, P., Seidle, H. F., Wojcik, M., & Brenner, C. (2006). Synthetic lethal and biochemical analyses of NAD and NADH kinases in Saccharomyces cerevisiae establish separation of cellular functions. *J Biol Chem, 281*(32), 22439-22445. doi:10.1074/jbc.M513919200

Bogdanov, M., Dowhan, W., & Vitrac, H. (2014). Lipids and topological rules governing membrane protein assembly. *Biochimica et Biophysica Acta (BBA) - Molecular Cell Research, 1843*(8), 1475-1488. doi:http://dx.doi.org/10.1016/j.bbamcr.2013.12.007

Bogdanov, M., Heacock, P. N., & Dowhan, W. (2002). A polytopic membrane protein displays a reversible topology dependent on membrane lipid composition. *Embo j, 21*(9), 2107-2116. doi:10.1093/emboj/21.9.2107

Bogdanov, M., Xie, J., Heacock, P., & Dowhan, W. (2008). To flip or not to flip: lipid–protein charge interactions are a determinant of final membrane protein topology. *The Journal of Cell Biology, 182*(5), 925-935. doi:10.1083/jcb.200803097

Booth, I. R., Miller, S., Muller, A., & Lehtovirta-Morley, L. (2015). The evolution of bacterial mechanosensitive channels. *Cell Calcium, 57*(3), 140-150. doi:10.1016/j.ceca.2014.12.011

Bordag, N., & Keller, S. (2010). Alpha-helical transmembrane peptides: a "divide and conquer" approach to membrane proteins. *Chem Phys Lipids, 163*(1), 1-26. doi:10.1016/j.chemphyslip.2009.07.009

Borges-Walmsley, M. I., McKeegan, K. S., & Walmsley, A. R. (2003). Structure and function of efflux pumps that confer resistance to drugs. *Biochemical Journal, 376*(Pt 2), 313-338. doi:10.1042/BJ20020957

Borst, P., & Elferink, R. O. (2002). Mammalian ABC transporters in health and disease. *Annu Rev Biochem, 71*, 537-592. doi:10.1146/annurev.biochem.71.102301.093055

Bratton, D. L., Fadok, V. A., Richter, D. A., Kailey, J. M., Guthrie, L. A., & Henson, P. M. (1997). Appearance of phosphatidylserine on apoptotic cells requires

calcium-mediated nonspecific flip-flop and is enhanced by loss of the aminophospholipid translocase. *J Biol Chem, 272*(42), 26159-26165.
Braun, P., & von Heijne, G. (1999). The Aromatic Residues Trp and Phe Have Different Effects on the Positioning of a Transmembrane Helix in the Microsomal Membrane. *Biochemistry, 38*(30), 9778-9782. doi:10.1021/bi990923a
Breukink, E., Demel, R. A., de Korte-Kool, G., & de Kruijff, B. (1992). SecA insertion into phospholipids is stimulated by negatively charged lipids and inhibited by ATP: a monolayer study. *Biochemistry, 31*(4), 1119-1124.
Broecker, J., Eger, B. T., & Ernst, O. P. (2017). Crystallogenesis of Membrane Proteins Mediated by Polymer-Bounded Lipid Nanodiscs. *Structure, 25*(2), 384-392. doi:10.1016/j.str.2016.12.004
Caffrey, M., & Feigenson, G. W. (1981). Fluorescence quenching in model membranes. 3. Relationship between calcium adenosinetriphosphatase enzyme activity and the affinity of the protein for phosphatidylcholines with different acyl chain characteristics. *Biochemistry, 20*(7), 1949-1961.
Cardew, A. S., & Fox, K. R. (2010). DNase I Footprinting. In K. R. Fox (Ed.), *Drug-DNA Interaction Protocols* (pp. 153-172). Totowa, NJ: Humana Press.
Chamberlain, A. K., Lee, Y., Kim, S., & Bowie, J. U. (2004). Snorkeling preferences foster an amino acid composition bias in transmembrane helices. *J Mol Biol, 339*(2), 471-479. doi:10.1016/j.jmb.2004.03.072
Chen, J., Lu, G., Lin, J., Davidson, A. L., & Quiocho, F. A. (2003). A tweezers-like motion of the ATP-binding cassette dimer in an ABC transport cycle. *Mol Cell, 12*(3), 651-661.
Chloupkova, M., LeBard, L. S., & Koeller, D. M. (2003). MDL1 is a high copy suppressor of ATM1: evidence for a role in resistance to oxidative stress. *J Mol Biol, 331*(1), 155-165.
Cho, W., & Stahelin, R. V. (2005). Membrane-Protein Interactions in Cell Signaling and Membrane Trafficking. *Annu Rev Biophys Biomol Struct, 34*(1), 119-151. doi:10.1146/annurev.biophys.33.110502.133337
Choudhury, H. G., Tong, Z., Mathavan, I., Li, Y., Iwata, S., Zirah, S., . . . Beis, K. (2014). Structure of an antibacterial peptide ATP-binding cassette transporter in a novel outward occluded state. *Proc Natl Acad Sci U S A, 111*(25), 9145-9150. doi:10.1073/pnas.1320506111
Clark, E. H., East, J. M., & Lee, A. G. (2003). The role of tryptophan residues in an integral membrane protein: diacylglycerol kinase. *Biochemistry, 42*(37), 11065-11073. doi:10.1021/bi034607e
Cornelius, F. (2001). Modulation of Na,K-ATPase and Na-ATPase Activity by Phospholipids and Cholesterol. I. Steady-State Kinetics. *Biochemistry, 40*(30), 8842-8851. doi:10.1021/bi010541g
Cronan, J. E. (1968). Phospholipid Alterations During Growth of Escherichia coli. *J Bacteriol, 95*(6), 2054-2061.
Cullis, P. R., & De Kruijff, B. (1978). The polymorphic phase behaviour of phosphatidylethanolamines of natural and synthetic origin. A 31P NMR study. *Biochimica et Biophysica Acta (BBA) - Biomembranes, 513*(1), 31-42. doi:http://dx.doi.org/10.1016/0005-2736(78)90109-8
Cullis, P. R., & de Kruijff, B. (1979). Lipid polymorphism and the functional roles of lipids in biological membranes. *Biochim Biophys Acta, 559*(4), 399-420.
Daniel Gietz, R., & Woods, R. A. (2002). Transformation of yeast by lithium acetate/single-stranded carrier DNA/polyethylene glycol method. In C.

Guthrie & G. R. Fink (Eds.), *Methods in Enzymology* (Vol. 350, pp. 87-96): Academic Press.
Dassa, E. (2011). Natural history of ABC systems: not only transporters. *Essays In Biochemistry, 50*, 19-42. doi:10.1042/bse0500019
Davidson, A. L., Dassa, E., Orelle, C., & Chen, J. (2008). Structure, function, and evolution of bacterial ATP-binding cassette systems. *Microbiol Mol Biol Rev, 72*(2), 317-364, table of contents. doi:10.1128/MMBR.00031-07
Davidson, A. L., & Maloney, P. C. (2007). ABC transporters: how small machines do a big job. *Trends Microbiol, 15*(10), 448-455. doi:10.1016/j.tim.2007.09.005
Dawaliby, R., Trubbia, C., Delporte, C., Noyon, C., Ruysschaert, J. M., Van Antwerpen, P., & Govaerts, C. (2016). Phosphatidylethanolamine Is a Key Regulator of Membrane Fluidity in Eukaryotic Cells. *J Biol Chem, 291*(7), 3658-3667. doi:10.1074/jbc.M115.706523
Dawson, R. J., & Locher, K. P. (2006). Structure of a bacterial multidrug ABC transporter. *Nature, 443*(7108), 180-185. doi:10.1038/nature05155
Dawson, R. J., & Locher, K. P. (2007). Structure of the multidrug ABC transporter Sav1866 from Staphylococcus aureus in complex with AMP-PNP. *FEBS Lett, 581*(5), 935-938. doi:10.1016/j.febslet.2007.01.073
de Vrije, T., de Swart, R. L., Dowhan, W., Tommassen, J., & de Kruijff, B. (1988). Phosphatidylglycerol is involved in protein translocation across Escherichia coli inner membranes. *Nature, 334*(6178), 173-175. doi:10.1038/334173a0
Dean, M., Allikmets, R., Gerrard, B., Stewart, C., Kistler, A., Shafer, B., . . . Strathern, J. (1994). Mapping and sequencing of two yeast genes belonging to the ATP-binding cassette superfamily. *Yeast, 10*(3), 377-383. doi:10.1002/yea.320100310
Dörr, J. M., Koorengevel, M. C., Schäfer, M., Prokofyev, A. V., Scheidelaar, S., van der Cruijsen, E. A. W., . . . Killian, J. A. (2014). Detergent-free isolation, characterization, and functional reconstitution of a tetrameric K+ channel: The power of native nanodiscs. *Proceedings of the National Academy of Sciences, 111*(52), 18607-18612. doi:10.1073/pnas.1416205112
Dörr, J. M., Scheidelaar, S., Koorengevel, M. C., Dominguez, J. J., Schäfer, M., van Walree, C. A., & Killian, J. A. (2016). The styrene–maleic acid copolymer: a versatile tool in membrane research. *European Biophysics Journal, 45*, 3-21. doi:10.1007/s00249-015-1093-y
Doshi, R., Woebking, B., & van Veen, H. W. (2010). Dissection of the conformational cycle of the multidrug/lipidA ABC exporter MsbA. *Proteins: Structure, Function, and Bioinformatics, 78*(14), 2867-2872. doi:10.1002/prot.22813
Dowhan, W. (1997). Molecular Basis for Membrane Phospholipid Diversity: Why Are There So Many Lipids? *Annu Rev Biochem, 66*(1), 199-232. doi:10.1146/annurev.biochem.66.1.199
Dowhan, W., & Bogdanov, M. (2002). Chapter 1 Functional roles of lipids in membranes *New Comprehensive Biochemistry* (Vol. Volume 36, pp. 1-35): Elsevier.
Dowhan, W., Bogdanov, M., & Mileykovskaya, E. (2008). CHAPTER 1 - Functional roles of lipids in membranes A2 - Vance, Dennis E. In J. E. Vance (Ed.), *Biochemistry of Lipids, Lipoproteins and Membranes (Fifth Edition)* (pp. 1-37). San Diego: Elsevier.

Dowhan William, B. M. (2002). Functional roles of lipids in membranes. *Biochemistry of Lipids, 4the Edition*.

Duquesne, S., Destoumieux-Garzon, D., Zirah, S., Goulard, C., Peduzzi, J., & Rebuffat, S. (2007). Two enzymes catalyze the maturation of a lasso peptide in Escherichia coli. *Chem Biol, 14*(7), 793-803. doi:10.1016/j.chembiol.2007.06.004

East, & Lee. (1982). Lipid selectivity of the calcium and magnesium ion dependent adenosine triphosphatase, studied with fluorescence quenching by a brominated phospholipid. *Biochemistry, 21*(17), 4144-4151. doi:10.1021/bi00260a035

El-Awady, R., Saleh, E., Hashim, A., Soliman, N., Dallah, A., Elrasheed, A., & Elakraa, G. (2017). The Role of Eukaryotic and Prokaryotic ABC Transporter Family in Failure of Chemotherapy. *Frontiers in Pharmacology, 7*(535). doi:10.3389/fphar.2016.00535

Elliott, J. I., Surprenant, A., Marelli-Berg, F. M., Cooper, J. C., Cassady-Cain, R. L., Wooding, C., . . . Higgins, C. F. (2005). Membrane phosphatidylserine distribution as a non-apoptotic signalling mechanism in lymphocytes. *Nat Cell Biol, 7*(8), 808-816. doi:10.1038/ncb1279

Epand, R. M. (1998). Lipid polymorphism and protein?lipid interactions. *Biochimica et Biophysica Acta (BBA) - Reviews on Biomembranes, 1376*(3), 353-368. doi:http://dx.doi.org/10.1016/S0304-4157(98)00015-X

Epis, S., Porretta, D., Mastrantonio, V., Comandatore, F., Sassera, D., Rossi, P., . . . Urbanelli, S. (2014). ABC transporters are involved in defense against permethrin insecticide in the malaria vector Anopheles stephensi. *Parasites & Vectors, 7*(1), 349. doi:10.1186/1756-3305-7-349

Fadok, V. A., Bratton, D. L., Rose, D. M., Pearson, A., Ezekewitz, R. A. B., & Henson, P. M. (2000). A receptor for phosphatidylserine-specific clearance of apoptotic cells. *Nature, 405*, 85. doi:10.1038/35011084

Fan, Z., & Makielski, J. C. (1997). Anionic Phospholipids Activate ATP-sensitive Potassium Channels. *Journal of Biological Chemistry, 272*(9), 5388-5395. doi:10.1074/jbc.272.9.5388

Feng, J., Wehbi, H., & Roberts, M. F. (2002). Role of tryptophan residues in interfacial binding of phosphatidylinositol-specific phospholipase C. *J Biol Chem, 277*(22), 19867-19875. doi:10.1074/jbc.M200938200

Fiedorczuk, K., Letts, J. A., Degliesposti, G., Kaszuba, K., Skehel, M., & Sazanov, L. A. (2016). Atomic structure of the entire mammalian mitochondrial complex I. *Nature, 538*, 406. doi:10.1038/nature19794

https://www.nature.com/articles/nature19794#supplementary-information

Fluman, N., & Bibi, E. (2009). Bacterial multidrug transport through the lens of the major facilitator superfamily. *Biochimica et Biophysica Acta (BBA) - Proteins and Proteomics, 1794*(5), 738-747. doi:http://dx.doi.org/10.1016/j.bbapap.2008.11.020

Foster, J. W., & Moat, A. G. (1980). Nicotinamide adenine dinucleotide biosynthesis and pyridine nucleotide cycle metabolism in microbial systems. *Microbiol Rev, 44*(1), 83-105.

Fribourg, P. F., Chami, M., Sorzano, C. O., Gubellini, F., Marabini, R., Marco, S., . . . Levy, D. (2014). 3D cryo-electron reconstruction of BmrA, a bacterial multidrug ABC transporter in an inward-facing conformation and in a lipidic

environment. *J Mol Biol, 426*(10), 2059-2069. doi:10.1016/j.jmb.2014.03.002
Fritz, R., Lanen, C., Chapeland-Leclerc, F., & Leroux, P. (2003). Effect of the anilinopyrimidine fungicide pyrimethanil on the cystathionine β-lyase of Botrytis cinerea. *Pesticide Biochemistry and Physiology, 77*(2), 54-65. doi:https://doi.org/10.1016/S0048-3575(03)00094-4
Fritz, R., Lanen, C., Colas, V., & Leroux, P. (1997). Inhibition of Methionine Biosynthesis in Botrytis cinerea by the Anilinopyrimidine Fungicide Pyrimethanil. *Pesticide Science, 49*(1), 40-46. doi:10.1002/(SICI)1096-9063(199701)49:1<40::AID-PS470>3.0.CO;2-Y
Gaede, H. C., Yau, W.-M., & Gawrisch, K. (2005). Electrostatic Contributions to Indole−Lipid Interactions. *The Journal of Physical Chemistry B, 109*(26), 13014-13023. doi:10.1021/jp0511000
Gallivan, J. P., & Dougherty, D. A. (1999). Cation-pi interactions in structural biology. *Proc Natl Acad Sci U S A, 96*(17), 9459-9464.
Galluhn, D., & Langer, T. (2004). Reversible assembly of the ATP-binding cassette transporter Mdl1 with the F1F0-ATP synthase in mitochondria. *J Biol Chem, 279*(37), 38338-38345. doi:10.1074/jbc.M405871200
Gassler, C. S., Ryan, M., Liu, T., Griffith, O. H., & Heinz, D. W. (1997). Probing the roles of active site residues in phosphatidylinositol-specific phospholipase C from Bacillus cereus by site-directed mutagenesis. *Biochemistry, 36*(42), 12802-12813. doi:10.1021/bi971102d
George, A. M., & Jones, P. M. (2012). Perspectives on the structure-function of ABC transporters: the Switch and Constant Contact models. *Prog Biophys Mol Biol, 109*(3), 95-107. doi:10.1016/j.pbiomolbio.2012.06.003
Gomez, B., & Robinson, N. C. (1999). Phospholipase Digestion of Bound Cardiolipin Reversibly Inactivates Bovine Cytochrome bc1. *Biochemistry, 38*(28), 9031-9038. doi:10.1021/bi990603r
Grabowska, D., & Chelstowska, A. (2003). The ALD6 Gene Product Is Indispensable for Providing NADPH in Yeast Cells Lacking Glucose-6-phosphate Dehydrogenase Activity. *Journal of Biological Chemistry, 278*(16), 13984-13988. doi:10.1074/jbc.M210076200
Granseth, E., von Heijne, G., & Elofsson, A. (2005). A study of the membrane-water interface region of membrane proteins. *J Mol Biol, 346*(1), 377-385. doi:10.1016/j.jmb.2004.11.036
Guse, A. H., & Lee, H. C. (2008). NAADP: a universal Ca2+ trigger. *Sci Signal, 1*(44), re10. doi:10.1126/scisignal.144re10
Gustot, A., Smriti, Ruysschaert, J. M., McHaourab, H., & Govaerts, C. (2010). Lipid composition regulates the orientation of transmembrane helices in HorA, an ABC multidrug transporter. *J Biol Chem, 285*(19), 14144-14151. doi:10.1074/jbc.M109.079673
Heijne, G. V. (1994). Membrane Proteins: From Sequence to Structure. *Annu Rev Biophys Biomol Struct, 23*(1), 167-192. doi:10.1146/annurev.bb.23.060194.001123
Hendrick, J. P., & Wickner, W. (1991). SecA protein needs both acidic phospholipids and SecY/E protein for functional high-affinity binding to the Escherichia coli plasma membrane. *Journal of Biological Chemistry, 266*(36), 24596-24600.

Herce, H. D., & Garcia, A. E. (2007). Cell Penetrating Peptides: How Do They Do It? *Journal of Biological Physics, 33*(5-6), 345-356. doi:10.1007/s10867-008-9074-3

Heye, U. J., Speich, J., Siegle, H., Steinemann, A., Forster, B., Knauf-Beiter, G., . . . Hubele, A. (1994). CGA 219417: a novel broad-spectrum fungicide. *Crop Protection, 13*(7), 541-549. doi:https://doi.org/10.1016/0261-2194(94)90108-2

Higgins, C. F. (1992). ABC Transporters: From Microorganisms to Man. *Annual Review of Cell Biology, 8*(1), 67-113. doi:10.1146/annurev.cb.08.110192.000435

Higgins, C. F., Hyde, S. C., Mimmack, M. M., Gileadi, U., Gill, D. R., & Gallagher, M. P. (1990). Binding protein-dependent transport systems. *J Bioenerg Biomembr, 22*(4), 571-592.

Higgins, C. F., & Linton, K. J. (2004). The ATP switch model for ABC transporters. *Nat Struct Mol Biol, 11*(10), 918-926. doi:10.1038/nsmb836

Hilgemann, D. W., & Ball, R. (1996). Regulation of Cardiac Na$^+$, Ca^{2+} Exchange and K$_{ATP}$ Potassium Channels by PIP$_2$. *Science, 273*(5277), 956-959.

Hill, D. J. T., O'Donnell, J. H., & O'Sullivan, P. W. (1985). Analysis of the mechanism of copolymerization of styrene and maleic anhydride. *Macromolecules, 18*(1), 9-17. doi:10.1021/ma00143a002

Hirama, T., Lu, S. M., Kay, J. G., Maekawa, M., Kozlov, M. M., Grinstein, S., & Fairn, G. D. (2017). Membrane curvature induced by proximity of anionic phospholipids can initiate endocytosis. *Nat Commun, 8*(1), 1393. doi:10.1038/s41467-017-01554-9

Hofacker, M., Gompf, S., Zutz, A., Presenti, C., Haase, W., van der Does, C., . . . Tampé, R. (2007). Structural and Functional Fingerprint of the Mitochondrial ATP-binding Cassette Transporter Mdl1 from Saccharomyces cerevisiae. *Journal of Biological Chemistry, 282*(6), 3951-3961. doi:10.1074/jbc.M609899200

Hohl, M., Briand, C., Grütter, M. G., & Seeger, M. A. (2012). Crystal structure of a heterodimeric ABC transporter in its inward-facing conformation. *Nat Struct Mol Biol, 19*(4), 395-402. doi:http://www.nature.com/nsmb/journal/v19/n4/abs/nsmb.2267.html#supplementary-information

Hollenstein, K., Frei, D. C., & Locher, K. P. (2007). Structure of an ABC transporter in complex with its binding protein. *Nature, 446*(7132), 213-216. doi:10.1038/nature05626

Houtkooper, R. H., Canto, C., Wanders, R. J., & Auwerx, J. (2010). The secret life of NAD+: an old metabolite controlling new metabolic signaling pathways. *Endocr Rev, 31*(2), 194-223. doi:10.1210/er.2009-0026

Hristova, K., & Wimley, W. C. (2011). A Look at Arginine in Membranes. *The Journal of Membrane Biology, 239*(1-2), 49-56. doi:10.1007/s00232-010-9323-9

Huang, W., Liao, G., Baker, G. M., Wang, Y., Lau, R., Paderu, P., . . . Xue, C. (2016). Lipid Flippase Subunit Cdc50 Mediates Drug Resistance and Virulence in Cryptococcus neoformans. *MBio, 7*(3). doi:10.1128/mBio.00478-16

Huijbregts, R. P., de Kroon, A. I., & de Kruijff, B. (2000). Topology and transport of membrane lipids in bacteria. *Biochim Biophys Acta, 1469*(1), 43-61.

Ikeda, M., Kihara, A., & Igarashi, Y. (2006). Lipid asymmetry of the eukaryotic plasma membrane: functions and related enzymes. *Biol Pharm Bull, 29*(8), 1542-1546.
Iyanagi, T. (2005). Structure and function of NADPH-cytochrome P450 reductase and nitric oxide synthase reductase domain. *Biochem Biophys Res Commun, 338*(1), 520-528. doi:10.1016/j.bbrc.2005.08.043
Jardetzky, O. (1966). Simple allosteric model for membrane pumps. *Nature, 211*(5052), 969-970.
Jeannot, K., Elsen, S., Kohler, T., Attree, I., van Delden, C., & Plesiat, P. (2008). Resistance and virulence of Pseudomonas aeruginosa clinical strains overproducing the MexCD-OprJ efflux pump. *Antimicrob Agents Chemother, 52*(7), 2455-2462. doi:10.1128/aac.01107-07
Jin, M. S., Oldham, M. L., Zhang, Q., & Chen, J. (2012). Crystal structure of the multidrug transporter P-glycoprotein from Caenorhabditis elegans. *Nature, 490*(7421), 566-569. doi:http://www.nature.com/nature/journal/v490/n7421/abs/nature11448.html#supplementary-information
Johnson, D. C., Dean, D. R., Smith, A. D., & Johnson, M. K. (2005). Structure, function, and formation of biological iron-sulfur clusters. *Annu Rev Biochem, 74*, 247-281. doi:10.1146/annurev.biochem.74.082803.133518
Jones, & George. (2004). The ABC transporter structure and mechanism: perspectives on recent research. *Cell Mol Life Sci, 61*(6), 682-699. doi:10.1007/s00018-003-3336-9
Jones, P. M., & George, A. M. (2015). The Nucleotide-Free State of the Multidrug Resistance ABC Transporter LmrA: Sulfhydryl Cross-Linking Supports a Constant Contact, Head-to-Tail Configuration of the Nucleotide-Binding Domains. *PLoS One, 10*(6), e0131505. doi:10.1371/journal.pone.0131505
Kanetis, L., Forster, H., Jones, C. A., Borkovich, K. A., & Adaskaveg, J. E. (2008). Characterization of genetic and biochemical mechanisms of fludioxonil and pyrimethanil resistance in field isolates of Penicillium digitatum. *Phytopathology, 98*(2), 205-214. doi:10.1094/phyto-98-2-0205
Kawai, S., Suzuki, S., Mori, S., & Murata, K. (2001). Molecular cloning and identification of UTR1 of a yeast Saccharomyces cerevisiae as a gene encoding an NAD kinase. *FEMS Microbiol Lett, 200*(2), 181-184.
Khandelwal, N. K., Chauhan, N., Sarkar, P., Esquivel, B. D., Coccetti, P., Singh, A., . . . Prasad, R. (2018). Azole resistance in a Candida albicans mutant lacking the ABC transporter CDR6/ROA1 depends on TOR signaling. *J Biol Chem, 293*(2), 412-432. doi:10.1074/jbc.M117.807032
Kispal, G., Csere, P., Guiard, B., & Lill, R. (1997). The ABC transporter Atm1p is required for mitochondrial iron homeostasis. *FEBS Lett, 418*(3), 346-350.
Kispal, G., Csere, P., Prohl, C., & Lill, R. (1999). The mitochondrial proteins Atm1p and Nfs1p are essential for biogenesis of cytosolic Fe/S proteins. *Embo j, 18*(14), 3981-3989. doi:10.1093/emboj/18.14.3981
Kleinschmidt, J. H., den Blaauwen, T., Driessen, A. J., & Tamm, L. K. (1999). Outer membrane protein A of Escherichia coli inserts and folds into lipid bilayers by a concerted mechanism. *Biochemistry, 38*(16), 5006-5016. doi:10.1021/bi982465w
Knowles, T. J., Finka, R., Smith, C., Lin, Y. P., Dafforn, T., & Overduin, M. (2009). Membrane proteins solubilized intact in lipid containing nanoparticles

bounded by styrene maleic acid copolymer. *J Am Chem Soc, 131*(22), 7484-7485. doi:10.1021/ja810046q

Kohli, A., Smriti, N., Mukhopadhyay, K., Rattan, A., & Prasad, R. (2002). In Vitro Low-Level Resistance to Azoles in Candida albicans Is Associated with Changes in Membrane Lipid Fluidity and Asymmetry. *Antimicrob Agents Chemother, 46*(4), 1046-1052. doi:10.1128/aac.46.4.1046-1052.2002

Korkhov, V. M., Mireku, S. A., & Locher, K. P. (2012). Structure of AMP-PNP-bound vitamin B12 transporter BtuCD-F. *Nature, 490*(7420), 367-372. doi:10.1038/nature11442

Koynova , T. (2013). Transitions between lamellar and non-lamellar phases in membrane lipids and their physiological roles. *OA Biochemistry, 1(1):9*.

Kozachkov, L., & Padan, E. (2011). Site-directed tryptophan fluorescence reveals two essential conformational changes in the Na+/H+ antiporter NhaA. *Proc Natl Acad Sci U S A, 108*(38), 15769-15774. doi:10.1073/pnas.1109256108

Kuchler, K., Goransson, H. M., Viswanathan, M. N., & Thorner, J. (1992). Dedicated transporters for peptide export and intercompartmental traffic in the yeast Saccharomyces cerevisiae. *Cold Spring Harb Symp Quant Biol, 57*, 579-592.

Kumar, A., Tyagi, N. K., Goyal, P., Pandey, D., Siess, W., & Kinne, R. K. (2007). Sodium-independent low-affinity D-glucose transport by human sodium/D-glucose cotransporter 1: critical role of tryptophan 561. *Biochemistry, 46*(10), 2758-2766. doi:10.1021/bi061696x

Kwan, T., Loughrey, H., Brault, M., Gruenheid, S., Urbatsch, I. L., Senior, A. E., & Gros, P. (2000). Functional analysis of a tryptophan-less P-glycoprotein: a tool for tryptophan insertion and fluorescence spectroscopy. *Mol Pharmacol, 58*(1), 37-47.

Lakowicz, J. R. (2006). Principles of Fluorescence Spectroscopy. (3), XXVI, 954. doi:10.1007/978-0-387-46312-4

Landau, E. M., & Rosenbusch, J. P. (1996). Lipidic cubic phases: A novel concept for the crystallization of membrane proteins. *Proceedings of the National Academy of Sciences, 93*(25), 14532-14535.

Lander, E. S., Linton, L. M., Birren, B., Nusbaum, C., Zody, M. C., Baldwin, J., . . . Szustakowki, J. (2001). Initial sequencing and analysis of the human genome. *Nature, 409*(6822), 860-921. doi:10.1038/35057062

Landolt-Marticorena, C., Williams, K. A., Deber, C. M., & Reithmeier, R. A. F. (1993). Non-random Distribution of Amino Acids in the Transmembrane Segments of Human Type I Single Span Membrane Proteins. *Journal of Molecular Biology, 229*(3), 602-608. doi:https://doi.org/10.1006/jmbi.1993.1066

Lange, C., Nett, J. H., Trumpower, B. L., & Hunte, C. (2001). Specific roles of protein–phospholipid interactions in the yeast cytochrome bc₁ complex structure. *Embo j, 20*(23), 6591-6600. doi:10.1093/emboj/20.23.6591

Larsson, O., Deeney, J. T., Bränström, R., Berggren, P.-O., & Corkey, B. E. (1996). Activation of the ATP-sensitive K Channel by Long Chain Acyl-CoA: A ROLE IN MODULATION OF PANCREATIC β-CELL GLUCOSE SENSITIVITY. *Journal of Biological Chemistry, 271*(18), 10623-10626. doi:10.1074/jbc.271.18.10623

Lazaridis, T. (2001). Hydrophobic Effect *eLS*: John Wiley & Sons, Ltd.

le Maire, M., Champeil, P., & Moller, J. V. (2000). Interaction of membrane proteins and lipids with solubilizing detergents. *Biochim Biophys Acta, 1508*(1-2), 86-111.
Lee, A. G. (2000). Membrane lipids: it's only a phase. *Curr Biol, 10*(10), R377-380.
Lee, A. G. (2003). Lipid–protein interactions in biological membranes: a structural perspective. *Biochimica et Biophysica Acta (BBA) - Biomembranes, 1612*(1), 1-40. doi:10.1016/s0005-2736(03)00056-7
Lee, J. Y., Yang, J. G., Zhitnitsky, D., Lewinson, O., & Rees, D. C. (2014). Structural basis for heavy metal detoxification by an Atm1-type ABC exporter. *Science, 343*(6175), 1133-1136. doi:10.1126/science.1246489
Leenhouts, Wijngaard, v. d., Kroon, d., & Kruijff, d. (1995). Anionic phospholipids can mediate membrane insertion of the anionic part of a bound peptide. *FEBS Lett, 370*(3), 189-192. doi:doi:10.1016/0014-5793(95)00823-R
Leighton, J., & Schatz, G. (1995). An ABC transporter in the mitochondrial inner membrane is required for normal growth of yeast. *Embo j, 14*(1), 188-195.
Leroux, P. (1994). Influence du pH, d'acides aminés et de diverses substances organiques sur la fongitoxicité du pyriméthanil, du glufosinate, du captafol, du cymoxanil et du fenpiclonil vis-à-vis de certaines souches de Botrytis cinerea. *Agronomie, 14*(8), 541-554.
Lewis, R. N. A. H., & McElhaney, R. N. (2013). Membrane lipid phase transitions and phase organization studied by Fourier transform infrared spectroscopy. *Biochimica et Biophysica Acta (BBA) - Biomembranes, 1828*(10), 2347-2358. doi:http://dx.doi.org/10.1016/j.bbamem.2012.10.018
Li, L., Vorobyov, I., & Allen, T. W. (2013). The different interactions of lysine and arginine side chains with lipid membranes. *J Phys Chem B, 117*(40), 11906-11920. doi:10.1021/jp405418y
Li, X.-Z., & Nikaido, H. (2009). Efflux-Mediated Drug Resistance in Bacteria: an Update. *Drugs, 69*(12), 1555-1623. doi:10.2165/11317030-000000000-00000
Li, X. X., Tsoi, B., Li, Y. F., Kurihara, H., & He, R. R. (2015). Cardiolipin and its different properties in mitophagy and apoptosis. *J Histochem Cytochem, 63*(5), 301-311. doi:10.1369/0022155415574818
Liang, J., Adamian, L., & Jackups, R., Jr. (2005). The membrane–water interface region of membrane proteins: structural bias and the anti-snorkeling effect. *Trends in Biochemical Sciences, 30*(7), 355-357. doi:10.1016/j.tibs.2005.05.003
Lill, R., Dowhan, W., & Wickner, W. (1990). The ATPase activity of secA is regulated by acidic phospholipids, secY, and the leader and mature domains of precursor proteins. *Cell, 60*(2), 271-280. doi:10.1016/0092-8674(90)90742-W
Lin, D. Y., Huang, S., & Chen, J. (2015). Crystal structures of a polypeptide processing and secretion transporter. *Nature, 523*(7561), 425-430. doi:10.1038/nature14623
Liu, Y., Cong, X., Liu, W., & Laganowsky, A. (2016). Characterization of Membrane Protein-Lipid Interactions by Mass Spectrometry Ion Mobility Mass Spectrometry. *J Am Soc Mass Spectrom*. doi:10.1007/s13361-016-1555-1
Locher. (2009). Structure and mechanism of ATP-binding cassette transporters. *Philosophical Transactions of the Royal Society B: Biological Sciences, 364*(1514), 239-245. doi:10.1098/rstb.2008.0125

Locher. (2016). Mechanistic diversity in ATP-binding cassette (ABC) transporters. *Nat Struct Mol Biol, 23*(6), 487-493. doi:10.1038/nsmb.3216
Locher, Lee, & Rees. (2002). The E. coli BtuCD structure: a framework for ABC transporter architecture and mechanism. *Science, 296*(5570), 1091-1098. doi:10.1126/science.1071142
Lodish, H., Berk, A., & Zipursky, L. S. (2000). Molecular Cell Biology (4th edition ed.). New York: W. H. Freeman.
Logothetis, D. E., Jin, T., Lupyan, D., & Rosenhouse-Dantsker, A. (2007). Phosphoinositide-mediated gating of inwardly rectifying K+ channels. *Pflügers Archiv - European Journal of Physiology, 455*(1), 83-95. doi:10.1007/s00424-007-0276-5
Lopez-Marques, R. L., Poulsen, L. R., Bailly, A., Geisler, M., Pomorski, T. G., & Palmgren, M. G. (2015). Structure and mechanism of ATP-dependent phospholipid transporters. *Biochim Biophys Acta, 1850*(3), 461-475. doi:10.1016/j.bbagen.2014.04.008
Lu, M. (2016). Structures of multidrug and toxic compound extrusion transporters and their mechanistic implications. *Channels, 10*(2), 88-100. doi:10.1080/19336950.2015.1106654
Luckey, M. (2014). *Membrane Structural Biology* (Second ed.). United States: Sheridan Inc.
Luzzati, V. (1997). Biological significance of lipid polymorphism: the cubic phases. *Current Opinion in Structural Biology, 7*(5), 661-668. doi:http://dx.doi.org/10.1016/S0959-440X(97)80075-9
Maeno, S., Miura, I., Masuda, K., & Nagata, T. (1990). *Mepanipyrim (KIF-3535), a new pyrimidine fungicide.* Paper presented at the Brighton Crop Protection Conference, Pests and Diseases-1990. Vol. 2.
Manajit, H.-H., Hermann, S., Gebhard, J., & Klaus, B. (1992). Interactions of phospholipids with the mitochondrial cytochrome-c reductase studied by spin-label ESR and NMR spectroscopy. *European Journal of Biochemistry, 209*(1), 423-430. doi:doi:10.1111/j.1432-1033.1992.tb17305.x
Marius, P., Zagnoni, M., Sandison, M. E., East, J. M., Morgan, H., & Lee, A. G. (2008). Binding of anionic lipids to at least three nonannular sites on the potassium channel KcsA is required for channel opening. *Biophys J, 94*(5), 1689-1698. doi:10.1529/biophysj.107.117507
Marquez, B. (2005). Bacterial efflux systems and efflux pumps inhibitors. *Biochimie, 87*(12), 1137-1147. doi:10.1016/j.biochi.2005.04.012
Masner, P., Muster, P., & Schmid, J. (1994). Possible methionine biosynthesis inhibition by pyrimidinamine fungicides. *Pesticide Science, 42*(3), 163-166. doi:10.1002/ps.2780420304
McAuley, K. E., Fyfe, P. K., Ridge, J. P., Isaacs, N. W., Cogdell, R. J., & Jones, M. R. (1999). Structural details of an interaction between cardiolipin and an integral membrane protein. *Proc Natl Acad Sci U S A, 96*(26), 14706-14711.
Mehmood, S., Corradi, V., Choudhury, H. G., Hussain, R., Becker, P., Axford, D., . . . Beis, K. (2016). Structural and functional basis for lipid synergy on the activity of the antibacterial peptide ABC transporter McjD. *Journal of Biological Chemistry*. doi:10.1074/jbc.M116.732107
Menezes, M. E., Roepe, P. D., & Kaback, H. R. (1990). Design of a membrane transport protein for fluorescence spectroscopy. *Proceedings of the*

National Academy of Sciences of the United States of America, 87(5), 1638-1642.
Milling, R. J., & Richardson, C. J. (1995). Mode of action of the anilino-pyrimidine fungicide pyrimethanil. 2. Effects on enzyme secretion in Botrytis cinerea. *Pesticide Science, 45*(1), 43-48. doi:10.1002/ps.2780450107
Miura, I., Kamakura, T., Maeno, S., Hayashi, S., & Yamaguchi, I. (1994). Inhibition of Enzyme Secretion in Plant Pathogens by Mepanipyrim, a Novel Fungicide. *Pesticide Biochemistry and Physiology, 48*(3), 222-228. doi:https://doi.org/10.1006/pest.1994.1023
Miyagi, H., Kawai, S., & Murata, K. (2009). Two sources of mitochondrial NADPH in the yeast Saccharomyces cerevisiae. *J Biol Chem, 284*(12), 7553-7560. doi:10.1074/jbc.M804100200
Mizushima, T., Ishikawa, Y., Obana, E., Hase, M., Kubota, T., Katayama, T., . . . Sekimizu, K. (1996). Influence of Cluster Formation of Acidic Phospholipids on Decrease in the Affinity for ATP of DnaA Protein. *Journal of Biological Chemistry, 271*(7), 3633-3638. doi:10.1074/jbc.271.7.3633
Moody, J. E., Millen, L., Binns, D., Hunt, J. F., & Thomas, P. J. (2002). Cooperative, ATP-dependent association of the nucleotide binding cassettes during the catalytic cycle of ATP-binding cassette transporters. *J Biol Chem, 277*(24), 21111-21114. doi:10.1074/jbc.C200228200
Morita, Y., Kataoka, A., Shiota, S., Mizushima, T., & Tsuchiya, T. (2000). NorM of vibrio parahaemolyticus is an Na(+)-driven multidrug efflux pump. *J Bacteriol, 182*(23), 6694-6697.
Morita, Y., Kodama, K., Shiota, S., Mine, T., Kataoka, A., Mizushima, T., & Tsuchiya, T. (1998). NorM, a Putative Multidrug Efflux Protein, of Vibrio parahaemolyticus and Its Homolog in Escherichia coli. *Antimicrob Agents Chemother, 42*(7), 1778-1782.
Morrison, K. A., Akram, A., Mathews, A., Khan, Z. A., Patel, J. H., Zhou, C., . . . Rothnie, A. J. (2016). Membrane protein extraction and purification using styrene-maleic acid (SMA) copolymer: effect of variations in polymer structure. *Biochem J, 473*(23), 4349-4360. doi:10.1042/bcj20160723
Mosbach, A., Edel, D., Farmer, A. D., Widdison, S., Barchietto, T., Dietrich, R. A., . . . Scalliet, G. (2017). Anilinopyrimidine Resistance in Botrytis cinerea Is Linked to Mitochondrial Function. *Front Microbiol, 8*(2361). doi:10.3389/fmicb.2017.02361
Munita, J. M., & Arias, C. A. (2016). Mechanisms of Antibiotic Resistance. *Microbiology spectrum, 4*(2), 10.1128/microbiolspec.VMBF-0016-2015. doi:10.1128/microbiolspec.VMBF-0016-2015
Murakami, S. (2008). Multidrug efflux transporter, AcrB--the pumping mechanism. *Curr Opin Struct Biol, 18*(4), 459-465. doi:10.1016/j.sbi.2008.06.007
Neumann, G., Winter, E., & Pittis, J. (1992). *Pyrimethanil: a new fungicide.* Paper presented at the Brighton Crop Protection Conference, Pests and Diseases-1992. Volume 1.
Nikaido, H., & Takatsuka, Y. (2009). Mechanisms of RND multidrug efflux pumps. *Biochim Biophys Acta, 1794*(5), 769-781. doi:10.1016/j.bbapap.2008.10.004
Nishiyama, K., Mizushima, S., & Tokuda, H. (1993). A novel membrane protein involved in protein translocation across the cytoplasmic membrane of Escherichia coli. *Embo j, 12*(9), 3409-3415.

O'Keeffe, A. H., East, J. M., & Lee, A. G. (2000). Selectivity in lipid binding to the bacterial outer membrane protein OmpF. *Biophys J, 79*(4), 2066-2074. doi:10.1016/s0006-3495(00)76454-x

O'Mara, M. L., & Tieleman, D. P. (2007). P-glycoprotein models of the apo and ATP-bound states based on homology with Sav1866 and MalK. *FEBS Lett, 581*(22), 4217-4222. doi:10.1016/j.febslet.2007.07.069

Ohvo-Rekilä, H., Ramstedt, B., Leppimäki, P., & Peter Slotte, J. (2002). Cholesterol interactions with phospholipids in membranes. *Progress in Lipid Research, 41*(1), 66-97. doi:https://doi.org/10.1016/S0163-7827(01)00020-0

Oldham, M. L., Hite, R. K., Steffen, A. M., Damko, E., Li, Z., Walz, T., & Chen, J. (2016). A mechanism of viral immune evasion revealed by cryo-EM analysis of the TAP transporter. *Nature, 529*(7587), 537-540. doi:10.1038/nature16506

Opperman, T. J., & Nguyen, S. T. (2015). Recent advances toward a molecular mechanism of efflux pump inhibition. *Front Microbiol, 6*, 421. doi:10.3389/fmicb.2015.00421

Outten, C. E., & Culotta, V. C. (2003). A novel NADH kinase is the mitochondrial source of NADPH in Saccharomyces cerevisiae. *Embo j, 22*(9), 2015-2024. doi:10.1093/emboj/cdg211

Pain, J., Balamurali, M. M., Dancis, A., & Pain, D. (2010). Mitochondrial NADH kinase, Pos5p, is required for efficient iron-sulfur cluster biogenesis in Saccharomyces cerevisiae. *J Biol Chem, 285*(50), 39409-39424. doi:10.1074/jbc.M110.178947

Panatala, R., Hennrich, H., & Holthuis, J. C. (2015). Inner workings and biological impact of phospholipid flippases. *J Cell Sci, 128*(11), 2021-2032. doi:10.1242/jcs.102715

Papadopoulos, J. S., & Agarwala, R. (2007). COBALT: constraint-based alignment tool for multiple protein sequences. *Bioinformatics, 23*(9), 1073-1079. doi:10.1093/bioinformatics/btm076

Parmar, M., Rawson, S., Scarff, C. A., Goldman, A., Dafforn, T. R., Muench, S. P., & Postis, V. L. G. (2018). Using a SMALP platform to determine a sub-nm single particle cryo-EM membrane protein structure. *Biochim Biophys Acta, 1860*(2), 378-383. doi:10.1016/j.bbamem.2017.10.005

Pasupuleti, M., Schmidtchen, A., & Malmsten, M. (2012). Antimicrobial peptides: key components of the innate immune system. *Critical Reviews in Biotechnology, 32*(2), 143-171. doi:doi:10.3109/07388551.2011.594423

Paulsen, I. T., Skurray, R. A., Tam, R., Saier, M. H., Jr., Turner, R. J., Weiner, J. H., . . . Grinius, L. L. (1996). The SMR family: a novel family of multidrug efflux proteins involved with the efflux of lipophilic drugs. *Mol Microbiol, 19*(6), 1167-1175.

Peetla, C., Bhave, R., Vijayaraghavalu, S., Stine, A., Kooijman, E., & Labhasetwar, V. (2010). Drug resistance in breast cancer cells: biophysical characterization of and doxorubicin interactions with membrane lipids. *Mol Pharm, 7*(6), 2334-2348. doi:10.1021/mp100308n

Pinkett, H. W., Lee, A. T., Lum, P., Locher, K. P., & Rees, D. C. (2007). An inward-facing conformation of a putative metal-chelate-type ABC transporter. *Science, 315*(5810), 373-377. doi:10.1126/science.1133488

Pollak, N., Dolle, C., & Ziegler, M. (2007). The power to reduce: pyridine nucleotides--small molecules with a multitude of functions. *Biochem J, 402*(2), 205-218. doi:10.1042/bj20061638

Postis, V., Rawson, S., Mitchell, J. K., Lee, S. C., Parslow, R. A., Dafforn, T. R., . . . Muench, S. P. (2015). The use of SMALPs as a novel membrane protein scaffold for structure study by negative stain electron microscopy. *Biochimica et Biophysica Acta (BBA) - Biomembranes, 1848*(2), 496-501. doi:https://doi.org/10.1016/j.bbamem.2014.10.018

Powl, A. M., East, J. M., & Lee, A. G. (2005). Heterogeneity in the binding of lipid molecules to the surface of a membrane protein: hot spots for anionic lipids on the mechanosensitive channel of large conductance MscL and effects on conformation. *Biochemistry, 44*(15), 5873-5883. doi:10.1021/bi047439e

Powl, A. M., East, J. M., & Lee, A. G. (2008). Anionic Phospholipids Affect the Rate and Extent of Flux through the Mechanosensitive Channel of Large Conductance MscL. *Biochemistry, 47*(14), 4317-4328. doi:10.1021/bi702409t

Prasad, T., Chandra, A., Mukhopadhyay, C. K., & Prasad, R. (2006). Unexpected Link between Iron and Drug Resistance of Candida spp.: Iron Depletion Enhances Membrane Fluidity and Drug Diffusion, Leading to Drug-Susceptible Cells. *Antimicrob Agents Chemother, 50*(11), 3597-3606. doi:10.1128/aac.00653-06

Puthenveetil, R., Nguyen, K., & Vinogradova, O. (2017). Nanodiscs and Solution NMR: preparation, application and challenges. *Nanotechnol Rev, 6*(1), 111-126. doi:10.1515/ntrev-2016-0076

Raetz, C. R. (1978). Enzymology, genetics, and regulation of membrane phospholipid synthesis in Escherichia coli. *Microbiol Rev, 42*(3), 614-659.

Raja, M., Spelbrink, R. E., de Kruijff, B., & Killian, J. A. (2007). Phosphatidic acid plays a special role in stabilizing and folding of the tetrameric potassium channel KcsA. *FEBS Lett, 581*(29), 5715-5722. doi:10.1016/j.febslet.2007.11.039

Rapedius, M., Soom, M., Shumilina, E., Schulze, D., Schönherr, R., Kirsch, C., . . . Baukrowitz, T. (2005). Long Chain CoA Esters as Competitive Antagonists of Phosphatidylinositol 4,5-Bisphosphate Activation in Kir Channels. *Journal of Biological Chemistry, 280*(35), 30760-30767. doi:10.1074/jbc.M503503200

Rasmussen, A., Rasmussen, T., Edwards, M. D., Schauer, D., Schumann, U., Miller, S., & Booth, I. R. (2007). The role of tryptophan residues in the function and stability of the mechanosensitive channel MscS from Escherichia coli. *Biochemistry, 46*(38), 10899-10908. doi:10.1021/bi701056k

Rebuffat, S., Blond, A., Destoumieux-Garzon, D., Goulard, C., & Peduzzi, J. (2004). Microcin J25, from the macrocyclic to the lasso structure: implications for biosynthetic, evolutionary and biotechnological perspectives. *Curr Protein Pept Sci, 5*(5), 383-391.

Rees, D. C., Johnson, E., & Lewinson, O. (2009). ABC transporters: the power to change. *Nat Rev Mol Cell Biol, 10*(3), 218-227. doi:10.1038/nrm2646

Rule, C. S., Patrick, M., & Sandkvist, M. (2016). Measuring In Vitro ATPase Activity for Enzymatic Characterization. *J Vis Exp*(114). doi:10.3791/54305

Saeui, C., Mathew, M., Liu, L., Urias, E., & Yarema, K. (2015). Cell Surface and Membrane Engineering: Emerging Technologies and Applications. *Journal of Functional Biomaterials, 6*(2), 454.

Saier, M. H., Jr., & Paulsen, I. T. (2001). Phylogeny of multidrug transporters. *Semin Cell Dev Biol, 12*(3), 205-213. doi:10.1006/scdb.2000.0246

Schaedler, T. A., Faust, B., Shintre, C. A., Carpenter, E. P., Srinivasan, V., van Veen, H. W., & Balk, J. (2015). Structures and functions of mitochondrial ABC transporters. *Biochem Soc Trans, 43*(5), 943-951. doi:10.1042/bst20150118

Schaedler, T. A., Thornton, J. D., Kruse, I., Schwarzländer, M., Meyer, A. J., van Veen, H. W., & Balk, J. (2014). A Conserved Mitochondrial ATP-Binding Cassette Transporter Exports Glutathione Polysulfide for Cytosolic Metal Cofactor Assembly. *Journal of Biological Chemistry*. doi:10.1074/jbc.M114.553438

Schagger, H., Hagen, T., Roth, B., Brandt, U., Link, T. A., & von Jagow, G. (1990). Phospholipid specificity of bovine heart bc1 complex. *European Journal of Biochemistry, 190*(1), 123-130. doi:10.1111/j.1432-1033.1990.tb15554.x

Schiffer, M., Chang, C.-H., & Stevens, F. J. (1992). The function of tryptophan residues in membrane proteins. *Protein Engineering, 5*(3), 213-214. doi:10.1093/protein/5.3.213

Schmidt, T., Suk, J. E., Ye, F., Situ, A. J., Mazumder, P., Ginsberg, M. H., & Ulmer, T. S. (2015). Annular anionic lipids stabilize the integrin alphaIIbbeta3 transmembrane complex. *J Biol Chem*. doi:10.1074/jbc.M114.623504

Schneider, C. A., Rasband, W. S., & Eliceiri, K. W. (2012). NIH Image to ImageJ: 25 years of image analysis. *Nat Meth, 9*(7), 671-675.

Schreiber, V., Dantzer, F., Ame, J. C., & Murcia, G. (2006). Poly(ADP-ribose): novel functions for an old molecule. *Nat Rev Mol Cell Biol, 7*. doi:10.1038/nrm1963

Schuber, F., & Lund, F. E. (2004). Structure and enzymology of ADP-ribosyl cyclases: conserved enzymes that produce multiple calcium mobilizing metabolites. *Curr Mol Med, 4*(3), 249-261.

Schueck, N. D., Woontner, M., & Koeller, D. M. (2001). The role of the mitochondrion in cellular iron homeostasis. *Mitochondrion, 1*(1), 51-60.

Schulze, D., Rapedius, M., Krauter, T., & Baukrowitz, T. (2003). *Long-chain acyl-CoA esters and phosphatidylinositol phosphates modulate ATP inhibition of K-ATP channels by the same mechanism* (Vol. 552).

Seddon, A. M., Curnow, P., & Booth, P. J. (2004). Membrane proteins, lipids and detergents: not just a soap opera. *Biochim Biophys Acta, 1666*(1-2), 105-117. doi:10.1016/j.bbamem.2004.04.011

Seeger, M. A., & van Veen, H. W. (2009). Molecular basis of multidrug transport by ABC transporters. *Biochim Biophys Acta, 1794*(5), 725-737. doi:10.1016/j.bbapap.2008.12.004

Seelig, A., & Seelig, J. (1977). Effect of a single cis double bond on the structures of a phospholipid bilayer. *Biochemistry, 16*(1), 45-50.

Segawa, K., Kurata, S., Yanagihashi, Y., Brummelkamp, T. R., Matsuda, F., & Nagata, S. (2014). Caspase-mediated cleavage of phospholipid flippase for apoptotic phosphatidylserine exposure. *Science, 344*(6188), 1164-1168. doi:10.1126/science.1252809

Senior, A. E., Al-Shawi, M. K., & Urbatsch, I. L. (1995). The catalytic cycle of P-glycoprotein. *FEBS Lett, 377*(3), 285-289. doi:https://doi.org/10.1016/0014-5793(95)01345-8

Senior, A. E., & Bhagat, S. (1998). P-Glycoprotein Shows Strong Catalytic Cooperativity between the Two Nucleotide Sites. *Biochemistry, 37*(3), 831-836. doi:10.1021/bi9719962

Sharma, S., & Davidson, A. L. (2000). Vanadate-induced trapping of nucleotides by purified maltose transport complex requires ATP hydrolysis. *J Bacteriol, 182*(23), 6570-6576.
Sharom, F. J. (2011). The P-glycoprotein multidrug transporter. *Essays Biochem, 50*(1), 161-178. doi:10.1042/bse0500161
Shi, F., Kawai, S., Mori, S., Kono, E., & Murata, K. (2005). Identification of ATP-NADH kinase isozymes and their contribution to supply of NADP(H) in Saccharomyces cerevisiae. *Febs j, 272*(13), 3337-3349. doi:10.1111/j.1742-4658.2005.04749.x
Shinzawa‐Itoh, K., Aoyama, H., Muramoto, K., Terada, H., Kurauchi, T., Tadehara, Y., . . . Yoshikawa, S. (2007). Structures and physiological roles of 13 integral lipids of bovine heart cytochrome c oxidase. *Embo j, 26*(6), 1713-1725. doi:10.1038/sj.emboj.7601618
Shyng, S.-L., & Nichols, C. G. (1998). Membrane Phospholipid Control of Nucleotide Sensitivity of K_{ATP} Channels. *Science, 282*(5391), 1138-1141. doi:10.1126/science.282.5391.1138
Sievers, S., Ernst, C. M., Geiger, T., Hecker, M., Wolz, C., Becher, D., & Peschel, A. (2010). Changing the phospholipid composition of Staphylococcus aureus causes distinct changes in membrane proteome and membrane-sensory regulators. *Proteomics, 10*(8), 1685-1693. doi:10.1002/pmic.200900772
Silhavy, T. J., Kahne, D., & Walker, S. (2010). The Bacterial Cell Envelope. *Cold Spring Harb Perspect Biol, 2*(5), a000414. doi:10.1101/cshperspect.a000414
Simmonds, A. C., East, J. M., Jones, O. T., Rooney, E. K., McWhirter, J., & Lee, A. G. (1982). Annular and non-annular binding sites on the (Ca2+ + Mg2+)-ATPase. *Biochimica et Biophysica Acta (BBA) - Biomembranes, 693*(2), 398-406. doi:http://dx.doi.org/10.1016/0005-2736(82)90447-3
Simmonds, A. C., Rooney, E. K., & Lee, A. G. (1984). Interactions of cholesterol hemisuccinate with phospholipids and calcium-magnesium ATPase. *Biochemistry, 23*(7), 1432-1441. doi:10.1021/bi00302a015
Sirangelo, I., Tavassi, S., Martelli, P. L., Casadio, R., & Irace, G. (2000). The effect of tryptophanyl substitution on folding and structure of myoglobin. *Eur J Biochem, 267*(13), 3937-3945.
Smith, P. K., Krohn, R. I., Hermanson, G. T., Mallia, A. K., Gartner, F. H., Provenzano, M. D., . . . Klenk, D. C. (1985). Measurement of protein using bicinchoninic acid. *Anal Biochem, 150*(1), 76-85.
Solbiati, J. O., Ciaccio, M., Farías, R. N., González-Pastor, J. E., Moreno, F., & Salomón, R. A. (1999). Sequence Analysis of the Four Plasmid Genes Required To Produce the Circular Peptide Antibiotic Microcin J25. *J Bacteriol, 181*(8), 2659-2662.
Srinivasan, V., Pierik, A. J., & Lill, R. (2014). Crystal structures of nucleotide-free and glutathione-bound mitochondrial ABC transporter Atm1. *Science, 343*(6175), 1137-1140. doi:10.1126/science.1246729
Srivalli, K. M. R., & Lakshmi, P. K. (2012). Overview of P-glycoprotein inhibitors: a rational outlook. *Brazilian Journal of Pharmaceutical Sciences, 48*, 353-367.
Srivastava, S. (2016). Emerging therapeutic roles for NAD+ metabolism in mitochondrial and age-related disorders. *Clinical and Translational Medicine, 5*(1), 25. doi:10.1186/s40169-016-0104-7

Starling, A. P., East, J. M., & Lee, A. G. (1993). Effects of phosphatidylcholine fatty acyl chain length on calcium binding and other functions of the calcium-magnesium-ATPase. *Biochemistry, 32*(6), 1593-1600. doi:10.1021/bi00057a025

Stroud, Z., Hall, S. C. L., & Dafforn, T. R. (2018). Purification of membrane proteins free from conventional detergents: SMA, new polymers, new opportunities and new insights. *Methods*. doi:10.1016/j.ymeth.2018.03.011

Sun, C., Benlekbir, S., Venkatakrishnan, P., Wang, Y., Hong, S., Hosler, J., . . . Gennis, R. B. (2018). Structure of the alternative complex III in a supercomplex with cytochrome oxidase. *Nature, 557*(7703), 123-126. doi:10.1038/s41586-018-0061-y

Suzuki, S., Green, P. G., Bumgarner, R. E., Dasgupta, S., Goddard, W. A., & Blake, G. A. (1992). Benzene Forms Hydrogen Bonds with Water. *Science, 257*(5072), 942-945. doi:10.1126/science.257.5072.942

Swartz, D. J., Weber, J., & Urbatsch, I. L. (2013). P-glycoprotein is fully active after multiple tryptophan substitutions. *Biochim Biophys Acta, 1828*(3), 1159-1168. doi:10.1016/j.bbamem.2012.12.005

Swinehart, D. F. (1962). The Beer-Lambert Law. *Journal of Chemical Education, 39*(7), 333. doi:10.1021/ed039p333

Technikova-Dobrova, Z., Sardanelli, A. M., & Papa, S. (1991). Spectrophotometric determination of functional characteristics of protein kinases with coupled enzymatic assay. *FEBS Lett, 292*(1), 69-72. doi:https://doi.org/10.1016/0014-5793(91)80836-R

Todisco, S., Agrimi, G., Castegna, A., & Palmieri, F. (2006). Identification of the mitochondrial NAD+ transporter in Saccharomyces cerevisiae. *J Biol Chem, 281*(3), 1524-1531. doi:10.1074/jbc.M510425200

Tonge, S. R., & Tighe, B. J. (2001). Responsive hydrophobically associating polymers: a review of structure and properties. *Adv Drug Deliv Rev, 53*(1), 109-122.

Trumpower, B. L., & Gennis, R. B. (1994). Energy transduction by cytochrome complexes in mitochondrial and bacterial respiration: the enzymology of coupling electron transfer reactions to transmembrane proton translocation. *Annu Rev Biochem, 63*, 675-716. doi:10.1146/annurev.bi.63.070194.003331

Tsukihara, T., Aoyama, H., Yamashita, E., Tomizaki, T., Yamaguchi, H., Shinzawa-Itoh, K., . . . Yoshikawa, S. (1996). The whole structure of the 13-subunit oxidized cytochrome c oxidase at 2.8 A. *Science, 272*(5265), 1136-1144.

Tucker, S. J., & Baukrowitz, T. (2008). How Highly Charged Anionic Lipids Bind and Regulate Ion Channels. *The Journal of General Physiology, 131*(5), 431-438. doi:10.1085/jgp.200709936

Ulmschneider, M. B., & Sansom, M. S. P. (2001). Amino acid distributions in integral membrane protein structures. *Biochimica et Biophysica Acta (BBA) - Biomembranes, 1512*(1), 1-14. doi:https://doi.org/10.1016/S0005-2736(01)00299-1

Valeur, B. (2001). Characteristics of Fluorescence Emission *Molecular Fluorescence* (pp. 34-71): Wiley-VCH Verlag GmbH.

Valiyaveetil, F. I., Zhou, Y., & MacKinnon, R. (2002). Lipids in the structure, folding, and function of the KcsA K+ channel. *Biochemistry, 41*(35), 10771-10777.

Van Der Does, C., & Tampé, R. (2004). How do ABC transporters drive transport? *Biological Chemistry* (Vol. 385, pp. 927).
Van Klompenburg, W., Nilsson, I., von Heijne, G., & de Kruijff, B. (1997). Anionic phospholipids are determinants of membrane protein topology. *Embo j, 16*(14), 4261-4266.
Van Meer, G., Voelker, D. R., & Feigenson, G. W. (2008). Membrane lipids: where they are and how they behave. *Nat Rev Mol Cell Biol, 9*(2), 112-124. doi:10.1038/nrm2330
Vance, D. E., & Vance, J. E. (2008). *Biochemistry of lipids, lipoproteins and membranes*: Amsterdam ; Oxford : Elsevier, 2008. 5th ed.
Vázquez-Ibar, J. L., Guan, L., Svrakic, M., & Kaback, H. R. (2003). Exploiting luminescence spectroscopy to elucidate the interaction between sugar and a tryptophan residue in the lactose permease of Escherichia coli. *Proceedings of the National Academy of Sciences, 100*(22), 12706-12711. doi:10.1073/pnas.1835645100
Velamakanni, S., Yao, Y., Gutmann, D. A., & van Veen, H. W. (2008). Multidrug transport by the ABC transporter Sav1866 from Staphylococcus aureus. *Biochemistry, 47*(35), 9300-9308. doi:10.1021/bi8006737
Verhalen, B., & Wilkens, S. (2011). P-glycoprotein Retains Drug-stimulated ATPase Activity upon Covalent Linkage of the Two Nucleotide Binding Domains at Their C-terminal Ends. *Journal of Biological Chemistry, 286*(12), 10476-10482. doi:10.1074/jbc.M110.193151
Verhoven, B., Schlegel, R. A., & Williamson, P. (1995). Mechanisms of phosphatidylserine exposure, a phagocyte recognition signal, on apoptotic T lymphocytes. *J Exp Med, 182*(5), 1597-1601.
von Heijne, G. (1989). Control of topology and mode of assembly of a polytopic membrane protein by positively charged residues. *Nature, 341*(6241), 456-458. doi:10.1038/341456a0
von Heijne, G. (1992). Membrane protein structure prediction: Hydrophobicity analysis and the positive-inside rule. *Journal of Molecular Biology, 225*(2), 487-494. doi:https://doi.org/10.1016/0022-2836(92)90934-C
Wallace, L. A., Burke, J., & Dirr, H. W. (2000). Domain-domain interface packing at conserved Trp-20 in class alpha glutathione transferase impacts on protein stability. *Biochim Biophys Acta, 1478*(2), 325-332.
Ward, A., Reyes, C. L., Yu, J., Roth, C. B., & Chang, G. (2007). Flexibility in the ABC transporter MsbA: Alternating access with a twist. *Proc Natl Acad Sci U S A, 104*(48), 19005-19010. doi:10.1073/pnas.0709388104
Ward, A. B., Szewczyk, P., Grimard, V., Lee, C. W., Martinez, L., Doshi, R., . . . Chang, G. (2013). Structures of P-glycoprotein reveal its conformational flexibility and an epitope on the nucleotide-binding domain. *Proc Natl Acad Sci U S A, 110*(33), 13386-13391. doi:10.1073/pnas.1309275110
Wen, P. C., Verhalen, B., Wilkens, S., McHaourab, H. S., & Tajkhorshid, E. (2013). On the origin of large flexibility of P-glycoprotein in the inward-facing state. *J Biol Chem, 288*(26), 19211-19220. doi:10.1074/jbc.M113.450114
Wheatley, M., Charlton, J., Jamshad, M., Routledge, Sarah J., Bailey, S., La-Borde, Penelope J., . . . Poyner, David R. (2016). GPCR–styrene maleic acid lipid particles (GPCR–SMALPs): their nature and potential. *Biochem Soc Trans, 44*(2), 619-623. doi:10.1042/bst20150284

Williamson, I. M., Alvis, S. J., East, J. M., & Lee, A. G. (2002). Interactions of phospholipids with the potassium channel KcsA. *Biophys J, 83*(4), 2026-2038. doi:10.1016/s0006-3495(02)73964-7

Xue, M., Cheng, L., Faustino, I., Guo, W., & Marrink, S. J. (2018). Molecular Mechanism of Lipid Nanodisk Formation by Styrene-Maleic Acid Copolymers. *Biophys J*. doi:10.1016/j.bpj.2018.06.018

Yankovskaya, V., Horsefield, R., Törnroth, S., Luna-Chavez, C., Miyoshi, H., Léger, C., . . . Iwata, S. (2003). Architecture of Succinate Dehydrogenase and Reactive Oxygen Species Generation. *Science, 299*(5607), 700-704. doi:10.1126/science.1079605

Yau, W.-M., Wimley, W. C., Gawrisch, K., & White, S. H. (1998). The Preference of Tryptophan for Membrane Interfaces. *Biochemistry, 37*(42), 14713-14718. doi:10.1021/bi980809c

Yeagle, P. L. (2016). Chapter 12 - Lipid–Protein Interactions in Membranes. In P. L. Yeagle (Ed.), *The Membranes of Cells (Third Edition)* (pp. 291-334). Boston: Academic Press.

Yerushalmi, H., Lebendiker, M., & Schuldiner, S. (1995). EmrE, an Escherichia coli 12-kDa Multidrug Transporter, Exchanges Toxic Cations and H+ and Is Soluble in Organic Solvents. *Journal of Biological Chemistry, 270*(12), 6856-6863. doi:10.1074/jbc.270.12.6856

Ying, W. (2006). NAD+ and NADH in cellular functions and cell death. *Front Biosci, 11*, 3129-3148.

Young, L., Leonhard, K., Tatsuta, T., Trowsdale, J., & Langer, T. (2001). Role of the ABC transporter Mdl1 in peptide export from mitochondria. *Science, 291*(5511), 2135-2138. doi:10.1126/science.1056957

Yu, H. Z., Xu, J. P., Wang, X. Y., Ma, Y., Yu, D., Fei, D. Q., . . . Wang, W. L. (2017). Identification of Four ATP-Binding Cassette Transporter Genes in Cnaphalocrocis medinalis and Their Expression in Response to Insecticide Treatment. *J Insect Sci, 17*(2). doi:10.1093/jisesa/iex017

Zasloff, M. (2002). Antimicrobial peptides of multicellular organisms. *Nature, 415*, 389. doi:10.1038/415389a

Zhang, G., & Feng, J. (2016). The intrinsic resistance of bacteria. *Yi Chuan, 38*(10), 872-880. doi:10.16288/j.yczz.16-159

Zhang, M., Mileykovskaya, E., & Dowhan, W. (2002). Gluing the Respiratory Chain Together: CARDIOLIPIN IS REQUIRED FOR SUPERCOMPLEX FORMATION IN THE INNER MITOCHONDRIAL MEMBRANE. *Journal of Biological Chemistry, 277*(46), 43553-43556. doi:10.1074/jbc.C200551200

Zhang, W., Bogdanov, M., Pi, J., Pittard, A. J., & Dowhan, W. (2003). Reversible Topological Organization within a Polytopic Membrane Protein Is Governed by a Change in Membrane Phospholipid Composition. *Journal of Biological Chemistry, 278*(50), 50128-50135. doi:10.1074/jbc.M309840200

Zhang, W., Campbell, H. A., King, S. C., & Dowhan, W. (2005). Phospholipids as Determinants of Membrane Protein Topology: PHOSPHATIDYLETHANOLAMINE IS REQUIRED FOR THE PROPER TOPOLOGICAL ORGANIZATION OF THE γ-AMINOBUTYRIC ACID PERMEASE (GabP) OF ESCHERICHIA COLI. *Journal of Biological Chemistry, 280*(28), 26032-26038. doi:10.1074/jbc.M504929200

Zheng, N., & Gierasch, L. M. (1996). Signal sequences: the same yet different. *Cell, 86*(6), 849-852.

Zhou, Y., Morais-Cabral, J. H., Kaufman, A., & MacKinnon, R. (2001). Chemistry of ion coordination and hydration revealed by a K+ channel-Fab complex at 2.0 A resolution. *Nature, 414*(6859), 43-48. doi:10.1038/35102009

Zloh, M., Kaatz, G. W., & Gibbons, S. (2004). Inhibitors of multidrug resistance (MDR) have affinity for MDR substrates. *Bioorg Med Chem Lett, 14*(4), 881-885. doi:10.1016/j.bmcl.2003.12.015

Zolnerciks, J. K., Andress, E. J., Nicolaou, M., & Linton, K. J. (2011). Structure of ABC transporters. *Essays Biochem, 50*(1), 43-61. doi:10.1042/bse0500043

Zolnerciks, J. K., Wooding, C., & Linton, K. J. (2007). Evidence for a Sav1866-like architecture for the human multidrug transporter P-glycoprotein. *Faseb j, 21*(14), 3937-3948. doi:10.1096/fj.07-8610com

Zou, P., Bortolus, M., & McHaourab, H. S. (2009). Conformational cycle of the ABC transporter MsbA in liposomes: detailed analysis using double electron-electron resonance spectroscopy. *J Mol Biol, 393*(3), 586-597. doi:10.1016/j.jmb.2009.08.050

Zou, P., & McHaourab, H. S. (2009). Alternating access of the putative substrate-binding chamber in the ABC transporter MsbA. *J Mol Biol, 393*(3), 574-585. doi:10.1016/j.jmb.2009.08.051

Zou, P., & McHaourab, H. S. (2010). Increased Sensitivity and Extended Range of Distance Measurements in Spin-Labeled Membrane Proteins: Q-Band Double Electron-Electron Resonance and Nanoscale Bilayers. *Biophys J, 98*(6), L18-L20. doi:10.1016/j.bpj.2009.12.4193